

This electronic thesis or dissertation has been downloaded from the King's Research Portal at <https://kclpure.kcl.ac.uk/portal/>



The geochemistry of chert formation in Upper Cretaceous chalks.

Clayton, Christopher John

The copyright of this thesis rests with the author and no quotation from it or information derived from it may be published without proper acknowledgement.

END USER LICENCE AGREEMENT



Unless another licence is stated on the immediately following page this work is licensed

under a Creative Commons Attribution-NonCommercial-NoDerivatives 4.0 International

licence. <https://creativecommons.org/licenses/by-nc-nd/4.0/>

You are free to copy, distribute and transmit the work

Under the following conditions:

- Attribution: You must attribute the work in the manner specified by the author (but not in any way that suggests that they endorse you or your use of the work).
- Non Commercial: You may not use this work for commercial purposes.
- No Derivative Works - You may not alter, transform, or build upon this work.

Any of these conditions can be waived if you receive permission from the author. Your fair dealings and other rights are in no way affected by the above.

Take down policy

If you believe that this document breaches copyright please contact librarypure@kcl.ac.uk providing details, and we will remove access to the work immediately and investigate your claim.

THE GEOCHEMISTRY OF CHERT FORMATION
IN UPPER CRETACEOUS CHALKS

Christopher John Clayton

Department of Geology
University of London King's College

and

Isotope Geology Unit
Institute of Geological Sciences
London

Thesis submitted for the
degree of Doctor of Philosophy,
University of London.

July 1984

BEST COPY

AVAILABLE

Variable print quality

5 box files of plates

not available .

Please contact the
University if required

ALL
MISSING
PAGES ARE
BLANK

**THESIS
CONTAINS
TAPE
CASSETTE**

**PLEASE CONTACT THE
UNIVERSITY IF YOU WISH TO
SEE THIS MATERIAL.**

**THESIS
CONTAINS
CD/DVD**

CONTAINS DISKETTE

UNABLE TO COPY

CONTACT UNIVERSITY

IF YOU WISH TO SEE

THIS MATERIAL

**THIS THESIS CONTAINS
MICROFILMS THAT COULD
NOT BE DIGITISED.**

**PLEASE CONTACT THE
UNIVERSITY IF YOU WISH TO
SEE THIS MATERIAL.**

Contains

Microfiche

CONTAINS MUSIC CD

UNABLE TO COPY

CONTACT UNIVERSITY

IF YOU WISH TO SEE

THIS MATERIAL

VOLUME CONTAINS CLEAR OVERLAYS

OVERLAYS SCANNED SEPERATELY AND

OVER THE RELEVANT PAGE.

MISSING PAGES
CONTAIN SLIDES
PLEASE APPLY
TO UNIVERSITY
IF REQUIRED

**THESIS
CONTAINS
VIDEO**

**DIAGRAM ON THIS
PAGE EXCLUDED
UNDER INSTRUCTION
FROM THE
UNIVERSITY**

**EXECUTIVE SUMMARY
ONLY AVAILABLE.
THE ACCOMPANYING
PORTFOLIO
CONTAINS SENSITIVE
INFORMATION**

NO CD/DVD

ATTACHED

PLEASE APPLY

TO

UNIVERSITY

MISSING

PRINT

**Thesis contains many
DVD'S CD'S unable to
copy.**

**If required please contact
the University.**

Volume 2

Volume 3

Volume 4

Volume 5

BEST COPY

AVAILABLE

Poor text in the original
thesis.

Some text bound close to
the spine.

Some images distorted

PAGE
NUMBERING
AS ORIGINAL

APPENDIX 1 NOT COPIED
ON INSTRUCTION FROM
UNIVERSITY

CONTAINS
MICROFICHE

UNABLE TO
DIGITISE

CONTACT
UNIVERSITY

**Page
missing**

**PAGE
NUMBERS
CUT OFF
IN
ORIGINAL**

PAGE/PAGES
EXCLUDED
UNDER
INSTRUCTION
FROM
UNIVERSITY

MISSING PAGES
REMOVED ON
INSTRUCTION
FROM THE
UNIVERSITY

PORTFOLIO NOT
AVAILABLE ON
INSTRUCTION FROM
UNIVERSITY

**CONTAINS
PULLOUTS**

TEXT BOUND INTO

THE SPINE

Text cut off in original

Volume 2 restricted access

ABSTRACT

Nodular cherts ("flints") in the Upper Cretaceous Chalk of western Europe are a product of early diagenetic silica precipitation which occurred 5-10 metres below the sediment surface. Trace element and stable isotope variations suggest that silicification proceeded in sediment of 75-80% porosity and was initiated by dissolution of the host carbonate at this depth. Paramoudras (round vertical columnar flints containing a cemented chalk core and central burrow) provide a vital clue to understanding such localised carbonate dissolution. Anaerobic bacterial sulphate reduction released excess sulphide (H_2S or HS^-) which diffused outwards to become oxidised at the oxic-anoxic boundary, as revealed by iron and manganese profiles. The resulting hydrogen ions dissolved the chalk sediment causing seeding of dissolved silica.

The more common "bedded" flint bands result from more widespread sulphate reduction and re-oxidation of resultant sulphide at the base of the oxic zone. Local porosity/permeability variations resulted in heterogeneous mixing of the sulphide and oxygen to produce the characteristic digitate-nodular form of most flints. Less marked permeability variations resulted in more regular "tabular" flints, and early stage compaction joints became the sites of "sheet" flint formation.

Petrological investigations indicate that silicification proceeded in the sequence: centripetal replacement of skeletal fragments, en-mass precipitation of opal-CT lepispheres, and

growth of interstitial chalcedony cement. Subsequent recrystallisation of the opal-CT to low-quartz reset the oxygen isotope signature of the chert to an extent depending on both temperature and rate of recrystallisation. Recrystallisation during deeper burial was partially closed system and resulted in exsolution of structure-bound water and lowered $\delta^{18}\text{O}$ and δD in the ratio 1:3.7.

Finally, during uplift of the Chalk, the black ("wet") silica of the chert underwent partial isotopic re-equilibration with meteoric waters, lowering $\delta^{18}\text{O}$ and δD in the ratio 1:14.

"Who led thee through that great and terrible
wilderness, wherein were fiery serpents, and scorpions,
and drought, where there was no water; who brought
thee forth water out of the rock of flint;"

God speaks to Moses,

Deuteronomy 9, 15

ACKNOWLEDGEMENTS

This work would not have been possible without the support and guidance of my patient supervisors Max Coleman and Nick Walsh whose help is greatly appreciated. I would also like to thank the numerous colleagues with whom I have worked in the field, and particularly Rory Mortimore, Chris Wood, Andy Gale, Ian Jarvis and Richard Bromley, who have made fieldwork both illuminating and frequently very entertaining.

I wish also to acknowledge my many friends and colleagues at King's College and the Institute of Geological Sciences for their help, advice and technical backup over the past few years, and Miss A. Grant Suttie who kindly typed the manuscript at considerable risk to mental integrity.

Finally, my very special thanks to Janet Macmillan for her constant support during the seemingly interminable writing of this wretched thing, and for lending a hand to plate 7A.

CONTENTS

1. INTRODUCTION	15
1.1 Outline of Project	15
1.2 Terminology	16
1.3 History of Flint Research	17
1.3.1 Early Theories of Flint and Chalk	17
1.3.2 Current Theories	20
1.4 Organisation of Thesis	24
2. CHEMICAL DIAGENESIS IN SEDIMENTS	26
2.1 Background	26
2.2 pH/Eh Variations	26
2.3 Organic Matter Oxidation	27
2.3.1 Aerobic Respiration	30
2.3.2 Nitrate Reduction	31
2.3.3 Fe^{3+} and Mn^{4+} Reduction	32
2.3.4 Sulphate Reduction	33
2.3.5 Bacterial Fermentation	37
2.3.6 Subsequent Reactions	38
2.4 Silica Diagenesis	39
2.4.1 Silica in the Oceans	39
2.4.2 Silica Diagenesis	42
a) Dissolution	42
b) Chert Formation	46
c) Precipitation of Opal-CT	46
d) Opal-CT - Quartz recrystallisation	50
3. SEDIMENTOLOGY AND FIELD RELATIONS OF UPPER CRETACEOUS CHALKS	52
3.1 The Upper Cretaceous of Western Europe	52
3.2 Chalk Sedimentation	54
3.3 Marl Seams, "Flaser" Beds and Griotte Chalks	59
3.4 Omission Surfaces, Nodular Beds and Hardgrounds	68
3.5 Laminated Beds	71

3.6 Flints	72
3.6.1 The Burrow-form - Nodular - Tabular Association	77
3.6.2 Ring Flints and Paramoudras	87
3.6.3 Sponge Flints and Flint Replaced Fossils	94
3.6.4 Carious and Incipient Flints	97
3.6.5 Sheet Flints	98
3.6.6 Summary of Flint Field Relations	102
3.7 Pyrite and Related Minerals	104
3.8 Other Authigenic Minerals	109
3.8.1 Phosphates	109
3.8.2 "Glauconite"	111
4. PETROGRAPHY AND MICROSTRUCTURE OF FLINT	114
4.1 Introduction	114
4.2 General Characteristics of Flint	115
4.3 Water Distribution in Flint	118
4.3.1 Theoretical Considerations	118
4.3.2 Determination of Water in Flint	121
a) Thermogravimetric methods	121
b) Infra-red Absorption Spectra	125
4.4 Microstructure of Black Flint	126
4.5 White Bodies	138
4.5.1 Petrology and Origin	138
4.5.2 Banded Flints	144
4.6 Late Stage Void-filling Fabrics	145
4.7 Other Constituents	147
4.7.1 Detrital Grains	147
4.7.2 Authigenic Grains	147
4.7.3 Carbonaceous Matter	148
4.8 Cortex and Patina Formation	149
4.9 Structure of the Flint Crust	154
4.10 The Structural Classification of Flints & Cherts	157
4.11 Summary	158

5. TRACE ELEMENT AND STABLE ISOTOPE VARIATIONS IN FLINT	163
5.1 Introduction	163
5.2 Trace Element Variations	163
5.2.1 Trace Elements Associated with Trapped Pore-waters	165
5.2.2 Trace Elements in Other Phases	169
a) Effect of White Bodies	169
b) The Brandon Flint	175
5.2.3 Clay Mineral Dilution During Silicification	182
5.2.4 Chemistry of the Cortex and Crust	186
5.3 Stable Isotope Variations	190
5.3.1 Background	190
5.3.2 Relevance of Flints to Other Cherts	193
5.3.3 Effect of White Body Formation	194
5.3.4 Stable Isotope Variations in Black Flint	200
6. GEOCHEMISTRY OF PARAMOUDRAS	211
6.1 Introduction	211
6.2 Minor and Trace Element Chemistry	213
6.2.1 Chalk Interior	213
a) Pyrite and Carbonate Chemistry	213
b) Other Diagenetic Reactions	221
6.2.2 Flint Chemistry	225
a) Calcite Association	225
b) Iron and Manganese	227
c) Non-carbonate Association	231
6.3 Stable Isotope Variations	234
6.3.1 Host Calcite	234
6.3.2 Cement	238
6.4 Mass Balance Constraints	241
6.5 Sulphate-sulphide Reflux Reactions	245
6.6 Summary	247
7. GEOCHEMISTRY OF BEDDED FLINT SERIES	252
7.1 Introduction	252
7.2 Chemical Variations in Chalk Samples	254
7.2.1 Variations Around the Flint Band	254
7.2.2 Variations higher in the Section	265

7.3 Stable Isotope Variations	269
7.4 Chalk-Flint Partitioning	277
7.5 The Rare Earth Elements	282
7.6 Variations Within the Flint	287
7.7 Discussion	292
 8. THE ORIGIN OF CHALK HARDGROUNDS	 296
8.1 Introduction	296
8.2 Chalk Rock Nodular Bed	298
8.3 The Clandon Hardground	303
8.4 The Suzanne Hardground	308
8.5 Discussion	313
 9. SYNTHESIS, DISCUSSION AND CONCLUSIONS	 316
9.1 Mechanism of Flint Nucleation	316
9.2 Microstructure and Growth History	321
9.3 Implications for Cretaceous Oceanography	327
9.3.1 Source of Silica in Flints	327
9.3.2 Rhythmicity of Flint Bands	330
9.3.3 Depth of the Redox Boundary	332
9.3.4 Regional Hardground Complexes	334
9.4 Relevance of Flints to Other Cherts	338
 APPENDICES	
 1. TERMINOLOGY OF THE SILICA MINERALS	 341
 2. THEORETICAL SETTLING RATES FOR CHALK CONSTITUENTS	 349
 3. METHODS USED IN TRACE ELEMENT DETERMINATIONS	 355
 4. DETERMINATION OF STABLE ISOTOPE RATIOS	 361
 REFERENCES	 367

LIST OF PLATES

1. Field Relations of Upper Cretaceous Flints	74
2. Influence of Sedimentary Structures on Flint Morphology	76
3. Preservation of Burrows in Flint	79
4. Influence of Burrows on Flint Morphology	82
5. Paramoudras and Carious Flint Bands	90
6. Preservation of Fossils in Flint and Typical Banded Flints	96
7. Structure and Field Relations of Sheet Flints	100
8. Major Characteristics of Flints and Pyrite Nodules	107
9. Macro-structure of Flints	117
10. Lepispheric Structure in Flints	128
11. Detail of Lepispheres, Chalcedony and Quartz Druse	131
12. Detail of Silicified Skeletal Fragments	133
13. Effects of Recrystallisation of Flint Structure	140
14. Structure of the Flint Cortex	151
15. Microstructure of the Crust of Flints	156

LIST OF FIGURES

2.1 Principal zones of bacterial oxidation during early diagenesis	29
2.2 Behaviour of dissolved silica during shallow burial	43
2.3 Schematic diagram showing transformation and diagenetic processes between silica minerals	47
2.4 Principal phase transformations of the silica minerals	49
3.1 Generalised Upper Cretaceous palaeogeography in western Europe	53
3.2 Eustatic variations in Cretaceous sea level	53
3.3 Stratigraphy of the Sussex White Chalk Formation	60
3.4 Upper Cretaceous stratigraphy in Northern England	61
3.5 Stratigraphy of the Maastrichtian type sections	62

3.6 Lithostratigraphy of the type Craie de Villedieu	63
3.7 North-South variations in flint morphology during the Turonian	84
3.8 Relationship between the Lichtenberg horizon and the Lanaye Chalk in the type Maastrichtian	84
3.9 Association of flints with channelling in Schiepersberg Chalk	85
3.10 Variation in form of the Romontbos flints	85
3.11 Structure of the Silicified Hardground, Craie de Villedieu	85
3.12 Morphological classification of flint types	88
3.13 a) Usual relationship of paramoudras and bedded flint	92
b) Complex shape of the Ashby Hill Pit paramoudra	
4.1 Types of bonding at the silica surface	119
4.2 Thermogravimetric curve of typical black flint	123
4.3 Infra Red absorption curve of Brandon black flint	123
4.4 Summary of flint diagenesis in the Chalk	159
5.1 Effect of grainsize on trace element extractions of flint	167
5.2 Variation of flint chemistry with colour in flint sub-samples	171
5.3 a) K vs Al in flint CL1/30	173
b) Sr vs P in same specimen	
5.4 Sample distribution in the Brandon flint specimen	176
5.5 Selected covariance diagrams for the Brandon samples	179
5.6 Distribution of Ca, Al, P and Na in the Brandon specimen	181
5.7 Clay mineral dilution effects associated with silicification	183
5.8 Comparison of trace elements in the crust of flints with those in the black flint and host chalk	189
5.9 δD vs $\delta^{18}O$ for cherts of various ages	192
5.10 Temperature dependance of the quartz-water oxygen isotope fractionation.	192
5.11 Sample distribution in flint CL2/7	195
5.12 H_2O vs $\delta^{18}O$ in flint CL2/7	197
5.13 δD vs $\delta^{18}O$ in CL2/7	197
5.14 Variation of $\delta^{18}O$ with % of lepispheres in Brandon flint	204
5.15 Structure bound water vs $\delta^{18}O$ of Brandon flint	204
5.16 δD vs $\delta^{18}O$ for all samples analysed in this study	205
5.17 Fig. 15 after correcting for late diagenetic overprint	209
6.1 Sample distribution in paramoudra CA/1	212

6.2	Minor and trace element variations in the chalk core of CA/1	216
6.3	" " " " " in the flint of CA/1	217
6.4	Explanation of anomalous Al distribution in the chalk samples	219
6.5	Dilution of clay minerals during lithification	219
6.6	Distribution of authigenic components in the chalk core	222
6.7	Distribution of Fe and Mn in the chalk and flint of CA/1	228
6.8	Schematic representation of the distribution of cement and present day porosity in the chalk core	228
6.9	Variation of Mn with calcite content in the flint samples	230
6.10	Comparison of Fe and Ca in the flint	230
6.11	Stable carbon and oxygen isotope ratios in the chalk core	236
6.12	Three component mixing curves for sources of carbonate in the core	
6.13	Postulated model of paramoudra formation	248
6.14	Summary of diagenetic reactions associated with paramoudra genesis	250
7.1	Lithostratigraphy and sample sites of the Chalk in West Clandon Pit, Surrey	253
7.2	Sample distribution for the main CLL series	255
7.3	Vertical variation in trace element concentration across a flint	258
7.4	Mg vs Na for the chalk samples	260
7.5	Detail of the Ti, K, Fe, Al and Si curves for part of fig. 7.3	261
7.6	Fe vs K for the chalk samples	264
7.7	Trace element variations in chalk samples above the main Clandon sample series	267
7.8	Vertical variation in $\delta^{13}\text{C}$ and $\delta^{18}\text{O}$ in the Clandon samples	270
7.9	$\delta^{13}\text{C}$ vs $\delta^{18}\text{O}$ for the same samples	273
7.10	$\delta^{13}\text{C}$ vs potassium content in Clandon chalks	274
7.11	Partitioning of trace elements between flint and chalk	280
7.12	REE distributions in samples from West Clandon Pit	285
7.13	Trace element variations on a vertical traverse through a flint	289
7.14	Proposed model for the origin of flints	294
8.1	General pattern of events during hardground formation in chalks	297
8.2	$\delta^{13}\text{C}$ vs $\delta^{18}\text{O}$ for nodule-matrix pairs from the Chalk Rock	300
8.3	Isotope variations within a single nodule	302
8.4	Isotope variations below the Clandon hardground	306

8.5	Variations in Suzannes lovelly rounded surfaces	309
8.6	$\delta^{13}\text{C}$ vs $\delta^{18}\text{O}$ in the Suzanne samples	312
8.7	The fluctuating $\text{O}_2\text{-H}_2\text{S}$ boundary model for hardground formation	314
9.1	Summary of diagenetic reactions in the Chalk	318
9.2	Proposed model of silicification in Upper Cretaceous chalks	320
9.3	Schematic growth history of flint nodules	322
9.4	Oceanographic control of flint and hardground distributions during the Upper Cretaceous	337

LIST OF TABLES

2.1	Predicted sequence of bacterial reactions in pelagic sediments	29
4.1	Infra Red absorption bands due to water in the silica struture	124
5.1	Distilled water extraction of powdered samples	166
5.2	a) Trace element concentrations in CL1/30 sub samples b) Linear correlation coefficients	170
5.3	Minor elements in Brandon flint	177
5.4	Linear correlation coefficients - Brandon flint	178
5.5	Potassium distribution in Malincourt flints and chalks	185
5.6	Trace element variations in Bridgewick flint fractions	187
5.7	Chemistry of flint crusts	187
5.8	TG and stable isotope data for Clandon flint	195
5.9	TG and isotope ratios in Brandon flint	202
5.10	Isotope ratios in Brandon flint after correcting for late diagenetic effects	202
6.1	Minor and trace elements in the chalk core of Caister paramoudra	214
6.2	" " " " " flint samples of the paramoudra	215
6.3	Linear correlation coefficients for trace elements in CA/1	226
6.4	Stable isotope ratios for paramoudra chalks and pyrites	235
7.1	Minor elements in Clandon chalks	256
7.2	" " " " flints	257

7.3	Porosity determinations on chalks	257
7.4	Minor elements in high zonal chalks at Clandon Pit	266
7.5	Stable isotope ratios in Clandon chalks	266
7.6	Flint/chalk partition coefficients for various trace elements	279
7.7	REE in Clandon flints and chalks	284
7.8	Minor elements in flint CL1/7	288
8.1	Isotope ratios in Chalk Rock nodules and host chalks	299
8.2	Variations within nodule 1	299
8.3	Stable isotope variations below the Clandon hardground	305
8.4	" " " " " Suzanne "	305
A3.1	Analytical precision for trace element determinations on flints and chalks	357
A3.2	Standard deviations of determinations on BDN samples	359
A3.3	Analytical precision of REE determinations	359
A4.1	Raw data for isotope analyses of samples from the Caister paramoudra	362
A4.2	Analytical reproducibility for BrF ₅ extractions on samples of Brandon flint	365

1. INTRODUCTION

1.1 OUTLINE OF PROJECT

Black nodular cherts (popularly known as flints) from the Cretaceous Chalk of western Europe have been studied for generations and were of continuous economic importance for over half a million years. Moreover, in the last 15 years, cherts have proved to be among the most important of all deep sea sedimentary rocks and a knowledge of the genesis and diagenesis of these deposits is proving fundamental to any understanding of the geological history of the oceans. Although much literature concerning petrological and mineralogical aspects of silica-rich sediments now exists (see Pisciotto, 1981, and Kastner, 1982, for recent reviews), the underlying chemistry of chert genesis is still largely unknown.

Nodular flints represent one end member of a morphologic sequence ranging from isolated nodular replacement cherts to laterally continuous massive bedded cherts. The genetic significance of this sequence is complex but in general terms the massive cherts represent an in-situ recrystallisation of more or less pure volcanic or biogenic siliceous deposits whereas the nodular forms apparently represent a significant spacial redistribution of silica, and chemical replacement of a host carbonate. It is common to find nodular cherts enclosed within massive bedded cherts implying that the chemical transformation giving rise to concretions of nodular chert predated the large scale in-situ recrystallisation of the main chert bed. The present work is a case story of the underlying chemistry of

nodular chert replacements in a carbonate-rich sediment. In particular, I set out to determine the causes and mechanism for localised carbonate-silica replacement, as opposed to simple silica redistribution or recrystallisation, and to relate this to other major diagenetic changes which have affected the Chalk.

1.2 TERMINOLOGY

Much confusion exists in the terminology of the chemical siliceous sediments, particularly in the translation of terms from English to French (and in many cases American). For convenience, the following definitions of flint and chert are used in this study:

CHERT - is a siliceous rock consisting predominantly of microcrystalline or cryptocrystalline non-clastic silica occurring as beds, nodular masses, or veins in sedimentary rocks (Smith, 1960). This definition includes flint, agate, silicite, hornstone, jasper, etc., but does not refer to colloidal or opaline rocks or vein quartz.

FLINT - is a variety of chert found in or derived from the Upper Cretaceous to Lower Eocene Chalk. It is characteristically homogeneous black and breaks with a conchoidal fracture but may also be partly or wholly white to grey with a flat fracture, or weathered white, grey, red, orange, yellow or brown. The name is retained here only because it is so well engrained in the literature, the term "Cretaceous nodular chert" being more explicit.

A full discussion of the terminology of siliceous sediments and rocks is given in Appendix 1.

1.3 HISTORY OF FLINT RESEARCH

1.3.1 Early Theories of Flint and Chalk

As mentioned above, investigations into the origin of flint and chalk have had a long history. Probably one of the earliest explanations of flint can be traced back to Theophrastus, Aristotle's successor at the Lyceum, who made a special study of minerals about 300 BC. Flints, and the curious forms these objects sometimes take, were well known at this time and could readily be explained by the then new theory of "plastic virtue". According to this concept, fossils and pseudofossils of all sorts were really partial failures of a vis plastica or "formative virtue" at work: the successes being represented by real live sea-urchins and fishes (Shepherd, 1972, p 25-6). Although fossils had already been correctly interpreted as the remains of dead animals many years earlier (e.g. by Anaximander, c.570 BC), this theory received much support and maintained some adherents until very recently. Indeed T.W. Shore (1900) remarked on how many country people were led to believe that flints "grew" in the soil, because of their apparent persistence, even after weeks of labour to clear them from fields.

As time went on, the plastic virtue theory fell from favour and more scientifically rigorous theories began to appear. By this time the spread of petrographic investigation of thin sections (e.g. Sorby, 1861; 1879) and the discoveries of the Challenger voyages (1872-1878) had already demonstrated the biogenic nature of the Chalk, and by the early 1890's the association of many flints with fossil sponges was well established (e.g. Cayeux, 1891). The

following thirty years saw the development of all the main theories of flint formation which found their way into student text books and popular accounts up until the scientific revolution which followed the launching of the Deep Sea Drilling Project in 1968.

About this time geologists first began to take a serious interest in the discoveries of contemporary chemists, and in particular the ability of silica to form colloidal gels was readily adopted as an important property in explaining flint genesis. The silica gel theory was taken up most notably by W.A. Tarr (1917, 1926) and R.M. Brydone (1920) who suggested that dissolved silica, supplied by rivers, was precipitated by "alkalic salts" to form more or less globular lumps of silica gel which fell periodically to the sea floor. Here they engulfed foraminifera and sponges, flowed into burrows and infiltrated the tests of echinoids. This theory was criticised on many accounts, not the least of which was that echinoderms are sufficiently motile to avoid such a fate.

Despite the many objections the silica gel theory became widely accepted and it was only in 1960 when Millot demonstrated that such reactions would not normally happen with the concentrations of silica found in natural waters, that the theory was discounted. However, the theory did become modified en-route by Illies (1949) into a more sophisticated form, involving gel formation at the boundary of oxidising and reducing conditions, within the sediment. Although this theory also fell into disfavour it is important as the first serious attempt to explain flints in terms of early diagenetic reactions occurring below the sediment surface.

In contrast to the syngenetic (i.e. on the sediment surface) and penecontemporaneous (within the newly deposited sediment) theories, many other workers turned to meteoric water infiltration during uplift as an explanation of flints. It had already been established (e.g. by Sollas, 1905) that siliceous sponges buried within the sediment provided an important source of silica (indeed before the introduction of petrology it had been widely assumed that all flints were simply overgrown fossil sponges; see discussions by Julien, 1880; Alloway Pankhurst c. 1895; Hill, 1911) so the problem became more one of how the silica in sponges could become segregated into flints.

Once again geologists turned to chemistry, and to the recently discovered phenomenon of Liesegang banding (e.g. Liesegang 1913, 1914). Dean (1918), Richardson (1919), and later Oakley (1939) were quick to apply these ideas to flint bands and pointed out that the downward diffusion of meteoric waters, as the Chalk was uplifted, could potentially redistribute the silica into a series of regularly spaced bands. Richardson (1919) even backed this up by demonstrating that the maximum development of flint in the English Chalk crudely followed present day topography, and these ideas were elaborated upon by Wroost (1936) who discussed the possible mechanism of silica replacing carbonate as a result of high levels of CO_2 in meteoric waters. This could dissolve the chalk, and in turn lead to silica (gel) precipitation as a consequence of the loss of CO_3^{2-} ions from solution.

Attractive as these theories were, they failed to explain the fine preservation of uncrushed fossils, delicate sponges, and occasionally the soft parts of organisms, and although they were

readily taken up by many leading geologists of the time (e.g. Arkell, 1933) they also were soon forgotten.

1.3.2 Current Theories

With the initiation of the Deep Sea Drilling Project in 1968, vast amounts of new data on oceanic cherts became available, and for the first time it was possible to investigate progressive diagenetic changes in continuous cores.

It rapidly became apparent that the Cretaceous-Eocene period represented a time of anomalous preservation of siliceous sediments (Heath and Moberly, 1971) and much discussion ensued as to the reasons for this (Gibson and Towe, 1971, 1975; Weaver and Wise, 1974, 1975; Froehlich, 1974; Leclaire, 1974). Many authors also made a clear distinction between "bedded cherts" which were associated with siliceous or argillaceous sediments and nodular cherts which (like flints) were associated with carbonate sediments, although the possible reasons for such a difference have been rather neglected amidst a spate of mineralogical studies on the cherts.

By far the most significant contribution of the D.S.D.P to chert research was the discovery of the "maturation" of biogenic opal (opal-A of Jones and Segnit, 1971) to disordered cristobalite (opal-CT) and then to quartz. Also important was the discovery that the opal-CT characteristically forms spherical aggregates of bladed crystals ("lepispheres" of Wise and Kelts, 1972) since this morphology provided an important link between on-land studies of flints and the better known deep sea cherts.

It is now well established that time and temperature are the main controls on the maturation of opal-CT to quartz although the

lithology of the host sediment exerts a significant control on the kinetics of the transformation (Isaacs, 1982; Pisciotto, 1981) and in the past has been proposed as the main control on mineralogy (Lancelot, 1973; Froehlich, 1974). Important in the confirmation of this theory were the experimental studies of Kastner et al. (1977) and Kaster and Keene (In prep. - quoted in Kastner, 1982 and pers.com, 1982) in which the opal-A to opal-CT and opal-CT to quartz transformation were demonstrated under laboratory conditions.

Geologists concerned with the origin of Cretaceous flints were slow to use the new data from the deep sea investigations. The presence of opal-CT in flints had been known for many years (e.g. "subsidiary cryptocrystalline silica" of Jensen et al., 1957; "badly crystallised low tridymite" of Buurman and van der Plas, 1971), and Leclaire et al. (1973) had described lepispheres ("spherules de cristobalite-tridymite"), but these were generally regarded as interesting associations of the silica rather than a major constituent.

In more recent years the maturation theory of opal-CT to quartz has been more widely accepted as an explanation of flint diagenesis (e.g. Hancock, 1975, Kennedy and Garrison, 1975), however, some authors still regard host lithology as the dominant control (Jeans, 1978), due largely to a poor understanding of the mineralogical nature of opal-CT.

Despite the widespread acceptance of the new theories, there is still no clear understanding of the causes of flint genesis, and indeed most authors tend to ignore the problem entirely.

Currently, only one theory of flint genesis is widely accepted - that proposed by Hakansson et al. (1974). These authors pointed out the close association of flints with organic structures and burrows, and also that flint bands closely followed bedding even when this was disrupted by synsedimentary slumps. The sites of flint formation therefore must have been determined very early in the diagenetic history of the Chalk. Conversely, synsedimentary reworking of flints was unknown (but see subsequent account by Voigt, 1979), and aragonitic fauna is only rarely found preserved in flint, so Hakansson et al. argue that the flints themselves must be the product of later diagenesis.

Importantly, the authors recognised that silica solubility is hardly affected by pH within the range normally expected in such an environment (cf Alexander et al., 1954; Krauskopf, 1959) and turn to a modification of Siever's (1962) "organic phase interaction" model as an explanation of flint genesis. According to this theory organic decay locally lowers pH enough to dissolve carbonate, but in the presence of the organic compounds the solubility of silica is reduced (Emery and Rittenburg, 1952; Siever, 1962). The silica is therefore immobilised in the form of organic-silica complexes at the sites of flint formation (i.e. the sites of flint formation are determined early) but the silica is only released after organic matter breakdown during later diagenesis, when it precipitates as lepispheres and eventually recrystallises to quartz. With the addition of more silica at depth a solid flint would form.

Elegant as this theory is, there are a number of serious problems. Firstly the absence of reworked flints does not necessarily imply that the flint did not exist at this time, merely that it was too friable to resist reworking (the discovery of rare reworked flints by Voigt (1979) is further evidence of this). Secondly, the absence of aragonitic fauna preserved in flints is not really surprising since flint formation of necessity involves carbonate dissolution, and the less stable aragonite would be expected to dissolve more readily than calcitic fossils. There is, therefore, no reliable evidence that flints have anything whatsoever to do with late diagenesis.

More importantly, in some cases (such as the paramoudras described by Bromley et al. 1975) organic matter decay, proposed as a cause of carbonate dissolution, clearly acts to precipitate carbonate under the same conditions. Also, tabular flints may be found in sediments which are devoid of bioturbation which is assumed to be the source of the organic matter.

Furthermore, if one considers the amount of organic matter required to form a complex with even 50% of the silica in a flint, one is led to consider that adsorption of organic matter on the silica is perhaps more viable.

Although the work of the above authors represents a major advance in understanding flint genesis, as it stands there are serious flaws. It is in the light of these problems, and with the large amount of new data on chemical diagenesis now available, that the present work is based.

1.4 ORGANISATION OF THESIS

A number of problems remain in understanding flint genesis.

- a) Why do flints grow in regular beds, reflecting bedding in the original sediment, and how do they acquire their characteristic range of morphology?
- b) How does the distribution, pattern and mechanism of silicification relate to other diagenetic reactions within the sediment, and how do these relate to contemporaneous sedimentology and oceanography?
- c) Are there systematic variations in stable isotope ratios and the distribution of trace elements in flints and what is their significance? Can either of these offer a guide to secular variations in ocean chemistry?

Chapters 2 and 3 of this work outline the geochemical and sedimentological framework of the study respectively, and attempt to place the Chalk and its flints in a context in which the results of this study can be related to other sedimentary units. Much of our current understanding of Chalk sedimentology is, as yet, unpublished and I am indebted to my many colleagues and co-workers for helpful discussion during the preparation of chapter 3.

Chapters 4 and 5 concentrate on the mineralogical and chemical variations within individual flint nodules and are aimed at understanding the diagenetic and growth history of the flints, subsequent to their formation. This provides useful background to understanding the timing of flint formation and leads into an investigation of the chemical environment in the sediment at the time of silification (chapter 6).

Curious barrel shaped flints called paramoudras proved to be critical in understanding flint genesis so the chemistry of these is discussed first, before extrapolation of the findings to the more normal bedded flints (chapter 7). After a brief discussion of hardground formation and it's relationship to flints (chapter 8), the final chapter discusses the oceanographic implications of the findings.

In order to leave the text as uncluttered as possible, full discussion of the analytical methods employed and analytical precision of the results have been appended.

2. CHEMICAL DIAGENESIS IN SEDIMENTS

2.1 BACKGROUND

The launching of the drilling vessel "Glomar Challenger" in 1968 initiated a major revival of interest in modern pelagic sediments and their diagenesis and recent years have seen an enormous and rapid influx of data on the chemistry of early diagenesis. As well as enabling quantification of chemical fluxes back into sea-water from sediments (of use for mass balance calculations), these data have provided a sound framework with which to interpret the diagenetic features of ancient sediments. The purpose of this chapter is to briefly review early work and to summarise current understanding of early diagenesis in pelagic sediments.

2.2 pH/Eh VARIATIONS

Early work on sediment chemistry concentrated on the definition and determination of pH and redox potentials in the pore waters of the sediment. It rapidly became apparent that oxic or aerobic sediments had very different chemical properties to reducing sediments, manifested in two ways. Firstly, elements which show a variable valency may show varying mobilities in the two sediment types as a result of differing mobilities of the element in each oxidation state. Thus, for example, Mn or Fe, will show a tendency to be concentrated in the oxic zone since on reduction they will change into the more mobile divalent state and migrate upwards to be fixed as the higher oxides under aerobic conditions. Secondly, different bacterial populations are operative in aerobic and anaerobic sediments, and

minerals whose genesis involves bacterial reactions (e.g. pyrite) will be confined to the appropriate level. Consequently, much work was dedicated to the application of thermodynamic principles to sediments based on pH and Eh controls, and stability diagrams were generated for most of the common, simple, minerals found in sediments (e.g. see Garrels and Christ, 1965; Stumm and Morgan, 1970).

Classification of sediments by pH and Eh alone is, however of only limited use. Although pH is easy to measure, it shows only very little variation in most sediments as a result of rapid buffering reactions, whereas Eh is practically impossible to measure accurately in situ. In addition, the redox potential for the change of valency state varies between elements and problems arise when a sediment is described as simply "reducing" or "oxidising" without reference to which range of elements this relates to. Numerous descriptions exist in the literature of so called "reducing" conditions where the assumption of merely an Eh below zero is either misleading or inadequate to explain the reaction(s) concerned. Even more problematic however is the fact that many reactions are subject to kinetic constraints and quite often thermodynamic equilibrium is never established.

Consequently, although pH-Eh diagrams may be of some use for understanding the paragenesis of minerals in certain, clearly defined, chemical environments, they are inadequate to provide a general framework in which to understand total sediment diagenesis, so alternative approaches are needed.

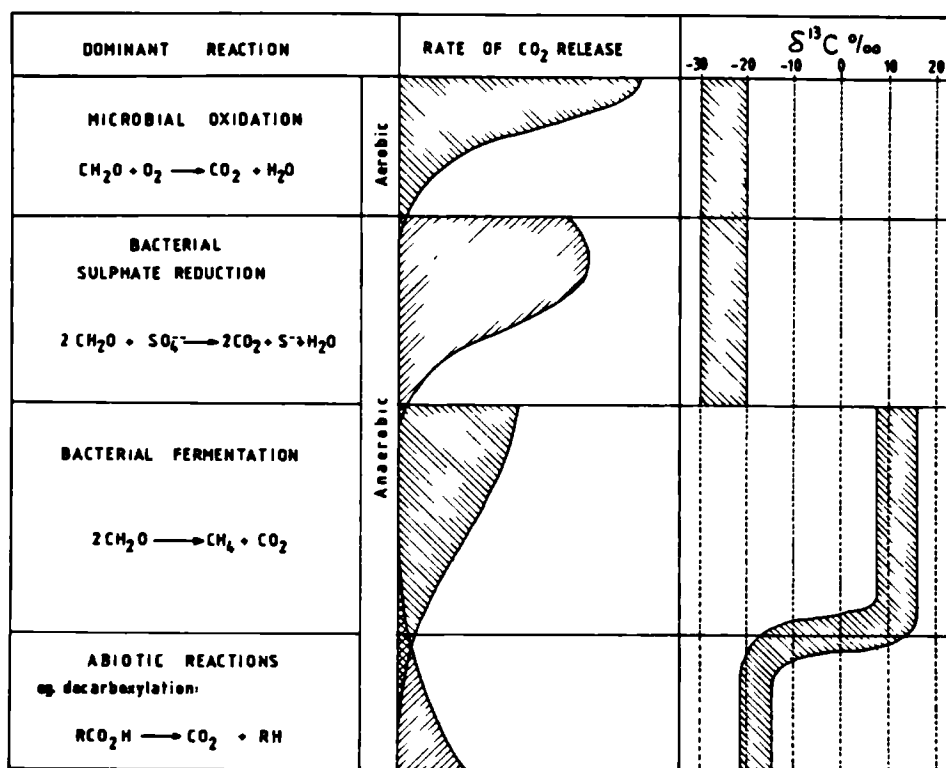
2.3 ORGANIC MATTER OXIDATION

In the absence of highly reactive inorganic material, such as volcanic ash or lavas, the most important cause of early diagenetic chemical changes in most pelagic sediments is the result of the

bacterial breakdown of organic matter. Berner (1981) has recently introduced a general chemical classification scheme based on the presence or absence of the main dissolved bacterial respiratory agents, O_2 and SO_4^{2-} . In essence, this is a formalisation of the early part of the depth related diagenetic sequence of Curtis (1977). According to these authors, organic matter is destroyed by bacterial action involving first dissolved oxygen and then dissolved sulphate as the organic matter is buried and the previous nutrient becomes depleted (fig. 2.1). Following this, when dissolved sulphate also runs out, the chemically bound oxygen in the organic matter acts as the electron acceptor - effectively a fermentation reaction. This sequence is in the order of the free energy yield per mole of oxidant utilised, and on this principle, other workers, have also included dissolved nitrate reduction (e.g. Berner, 1971, 1980; Stumm and Morgan, 1970). The classification is particularly useful in view of recent work (e.g. Irwin, Curtis and Coleman, 1977; Coleman and Raisewell, 1981) which has described the isotopic "tracing" of the products of these reactions (see fig. 2.1).

With respect to pelagic sediments, a more refined description of the series of events (table 2.1), has been postulated by Froelich et al. (1979) and the general applicability of this was confirmed by their own data and by subsequent measurements (e.g. Emerson et al. 1980; Grundmanis and Murray, 1982).

The relative importance of each reaction is controlled by the rate at which the previous nutrient is used up. This in turn is controlled by such factors as sedimentation rate, porosity and permeability variations, and the degree of biological and physical reworking of the sediment. In general, rapidly deposited fine grained sediments, such as shales, will pass rapidly into the

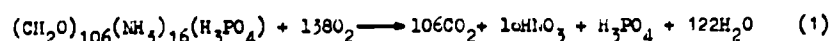


Not to scale

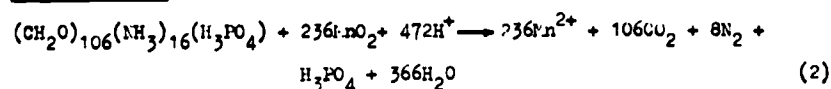
Figure 2.1 Principal zones of bacterial oxidation during early diagenesis

Table 2.1 Predicted sequence of bacterial reactions in pelagic sediments according to Froelich *et al.* (1979)

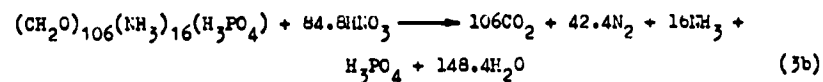
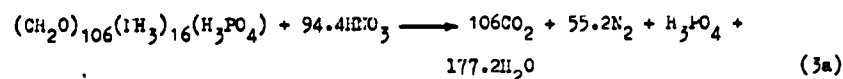
Dissolved oxygen reductions:



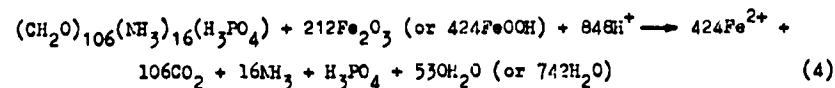
Mn⁴⁺ reductions:



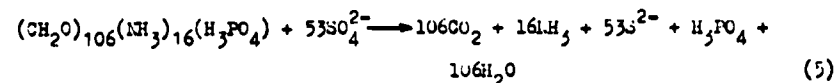
Dissolved nitrate reductions:



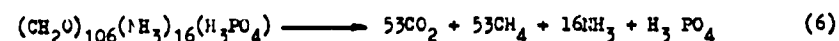
Fe³⁺ reductions:



Dissolved sulphate reductions:



Bacterial fermentations:



sulphate reduction and fermentation zones whereas slowly deposited sediments (such as most limestones and pelagic oozes), or coarse grained clastic sediments, allow sufficient oxygen supply to oxidise more or less all of the organic matter before significant burial. In pelagic sediments therefore, the upper 10 metres or so may remain aerobic, but in organic-rich shales, only the top few millimetres may be involved.

This series of reactions is now accepted as a working theory for the study of early diagenesis of organic matter and it is relevant here to discuss the individual reactions in more detail. Problems arise, however, in that the composition of the organic matter being oxidised is highly variable, but for convenience, the average composition obtained by Redfield (1958) is usually adopted, based on a C:N:P ratio of 106:16:1. For simplicity, however, organic matter is also sometimes approximated by the empirical formula for carbohydrate, $(CH_2O)_x$.

2.3.1 Aerobic Respiration

Organic matter degradation by the action of aerobic bacteria is the main process occurring in pelagic sediments. Aerobic bacteria are active throughout the water column in normal ocean systems and are the prime bacteria operating on organic matter at the sediment-water interface. In addition, such reactions occur within the sediment, down to a depth where dissolved O_2 becomes sufficiently depleted that the concentration is unable to support a viable bacterial population. This depth will be controlled by such factors as oxygen availability in the overlying waters, quantity of organic matter within the sediment, and the local effects of aeration by bioturbation (Aller, 1982).

The main products of these reactions are CO_2 and H_2O which usually diffuse back into the overlying water column, resulting in oceanic bottom waters which are depleted in dissolved oxygen and enriched in CO_2 relative to the bulk of the ocean water. In rapidly deposited shelf sediments, aerobic respiration only occurs in the top few mm or cm of the sediment (if at all), but in most pelagic sediments the aerobic zone extends down several tens of cms or even metres. This is a result of the low organic content (related to surface productivity and sedimentation rate) which favours the destruction of most of the labile organic matter at, or very near to, the sea floor (Menzel, 1974; Emerson and Bender, 1981). The reaction products usually diffuse easily back into overlying bottom waters but may cause local dissolution of biogenic calcite (e.g. Aller, 1982) and such reactions in highly restricted micro-environments have been invoked as a cause of silicification of shell material by Holdaway and Clayton (1982).

2.3.2 Nitrate Reduction

When dissolved oxygen concentrations approach low levels, manganese and nitrate reduction become the most important processes, the relative order of the two depending on the detail of the reactions occurring at the time (Froelich et al., 1979; Emerson et al., 1980; Table 2.1, this work).

Nitrate diagenesis has been well studied by Froelich et al., (1979), Emerson et al., (1980), and Rosenfeld (1981). Pure nitrate reduction of organic matter releases a mixture of CO_2 , ammonia, and free nitrogen but it is difficult to be sure of the importance of ammonia because additional amounts are released from organic matter by sulphate reduction (Emerson et al., 1980), and

subsequent reactions (Rosenfeld, 1981). In addition, organic nitrogen is also released as nitrate by aerobic respiration (Grundmanis and Murray, 1982). Model calculations by Knauer et al., (1979), Bishop et al., (1977), and Rosenfeld (1981) suggest that organic bound nitrogen is released in preference to organic carbon during oxidation, but Grundmanis and Murray (1982) have found a constant C:N ratio for residual decaying organic matter in their study.

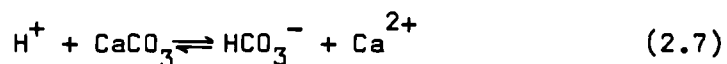
Within these limitations, it is generally believed that nitrate reduction of organic matter may result in a small amount of carbonate dissolution (Froelich et al., 1979; Emerson et al., 1980). The magnitude of this effect probably depends very much on local conditions but is never very great.

2.3.3 Fe³⁺ and Mn⁴⁺ Reduction

After dissolved oxygen and, to some extent nitrate, concentrations drop to a sufficiently low level, organic matter oxidation continues with Mn⁴⁺ and Fe³⁺ acting as the ultimate electron acceptor for the process. The Mn²⁺ and Fe²⁺ released in this way are highly mobile and will usually migrate towards oxic conditions to reprecipitate as the higher oxides. This is the basic process leading to the formation of deep-sea ferro-manganese nodules and crusts (e.g. see discussion in Berner, 1971, p.103), which are in turn important sinks for numerous metallic trace elements (Cronan and Moorby, 1981; Balistrein and Murray, 1982).

The detail of the processes involved are complicated by the variable importance of bacterial action (Emerson, 1982) compared with inorganic reduction and by kinetic constraints (e.g. Balzer, 1982; Emerson et al., 1982) but there is evidence that the reactions are

best represented as in Table 2.1. The CO_2 released by the processes could theoretically lead to calcite dissolution but the effect is offset by the high consumption of H^+ . This causes a shift in the general carbonate equilibrium:



and may result in a net precipitation of carbonate in both cases. Such reactions may be important in the explanation of the precipitation of Mn-rich carbonates in some slowly deposited sediments (e.g. Pedersen and Price, 1982; Coleman, Fleet and Donson, 1982).

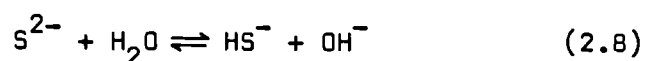
2.3.4 Sulphate Reduction

Oxidation of organic matter involving the bacterial reduction of dissolved sulphate is one of the most important reactions occurring in anaerobic sediments.

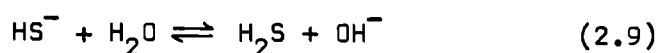
Such reactions are principally the result of bacteria of the genus Desulfovibrio which utilise dissolved sulphate as an oxidising agent for organic matter breakdown, liberating dissolved sulphide and carbon dioxide (Table 2.1). In some anoxic waters, these reactions may initiate during sedimentation (e.g. The Black Sea; Ross and Degens, 1974) but they are more usually confined to the interstitial waters of organic-rich sediments below the level of the other possible nutrients (principally oxygen). The environment which best favours this is one of quiet water where low density organic detritus can settle out or be "burrowed-in" without excessive reworking and consequent oxidation by aerobic bacteria. The low sedimentation rate of most carbonate sediments does not favour high levels of sulphate reduction but in some such sediments (e.g. Cretaceous chalks - see ch.3), there is evidence that it was

important, presumably as a result of the emplacement of organic matter at depth by the burrowing activities of the benthos.

The empirical products of sulphate reduction are dissolved sulphide and carbon dioxide (Table 2.1), but at the pH of most sediments (7-8), S^{2-} is unstable, and what is effectively hydrolysis, results in the stable monovalent ion HS^- or neutral H_2S species:



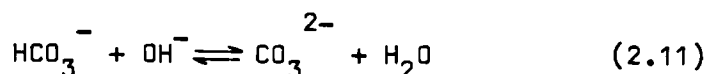
and



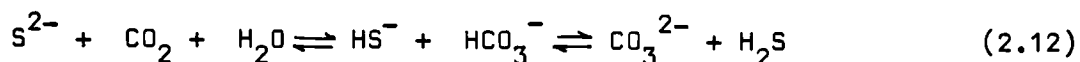
The hydroxyl ions released by this reaction would be buffered by the CO_2 released at the same time as the S^{2-} :



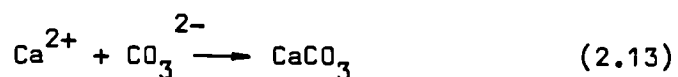
and



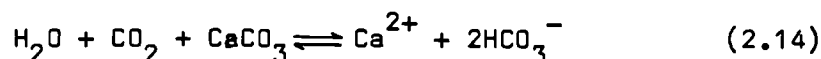
and the net reaction for sulphate reduction products therefore becomes:



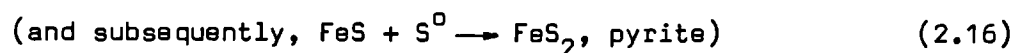
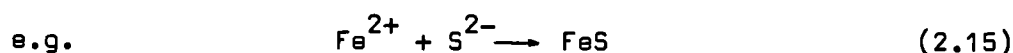
Loss of H_2S from the system will cause a shift of equilibrium to the right of equation 2.12 which, in the presence of dissolved Ca, may result in calcite precipitation:



If H_2S or HS^- are not lost from the system, however, equilibrium may shift to the left resulting in a certain amount of carbonate dissolution by the carbonate buffering reactions:



If S^{2-} is lost, for instance, such as if it became fixed by iron to form iron sulphides:

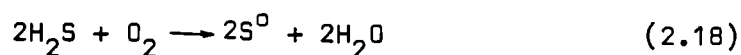
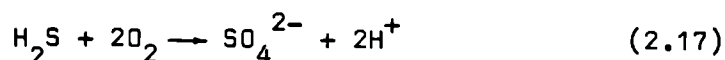


equilibrium would move to the left of eq. 2.12., although in practice, pyrite formation is more complicated than this and may involve a number of intermediates (see Pyzic and Sommer, 1981; and Goldhaber and Kaplan, 1974, for discussion). The overall effect however is that carbonate precipitation is controlled by the acidity (or more precisely the OH^- concentration) which in turn is dependant on the Eh, via iron buffering of the bacterially produced sulphide. Iron is introduced into sediments as structural iron in detrital minerals or as oxides or hydroxides, usually adsorbed on the surface of clay minerals (Carroll, 1958), and it is this iron which, on burial, becomes available for pyrite formation (e.g. see Suthill, Turner and Vaughan, 1982). In clay-rich sediments therefore, iron is generally freely available (within the kinetic constraints of releasing the iron from clays) and pyrite formation is widespread (e.g. see Coleman and Raisewell, 1981 and In Press). In clay-poor sediments however, such as chalks, iron is very limited and little

pyrite would form, resulting in an excess of H_2S and possible carbonate precipitation.

Evidence for the precipitation of calcite by sulphate reduction reactions can be obtained from stable isotope studies. The CO_2 released is the only carbon bearing species formed and it therefore inherits the isotopic composition of the organic precursor ($\sim -25\%$ PDB), which is often detectable in the calcite precipitates formed by the process (e.g. Irwin, Curtis and Coleman, 1977). However, the extreme value of -25% is rarely reached since precipitation occurs when the solubility product of the calcite is exceeded, irrespective of the source of the carbonate. This means that the cement formed will be composed of a mixture of biogenic carbonate and pre-existing dissolved marine carbonate ($\delta^{13}C \sim 0\%$ PDB), and will have an isotopic composition somewhere between the two.

The fate of the excess H_2S in sediments is not well known at present but in general terms, it is assumed to diffuse away from the sites of sulphate reduction towards more oxygenated conditions where it is reoxidised to sulphate or elemental sulphur (e.g. see Benmore, Coleman and McArthur, 1983):

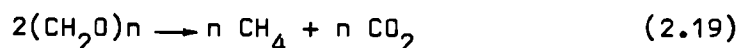


The reactions are believed to be biologically mediated (by the Thiobacilli bacteria) although they will also occur rapidly in the absence of micro-organisms. Elemental sulphur, where it is released, may subsequently be incorporated into pyrite (by reaction with iron monosulphides, eq. 2.16) but in pure carbonate sediments this is

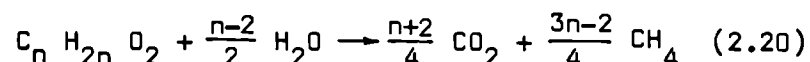
probably not the case since monosulphides were not abundant because of the low iron content. The absence of elemental sulphur in most sediments may suggest that in these environments, dissolved sulphate is the end product of sulphide oxidation rather than elemental sulphur.

2.3.5 Bacterial Fermentation

Below the zone of sulphate reduction, bacterial organic matter destruction proceeds using the oxygen contained within the organic matter itself. The process is essentially a fermentation reaction so the precise stoichiometry depends strongly on the nature of the organic matter available. For example, for carbohydrates the reaction can be represented as:

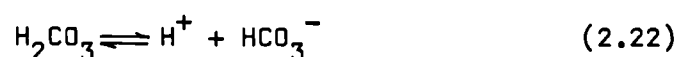


but for fatty acids it becomes:



(e.g. see Carrothers and Kharaka, 1980)

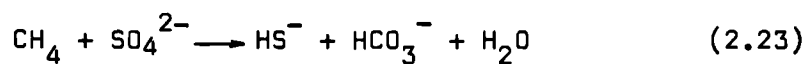
In all cases, the main products are methane, carbon dioxide and small amounts of nitrogenous and phosphatic compounds (Table 2.1). In solution the CO_2 is slightly acidic due to the dissociation of carbonic acid:



so the effect is a slight increase in acidity which may promote calcite dissolution.

Methane formed by this process may be very strongly depleted in ^{13}C (up to -75‰ PDB) leaving the CO_2 enriched in ^{13}C by up to 15‰. Irwin *et al.*, (1977), and Coleman *et al.*, (1979) have suggested that carbon from this source can be identified isotopically in diagenetic carbonates (concretions etc.) but the mechanism(s) whereby the CO_2 released can lead to calcite precipitation rather than dissolution is not discussed.

One important consequence of methane production at this level is that it may diffuse upwards into the sulphate reduction zone and become oxidised, possibly bacterially, by dissolved sulphate, according to the general reaction:



The effect of this would be to increase the apparent rate of sulphate reduction (as measured by sulphate depletion), and to release bicarbonate which is even more depleted in ^{13}C than normal sulphate reduction bicarbonate. Recent work (e.g. Devol and Ahmed, 1981; Reeburgh, 1980) suggests that this reaction may account for consumption of a considerable proportion of the downward sulphate flux in many sediments.

2.3.6 Subsequent Reactions

Reactions occurring below the zone of fermentation can scarcely be referred to as "early diagenetic" since they are largely the result of the higher temperature associated with deep burial.

One particular group of reactions worthy of mention, however, are decarboxylation reactions of the form:



Although very variable, carbon dioxide released by this process is usually quoted as having a $^{13}C/^{12}C$ ratio of between -10 and -25‰, and this can sometimes be detected in diagenetic carbonate concretions (Coleman et al., 1979). Although this may be an important source of carbonate in organic-rich sediments (such as the Kimmeridge Clay: Irwin et al., 1977) it probably plays a negligible role in organic-poor calcareous sediments such as the Chalk.

2.4 SILICA DIAGENESIS

The geochemical behaviour of silica in sediments is obviously of considerable interest in any discussion of chert genesis, and it is therefore considered in some detail here. Full discussion of the structure of the silica crystal lattice will however be left until chapter 4 ("Petrology and Microstructure of Flint").

2.4.1 Silica in the Oceans

The marine geochemistry of silicon has received much interest recently because of its biochemical importance in the marine production cycle in the form of phyto- (diatoms and silicoflagellates) and zooplankton (radiolarians).

Dissolved silica is present in ocean waters predominantly as the undissociated monomer variously referred to as "silicate" or

"reactive silica" in oceanographic accounts or "silica" in geochemical work. In this form, the silica is fully hydrolysed, probably as $\text{Si}(\text{OH})_4$ tetrahedra, and below pH9 is only very slightly dissociated to form a weak acid, $\text{pK}_a = 9.41$; (Wollast, 1974). Recent evidence suggests also the presence of tetrahedral silica dimers (Cary et al., 1982), and in concentrated solutions silica may be polymerised in the form of spiraling chains of tetrahedra (Hauser, 1955). In the presence of high concentrations of some anions, however, depolymerisation may occur (e.g. Folk and Pitman, 1971); and see discussion in Crerar et al., 1981).

The concentration of dissolved silica in the oceans is variable but is always less than $170 \mu\text{mol/l}$ ($\sim 10 \text{ ppm}$), substantially less than the equilibrium solubility of 1.8 mmol/l (Stober, 1967). The concentration varies with depth and characteristically shows a surface minimum due to extraction of silica by plankton (principally diatoms and radiolarians), with higher concentrations at depth as a result of the dissolution of sinking tests. In shelf environments, further silica removal may occur as a result of the growth of siliceous sponges and even gastropods (Lowenstam, 1971). There is therefore a considerable flux of particulate biogenic silica towards deeper parts of the ocean, and model calculations, (e.g. Eriksson, 1962), suggest that this is partially balanced by an upward flux of dissolved silica.

Structurally, the cell walls of siliceous organisms consist of hydrated amorphous SiO_2 referred to as "Opal-A" (Jones and Segnit, 1971) or simply "biogenic opal" by many authors. The lattice is composed of a more or less random network of silica tetrahedra ordered on a short range as cristobalite. Such ordering does not exceed a few tens of \AA and the X-ray diffraction spectrum shows a

single broad low-intensity reflection centred around 4\AA (Calvert, 1966; Mizutani, 1966; Kamatani, 1971; fig 2.4, this work). This is similar to silica glasses and gels (e.g. Cartz, 1964), and precious opals (Jones, Sanders and Segnit, 1964). Chemically, biogenic opal is believed to be very pure (Calvert, 1974) but contamination difficulties have prevented unequivocal verification of this.

Silica accumulation is primarily controlled by surface productivity which is in turn controlled by oceanic circulation patterns. Chief areas of productivity are the sub-polar and equatorial regions and areas of coastal upwelling in the eastern boundary currents (Sverdrup, 1938; Wooster and Reid, 1963). In the sub-antarctic, intense vertical mixing leads to highly fertile surface waters which therefore sustain a high rate of phytoplankton production (i.e. diatoms). In the North Pacific, similar conditions are produced by the slow upwelling of deep water, and in the North Atlantic, although feeding the deep water current of North Atlantic Deep Water, winter mixing produces high nutrient concentrations in surface waters. Coastal upwelling in lower latitudes is the result of transport of surface waters away from the continents and the nutrients brought up from depth sustain high levels of zooplankton (i.e. radiolarians), feeding on the phytoplankton produced.

Although high surface productivity is adequate to keep dissolved silica levels in surface waters well below the equilibrium solubility, only a small proportion is ever deposited because of rapid dissolution as the silica sinks. Indeed, Calvert (1968) and Lisitzin (1971) have calculated that between only 1 and 10% of the silica fixed in the euphotic zone by diatoms actually reaches the bottom sediments. Conversely, the more robust radiolarian tests are better

preserved, with the result that these are the main siliceous component of most biogenic sediments.

The mechanism of silica dissolution in the oceans has been extensively studied and modelled (e.g. see Van Lier et al., 1960; Stober, 1967; Hurd, 1973; Wollast, 1974, and references therein) and is thought to be a surface reaction controlled process. Incorporation of radiolarians in faecal pellets of deeper water zooplankton (particularly copepods) results in more efficient sedimentation and it is likely that most of the silica reaching the bottom is introduced in this form (Schrader, 1971).

2.4.2 Silica Diagenesis

a) Dissolution

The pore waters of most sediments are considerably undersaturated with respect to amorphous silica, so dissolution of biogenic silica continues after deposition both within the sediment, and particularly at the sediment-water interface. Consequently, dissolved silica concentrations in pore waters increase considerably with burial (fig. 2.2) and reach levels considerably higher than those of the overlying bottom water, resulting in a significant flux of silica back into the oceanic reservoir (Calvert, 1974). High levels of dissolved silica in pore waters are therefore common in many sediments but only a proportion of this will be permanently fixed in the sediment as chert.

The solution chemistry of the dissolved silica is complex in that kinetic constraints are generally prevalent to changes in thermodynamic equilibrium, and the resulting effects have caused much confusion in earlier studies. For all practical purposes, on

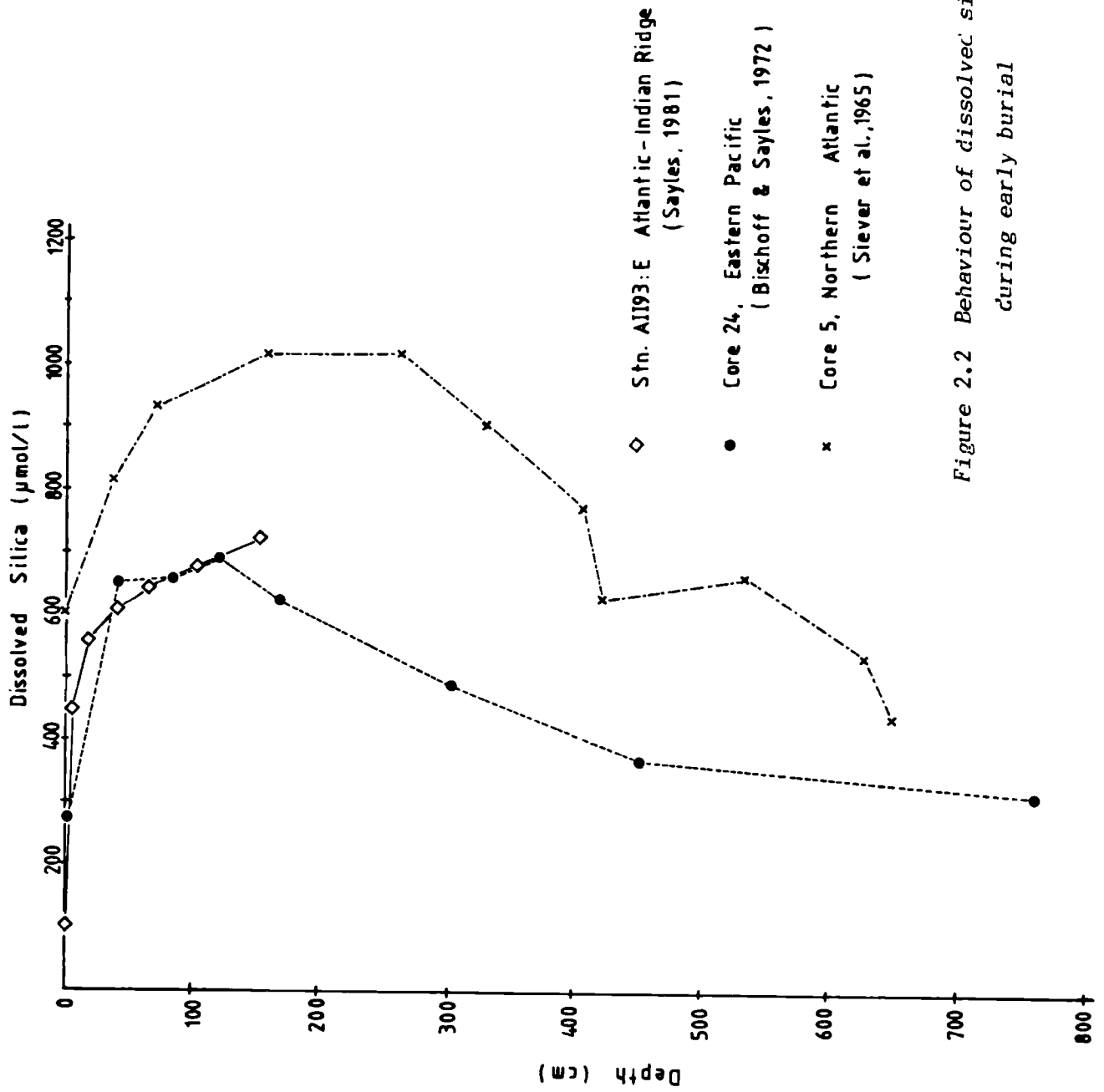


Figure 2.2 Behaviour of dissolved silica during early burial

normal laboratory time scales, the apparent equilibrium solubility of amorphous silica ($\sim 1.8 \text{ mmol/l}$) is real in that it can be approached from either the oversaturated or undersaturated state. From a thermodynamic point of view, however, the equilibrium solubility should be that of the most stable solid silica phase, quartz ($\sim 100 \text{ } \mu\text{mol/l}$). The discrepancy here is a consequence of the kinetic behaviour of dissolved silica and the observed solubility of amorphous silica is in fact a metastable equilibrium. Over geologic time periods, almost all of the silica will eventually reprecipitate, usually as cristobalite (Wollast, 1974). In reality, the apparent solubility is the result of a dynamic equilibrium between the dissolution of disordered silica and precipitation of a more ordered silica in its place. The apparent solubility is therefore directly related to the Arrhenius activation energy for dissolution of the solid material, which itself is a function of the structural disorder of the surface of the silica.

This behaviour has three important consequences. Firstly, the laboratory solubility of any silica will depend on the source of the silica, since different production methods result in silica with different degrees of structural disorder. Secondly, it leads to an "ageing" effect of silica with time as the amorphous surface of siliceous tests are progressively replaced by more ordered silica (e.g. see Willey, 1980, 1982). This results in a considerable variation in the physical and chemical properties of biogenic opal with time, and older siliceous sediments are characterised by a lower "equilibrium" solubility, lower surface area, and greater structural order (Hurd et al., 1979, 1981; and Hurd and Theyer, 1975, for effects; Willey, 1980 for laboratory investigations). Thirdly,

it means that the pore-waters of a sediment may be simultaneously "undersaturated" with respect to amorphous silica and highly supersaturated (by up to an order of magnitude) with respect to quartz. The rapid precipitation of silica to form cherts can not, then, be the result only of a shift in thermodynamic equilibrium (e.g. a large drop in pH). The only alternative here is that it must be a kinetic effect attributable to the action of some kinetic "bridge" which acts as a catalyst to the precipitation of crystalline silica. This is a critical point to any understanding of chert genesis but is almost invariably ignored in publications on silicification.

More problematic is the nature of this kinetic bridge. It has long been known that organic matter forms a very important substrate for silica precipitation (e.g. Francis et al., 1978 a and b), and indeed organic-silica complexation has been suggested as an important step in flint formation (Håkansson et al., 1974; Bromley et al., 1975). On the grounds of mass balance considerations, however, this can be discounted (see chapter 1).

Dissolved metallic cations are another possibility (e.g. see Marshall and Warakowski, 1980) but the effects of these are only small, and although Kastner et al., (1977) have found $Mg(OH)_2$ to be an important nucleating agent for sedimentary silica, dissolved cations alone cannot account for silica precipitation on the scale of widespread chert formation. One dissolved species which can, however, is carbonate ions. Mathews (1972) has found carbonate to be a very effective mineralizing agent in silica solutions and a similar effect has been noticed by Lovering and Patten (1962), who found silica to be precipitated on the addition of CO_2 . In this respect, it is important to note that dissolved carbonate is generated at any site of carbonate dissolution, so providing dissolved silica is abundant,

a chert could form anywhere that carbonate is dissolving. Furthermore, although the mechanism involved is not known in detail, it probably involves a certain amount of hydroxyl consumption (Iler, 1979, p.84) which will in turn lead to more carbonate dissolution: a simple feedback mechanism.

b) Chert Formation

Much literature exists on the mineralogical and petrological aspects of silica precipitation in cherts, obtained largely from the Deep Sea Drilling Project (Calvert, 1971 a and b; Heath and Moberly, 1971; Von Rad and Rosch, 1972; Heath, 1973; Knauth and Epstein, 1976; and others) so only an outline will be given here.

The general pattern of chert formation is shown in Fig. 2.3, after Von Rad et al., (1978). Early precipitation of silica occurs in two ways: the local precipitation of quartz as a replacement of calcitic microfossil tests, and probably also in some intraparticulate pores; and larger scale precipitation of dense opal-CT (disordered low cristobalite) as a replacement and in pore spaces, to form a "porcellanite" (porcellanous chert). There then follows a time dependent ordering of the opal-CT crystal lattice followed by diagenetic alteration to quartz (fig. 2.4).

c) Precipitation of Opal-CT

Although small amounts of silica precipitate directly as quartz, such as in the replacement of microfossils (Kastner et al., 1977; Von Rad, Riech and Rosch, 1978) and free precipitation in pores (Heath and Moberly, 1971; Von Rad and Rosch, 1972), most silica in cherts is in the form of low cristobalite, usually termed opal-CT (see appendix). According to Jones and Segnit (1972),

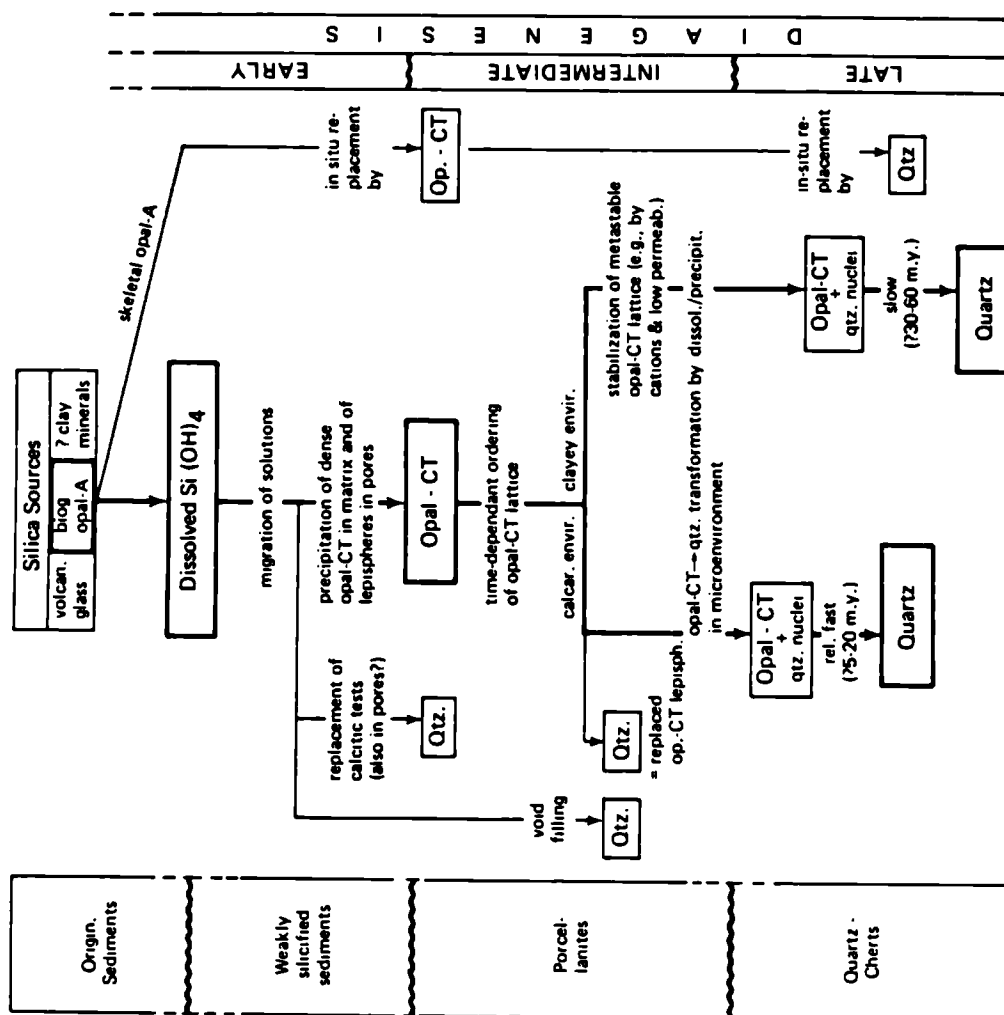


Figure 2.9 Schematic diagram showing transformation and diagenetic processes between opal-A, opal-CT, and diagenetic quartz (modified from von Rad et al., 1978).

this is because the lowest energy state for the polymerisation of silica tetrahedra is in the form of six membered unconstrained rings. On precipitation, coalescence of these rings will produce extended sheets with elements of both cristobalite and tridymite symmetry, with a dominance of the cristobalite structure. In practice this is probably a little simplistic and Wollast (1974), based on the experimental data of Stober (1967), has offered a more feasible explanation on purely kinetic grounds.

The resulting mineral is a unidimensionally disordered low cristobalite with a distinctive X-ray diffraction pattern in which some of the characteristic tridymite peaks appear at the expense of some of the cristobalite peaks. The most characteristic features are two rather broad reflections at about 4.05\AA and 2.49\AA with a subsidiary reflection at $4.25 - 4.30\text{\AA}$ (fig. 2.4). The 4.05\AA peak (corresponding to the $d(101)$ spacing) is of considerable interest since, with time, opal-CT shows a progressive ordering of the structure reflected in a sharpening of this peak associated with a smooth non-linear shift in the d -spacing from 4.10\AA to 4.04\AA (Pisciotta, 1981; Isaacs, 1982).

Crystallographically, opal-CT precipitates as small silica spherules (termed "lepispheres" by Wise and Kelts, 1972), around $10-15\text{ }\mu$ in diameter, composed of fine pseudo-hexagonal bladed crystals, $300-500\text{\AA}$ thick, flattened on (0001) (Weaver and Wise, 1972; Wise and Kelts, 1972; Florke, 1976; Oehler, 1973). There is abundant evidence that cristobalite lepispheres are an important component of deep-sea cherts (e.g. see Lancelot, 1973; Kastner, Keene and Gieskes, 1977; Von Rad and Rosch, 1972), but although some workers have suggested that coalescence of lepispheres may form the main component in the porous porcellanite fabric of "young" cherts (e.g.

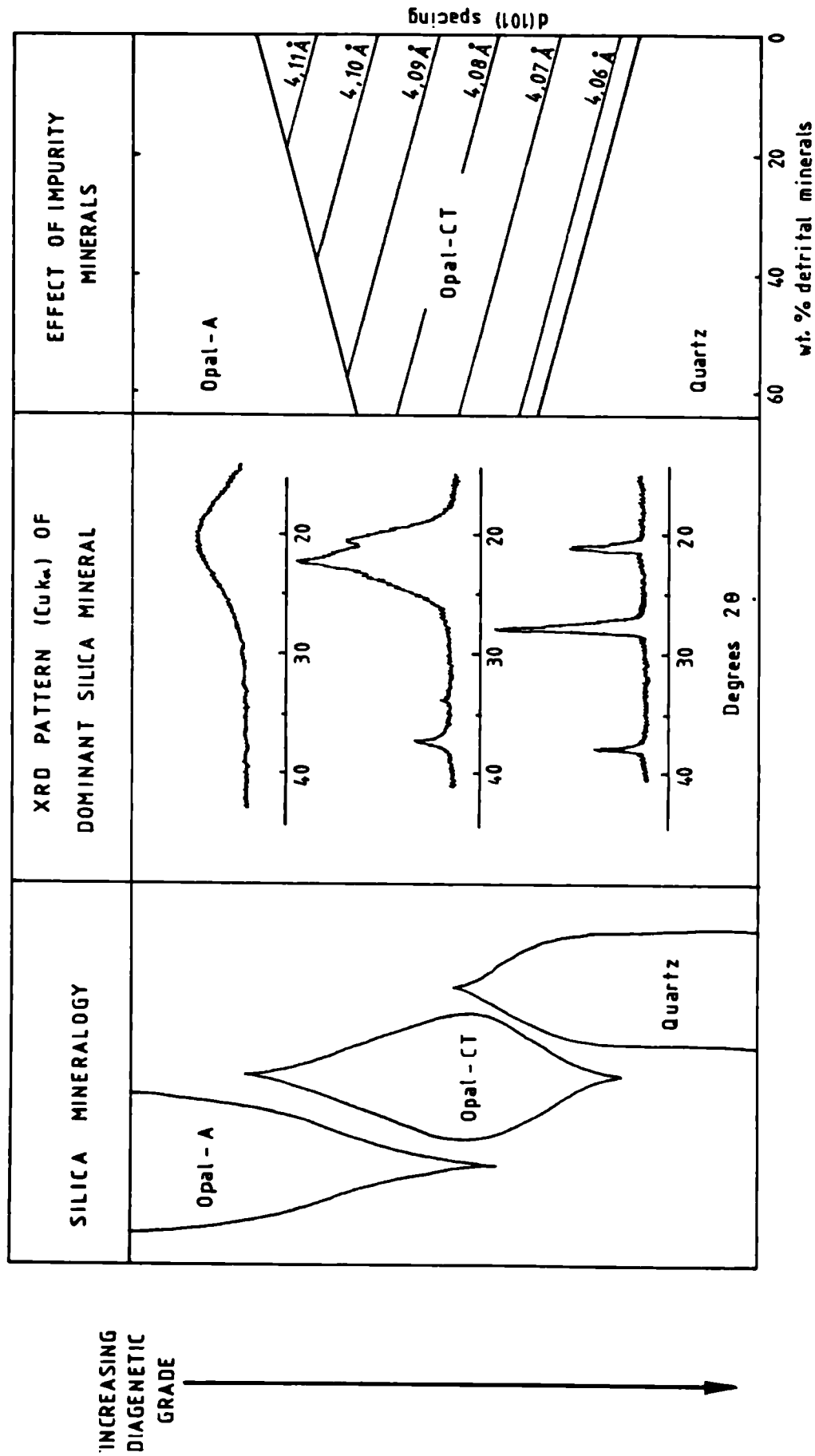


Figure 2.4 Principal phase transformations of the silica minerals during diagenesis.
After Isaacs, 1982 and Pisciotto, 1981

Calvert, 1974) it is generally held that opal-CT occurs more commonly as a cryptocrystalline cement, interstitial to the matrix (e.g. Pisciotto, 1981; Heath and Moberly, 1971). The relationship of porcellanite fabric to that of homogeneous granular microcrystalline quartz chert is unclear.

d) Opal-CT - Quartz Recrystallisation

Although it is obvious that the opal-A - opal-CT transformation takes place via a solution-redeposition process, the nature of the opal-CT to quartz transformation is more controversial. This transition is, however, of great importance since a solid state transformation would be expected to preserve Si-O bonds and thus the oxygen isotope composition of the opal-CT, (reflecting the composition of very early diagenetic pore-waters and to some extent, marine bottom-water temperatures). Quartz occurs in cherts dominantly as granular microcrystalline quartz (Knauth and Epstein, 1975) with a smaller amount of coarser "megaquartz" infilling later stage voids. A solid state (zero-order) reaction was first suggested for the change by Ernst and Calvert (1969) and Heath and Moberly (1971), but a solution-redeposition mechanism is suggested by the hydrothermal experiments of Carr and Fyfe (1958), and T.E.M. studies of Stein and Kirkpatrick (1976; who incidentally worked on Ernst and Calverts experimental products). More recent work, e.g. Mizutani (1966), and the isotopic results of Murata and Larson (1975), Murata et al., (1977) and Pisciotto (1981), in the Monterey formation of California, Knauth and Epstein (1975) on deep sea cherts, and experimental data of Kastner (1982, and pers. com.) suggest a solution-redeposition mechanism. All this work is, however, based on whole-rock analyses and no attempt has yet been made to confirm that this is true for all types of opal-CT in cherts (i.e. lepispheres and interstitial material).

The rates of the transformation are controlled both by temperature and the trace element composition of interstitial solutions. Typically, chert maturation will be more rapid in areas of high heat flow but is retarded by the absence of metallic trace elements (fig. 2.4). This latter point is in contrast to the effect on the opal-A - opal-CT change which is retarded by the presence of trace elements (Issacs, 1982, and fig. 2.4, this work).

The overall pattern of silica diagenesis is thus as shown in fig. 2.4, with an initial precipitation as quartz or opal-CT, and a slow maturation sequence to quartz cherts. The relevance of this to Upper Cretaceous flints is discussed in chapters 4 and 5.

3. SEDIMENTOLOGY AND FIELD RELATIONS OF UPPER CRETACEOUS CHALKS

3.1 THE UPPER CRETACEOUS OF WESTERN EUROPE

The Upper Cretaceous of Western Europe represents a period of high sea level stands following major eustatic sea level rises during the mid-Cretaceous. During this time, the general paucity of exposed land masses and arid climate produced very limited detrital input into the extensive shelf seas of the area, resulting in extensive deposits of high purity pelagic carbonates: the Cretaceous Chalk.

Chalk sedimentation began early in the Cenomanian stage (~98 my) with marly chalks, and in most areas continued until the great marine regressions of the Maastrichtian, about 65 my ago. White chalk sedimentation was confined to three depositional basins in Western Europe (fig. 3.1): the Wessex-Paris Basin (corresponding to the "Southern Province" in the British Isles); the Anglo-Dutch Basin to the north ("Northern Province" of the British Isles and passing laterally into the North Sea Graben system, and across into the Danish-Polish basin system); and the more southerly Aquitaine Basin of Southern France. Sedimentation in these areas was dominated by pure white pelagic carbonates (coccolith oozes) but in deep basins and troughs (e.g. Central Graben of the North Sea, South Celtic Sea Basin etc.) the sediment may contain a much higher clastic content (e.g. see Hancock and Scholle, 1975). Over structural highs and around coastlines the sedimentary sequence is highly condensed (e.g. see Bromley and Gale, 1982, for sedimentation over the

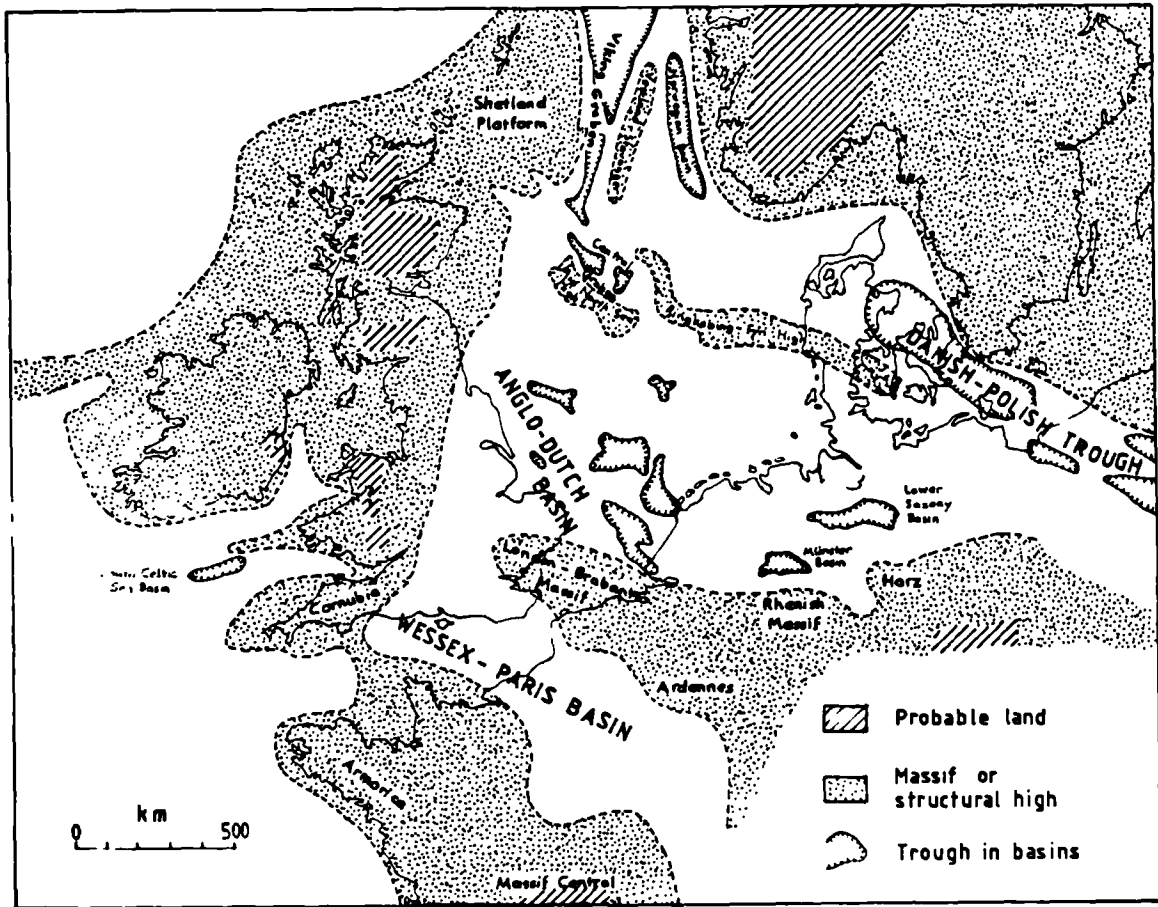


Figure 3.1 Generalised palaeogeography during Upper Cretaceous times (approx mid-Turonian) in Western Europe. After *l'encock*, 1975, *Gale pers con* and authors own observations.

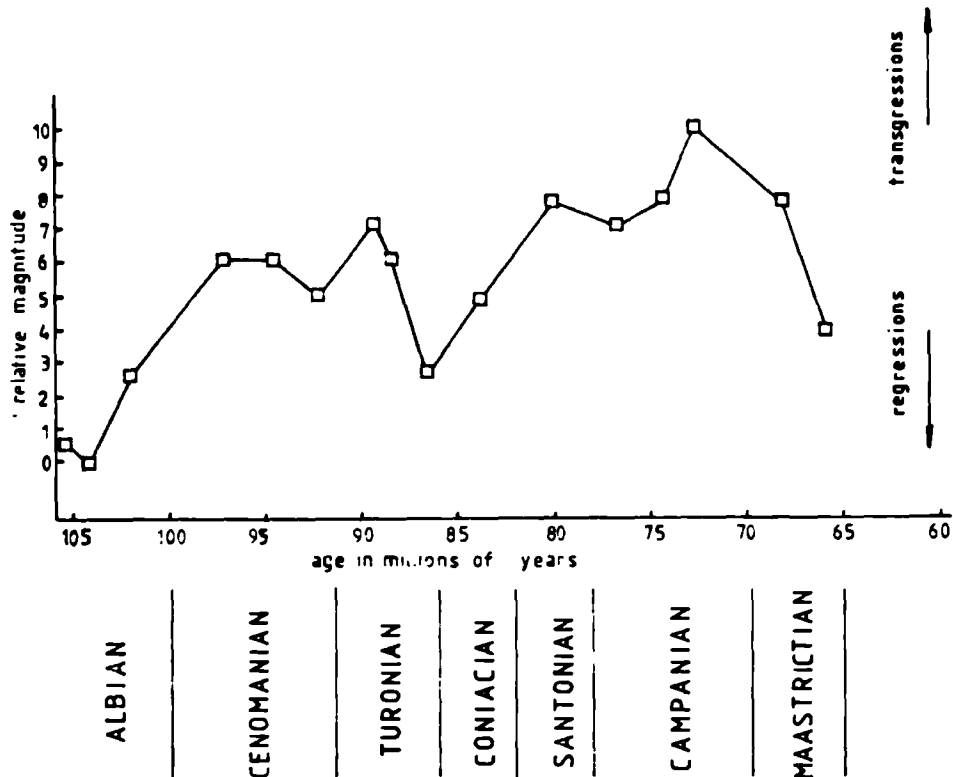


Figure 3.2 Eustatic variations in Cretaceous sea level. Data from *Hancock and Kauffman*, 1979, replotted to time scale of *van Hinte*, 1976.

London-Brabant Massif) and may develop into glauconite-rich facies in some areas (e.g. Fletcher, 1977, for Northern Ireland; Jarvis, Gale and Clayton, 1982 for south-west margin of the Paris Basin). In general, the pure coccolith oozes of the open basins pass into "tuffaceous" (i.e. bioclastic-rich) chalks nearer land (e.g. Turonian "Tuffeau de Touraine" of Touraine area of Central France, Robaszynski et al., 1982; much of Maastrichtian chalk in type area, Felder 1975 and 1976).

Geochemical investigations reported in this work were carried out almost exclusively in the pure coccolith chalks of the Wessex-Paris Basin in Southern England but field observations have been more extensive. The descriptions here are based primarily on the author's own observations but the views expressed have been greatly influenced by discussions with numerous co-workers whose valuable contributions are greatly appreciated.

3.2 CHALK SEDIMENTATION

Pure Cretaceous chalk is composed mostly of low-Mg calcite, dominantly the skeletons of planktonic algae: coccoliths and rhabdoliths. In addition, small amounts of clay minerals and silt grade quartz grains occur (generally < 2%), a variable quantity of macro-faunal fragments such as Inoceramus prisms, echinoderm fragments and bryzoan debris, and a little authigenic mineral matter, particularly iron sulphides, phosphates and "glauconite". Microfauna, such as foraminifera and calcispheres may also be important locally (e.g. calcisphere-rich chalks associated with nodular beds: Mortimore, 1979). In this context, the Chalk falls within the definition of a "pelagic sediment" (i.e. pertaining to the open sea),

but is unique in that it forms extensive shelf sediments rather than the deeper water deposits usually associated with pelagic sedimentation.

In addition to the above components, biogenic siliceous particles and aragonitic fauna were probably also important in the original sediment but have since dissolved. Aragonitic fauna are common where early diagenetic lithification has preserved a mould of the shell, and similar preservation can (rarely) be found in flints. Originally siliceous sponges and disaggregated spicules occur now as calcitic replacements throughout much of the Chalk and these, as well as rare radiolarians, often maintain their siliceous mineralogy when preserved in flint. Siliceous organisms were undoubtedly very common constituents of the original sediment but as explained in Chapter 2, their presence in the sediment would have been short lived as spontaneous dissolution of the biogenic opal would occur on burial, leading to high levels of dissolved silica in pore waters. This silica is probably now represented in the flints, although the absence of these does not necessarily imply an original absence of biogenic silica.

Water depth estimates for the Chalk vary greatly but are now generally quoted as between 100 and 600 m (Hancock, 1975). The maximum depth of 300 m suggested by Kennedy and Garrison (1975) was based on the assumption of a tectonically stable outer shelf but this is now known to be false (e.g. see Mortimore, 1979 and 1983; Hancock and Scholle, 1975; Colbeaux et al., 1980; Robaszynski, 1981, and related papers). The estimate of 250 m for the tuffaceous chalks of the Maastrichtian (Hakansson et al., 1974), is probably a reliable estimate for such sediments, suggesting slightly deeper water for the pure coccolith chalks. Over

structural highs, usually associated with hardground formation, water depths of nearer 100 m are usually suggested (e.g. Reid, 1962; Bromley, 1965 and 1970; Kennedy, 1970).

Coccoliths live exclusively in the surface waters of the ocean and their small size results in very slow sedimentation of dead organisms. Theoretical calculations by the author (see Appendix 2) suggest settling rates in the order of 4×10^{-5} m/sec for coccospheres and 8×10^{-6} m/sec for coccolith discs which result in sinking times of around 60 days and 9 months respectively, for a 200 m water depth. During this time the sinking organic detritus would be expected to pass through the digestive systems of higher organisms (e.g. copepods) several times so it is likely that most of the material would have been carried to the bottom predominantly in the form of faecal pellets, (see Scrader, 1971, for modern analogy). This suggestion is strongly supported by the occasional presence of loosely packed pelletal chalk in burrows, and the common occurrence of phosphates in the form of faecal pellets (e.g. Jarvis, 1980). However, in most cases the pellets must have been broken down by bacterial action and physical reworking very early in the diagenetic history of the chalk.

Intense bioturbation has generally destroyed most of the original bedding lamination of the chalk but it is still possible to tell something of contemporary bottom conditions. In general, the sediment has been regarded as a "semi-fluid" (e.g. Kennedy and Garrison, 1975) but this has not been substantiated by more recent work. The assumption of a soft sea floor was based mainly on faunal evidence such as the development of frills and spines in bivalves and brachiopods, supposedly as sediment traps, large scale encrustation of hard substrates, and the development of

"unconventional" root-like pedicles on some brachiopods. Frills and spines, however, are also common on reef-dwelling organisms and Jarvis, Gale and Clayton (1982) have found similar adaptations in the firm substrate fauna of the Craie de Villedieu. Large scale encrustation of hard substrates involves the development of an entirely independent ecosystem and this will occur irrespective of surrounding sediment type (e.g. it occurs over most of the North Sea at present), and many seaweeds and mussel species attach themselves by root-like systems in all sediment types, even on hard substrates. Conversely, the presence of cutting and "packing" spines on some Chalk echinoids (Gale and Smith, 1982 and A.S. Gale pers. com.), and the common preservation of firm substrate burrows (Bromley, 1967 and 1975) and surface-dwelling fauna (Inoceramid bivalves, regular echinoids, lobsters and asteroids etc.) suggest a firm substrate. In addition, early stage compaction jointing (see section 3.6.5), and the laboratory studies of R.N. Mortimore (pers. com.) suggest a fairly stable substrate (although with a slight tendency for thixotropy), even in sediment of 70-80% porosity. The absence on carbonate grains of surface electrical charges, such as those associated with clays, probably resulted in the Chalk behaving more like a silt or fine sand than a clastic mud.

Average sedimentation rates for the Chalk are very difficult to estimate because the effects of subsequent compaction are only poorly known, and most of the time represented by the sediment pile was taken up in non-deposition ("omission") planes, usually reflected as bedding planes. Estimates usually concentrate at around $2-3 \text{ cm}/10^3 \text{ years}$ (e.g. Kennedy and Garrison, 1975, and references therein) for white chalks but may be much higher (e.g. $15 \text{ cm}/10^3 \text{ years}$: Hakansson et al., 1974) for bioclastic-rich chalks. Such slow

sedimentation rates are incompatible with the burial of some of the fauna found in the chalk before it could be destroyed by bioerosion (e.g. 2000 years to bury a Micraster) suggesting that short periods of much more rapid sedimentation alternated with long periods of non-deposition. This was presumably the result of lateral sediment movement on the sea-floor since even under exceptional conditions, coccolith production would be unlikely to exceed a few cms/ten years. Lateral movement is also suggested by the air weathered sections of the Northern Province where bedding on the scale of 5-10 cm is common (pl. 2B). Fine horizontal laminations are usually visible within the beds suggesting that intense sediment reworking by current activity was dominant over the burrowing activities of the benthos - a feature also apparent from flint morphology (see below). In the Southern Province, and the south of the Northern Province (i.e. in Norfolk), current activity was less intense and bioturbation has destroyed almost all traces of primary bedding.

Sediment re-deposition is indicated in the Southern Province also, by the presence of normal and reverse graded units (suggestive of turbiditic and grain flows respectively) and by the great variation in isopachytes over the structurally unstable Sussex area (R.N. Mortimore, pers. com. and 1983). Synsedimentary slump movements are also known in the Chalk (e.g. Kennedy and Juignet, 1974; Gale, 1980) and a conglomerate containing Greensand boulders up to $\frac{1}{2}$ m across occurs in the Turonian of Winterbourne Abbas, Devon. This latter feature is adjacent to the Winterbourne Abbas Fault (see I.G.S. 1 inch sheet 327) suggesting synsedimentary tectonic activity.

Overall therefore, at least in England, the Chalk sedimentary regime probably bore more resemblance to a silt or fine sand covered tidal shelf system than to a quiet soupy "great white sludge".

3.3 MARL SEAMS, "FLASER" BEDS, AND GRIOTTE CHALKS

The presence of clay rich horizons in the Chalk has aroused much interest and discussion, largely as a result of their potential importance as stratigraphical marker beds. Although some minor marls are of only local extent, others, such as the Lewes Marl of Sussex (fig. 3.3), may be traced over all of the Wessex region, into Northern France, and possibly even into the Northern English Basins (C.J. Wood and R.N. Mortimore, pers. com.). Individual marls may often exhibit local variations in lithology and fauna but overall their general character and position with respect to flint bands and hardgrounds is usually constant, over large distances. Despite this very little is known about their genesis.

In some cases, marls take the form of clearly defined dark grey-green regular clay seams, up to 25 cm thick, sometimes finely laminated. More often, the marls occur as fine streamers of clay, lying dominantly in the plane of bedding, enclosing either hardened or soft white chalk "islands" or nodules. This latter texture is essentially that of a "griotte" limestone (e.g. Ammonitico Rosso facies of Tethyan Jurassic, Jenkyns, 1974; Griotte and Cephalopodenkalk of Variscan Geosyncline, Tucker, 1974) although the misleading term "flaser-chalk" is a more common description. In three dimensions the white chalk "islands" can usually be seen to be infilled Thalassinoides burrow systems which have become flattened by a combination of compaction and sub-surface dissolution (Mortimore, 1979). In extreme cases, the burrow infills may be reduced to highly flattened lenticles which may extend laterally into streamers of clay (e.g. see pl.2b of Hancock, 1975). Such griotte chalks are more characteristic of the

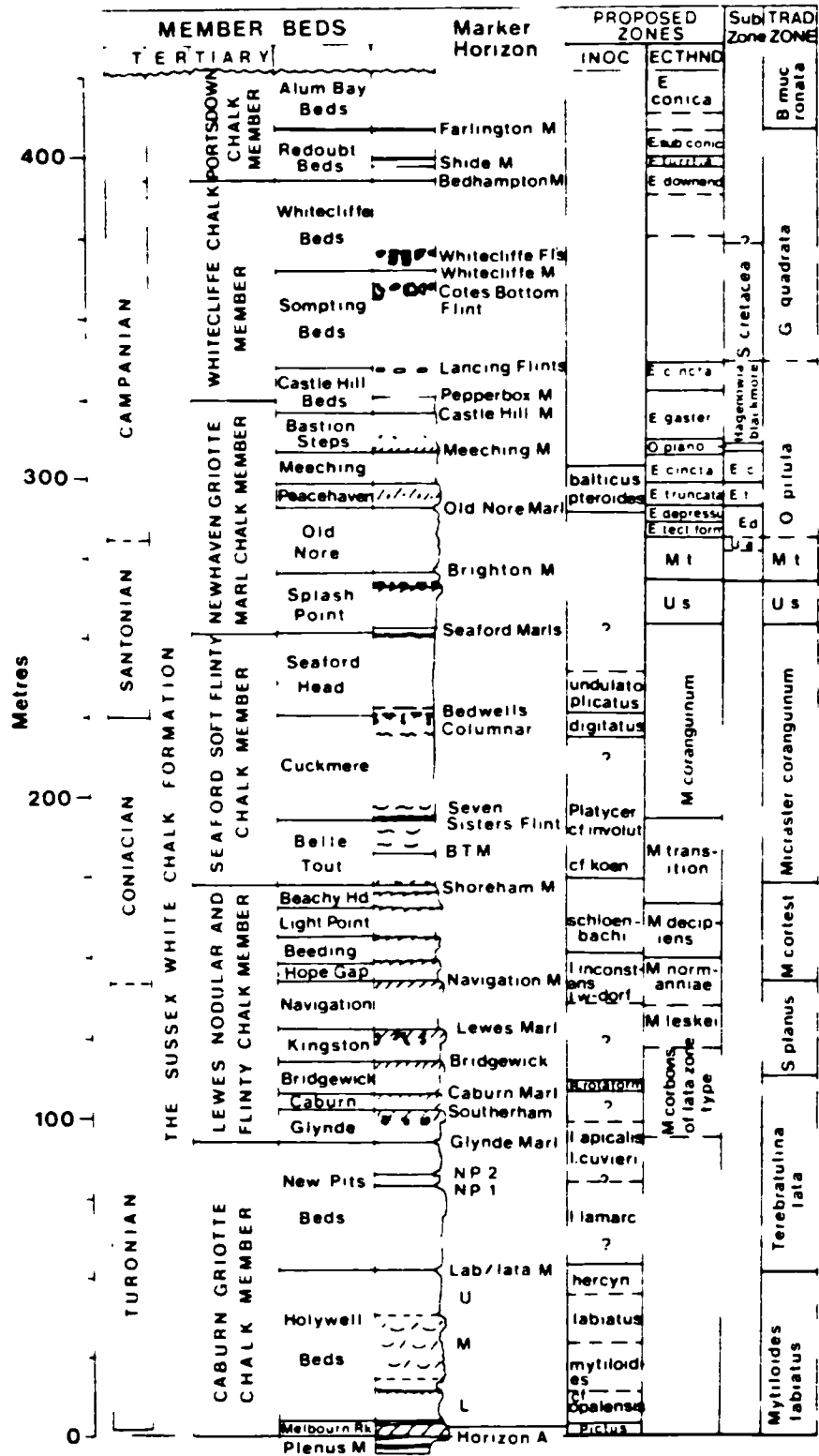


Figure 3.3 Stratigraphy of the Sussex White Chalk Formation: Lewes and Whitecliffe stratotypes. Northmore, Pers. Com.

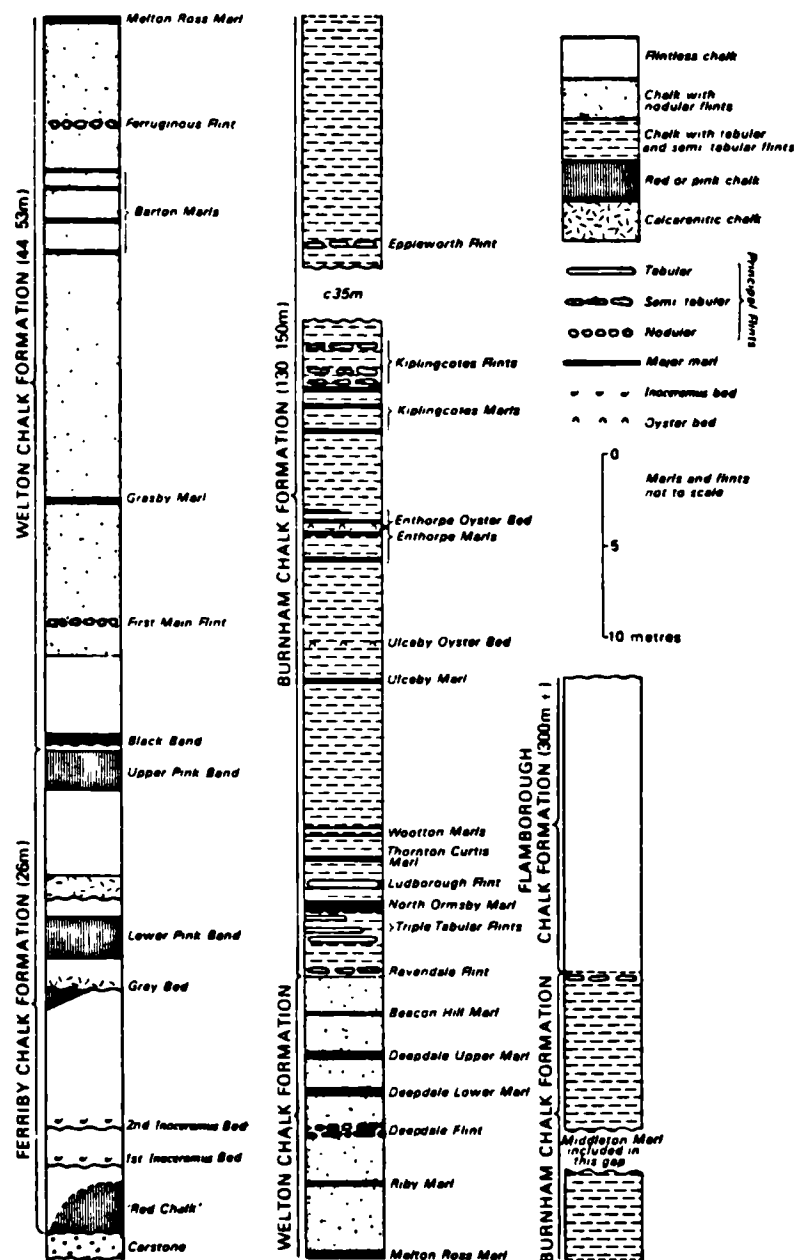


Figure 3.4 Generalised section of the Chalk in northern England showing the four component formations and the marker horizons. From Wood and Smith, 1978. Reproduced by permission of the authors.

**Felder
(1975)**

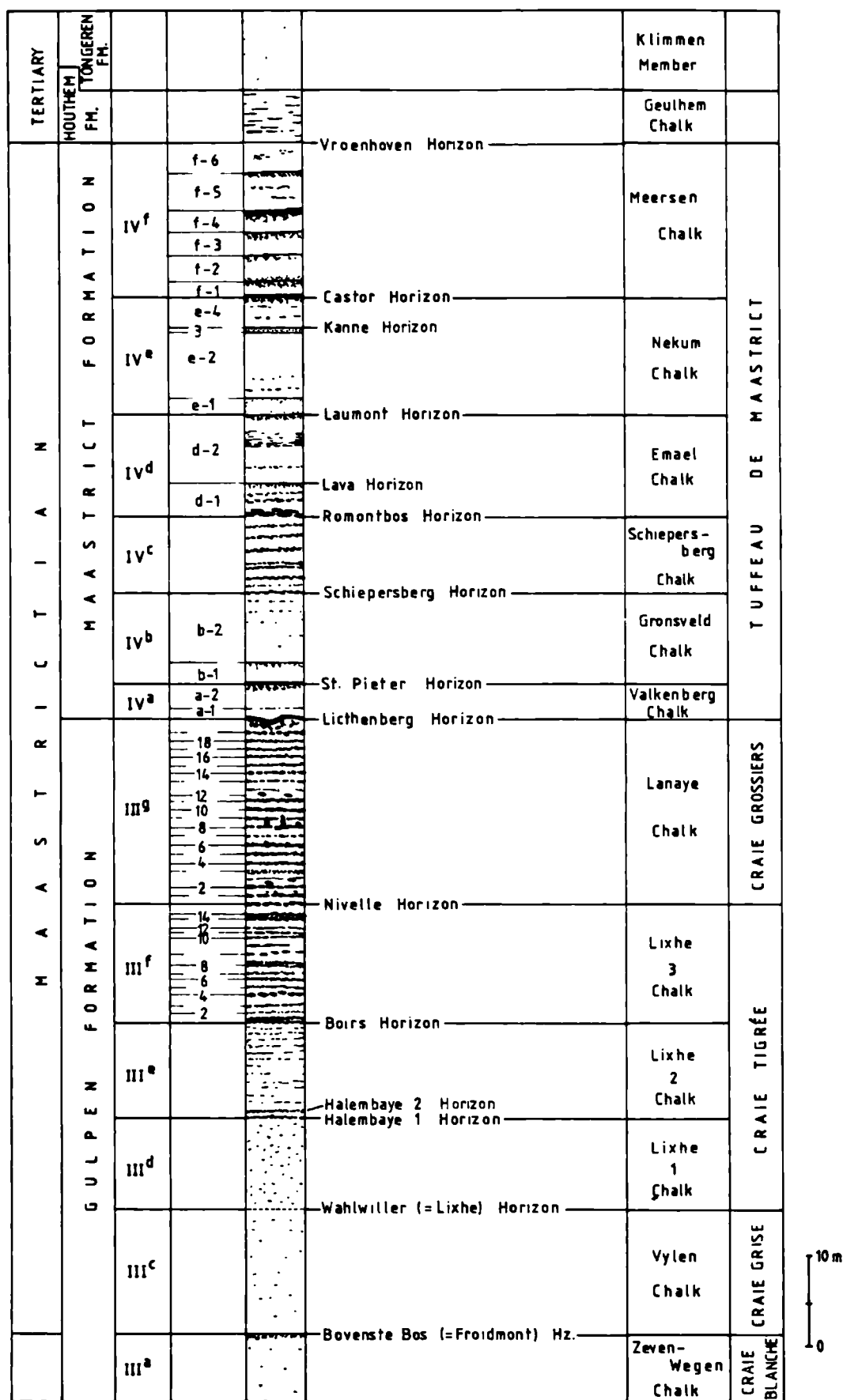


Figure 3.5 Lithostratigraphy of the Maastrichtian type sections.

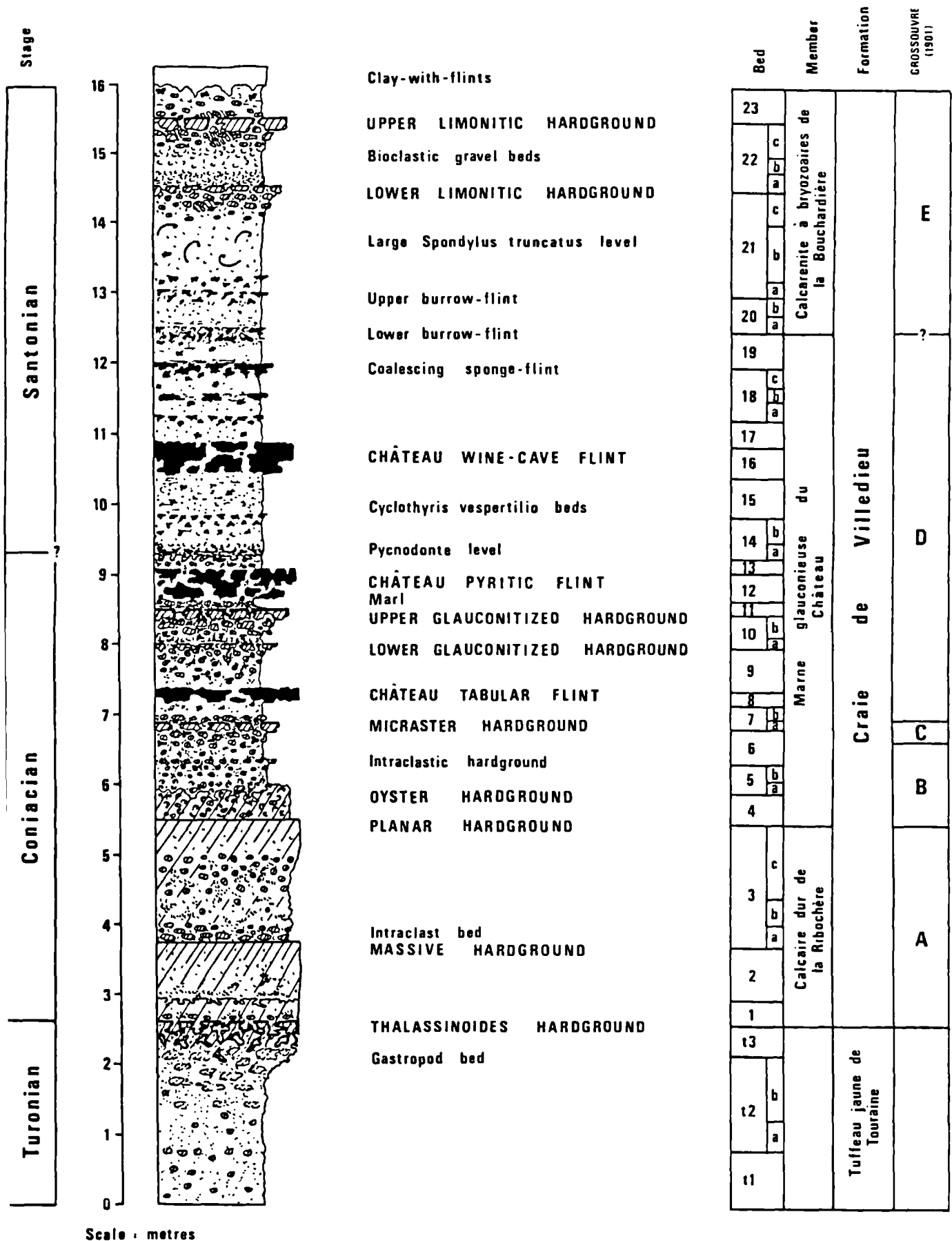


Figure 3.6 Lithostratigraphy of the Craie de Villedieu. From Jarvis et al., 1982

Southern Chalk Basin; marls in the Northern Province and in other areas tend to be more regular. This is probably a reflection of the extent of bioturbation in the Southern Province chalks which is absent from the more intensively reworked Northern chalks (see above).

Explanations of marl genesis in chalks have tended towards speculation rather than deduction but two broad schools of thought have developed: the marls may be entirely the result of sub-surface dissolution (i.e. diagenetic); or they are the result of oceanic events or ash falls (i.e. sedimentary).

In most cases, sub-surface dissolution is clearly a contributory factor to marl genesis and this is commonly attributed to deep burial (e.g. Kennedy and Garrison, 1975; Jeans, 1973). However, it is not uncommon for the dissolution fabric to be cut by early stage conjugate compaction joints (e.g. pl. 2d of Hancock, 1975), and vertical slickensides are commonly present where the hardened nodules have moved against each other under compactional stresses. In addition, the author has observed Thalassinoides burrows which truncate the clay seams. All of these points suggest that dissolution was a very early event and the most likely cause of this is the CO_2 released by bacterial oxidation of organic matter (see chapter 2). The very shallow burial under which this occurred is compatible with oxidation by aerobic bacteria (cf. Aller, 1982; Grundmanis and Murray, 1982).

Sub-surface dissolution is probably the cause of marl seam formation in the Maastrichtian Lanaye Chalk of the Maastricht area (fig. 3.5). The Lanaye Chalk represents a brief period of relatively stable chalk sedimentation during which approximately 30 m of slightly tuffaceous chalk was deposited. About 20 regularly spaced flint bands occur within this unit but at two levels (between

flints 9 and 10, and 13 and 14), the expected position of a flint band is occupied by a moderately well-developed marl, (fig. 3.5, pl. 1A). It is possible that pre-existing marl seams here have inhibited flint formation, but in view of the fact that these are the only two well developed marls present and both coincide exactly with the expected position of a flint, it is perhaps rather optimistic to attribute this to chance. More likely, carbonate dissolution occurred at these sites by whatever process usually initiates flint formation (see chapter 1), but for some reason, this did not result in silica precipitation. The result was not therefore a flint, but a marl seam, generated by a concentration of the insoluble residue of the pre-existing chalk.

Although shallow burial dissolution alone can apparently result in marl seams, there is conversely, abundant evidence that most marls were original sedimentary features. Marls are commonly burrowed down into the underlying white chalk, and, as explained above, white chalk from above is often burrowed into marl seams. In some cases, subsequent erosion has entirely removed the marl seam but left marl burrow fills in the underlying white chalk. Marls also typically contain a different fauna from the surrounding chalk and M. Hart (pers. com.) has found that the presence of some major marls is reflected in a temporary change of the foraminiferal assemblage in the overlying chalk. This latter point is suggestive of a catastrophic oceanic event such as a volcanic ash fall or an anoxic event.

Numerous explanations have been suggested to account for such clay concentrations on the sea floor, but the most likely are: an increase in clastic supply to the oceans; a decrease in carbonate production in oceanic surface waters; or an increase in sea-floor or

water column dissolution rate.

Increased clastic input is unlikely to be the result of a change in continental weathering regime since exposed land area was minimal over most of central Europe and weathering would be unlikely to distribute clay into such widespread and regular marls. Argillisation of volcanic ash falls is a more likely way of increasing the clastic content, and this is particularly likely in view of the widespread presence of ash bands in the lower and mid-Cretaceous (Jeans et al., 1982). Such an origin would also explain the faunal catastrophe associated with major marls (see above) and is inherently suited to the production of widespread and contemporaneous marls. Despite much observation, however, direct evidence of a volcanic origin has not been found. Relic shards are absent in all material so far studied, and indeed, many marls do not contain any material coarser than clay grade.

A decrease in carbonate production or increase in carbonate solution are effectively inseparable in terms of effect as either of these will produce an elevation of the carbonate compensation depth. Such an origin for many marl seams is a very good explanation of the observed features and has been suggested by Ernst (1978) as a cause of marls in the German Lagerdorf Chalk section where they coincide with extensively bioturbated layers ("Grabganglagen"), rich in benthonic foraminifera. Oceanic anoxic events are well known for having such an effect on surface production in the Cretaceous and at least one major marl - the basal Turonian Black Band of Yorkshire and Lincolnshire (fig. 3.4) - has already been attributed to such an event (Jenkyns, 1980). Almost identical, but more dramatic sedimentary changes at the Cretaceous - Tertiary boundary have been interpreted as possible evidence for an extra-terrestrial

cause but this has not gained widespread acceptance amongst specialists in Chalk sedimentology.

Anoxic events are associated with the burial of anomalous amounts of organic matter which, upon return to oxic conditions would become the natural centre for bacterial decay reactions. These reactions could then explain the observed subsequent carbonate dissolution, particularly where the sediment became aerated by burrow networks. Furthermore, depletion of oxygen in the water column would also explain the associated faunal crisis, and the anomalous benthonic fauna.

The effect of oceanic anoxic events on the carbon isotope balance in the oceanic carbon reservoir is a critical aid in any understanding of marl genesis by this process but data are rather limited at present. Scholle and Arthur (1980) have recently published crude $^{13}\text{C}/^{12}\text{C}$ ratio curves for the Cretaceous which they believe reflect transient deviations in organic carbon-dissolved carbonate balance in the oceans, but detailed investigations of isotope variations across individual marls have not yet been carried out.

In summary, Chalk marl seams may in some cases be the result solely of shallow sub-surface carbonate dissolution but are more usually of primary origin and subsequently modified by dissolution. The ultimate origin of marls is unclear but is most likely the effect of either argillisation of volcanic ash falls or changes in the marine organic production cycle, such as could be associated with an anoxic event. There is insufficient evidence to differentiate between the two at present but carbon isotope studies are seen as an important next step. An origin due to a meteorite impact or a similar act of God is probably of only rare importance, if at all.

3.4 OMISSION SURFACES, NODULAR BEDS AND HARDGROUNDS

"Hardground" is a sedimentological and ecological interpretative term used to describe omission surfaces (i.e. non-depositional surfaces) at which early diagenetic cementation has produced a lithified sea floor (Bromley, 1978; Bromley and Gale, 1982). Hardgrounds, and the underlying indurated chalk (infelicitously termed "chalkstone" by the above authors) are conspicuous features of Cretaceous Chalk sections, and are of great stratigraphic value.

Chalk hardgrounds are typically heavily glauconitised and phosphatised, and are often extensively stained by limonite, probably formed by the weathering of pyrite at outcrop. In detail, the hardground may also be bored and encrusted by organisms adapted to a hard sea floor, and Bromley (1967) has demonstrated an ecological succession within crustaceans as the population modified their burrowing behavior as the hardening proceeded. Generally, hardgrounds occur in groups at any one stratigraphic level (e.g. Kingston⁹ Hardgrounds of Sussex; fig. 3.3) but in other cases isolated individual hardgrounds may be correlated over large areas (e.g. the Clandon hardground, fig. 7.1, can be correlated with a hardground at North Barn in Dorset, and is represented on the Kent coast by Barrois' Sponge Bed, an iron stained nodular bed (A.S. Gale, pers. com.)).

The sequence of events leading to hardground formation has been extensively discussed by Voigt (1959) and Bromley (1967, 1968, 1975, 1978), and recently reviewed by Kennedy and Garrison (1975). Hardground genesis starts with a break in sedimentation which produces an omission surface with a characteristic suite of burrows. Lithification begins at localised sites between Thalassinoides

burrows and continued cementation results in a nodular chalk (pl. 2c). Burrows formed at this stage avoid the hard nodules and Thalassinoides systems may remain open during the process, suggesting that cementation occurred within a few metres of the surface. Further cementation results in a more intensely hardened nodule bed and eventually a solidly lithified unit (e.g. pl. 2e). The surface morphology of a hardground is dependent on the intensity of erosion after the sub-surface lithified bed is exhumed. Small amounts of erosion remove only the top levels of the unit, to reveal a highly convoluted surface, controlled by the distribution of open burrows (i.e. Thalassinoides) and borings (particularly of the boring sponge Entobia: Bromley, 1970). More intense erosion will usually remove all topography above the lower Thalassinoides chamber system resulting in a planar hardground (e.g. the Clandon hardground, fig. 7.1). Erosion is largely by biological agents but current scour and lateral movements on inclined surfaces may also be important (Jarvis, Bromley and Clayton, 1982).

All stages of the above morphological sequence are preserved in various places but it is rare to find them all together within one unit. More usually, multiple hardgrounds may be present within a single lithified unit (e.g. the Chalk Rock: Bromley and Gale, 1982) and this passes laterally into units of nodular chalk (e.g. Bridgewick - Lewes series in Sussex) and eventually unlithified units with omission surfaces. Although the morphological sequence: omission surface - nodular bed - hardground is a true genetic sequence, it would appear that the end point of this sequence varies geographically (? water depth effect). This implies that the common assumptions of hardgrounds forming as a consequence of a

break in sedimentation (Kennedy and Garrison, 1975; Gale, 1980), or associated with coarser sediments (Jarvis, 1980), are false, and some external factor must exert an influence.

The genesis of hardground groups is intimately related to sedimentary thinning and condensation, over massifs or onto oceanic margins, and is also strongly stratigraphically controlled. For example, the late Turonian was a period of extensive lithification over the London platform (R.G. Bromley and A.S. Gale, pers. com.) and coincides with a major period of penecontemporaneous cementation on the south-west margin of the Paris Basin (Jarvis, Gale and Clayton, 1982). This period also coincides with a marine regression (fig. 3.2) and Kennedy and Garrison (1975) have suggested that this is an essential feature. Hardgrounds also developed over the margins of the Maastricht area during the Maastrichtian regression where they can be traced laterally into normal flinty chalks in the deeper part of the basin. Interestingly, A.S. Gale (pers. com.) has recently found that the main zone of cementation over the London Platform migrates away from the highest part of the succession, progressively, during the Turonian regression. If true, this would suggest a very specific water depth control on such lithification.

The mechanism of cementation is only rarely considered in descriptions of chalk hardgrounds. Kennedy and Garrison (1975) have suggested that the cement was originally high-magnesian calcite, however, this must be considered as dubious since it is based on direct analogy with the cement in modern hardgrounds, which morphologically, petrologically, mineralogically and geographically bear very little resemblance to Chalk hardgrounds. Scholle and Kennedy (1974) have produced carbon and oxygen isotopic

evidence that the cement is derived directly from sea-water, although the present author has found that this is not generally the case (see chapter 8). Perhaps the most extensive discussion of hardground formation is that of Jeans (1980), who envisages that lithification of the sediment took place by the precipitation of ferroan calcite, caused by bacterial ammonification and sulphate reduction. This interpretation is rather more compatible with our current knowledge of early diagenesis (see chapter 2) and implies localised areas of sulphate reduction between the oxidising environments of the Thalassinoides burrows. The Jean's model is discussed in more detail in the light of isotopic data in Chapter 8.

3.5 LAMINATED BEDS

One particularly interesting fabric in Chalk sediments is the development of thin undulating laminated beds well described by Mortimore (1979).

Laminations occur on the 1-2 mm scale in 5-10 cm thick undulating beds, usually with sharp upper and lower boundaries. Such beds can usually be traced over tens to hundreds of metres but in rare cases may be continuous over more than a kilometre. Typically, they are associated with coarser (~0.5 mm) bioclastic material but it is unclear to what extent this is due to the laminations being visible only in such sediment.

In England, laminated beds are most common in the Northern Province where they may be pervasive throughout the entire section of some localities (e.g. pl. 28). This has been attributed by Hancock (1975) to a weathering effect associated with the hardness of the chalks, but is considered by the present author to represent true sedimentary differences, indicative of higher intensity bottom currents in the Northern Basin.

In the Southern Province, laminated beds are rarer, more stratigraphically confined, and often include brecciated flints and shattered hardened chalk nodules. These are interpreted by Mortimore (1979) as "soft" sediment deformation features associated with inter- and intra- bed sliding under confining pressures associated with shallow to medium burial conditions, although some may represent true sedimentary features ("quasi-turbidites" of Mortimore, 1979). According to Mortimore (pers.com.), the crude stratigraphic control on laminated bed development reflects seismically active periods and consequently they show a close association with sub-horizontal "sheet flints" (sec. 3.6.5).

3.6 FLINTS

Although vast quantities of literature exist on possible origins of flint, systematic studies of variation in flint morphology have been rather limited.

The range of flint morphologies is almost as great as the list of suggested origins but a few general patterns are visible. The detailed classifications are to a large extent subjective, but on the evidence of field relations, most flints in flint bands can be considered to be morphological intermediates between three end members: burrow-form flints ; tabular flints; and paramoudra/ring flints. In addition, isolated flints may form around localised fossil remains (especially sponges) or in fractures in the chalk ("sponge flints" and "sheet flints" respectively). "Carious" flints and "incipient" flints represent morphological modifications to any of the above forms.

Plate 1

- A. *Typical nodular flint series. Maastrichtian Lanaye Chalk, Maastricht. Arrows pick out a gap in the otherwise regular bands of flint, now occupied by a thin ?diagenetic marl seam.*
- B. *Typical tabular flint series. The "Triple Tabulars" of the Burnham Chalk Formation of northern England.*
- C. *Detail of a thalassinoidean-form semi tabular flint. 1st flint below Eppleworth flint band (Burnham Chalk Formation), Eppleworth Quarry, Yorkshire.*
- D. *Detail of the lower surface of the middle Triple Tabular. Note the relic traces of bioturbation reflected in bulbous nature of the flint's lower surface.*
- E. *Typical small paramoudra in the Maastrichtian Lanaye Chalk, ENCI quarry, Maastricht.*

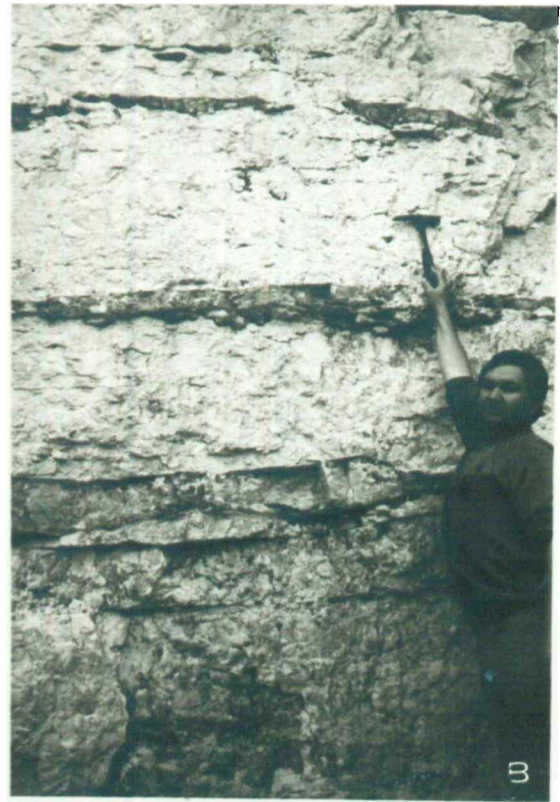


Plate 1

Plate 2

- A. *Traces of bedding picked out on weathered surface of a giant nodular flint band. The Romontbos Flints, Maastrichtian, Schiepersberg Quarry, Cadier en Keer, Maastricht.*
- B. *Association of tabular flints with well bedded chalks in the Burnham Chalk Formation of Lincolnshire.*
- C. *Nodular flints occupying lower part of burrows beneath a nodular bed in the Lewes Chalk Member, Beachy Head, Sussex.*
- D. *Another view of the unit seen in C, but with chalk-marl contrast picked out using a yellow filter. Note how the flints are confined to the marly chalk between the white chalk nodules.*
- E. *Slender burrow-form flint (Thalassinoides) occupying a burrow in a Lower Maastrichtian hardground. Halembaye quarry, N. Belgium.*
- F. *Detail from D.*

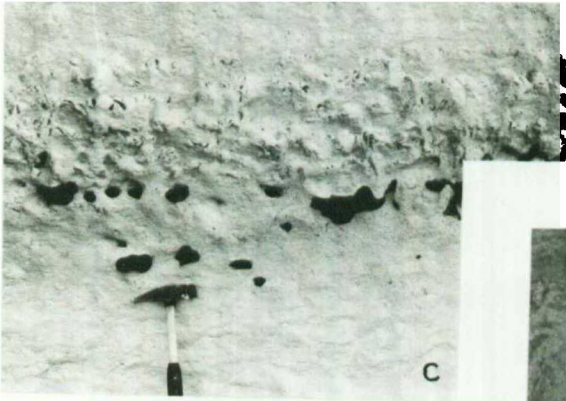


Plate 2

3.6.1 The Burrow-form - Nodular - Tabular Association

By far the most common forms of flint bands are morphologically intermediate between slender, digitate burrow-form flints and smooth sided horizontal tabular flints.

These are usually confined to fairly evenly spaced discrete bands although true burrow-form flints tend to have a more scattered character. The primary control on morphology in this group appears to have been the homogeneity of the original sediment, and in particular the compaction induced porosity contrast between burrow-sites and the enclosing sediment.

Burrow-form flints are siliceous replacements of bioturbation structures in the original sediment. Crustacean burrows of the ichnogenus Thalassinoides are by far the most important, but Zoophycos flints also occur, and more rarely Chondrites and Planolites may be found. In some cases, the burrow may be intricately preserved with fine detail of spreite and multiple reworking of burrow walls clearly visible (pl. 3B, C and G), but at other times, the flint has overgrown the burrow and replaced the adjacent chalk also.

Thalassinoides flints are particularly well developed below omission surfaces and hardgrounds where they may extend down 4-5 metres below the surface. Below hardgrounds, silicification is unable to extend into the hardened chalk but entirely replaces the burrow-fill (pl. 2E). Where the porosity contrast between burrow and matrix was not so great, silicification has extended beyond the burrow walls, although it is common to find the original burrow wall preserved inside the flint as a thin chalky zone of "chalk-meal" (pl. 3F) or even the burrow left entirely hollow (termed

Plate 3

Burrow Form Flints

- A. Slender thassinoides flint excavated from the hardground shown in plate 2E. The flint replaced the soft chalk infilling of the burrow after the hardground became buried.
- B. Part of the central vertical tube and uppermost whirl of a Zoophycos burrow preserved in flint. Englebel Quarry, northern Belgium.
- C. Plan view of a flat Zoophycos burrow. Note the delicately preserved spreite.
- D. Vertical "Thalassinoides" burrow reworked by Zoophycos. Maastrichtian Vijlen Chalk, N. Belgium.
- E. Unusual flint specimen from southern England which apparently represents the preferential preservation of the hard parts of an organism while the organism as a whole has perished. M.L. Coleman (pers.com.) has suggested that specimens such as this may have given rise to the term "Cockoliths" for the constituents of the Chalk. Specimen donated by I. Higginbottom.
- F. Typical burrow form flints from the Lewes Flint Series. Note the preservation of the original burrow wall as a chalky anulus within the flint. Bridgewick quarry, Sussex.
- G. Trace of ?Zoophycos in flint pebble from Nerlu quarry, nr. Peronne, France.

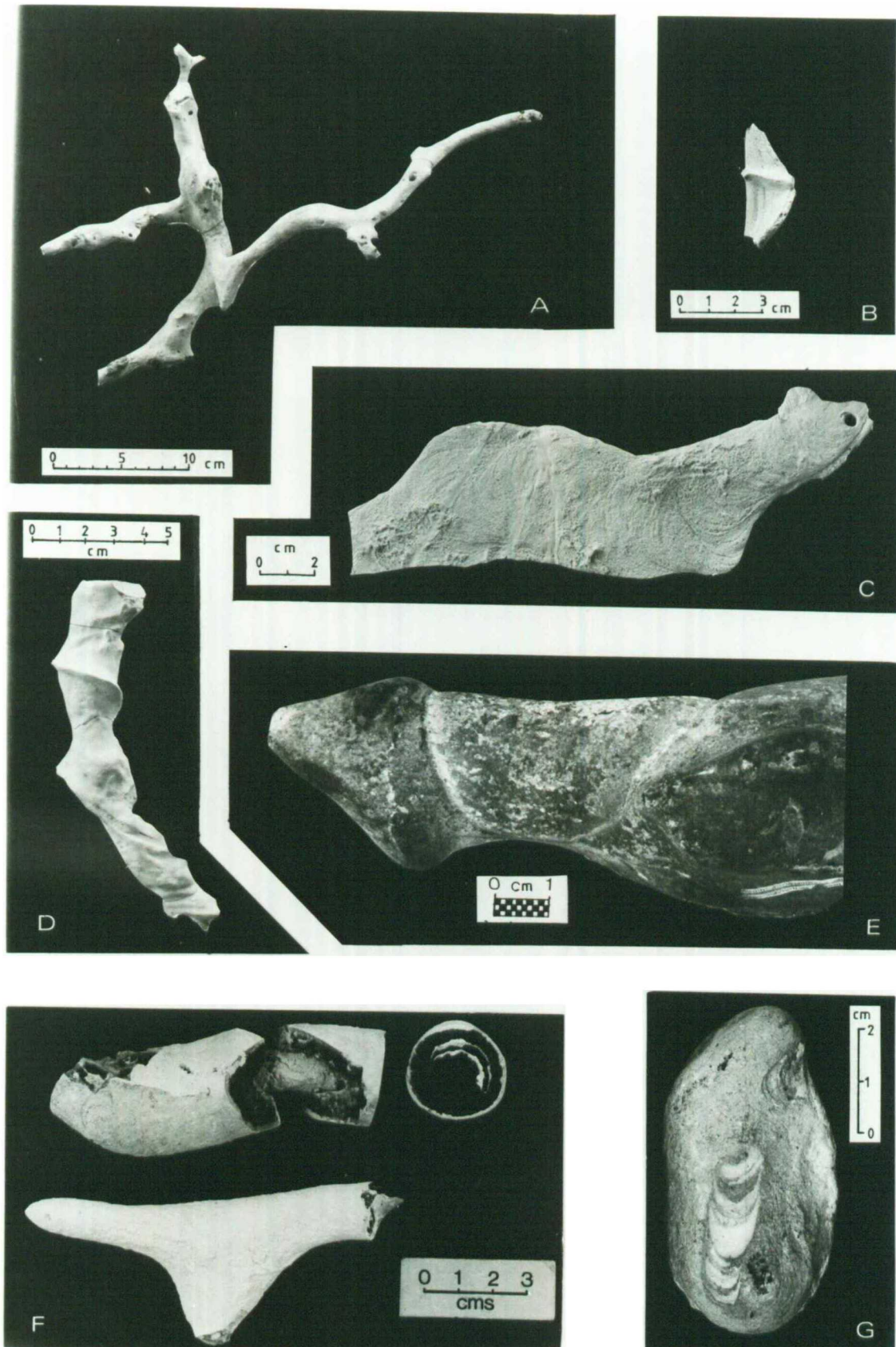


Plate 3

"tubular flints"). At other times, the burrow is so completely overgrown as to be hardly recognisable as such, and these grade into the better known nodular and semi-tabular flints. Where bioturbation is absent or very poorly developed, the nodular structure tends to break down altogether and tabular flints form, such as in the well bedded chalks of the Northern Province. However, even in tabular flints slight traces of bioturbation often produce a bulbous character to the bottom of the flint (pl. 1D) and in some cases (such as the Eppleworth Flint of northern England) the flint may locally jump level within a particular bed in response to the presence of Thalassinoides chamber systems.

Although the distribution of burrows is a major influence on flint morphology it is clear that the genesis of the flints is not dependent on the presence of the burrows themselves. Rather, the porosity, or more correctly the permeability, contrast between burrows and their host must serve to restrict the passage or the mixing zone of externally derived silicification solutions. This is further reflected in the position of silicification within the burrow networks. Sometimes, (e.g. in the uppermost Lanaye flint in the Maastrichtian - fig. 3.5) the flints form low in the burrow system but in other cases (e.g. below the St. Pieter Horizon just above), flints form in the top of the burrows and pass into incipient flints (see below) lower down. In some cases, the position within the burrow system even varies along the outcrop.

The effect of this permeability control on flint morphology is also apparent where silicification has occurred in distinctly bedded chalks. In these cases, curious shapes may be produced by the partial confinement of flints to one or two beds (e.g. pl. 1C and fig. 3.10) or a banded morphology may develop in larger specimens

Plate 4

- A. *Combined tabular/paramoudra flint, Welton Chalk Formation, Lincolnshire. Actual size about 34A.*
- B. *Completely silicified paramoudra. Note the higher concentration of silica immediately adjacent to the central burrow. Burrow itself is not visible in this picture but is picked out by pyrite and glauconite in the specimen itself.*
- C. *Chondrites burrows preserved in a sponge flint from West Clandon Pit Surrey.*
- D. *First generation burrow-form flint overgrown by a second generation tabular flint. Brandon flint Series, Brandon, Norfolk.*
- E. *Chalk breccia preserved if a tabular flint, just above Ravendale flint, West Ravendale Quarry, Lincolnshire.*

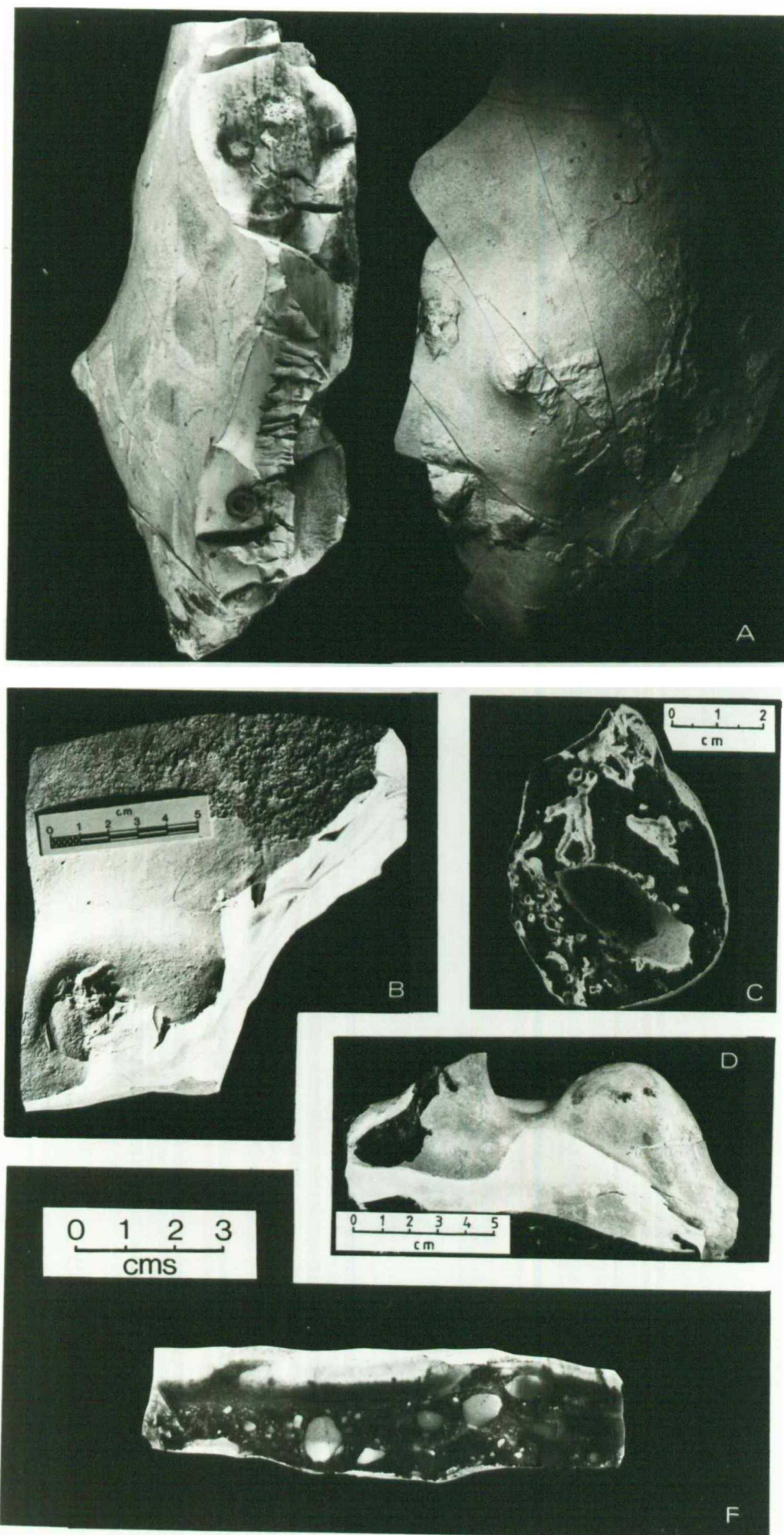


Plate 4

(pl. 5A and B). Laminations within beds are often visible in flints as either lines of recrystallisation structures ("white bodies" - see chapter 4 and pl. 9), or thin lines of localised pyrite micro-nodules picking out particularly organic-rich laminations.

Because flint morphology depends so strongly on sediment type, the morphology of individual flint bands may vary laterally if the sedimentology of the host sediment changes. This is well exemplified by the variation in flint morphology in the English Turonian (fig. 3.7). In Sussex, the Southerham and Bridgewick flints are typically nodular. When traced into the main part of the Northern Province, in Lincolnshire and Yorkshire, the flints at this level are generally well developed tabular forms (approximately the level of the Triple Tabular Flints, fig. 3.4: C.J. Wood and R.N. Mortimore, pers. com.). However, towards the southern margin of the Northern Province, in Norfolk, the flints are of identical morphology to those of the Southern Province, reflecting the bioturbated nature of the sediment here. A little later, towards the end of the Turonian regression (fig. 3.2), sedimentation in Sussex became more sporadic resulting in better developed omission surfaces and the formation of burrow-form flints in the Hitch Wood Hardground over the London Platform (see Bromley and Gale, 1982) and pass into a series of carious flints in Lincolnshire. As explained below (see 3.6.4), the carious nature probably reflects the presence of abundant organic rich Chondrites burrows, although the significance of this is unclear at present.

The association of burrow-form flints with omission surfaces means that these may be important markers of erosion surfaces. This is quite common on the small scale where burrow-form flints may form below erosion channels in the chalk (e.g. fig. 3.9) but

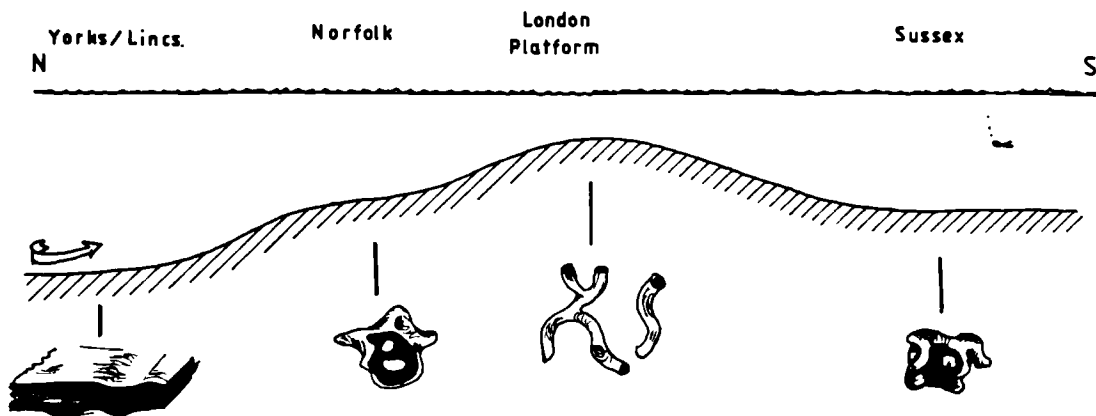
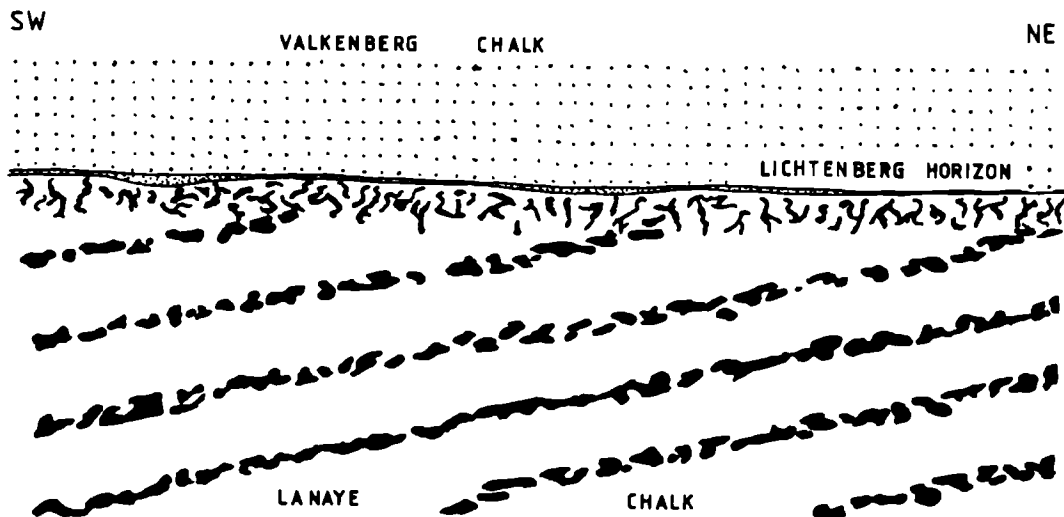


Figure 3.7 Relationship of flint morphology to depositional setting during the Turonian

Figure 3.8 Lanaye Chalk - Valkenberg Chalk relationships in the Maastrichtian type area. See text for discussion.



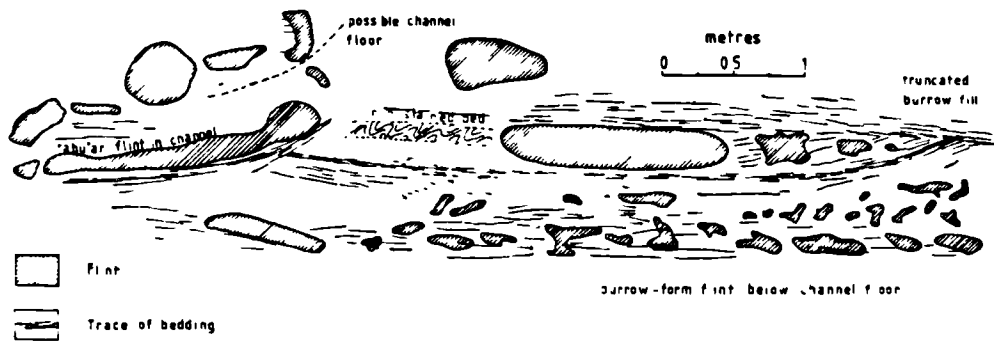


Figure 3.9 Association of flints with channelling in the Schiepersberg horizon (Maastrichtian), Nekami quarry, Maastricht.

Figure 3.10 (below left) Variation in form of the Romontbos Flints in the Maastrichtian type area.

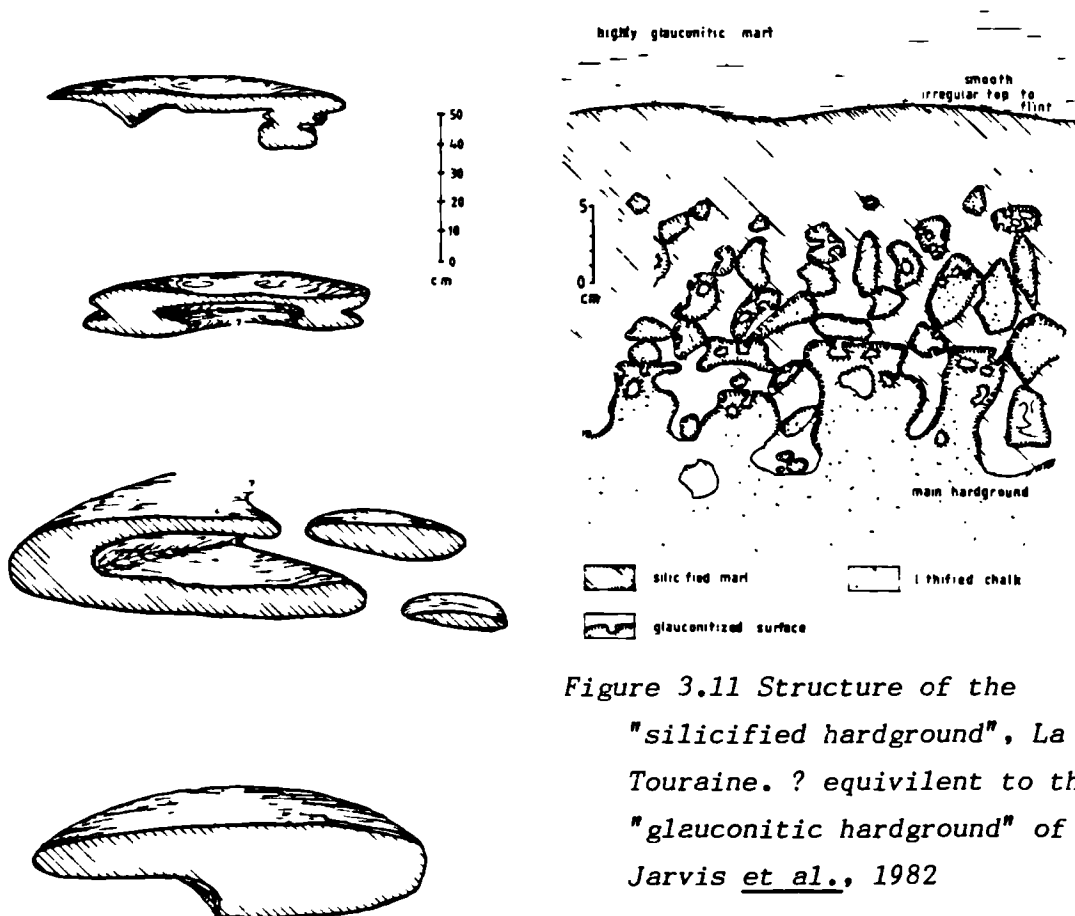


Figure 3.11 Structure of the "silicified hardground", La Paterne, Touraine. ? equivalent to the "glauconitic hardground" of Jarvis *et al.*, 1982

is more dramatically seen where large scale regional erosion surfaces are developed such as below the Lichtenberg Horizon in the Maastrichtian of southern Holland (fig. 3.8). At ENCI quarry, south of Maastricht, the Lanaye Chalk contains 19 flint bands, all nodular or semi-tabular other than the top one which is a Thalassinoides flint, related to the overlying Lichtenberg Horizon. However, a few km to the south-west, on the banks of the Albert Canal, 23 flint bands are present, again with only the top one of burrow-form type, and in East Limbourg the Lichtenberg Horizon cuts down further into the Lanaye Chalk, still with its associated burrow-form flint.

Where silicification occurs in conjunction with hardgrounds, it clearly post dates lithification, and flints occur in the burrows, or more rarely, as tabular flint on top of the hardground, replacing only the unlithified chalk here (fig. 3.11). There is, however, evidence that flint genesis was itself an early diagenetic, pre-compaction event. Vertical slickensides can sometimes be found in chalk adjacent to flints and sometimes sheared "compaction cones" occur on top of them. Marls may occasionally be compacted around the more solid flint and in rare cases a marl may even expand when it passes into a flint. It is also possible to find rare moulds of aragonitic fauna in flint, and the common occurrence of pyrite coated fractures in specific flint bands probably suggests an origin above the zone of sulphate reduction.

Conversely, there are very few reported cases of flints which show any evidence of reworking within the Cretaceous (e.g. encrusting or boring fauna, glauconite coatings, chink-marks etc). Voigt (1979) has reported rare reworked Maastrichtian flints (? from the Lanaye Chalk, see above) and D. Ward (In Mortimore, 1979) has found a similar

specimen at Downend (see Gale, 1980, for description of synsedimentary erosion here), but these are isolated occurrences and even where major channeling occurs, reworked flints are absent. This has been interpreted as evidence that although the sites of flint formation were determined early, the flints themselves are a product of late diagenesis, (Håkansson et al., 1974; Bromley et al., 1975). An alternative, not discussed by these authors is that the flints were present (see evidence for pre-compaction origin above) but were in a form in which the silica was easily disaggregated on reworking. Importantly, English flints at least, had obviously hardened before the Paleocene when they were reworked into the Bull-head Bed at the base of the Thanet Beds of Kent.

3.6.2 Ring Flints and Paramoudras

Formation of flints of the burrow-form - nodular - tabular series involves diffusion and/or mixing of solution within the sediment, concentrated around the higher permeability chalks associated with bioturbation structures. Conversely ring flints and paramoudras occur as a direct consequence of reactions occurring because of the presence of the burrow. Thus, in this group, the burrow actually causes silicification but in the above it only modifies the form of the flint, which would still form in the absence of the burrow. All intermediates exist between these flints and the burrow form - tabular series and the morphology of any flint can therefore be represented on a triangular composition diagram as in fig. 3.12.

Paramoudras have been described in great detail by Bromley et al., (1975) so only a few relevant aspects are discussed here. Paramoudras

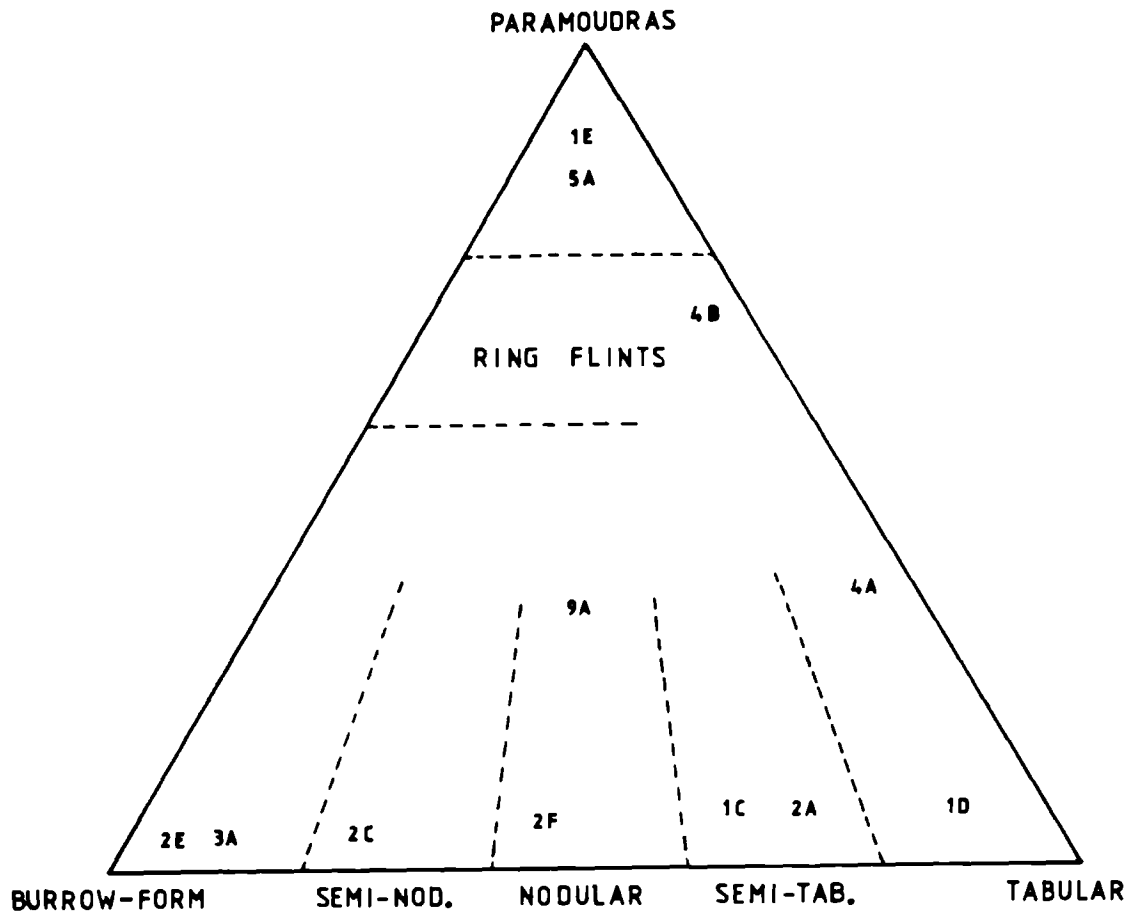


Figure 3.12 Schematic representation of the variation in flint morphology with respect to the three end members. Labels refer to plate numbers which represent the various types. Absence of types intermediate between burrow form and paramoudra is probably due to non-recognition rather than non-existence.

Plate 5

- A. *Three views of a short paramoudra showing the central burrow and the lithified chalk core. Reproduced from Bromley et al., (1975).*
- B. *Large, complex paramoudra in Coniacian chalk of Ashby Hill Quarry. This specimen was incorrectly figured reversed by Hancock (1975) as an example of cross-bedding but the inclined bedding is in fact the result of a fracture at the base of the upper half of the paramoudra.*
- C. *Carious tabular flint. Between Wooten Marls and Ulceby Marl, Burnham Chalk Formation, Church Top Farm, Elkington.*
- D. *Secondary banding in a Maastrichtian flint from the Lanaye Chalk of ENCI Quarry, Maastricht. Bands are due to cortication, apparently associated with the infiltration of fresh water into the flint structure.*
- E. *Detailed view of a carious flint associated with the specimen shown in pl. 5C. Note how the chalky silica is convex into the black flint (the opposite to "incipient flints").*



Plate 5

are large barrel or pear shaped flints characterised by a central pyritised and/or glauconitised burrow, surrounded by a lithified chalk core, within the flint (pl. 5A). These may be 1-2 m in diameter and several metres in height, either in a continuous column or as a superimposed series of short paramoudras or "potstones". The origin of paramoudras appears to be related to reactions occurring in the central burrow (Bathichnus paramoudrae Bromley, Schultz and Peake (1975)) and the outward diffusion of products from these reactions have caused pyritisation and glauconitisation, calcite cementation, and silicification, at successive sites away from the burrow. At other times, the chalk core may be fragmentary or absent although the relationship of silicification to burrow is still apparent. In these cases preferential silicification also occurs immediately adjacent to the burrow, as well as in the usual annulus at a distance from it (see pl. 4B).

Where paramoudras meet normal flint bands, the flints generally die out adjacent to the paramoudra, although the paramoudra itself is often better developed at these levels. Conversely, the paramoudra will often combine with the lowest flint band it meets, and in small examples this gives the appearance of vertical flint columns rising from flint bands, cutting through, but not touching higher flint bands (e.g. Bedwell's Columnar Band in Kent, Lanaye flint 8 of Maastrichtian shown in pl. 1E). This suggests that paramoudras form above the level of normal flints (fig. 3.13a) and this is confirmed by the complex shape of the paramoudra in pl. 5B which has apparently continued to grow in its' upper part, but not the lower part, when the horizontal silicification zone of normal flints shifted from the lower to the upper position (see fig. 3.13b). The vertical superimposition of multiple small paramoudras suggests

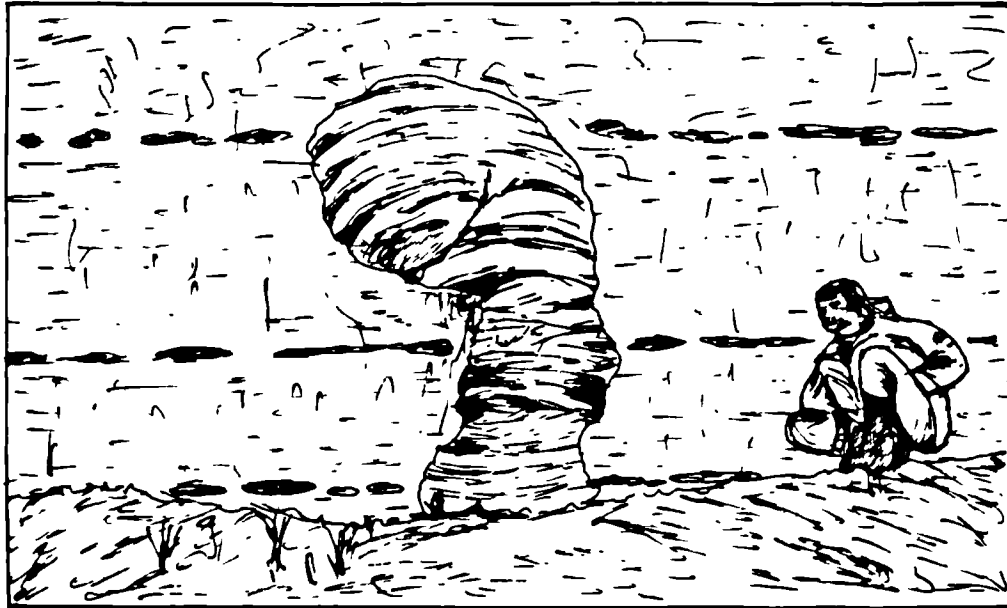
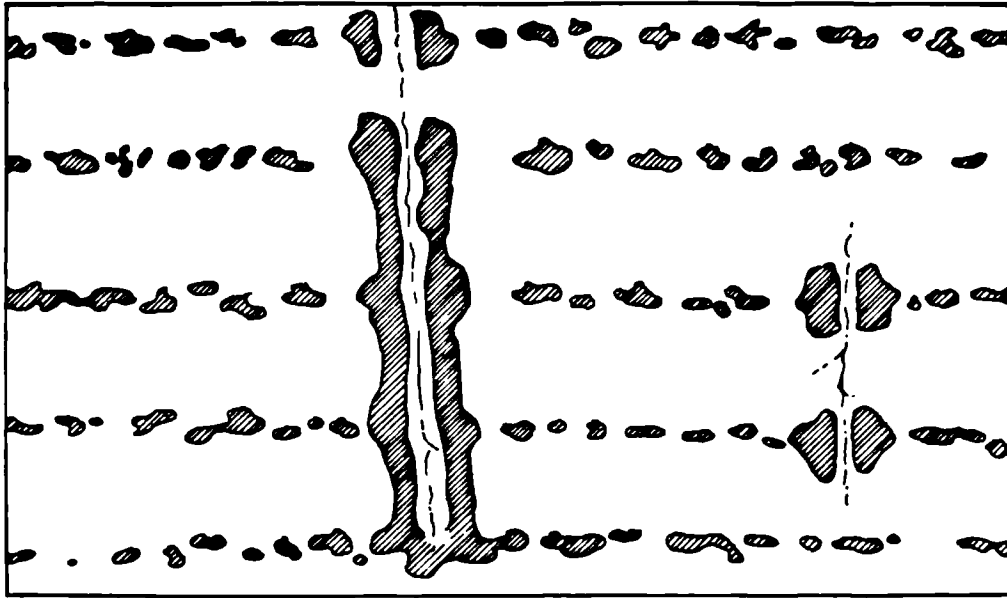


Figure 3.13 a) Top. Usual relationship of paramoudras to bedded flints. Note how paramoudra passes through higher flint bands but combines with basal flint band. b). Unusual paramoudra which apparently was "rejuvenated" part way through growth, resulting in a massive top part but slender lower column. Ashby Hill Quarry, Lincolnshire.

that the Bathichnus burrow was still an important cause but could only initiate silicification where the process was augmented by normal diffusive/mixing silicification reactions. In this respect, it is important to note that the burrow can often still be traced between the potstones, picked out by hardened chalk, without the surrounding flint.

Ring flints or "flint rings" are essentially similar to flat paramoudras, lying in the plane of normal flint bands. Typically, a single ring may be 1-5 metres in diameter and consists of a circle of irregular nodules, frequently linked (Peake and Hancock, 1970). Within the ring the chalk may be locally lithified and in cases, a central burrow can be found. Sometimes 2 or more rings may be concentric, or may have a paramoudra at the centre. This is presumably some form of Liesegang phenomenon suggesting that the diffusion of products away from a central burrow was an important process. It is likely than many apparently "normal" flint bands include a flint ring component but this is not obvious unless the flint is seen in plan.

Ring flints and paramoudras show a broad stratigraphic confinement in different areas, concentrating particularly in Campanian and Maastrichtian deposits. Presumably, this distribution is related to the presence of the right type of burrow (i.e. Bathichnus). The origin of the burrow is not yet known (see discussion in Bromley et al., 1975), but Nygaard (1982) has observed that Bathichnus burrows usually cut across the sheared remains of other burrows, and has suggested that the structure is an escape feature made by some animal adapted to living in unstable substrates. Indeed, the concentration of paramoudras and solid flint cylinders in the Coniacian of the Normandy coast does coincide with chalks which contain other evidence of lateral displacement (see section 3.6.5,

below) and the Maastrichtian of Denmark and nearby regions was clearly an unstable sedimentary environment at the time paramoudras formed here. However, the palaeoichnology of paramoudras is not well known at present, and the possibility of more than one type of burrow, and cause, cannot be ruled out.

3.6.3 Sponge Flints and Flint Replaced Fossils

Scattered more or less randomly amongst flint bands, and unrelated to them, are isolated spherical or sub-spherical flint nodules which usually enclose fossil sponges (see pl. 6C and E). Similar forms include replacements of many other groups of fossils (e.g. bryozoans, pl. 6B and some isolated burrows) and particularly echinoderms (pl. 6A and D). It is important to note the distinction between this type of replacement (i.e. by flint in its strict structural sense - see next chapter) and simple silicified fossils, which may form by a completely different process. Flint replaced specimens are typically enclosed in, or infilled with flint and if any silicification of the shell material is present it clearly initiates at the edge of the grain, implying silicification by a solution originating outside the skeletal calcite. Isolated silicified fossils, however, are replaced from the inside outwards by solutions generated within the skeleton (Holdaway and Clayton, 1982).

Where these flints coincide with normal flint bands they are enclosed within it, similar in nature to burrow-form flints in nodules (see above), indicating that they form nearer to the sediment surface. Presumably, such flints are analogous in origin to paramoudras and form around localised sites of organic matter concentration, above the level of more widespread silicification.

Plate 6

Fossils in Flint

- A. *Sediment infilled echinoids in Maastrichtian flint from Denmark. Note the (sideways on) geopetal filling in the central test, overlain by a layer of drusy quartz.*
- B. *Silicified bryozoans from the Maastrichtian of Stevns Klint, Denmark. The flint has replaced chalk infillings along the axes of the fossils and spread out to replace the wall.*
- C. *Sponges preserved in flint. Note how the sponge structure is preserved in fine detail in the upper specimens.*
- D. *Echinoid partially infilled with flint. West Clandon Pit. Test was crushed after flint formed.*
- E. *Banded flints. The Upper specimen appears to be controlled by a burrow but the lower specimen has formed around a sponge.*
- F. *Banding resulting from the cortication process. Loose specimen from beach under Beachy Head, Sussex.*

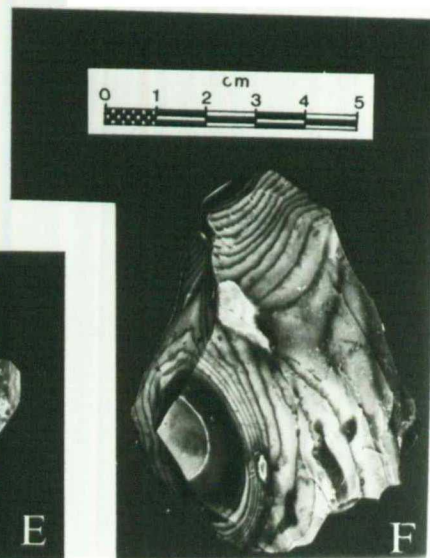
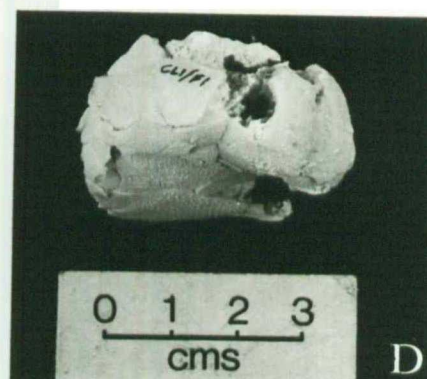
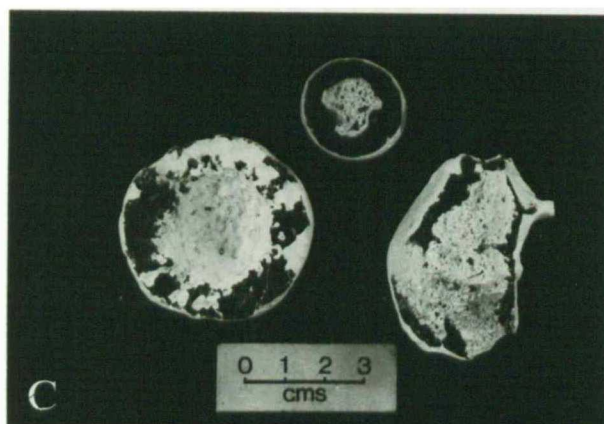


Plate 6

3.6.4 Carious Flints and Incipient Flints

Carious flints (= "chalky" or "rotten" flints) consist largely of a ramifying network of friable white silicified chalk within the normal black flint (pl. 5C). Carious nature is most characteristically developed in tabular flints but carious nodules and even carious paramoudras also occur. Such flints may be easily correlated across large distances and may be characteristic of specific stratigraphic intervals (e.g. the flints in lower half of the beds between the Wootton Marls and the Ulceby Marl of northern England: Wood and Smith, 1978; fig. 3.4 of this study), although isolated carious bands may occur within otherwise normal flint bands (e.g. at Clandon Pit, fig. 7.1).

In some cases the carious nature apparently represents sponge skeletons but more often the structure is obviously formed around burrow systems, especially Chondrites (e.g. pl. 4C). In detail, the boundary of the chalk and flint is scalloped inwards towards the black flint, concentrating around the burrows (pl. 5E). Clearly, either the flint is being corroded by solutions flowing through the burrows, or some chemical agent originating within the burrows has inhibited silicification here. Petrographically, the silicified chalk is the same as the white "crust" found around normal flints (see chapter 4) which forms where the specific chemical environment necessary for normal flint formation does not reach sufficient intensity. This suggests an inhibition effect to silicification associated with the burrows. In view of the connection with both burrows and sponges, some reaction connected with the presence of organic matter concentrations appears likely (e.g. the preservation of burrow walls as chalk-meal within burrow-form flints described above).

Similar to carious flints are incipient flints which also consist of poorly silicified chalk with enclosed areas of black flint. All intermediates exist between friable white, slightly siliceous chalks and solid black flints with only relic patches of crustose material, but unlike carious flints, the black material is scalloped into the white. In some cases, such as the Maastrichtian Gronsvelt Chalk (fig. 3.5) there is an increase in the normal flint content of nodules as the sequence is ascended, related to a decrease in the grain-size of the host chalk.

Compositionally, the silicified chalk of incipient flints is the same as the white "crust" of normal flints and the ramifying white silicified chalk in carious flints suggesting that incipient flints represent silicification in an environment not fully conducive to normal flint formation. However, in contrast to carious flints, this represents non-attainment of the correct chemical environment, rather than local inhibition.

3.6.5 Sheet Flints

In some areas, either cross cutting the normal stratigraphy of the Chalk at a high angle, or sometimes parallel to it, are thin tabular flints, apparently occupying joints (pl. 7E). These are here termed "sheet flints" to avoid confusion with normal tabular flints. Since the early days of Chalk research these have usually been regarded as of late, and usually Tertiary, origin because of the cross-cutting relationship with normal flint bands, and this idea has been perpetuated by most modern workers. There is, however, much evidence that these flints formed at about the same time as the other flints.

Plate 7

Field Relations of Sheet Flints

- A. Sheet flint which has undergone secondary fracturing as a result of re-juvenation of the fracture surface. Seaford Head.
- B. Confluence of sheet flint and nodular flint. Note how the two join perfectly with no trace of the edge of the fracture. This indicates that the two grew more or less simultaneously.
- C. Hand specimen to show a combined nodule and sheet flint. The arrows pick out the trace of the fracture which caused silicification. Again there is no trace of a join between the two flint types.
- D. Swarm of oblique sheet flints in Coniacian section east of Dieppe, France. Swarms of sheet flints such as this commonly formed on the flanks of palaeohighs as a consequence of shallow burial inter- and intra-bed sliding downslope.
- E. Sheet flint which has been offset by a sub-horizontal shear (unsilicified). Seaford Head, Sussex.
- F. Once vertical thalassinoidean burrow-form flint which has been sheared by two horizontal fractures. The fractures themselves are now occupied by thin sheet flints (barely visible between the hammer and the burrow), and these preserve traces of Zoophycos on their surfaces. Top Campanian, Englebel quarry, Northern Belgium.

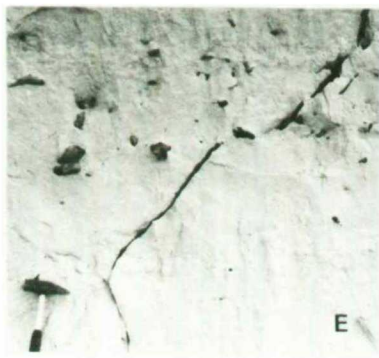
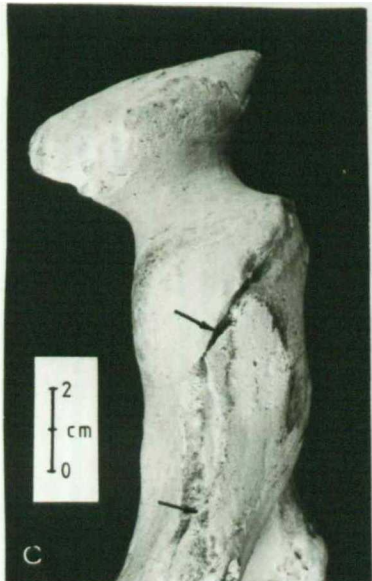
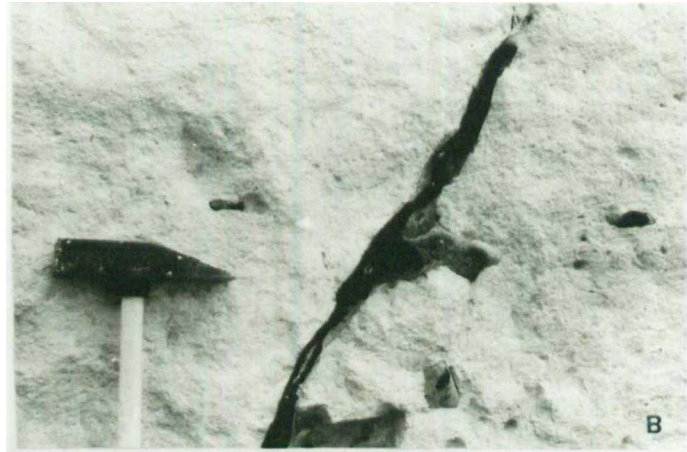
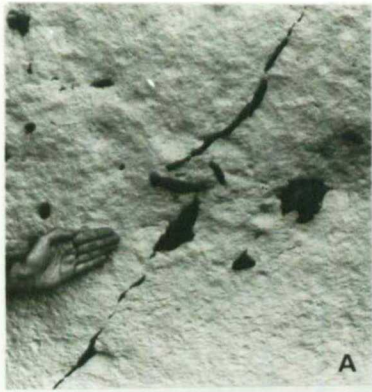


Plate 7

First, the assumption that the flint is infilling a fracture is untrue. Rather, the flint has replaced the wall rock to the fracture, the fracture itself usually remains unreplaced as a chalky crack running through the centre of the flint. Second, in detail (see next chapter) sheet flints are of identical micro-structure to normal flints, which are clearly of replacement origin (see chapter 4) and, furthermore, combine with them when they meet. Even on the microscopic scale, the boundary between the two is not visible, although the central chalk fissure of the sheet flint may be continuous through the object (pl. 7B and C). This would imply that both flints were in existence at the time of the opal -CT - quartz recrystallisation, and this is confirmed by the comparable oxygen isotope composition of the two (see chapter 5). The timing of this is not well known but by analogy with other cherts in pure carbonates, it was probably in the order of 5-10 m.y. after formation, well before the Tertiary for most of the southern England flints.

A further point of interest is that the flints do not occupy all joints: they are confined to early stage compaction joints, associated with shallow burial and lateral sediment movement. As such, the flints tend to occupy conjugate joint sets, and sub-horizontal fractures, and show a broad stratigraphic confinement to levels which are also characterised by laminated beds and, frequently, paraconformity development ("seismically active periods" of Mortimore, 1979). Additional subsequent movements often also result in fracturing of the sheet flints (pl. 7A), and these brecciated flints may sometimes be strung out along laminated beds.

Interestingly, flints in conjugate joint sets tend to occupy only one set of the joints available (i.e. all dip the same way: pl. 7D). This reflects some form of lateral movement associated with the

jointing, resulting in one joint set being more open than the other. Where this occurs the sense of movement is always away from contemporary structural highs (sensu Mortimore, 1983). A recent exposure at Seaford Head, Sussex, even showed a prominent horizontal sheet flint with high angle sheet flints occupying secondary splay faults associated with it. In other cases, rejuvenated movement may extend the fracture upwards (due to the original fracture being a plane of weakness) and this also may subsequently be the site of silicification. In this way, individual sheet flints may be in excess of fifteen metres long, although any single part of the flint probably formed only five to ten metres below the surface.

Where extensive lateral movement has occurred, such as in the Vijlen Chalk of north Belgium (fig. 3.5) small scale sheet flints commonly form along horizontal Zoophycos burrows, presumably because these represent planes of weakness. At times these may have also sheared vertical burrow-form flints (pl. 7F), indicating the sense of movement, and thus, contemporary topography.

As explained above, flint formation probably involves a degree of flow and/or mixing of some form within the sediment, and this is controlled by permeability irregularities in the sediment. It is not surprising therefore that penecontemporaneous fractures in the chalk sediment also acted as pathways for such flow, again resulting in silicification of the adjacent chalk (in this case, the walls of the fracture). Indeed, sediment pore-water overpressuring probably played an important part in the generation of these fractures (Jones, Bedford and Clayton, Unpublished data) so pore-water flow within these fractures would be inevitable.

3.6.6 Summary of Flint Field Relations

From the above discussion, a number of general points are

obvious. Flint bands formed parallel to the contemporaneous sea floor as a result of early diagenetic reactions, sometimes associated with organic matter decay, but were probably not able to survive reworking until deeper burial. In many cases, however, they must have been rigid enough to resist compaction very soon after they formed as the chalk is often sheared around them.

Morphologically, most bedded flints are intermediates in a continuous series ranging from slender branched thalassinoidean flints, through semi-nodular, nodular, and semi-tabular flints, to solid tabular flints. In these forms, the morphology is controlled by bioturbation induced permeability variations in the chalk which have modified the flow and/or mixing patterns of externally derived solutions. A third end member in the series is represented by ring flints and paramoudras. These form as a consequence of the outward diffusion of chemical species originating from within the burrows themselves, probably reacting with an externally derived chemical species sometimes causing silicification in the form of Liesegang bands. All morphologies of flint in flint bands can be explained by a mixture of these three end members and their form can be represented on a triangular compositional diagram (fig. 3.12). Other flints form around localised concentrations of organic matter, above the level of normal flint bands, or by pore-water mixing processes in early stage compaction joints. Sometimes, however, concentrations of organic matter appear to have locally inhibited silicification and a carious flint forms.

Such variations in flint morphology closely reflect the sedimentary environment of the original sediment and study of flint morphology may therefore be of considerable use in sedimentological investigations.

3.7 PYRITE AND RELATED MINERALS

Iron sulphides in the Chalk occur in two forms: concretions of either radiating acicular crystals or tabular "arrow-head" twins; or as microscopic grains, disseminated throughout the sediment.

The presence of disseminated sulphides in the Chalk has been largely overlooked because they are readily oxidised above the water table. If present in high concentrations, the oxidised iron species (limonite s.l.) may stain the chalk yellow or pale orange, but in the concentrations usually found in the Chalk (<1%) they are largely invisible. In fresh sections, however, such as boreholes, and more rarely in deep quarries, the sulphides remain unoxidised and may impart a pale bluish-grey colouration to the sediment. In some cases, the downward migrating oxidation front can be seen, cross cutting the stratigraphy with white chalk above and grey below. The slight discolouration often associated with hardgrounds, nodular beds and some burrows may also have a similar origin.

The morphology and mineralogy of this material is unknown at present but its rapid oxidation on exposure to aerobic conditions (<2 hours in some cases) may be an indication that iron monosulphides are the major phases present, rather than the more stable pyrite. In a preliminary XRD study of the unoxidised insoluble residue (dissolution in 2N acetic acid, buffered at pH 3.95) from Maastrichtian Lanays grey chalk, the author has identified pyrite and traces of marcasite, but any other sulphides which were present were below the detection limit of this method. It is also possible that any monosulphides became oxidised during the dissolution process used to separate the residue. By analogy with clay rich sediments, this material would be expected to be framboidal (c.f. Raisewell

and Plant, 1980; Pollastro, 1981; Hudson, 1982) but this has not been confirmed.

Larger masses of sulphides are fairly common throughout most of the Chalk. These were originally described as "marcasite" on the evidence of crystal morphology but X.R.D. usually reveals a pyrite lattice. Jeans (1973) has reported the presence of marcasite as well as pyrite but he gives no details of the morphology of the material analysed.

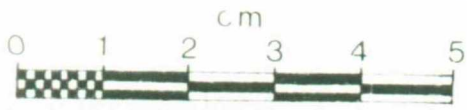
"Arrow-head" concretions consist of complex twins of tabular orthorhombic crystals, probably of true marcasite mineralogy. These are generally rare, but may be common locally, particularly in the Lower Chalk (e.g. at Folkestone, and across the Channel at Le Petit Blanc Nez).

Throughout most of the Chalk, however, iron sulphide concretions are smoother surfaced rounded (e.g. pl. 8D and F) or elongated in form. These also may show traces of apparently orthorhombic crystals on the surface, suggesting an original marcasite mineralogy, but Bannister (1932) has suggested that these are really cubic crystals, elongated along an axis perpendicular to the (111) plane. Internally, these form silvery gold radiating acicular crystals, (pl. 8D), frequently with a fine (<.2 mm) granular pyrite core, up to about 5 mm across.

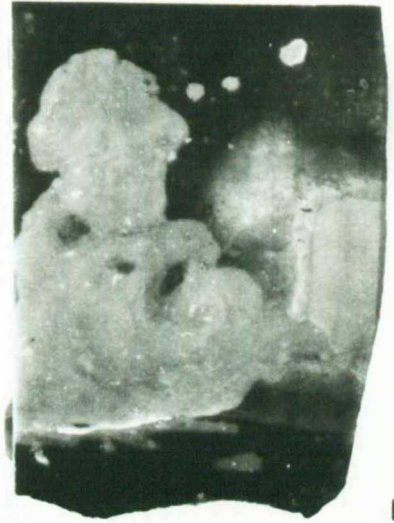
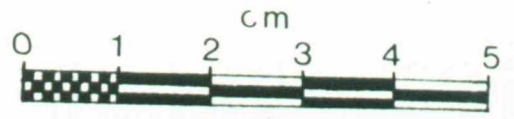
These pyrite concretions usually show a close relationship to the sites of early concentrations of organic matter such as burrows (especially Thalassinoides, Chondrites and the central Bathichnus burrow of paramoudras) and buried sponges (e.g. pl. 8C), although this association is not always visible in homogeneous white chalks. Isolated small nodules of sulphide may also occasionally be present within flint, often picking out local bedding laminations rich in organic matter (pl. 9C), but usually when large amounts of pyrite

Plate 8

- A. *Thin flake of Brandon flint showing the presence of numerous "black bodies", containing specks of organic matter. Light streak high on left is an opaque white body. Turonian, Brandon Norfolk.*
- B. *Flint CL2/7, West Clandon Pit, Surrey. Large well formed white body in centre was the main subject of stable isotope investigations described in chapter 5.*
- C. *Pyritised sponge. Cenomanian, Asham Cement Works, Sussex.*
- D. *Typical radial pyrite nodule. ?Santonian, Beachy Head, Sussex.*
- E. *Brecciated flint which has been re-cemented with pyrite. The fracturing is believed to be the result of high H_2S pressures in the sediment after the flint became solid.*
- F. *Curious tri-lobate pyrite nodule from the Santonian of Seaford Head, Sussex.*



A



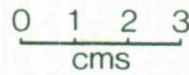
B



C



D



E



F



are found in association with flint the pyrite postdates silification and occupies voids and fractures within shattered flint (pl. 8E). Such pyritic flints may often be traceable over large areas and they make useful marker beds (e.g. Ferruginous Flint of Wood and Smith, 1978; Pyritic Fracture Flint of Jarvis, Gale and Clayton, 1982).

Nodular pyrite in the Chalk has been attributed by Jeans (1973, 1980) to late stage "non-intrinsic" diagenesis, related to a "downward movement of reducing conditions within the sulphate bearing pore-waters of the sediments" (?). This idea of a late origin was supported by Kennedy and Garrison (1975) who attributed it to "late stage remobilisation of sulphides and their re-deposition as pyrite (and rarely marcasite)". However, neither work discusses the possible mechanism(s) for these reactions. The close association with the original sites of organic matter, the concise stratigraphic confinement of pyritic flints and the occurrence of rare pyrite within flints (i.e. predating silicification) all suggest an early origin. Although a late origin for some of the pyrite cannot be conclusively ruled out, it is more likely that Chalk pyrite is fairly early diagenetic in origin, presumably related to bacterial sulphate reduction. The pyrite/flint relationship therefore suggests that flint formation occurred above the main zone of sulphate reduction although local high concentrations of organic matter above this level may have induced local sulphate reducing conditions prematurely, and predating silicification. The disseminated sulphide attests to widespread, but not necessarily intense, sulphate reduction in the sediment, and if the above hypothesis is true, such sulphide generation should post-date flint formation (see chapter 7).

The "sulphidisation" model of Jeans (above) is based on the irregular nature of the boundary of red ("limonitic") chalk with

overlying white-grey pyrite bearing chalk in the Red Chalk of the Lincolnshire/Yorkshire area (Jeans, 1973, 1980). In view of the above evidence, it is suggested here that this boundary is more likely to be the result of the upward migration of aerobic conditions (fed by oxygenated meteoric waters in the underlying, highly permeable, Carstone) rather than the "downward migration of reducing conditions" suggested by Jeans. Indeed, it may not be coincidence that the main, and only extensive, development of red chalks in Britain coincides exactly with the only place that the Chalk overlies a ferruginous sandstone. .

3.8 OTHER AUTHIGENIC MINERALS

3.8.1 Phosphates

Phosphates are widespread accessory minerals in the Chalk, occurring as skeletal remains (vertebrate teeth, fish scales etc.) and as authigenic and replacement phosphatic grains. These are not usually found in any significant concentrations but in some cases, phosphate may be a major component of the sediment. Mineralogically, these consist almost entirely of carbonate-fluorapatite but are usually referred to simply as "phosphate" or "collophane" in most publications.

Concentrations of phosphates in the Chalk are usually closely associated with hardground development, occurring most characteristically as lustrous brown coatings and crusts on hardground and intraclast surfaces. This is usually associated with a certain amount of replacement of adjacent lithified chalks. Reworked phosphatic lithoclasts and bioclasts often form a lag or phosphatic marl above hardgrounds. Different generations of phosphate are often visible as differing shades of brown, and by the phosphatisation of encrusting fauna and walls of borings, which has

post-dated a previous phosphatisation episode (Hancock, 1975; Jarvis, Bromley and Clayton, 1982). Several different morphological types of phosphate may be found in association in many places, with for example, shiny phosphate veneers on hardgrounds (considered by Jarvis (1980) to be "of potential algal origin") overlain locally by a finely laminated hard micritic phosphatic crust, and covered by a thick deposit of pelletal phosphate. Such an association is particularly common in Senonian (Coniacian-Campanian) of the Anglo-Paris Basin, where pelletal phosphatic chalks accumulated in small (1 km long) erosional cuvettes, floored by intensely phosphatised hardgrounds (Jarvis, 1980).

The primary source of dissolved phosphate in most sediments is the release of organic bound phosphorus during bacterial decay of organic matter (Krom and Berner, 1981, and references therein). Phosphates therefore form preferentially in regions of intense upwelling where the high nutrient concentrations brought up from depth can maintain a prolific biota, resulting in a high flux of organic matter to the sediment. In addition, an adequate supply of dissolved carbonate and sulphate are essential for phosphate formation. Within these constraints, phosphates can form in a number of chemical environments, such as by replacement of pre-existing carbonates near the sediment surface, within the sediment at the oxic-anoxic boundary (Benmore, pers. com.), or in anoxic muds (Bremner, 1980). The genesis of the phosphatic chalks of the Anglo-Paris Basin has been attributed by Jarvis (1980) predominantly to replacement of faecal pellets at, or near to, the sediment surface during periods of increased current activity and intense upwelling. In this case, it is associated with a marine regression but other mechanisms for different types of Chalk phosphates cannot be ruled out.

3.8.2 "Glauconite"

True mineral glauconite - a high iron potassium aluminosilicate of part dioctahedral and part trioctahedral mica structure - is not found in the Chalk. However, a range of green clay minerals probably of mixed layer illite/smectite structure, occur frequently and are commonly referred to as "glauconite" by most workers (see Jeans et al., 1982).

In this sense, glauconite occurs most commonly as a replacement or coating associated with omission surfaces and hardgrounds, although small rounded pelletal grains are also common and may locally make-up a high proportion of the sediment (e.g. Hibernian Greensand of Antrim, Craie de Villedieu of Touraine). Hancock (1975) has further pointed out that glauconite probably also occurs throughout normal white chalks but in concentrations too low to be detected by XRD.

Hardgrounds and associated intraclasts very commonly bear a very striking bright green crust of glauconite in addition to phosphate. In addition, Kennedy and Garrison (1975) have found textural evidence (for example replacement of foraminiferal tests and coccolith-rich matrix) that glauconite precipitation is associated with a concomitant dissolution of calcite and have pointed out that the most intense glauconitisation occurs at the sediment surface and dies out inwards. Jeans (1980), however, has reported Liesegang banding of glauconite, fading out away from the hardground top surface or walls of burrows and borings, and interprets this as an indication of the diffusion of iron from seawater into the sediment. In all cases, glauconitisation is a very early phenomenon and glauconitised surfaces and intraclasts are commonly encrusted and bored after the initial phase of

precipitation. Glauconite shows a close association with phosphates in the Chalk, an extensive period of glauconitisation predating phosphatisation in most cases (Kennedy and Garrison, 1975; Jarvis, Bromley and Clayton, 1982).

Granular glauconite commonly occurs in low concentrations in the coarse lag above hardgrounds but is particularly common around the margins of the Cretaceous Sea (e.g. Greensands of southern England and Antrim, Craie de Villedieu of south-west Paris Basin). Much of this material is clearly a replacement of faecal pellets (Kennedy and Garrison, 1975) but Jeans et al. (1982) have presented convincing evidence that the main component of some of these large scale accumulations are of volcanic derivation, forming as a replacement of lava particles, particularly of mafic composition.

The presence of both Fe^{2+} and Fe^{3+} in the glauconite lattice suggests that it forms under intermediate or fluctuating redox conditions (Berner, 1971). An Eh of approximately zero, and slightly alkaline conditions are generally now accepted as optimum (McRae, 1972). Glauconite will therefore tend to form around the oxic-anoxic boundary or under local reducing conditions within a generally oxidising environment.

A further complication is that glauconitisation is clearly a very slow process which is usually reflected in the requirements of an extended period of non-deposition at hardgrounds in order for glauconite to form (Kennedy and Garrison, 1975). However, this is probably a little misleading as the requirement is really only the maintenance of a stable state under the right Eh conditions. A break in sedimentation is of course an efficient mechanism for producing this, and allows glauconite to form between the oxidising environment of the burrow and the reducing conditions within the

sediment, but this is not necessarily the only situation where it can occur. The proximity of open sea water is important, however, as a source of potassium, but the source of dissolved aluminium is unknown at present.

4. PETROGRAPHY AND MICROSTRUCTURE OF FLINT

4.1 INTRODUCTION

Cretaceous flints are clearly closely related genetically to modern deep sea cherts, but the reasons for such segregation of silica are still unknown. Before this problem can be considered it is necessary to establish a petrographic grounding on which to base the chemical data. The deductions of Leclaire et al., (1973) and Froelich (1974), and detailed studies of Micheelsen (1966) and Aubry (1975) have greatly improved our knowledge of flint formation but there still exists important gaps in our knowledge: what is the origin of "granular microcrystalline quartz" (e.g. see Knauth and Epstein, 1975, 1976) and how does this fabric relate to lepispheres?; do the different silica phases in flint have a different chemistry and how does this change during diagenesis?; and do the relative proportions of the different silica types vary within flint nodules, laterally along flint bands, or stratigraphically between flint bands?

The diagenetic history and "fabrogenesis" of flint can be studied from two different aspects : first, the petrology and physical properties of the material, and second, the chemistry of the material and its constituent phases. The latter approach is the subject of the next chapter, whilst this section will consider the properties of the siliceous components of flint.

4.2. GENERAL CHARACTERISTICS OF FLINT

Two typical flint nodules are shown in pl. 8, A and B. The bulk of the flint is composed of homogeneous black or dark brown vitreous silica, often with a bluish tint in fresh specimens, usually referred to as "black-flint" (e.g. Micheelsen, 1966). This is what is usually envisaged when the term "flint" is used. It is characterised by a clean conchoidal fracture and homogeneous sub-vitreous lustre on fracture surfaces.

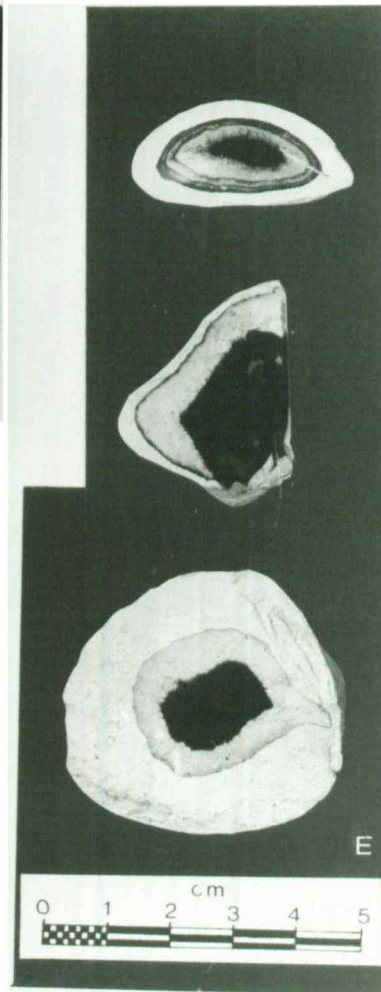
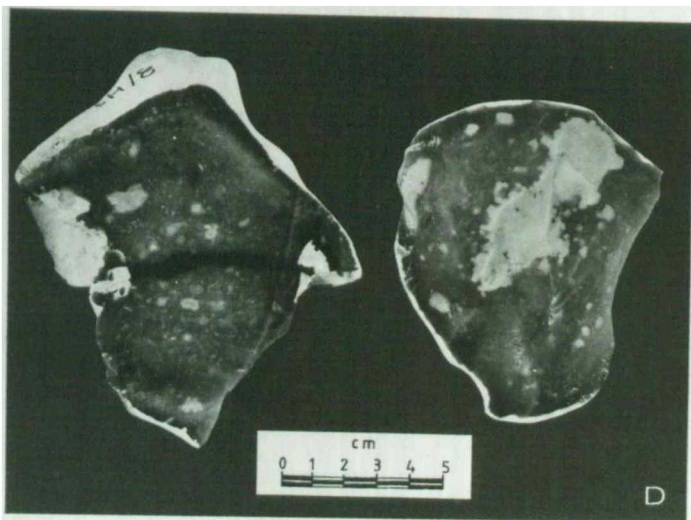
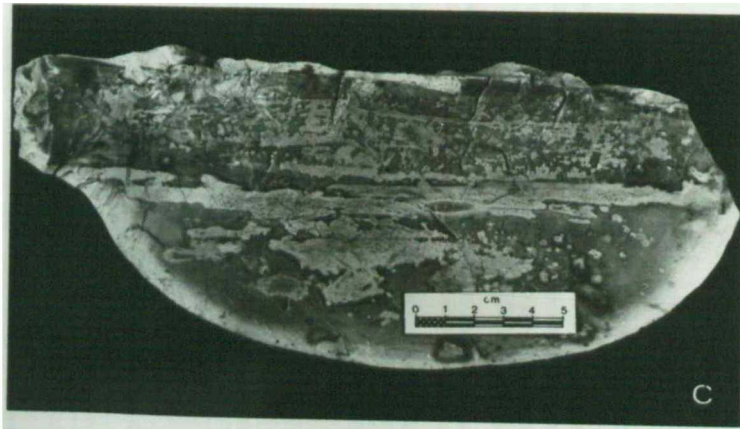
Within the black-flint, particularly near the middle of nodules or tabular units, it is common to find patches and spots of grey or white material variously referred to as "grey flint", or "grey-cores". However, these objects are not the only manifestation of grey coloured flint, nor are they always found in the middle of flints, so these terms are somewhat misleading and best avoided. The informal term "white bodies" is used for descriptive purposes in this work but no attempt is made to define this on a strict basis. In addition to these and often associated with them, it is common to find pockets and veins of coarse fibrous quartz (chalcedonic quartz) and druse (coarse euhedral crystals) within flint, present as a late stage cement.

Around the outer edge of flints, and the internal margins of carious flints (see section 3.6.4) a rind of white material is present which on close inspection can usually be seen to consist of two parts. The more external component shows a diffuse outer boundary, grading into the surrounding chalk, with a sharp smooth inner boundary. It is composed of a mixture of silica and carbonate, and is referred to here as the "crust" of the flint and corresponds to the "patine silico-calcaires" of Cayeux (1930) and Aubry (1975).

Plate 9

Macrostructure of Flints

- A. *Large nodular flint from the Burnham Chalk Formation of Lincolnshire. The horizontal bands are a reflection of the bedding in the original chalk.*
- B. *Interior of a Santonian flint from Beachy Head showing the coarse chalcedony and drusy quartz lining often found in voids within white bodies.*
- C. *Cross section of a flint similar to that shown in A. Note how the white bodies are strongly controlled by the bedding traces. Where bedding is absent (as in most of the southern England sections) white bodies are controlled by burrow structures.*
- D. *Sections of two flints to show typical structure of white bodies in nodular flints. Note also the horizontal black band across the left hand specimen which may represent the remains of a soft bodied organism.*
- E. *Sections of three flints to show the differentiation of the cortex from the crust (on the outside). Note how the two are separated by a thin dark band of normal silica. The upper specimen has developed a banded cortex.*



inside the crust is the "cortex" ("patine siliceuse " of above authors) which has an irregular, often scalloped boundary with the black flint. The cortex is wholly or almost wholly siliceous and is obviously a weathering product of the black flint.

The silica in flint is now almost entirely quartz, although many authors have also reported the presence of opal-CT (e.g. Jeans, 1978; Jarvis et al., 1982; "cristobalite-tridymite" of Leclaire et al., 1973; and Froelich, 1974; "subsidiary cryptocrystalline silica" of Jensen et al., 1957). This is of course, not unexpected in view of the well known maturation series of opal-CT to quartz found in deep-sea cherts (see discussion in section 2.4.2) and would imply a similar diagenetic history for Cretaceous flints. In addition, many authors have pointed out the presence of chemically bound water in flint, most notably Weymouth and Williamson, 1951; Midgley, 1951; Michelsen, 1966; and Knauth and Epstein, 1975). This water is of critical importance in understanding the physical properties of flint (e.g. see Micheelsen, 1966) and the diagenetic history of other cherts (e.g. Knauth and Epstein, 1975, 1976) so it is relevant to consider it in some detail in this study before giving a description of the different silica types in flint.

4.3 WATER DISTRIBUTION IN FLINT

4.3.1 Theoretical Considerations

Water is associated with the silica lattice either as surface- or defect-bound hydroxyl groups, as water molecules hydrogen-bonded to these groups, or as free molecular water in fluid inclusions (Iler, 1979). Silica groups exist almost entirely in the tetrahedral state (fig. 4.1a) and in the solid material

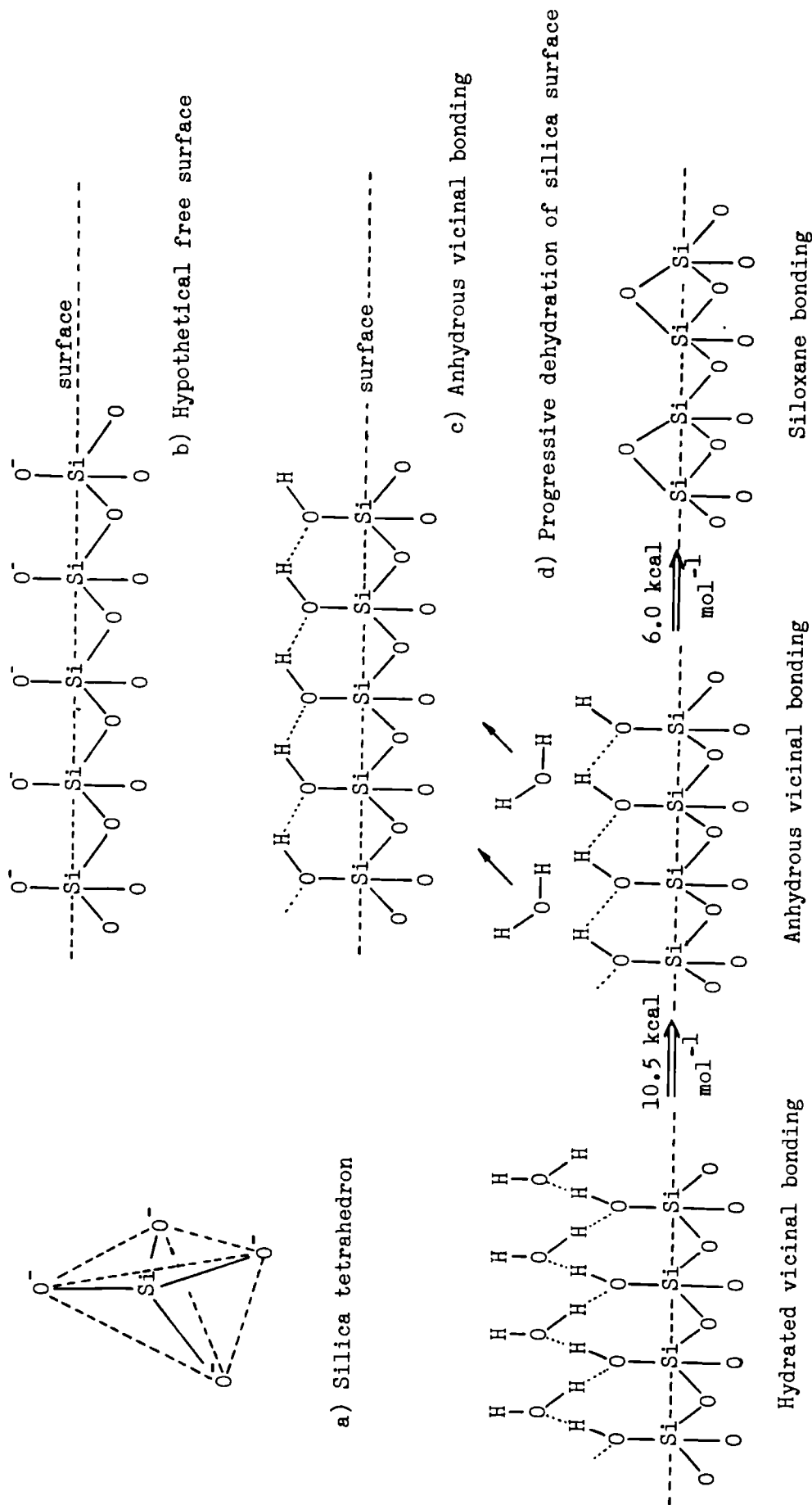


Fig. 4.1 Bonding style at the silica surface.

this leaves vacant oxygen bonds at the surface of the silica grain (fig. 4.1b). These free bonds are usually satisfied by strongly bound hydroxyl groups to form a chemisorbed layer attached by silanol (i.e. Si-OH, fig. 4.1c) bonds although, in theory, any monovalent anionic group could replace the hydroxyl ion. The hydroxylated surface is generally overlain by two or more layers of molecular water, hydrogen bonded to the hydroxyl groups ("physical absorption", fig. 4.1d), passing into free molecular water within a few molecules of the silica surface. Siliceous materials with a high surface area (i.e. very fine grain-size) therefore are associated with a high water content but more coarsely crystalline material has a much lower content.

In the absence of any physically absorbed water, adjacent silanol groups become mutually hydrogen bonded to each other (vicinal bonding) and only high temperature outgassing under vacuum can cause dehydration of the surface. When these bonds are broken, however, molecular water is formed by a combination of two adjacent hydroxyl groups, and the associated silicon atoms then share the residual oxygen atom (siloxane bonding, fig. 1d). The overlying physically absorbed water is more easily lost, although the mechanism involved is more complicated than would be expected (see discussion of bonding energies in these layers in Iler, 1979; p. 637 et. seq.). Additionally, any structural disorder in the silica is reflected in the distribution of the attached silanol groups and overlying layers, which will show a less ordered, and therefore less strongly bonded pattern. This will be reflected in the dehydration characteristics of the silica and will produce a shift towards longer wavelengths in the associated infra-red absorption peaks (see below).

4.3.2 Determination of Water in Flints

a) Thermogravimetric Methods

The most useful method of measuring the water content, and its distribution in flints is by thermogravimetric (T.G.) analysis, although Micheelsen (1966) is the only author to have reported extensive use of this.

A typical T.G. weight-loss curve is shown in fig. 4.2 where three distinct reactions are apparent: a low temperature rapid water loss, complete below 200°C (reaction I); a slower but generally more pronounced weight loss, initiating between 200 and 300°C with a peak at $4-500^{\circ}\text{C}$ (reaction II); and a sharp rapid weight loss at about 650°C (reaction III). Subsequently, a very slow progressive weight loss continues until the end of the heating cycle (reaction IV).

Reaction I occurs between room temperature and 200°C and typically accounts for a weight loss in the specimen of between zero and 0.5%. This is a reversible reaction whose magnitude depends on laboratory humidity at the time of determination (e.g. Micheelsen (1966) has demonstrated a similar weight loss due to isothermal dehydration) suggesting that it represents the loss of loosely bound molecular water absorbed on grain boundaries or in fairly large water-filled pores. Knauth (1973) has also found that the water given off by this reaction is highly susceptible to isotopic exchange with deuterated water. The water is presumably also lost at room temperature when the specimen is kept under vacuum (see next chapter) but apparently it is re-absorbed so rapidly that attempts to test this have been unsuccessful.

Reaction II occurs between 200 and 700°C and accounts for the main weight loss in carbonate-poor samples (see below). This

reaction probably corresponds to the breakdown of Si-OH bonds and loss of the immediately overlying physically absorbed water. The extended temperature range reflects the broad range of bonding energies and a certain time-lag associated with diffusion of the water away from its source. Interestingly, the early part of this reaction coincides with a decrease in the refractive index of the sample (Waymouth and Williamson, 1951) which may suggest that water redistribution predates actual loss from the sample (see discussion of water distribution in white bodies, below). This is compatible with the discovery by Micheelsen (1966) that the weight loss is delayed until higher temperature if coarse flint chips are heated, instead of powder (see his fig. 6, curve 9).

Reaction III occurs between 650 and 750°C and coincides with the decomposition temperature of calcite. This suggests that the weight change corresponds to the loss of CO₂ from relic carbonate grains in the flint which has been confirmed by Micheelsen (1966) who has found the start of the reaction is delayed until 720°C in a CO₂ atmosphere. Estimates of carbonate content based on this weight loss compare reasonably well with estimates based on determination of the Ca content by I.C.P. spectroscopy (see Appendix 3).

Reaction IV is a slow prolonged weight loss which is not completed below the upper temperature limit of the T.G. furnace (~1200°C). This weight loss occurs in all silica types so far studied and step heating studies suggest that it is dependent on temperature rather than time. According to Micheelsen (1966) this is attributable to the breakdown of traces of organic matter within the flint grains but a similar effect in silica gel has been attributed by McDonald (1958) to the presence of relic strongly

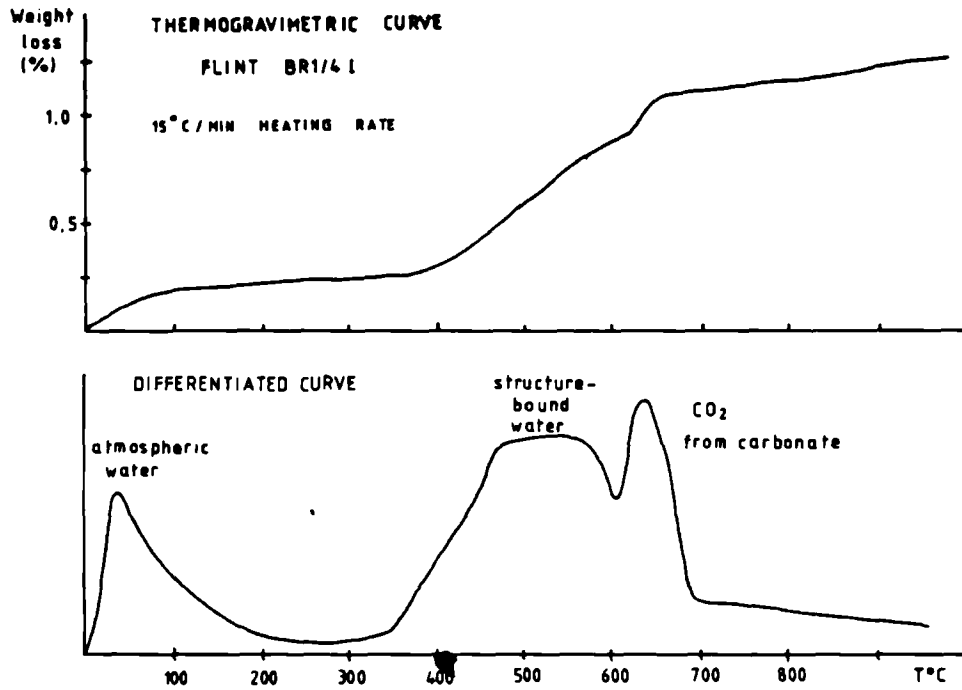


Figure 4.2 Thermogravimetric curve for typical black flint. Flint BR1/4, Bridgewick quarry, West Sussex. Bridgewick flint series.

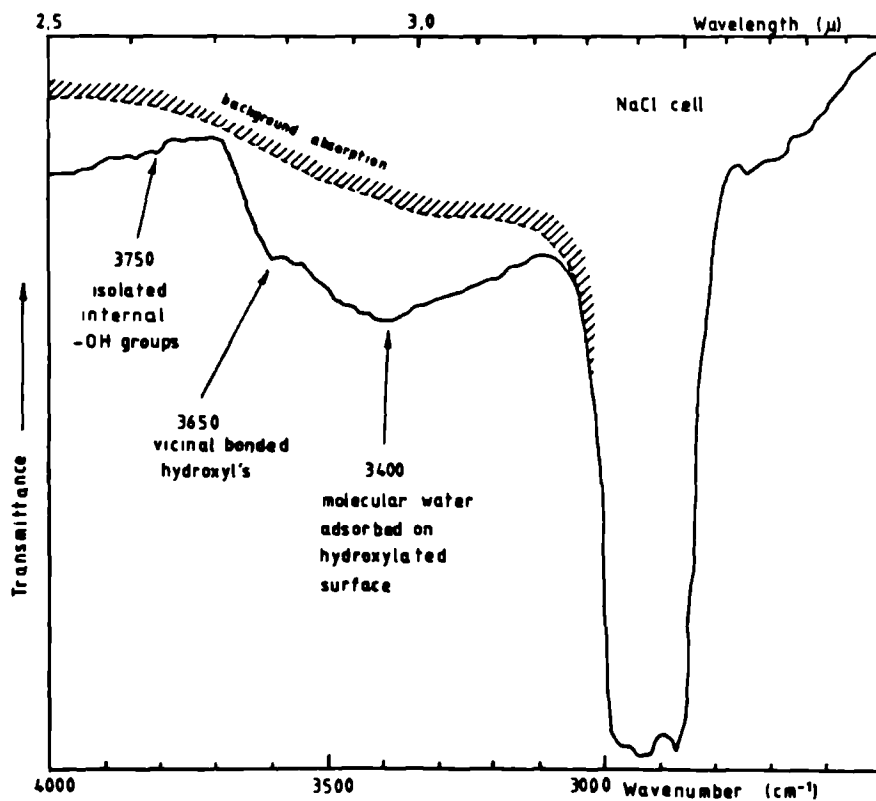


Figure 4.3 Infra red adsorption spectrum for Brandon black flint (BDN). Background absorption is due to mulling agent. See table 4.1 for assignment of peaks.

Table 4.1

*Infra-Red Absorption Bands of Water and Hydroxyl Groups
in Silica*

<u>Absorption (cm^{-1})</u>	<u>Assignment</u>	<u>Reference</u>
3389	molecular water	Jones 1978
3500	hydroxyl groups in qtz.	"
3500	H-bonded hydroxyl in quartz	Dodd & Frazer 1967
3400-3500	H ₂ O on hydroxyl groups	Iler 1979
3540-3550*	Paired hydrox. on surface	"
3650	Bulk hydroxyl, perturbed	Parke, 1974
3650-3660	Vicinal bonded internal -OH	Iler 1979
3740-3750@	Unperturbed Si-OH bonds	Parke 1974
3745-3750*	Free -OH on surfaces	Iler 1979

* Probably not present in flint structure

@ Probably present only along lattice defects

bound isolated -OH groups. Structurally, this latter explanation is of greater consequence, but quantitatively it accounts for only a very small fraction of the -OH groups and it apparently makes little difference to the hydrogen isotopic composition of the total structural water (see chapter 5).

b) Infra-Red Absorption Spectra

Infra-red (I.R.) spectroscopy is a valuable tool for determining the structural role of water and hydroxyl groups in silicates and offers greater refinement than is possible by thermogravimetry.

Of particular interest to this study is the $3000-4000\text{ cm}^{-1}$ frequency range (approximately $2.5 - 3.5\mu$ wavelength range) where stretching vibrations associated with hydroxyl and water groups cause a range of strong absorptions. (Parke, 1974; Jones, 1978). The absorption associated with typical black-flint is shown in fig. 4.3 and the interpretation of the peaks is shown in the accompanying table (4.1). The absorption pattern agrees well with the theoretical distribution (sec 4.3.1). A distinct peak occurs at around 3650 cm^{-1} which corresponds to internal -OH groups associated with lattice defects, and this is superimposed on a much broader absorption around 3400 cm^{-1} which represents the effects of hydrogen bonding between hydroxyl groups and with the associated physically absorbed water. The broadness of the peak here reflects the wide range in bond energy associated with the structural disorder of the silica. The near absence of a peak at 3750 cm^{-1} , due to isolated -OH groups on the silica surface is probably due to the influence of hydrogen bonding with the overlying water.

4.4 MICROSTRUCTURE OF BLACK FLINT

In 30 μ thin sections, black flint is generally clear to pale grey and displays the characteristic "pinpoint" extinction of very fine grained siliceous rocks (a result of the superimposition of several individual small grains, see pl. 10E). The refractive index and birefringence of the material is usually somewhat less than that of quartz (1.540 and .001 - .003 respectively) and this, together with the black colour of thick pieces of flint, has been attributed to the light dispersive effects of the very fine grain size, and about 1% of water in the structure (Micheelsen, 1966). In the past, the dark colour has often been attributed to the presence of organic matter, although it is now thought that this is of only rare importance, in isolated dark patches (see below).

Because of the fine grain size of the flint, thin sections are of limited use (see pl. 10E) and reflected light and electron microscopy of acid etched specimens have proved more productive. Etching times of between 30 seconds and 4 minutes in 40% HF at room temperature are sufficient to pick out most details but often a number of etchings on each specimen are necessary because of the wide variation in dissolution rate for the different siliceous components.

Etched black flint can be seen to be composed of at least three, and often up to six different siliceous phases (= morphologies and/or generations). The main framework of flint consists of silicified skeletal fragments (especially microfossils) and small (up to 20 μ) spherical aggregates of low quartz resembling, and probably pseudomorphing, opal-CT lepispheres, with an interstitial cement of micro-fibrous quartz, here termed "interstitial" or

Plate 10

Microstructure of Black Flint

- A. *Typical open lepispheric structure seen in acid etched Brandon black flint. View shows a silicified foram test containing lepispheres, cemented with interstitial chalcedony.*
- B. *Unetched sample of the same flint. Lepispheres are just visible as vague rounded objects protruding from the surface.*
- C. *Low power optical micrograph of a specimen of Clandon flint. Note how the structure is composed almost entirely of lepispheres with rare silicified foram fragments.*
- D. *Etched specimen of a coalesced lepispheric flint from an archaeological excavation in North Wales (Clayton, 1984). Lepispheres are visible only where they protrude into rare voids, such as in the foram chambers seen here.*
- E. *Transmission micrograph of an open lepispheric flint. Elongate objects are silicified macrofossil fragments, specular appearance of the groundmass is due to superimposed grains of quartz in lepispheres.*

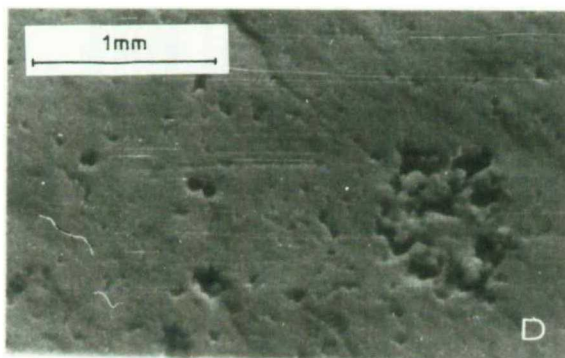
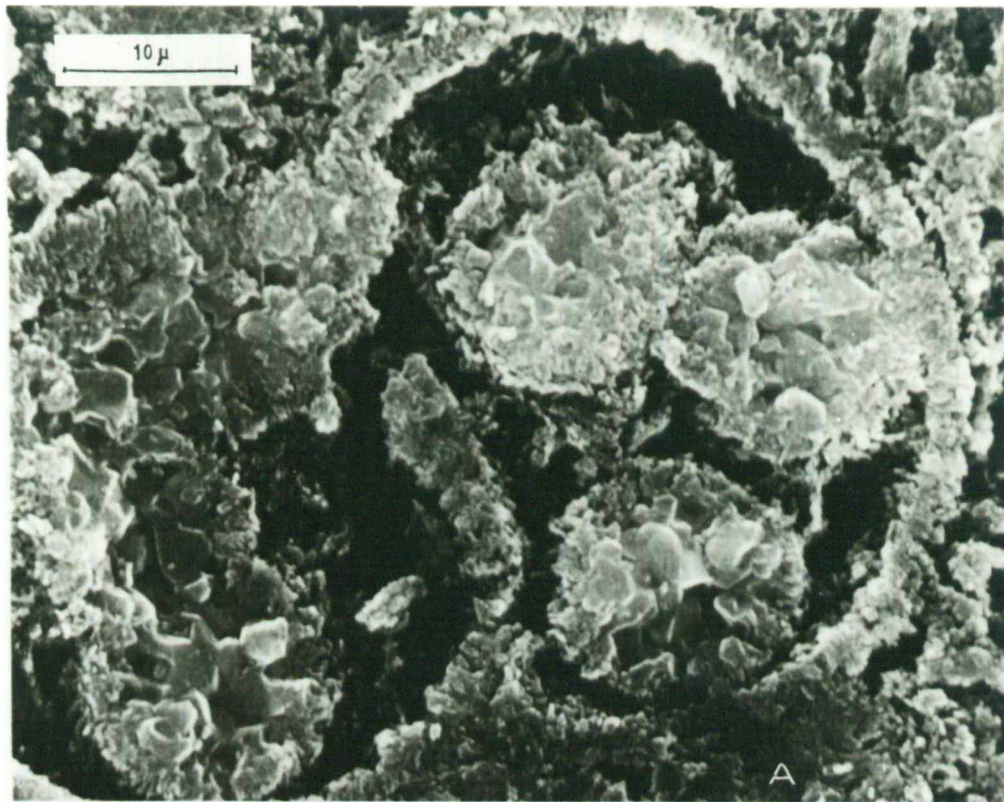


Plate 10

"type-1" chalcedony (see pl. 10A and C). In addition, small voids may contain chalcedonic quartz and quartz druse. In some specimens, small detrital quartz grains may also be common, and numerous other mineral grains may occur in some flints.

Silicified skeletal fragments in flint occur on two scales. Large fragments are typically replaced by chalcedonic quartz and druse, which represents a void filling fabric and is discussed later. Smaller skeletal fragments, particularly foraminifera and sponge spicules are usually preserved in much finer detail and are of more widespread occurrence.

Silicification of skeletal material marks the first main stage of flint growth. Unlike replacement of isolated skeletal fragments in micritic limestones (see Holdaway and Clayton, 1982), silicification initiates around the periphery of the fragment, migrating progressively inwards with time. The presence of lepispheres adhering to the surface of already silicified specimens suggests that replacement at least started, before the lepispheres were formed. Conversely, replacement postdated the growth of syntaxial overgrowths on the calcite prisms of the walls of some foraminifera (pl. 12C).

In thin section, this silica appears fibrous and may be either length fast or length slow, with a preference for the former (pl. 10A, 11D and 12C) although it is likely that one apparently bladed crystal seen in the SEM corresponds to several of the "fibres" seen in optical light (i.e. fibrous sub-grains of bladed crystals). Typically the grains are 1-2 μ thick, about 2-3 μ wide and up to 20 μ in length, but their size is highly variable in different environments. Individual grains are generally orientated with their long axis perpendicular to the surface of the skeletal fragment,

Plate 11

Constituents of Lepispheric Flint

- A. Detailed view of a quartz lepisphere from pl.10A. Note the interlocking grains and the gradual transition to chalcedony around the edge.
- B. Quartz druse in a void in a Santonian flint. This is the last silica phase to form in flints and corresponds to the deepest stage of burial.
- C. Detail of a coalesced lepispheric flint in which the constituent grains of lepispheres comprise the bulk of the silica to give a novaculite type structure.
- D. Silicified foram.chamber containing fibrous type 1 chalcedony and a somewhat tatty lepisphere.
- E. Detail of a single lepisphere grain. Striations on the edge of the grain reflect the constituent quartz plates of which the grains are composed.
- F. Type 4 chalcedony in a chalcedonic chert from the Tertiary of the Dordogne ("Meuliere"). cf the recrystallised chalcedony in pl. 13B.

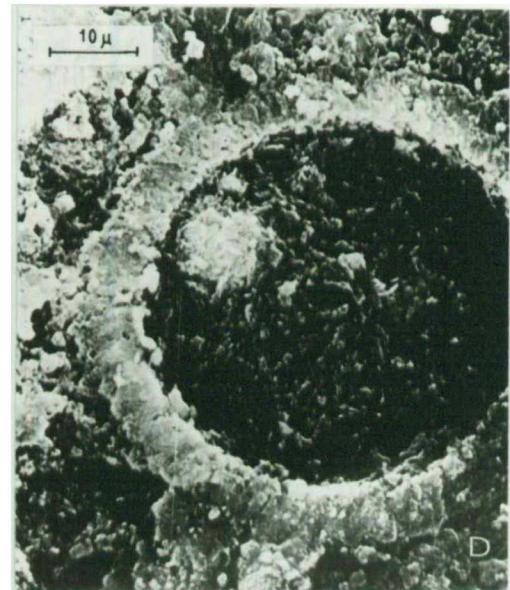
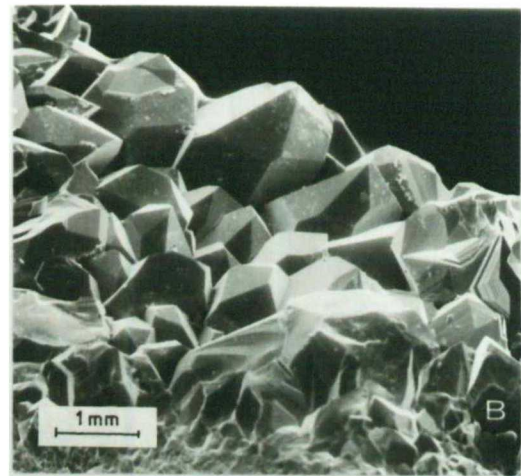
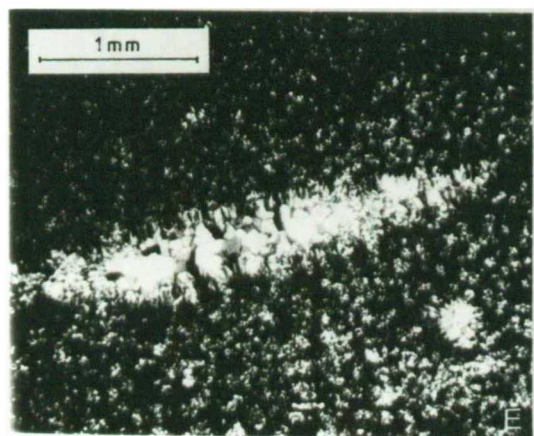
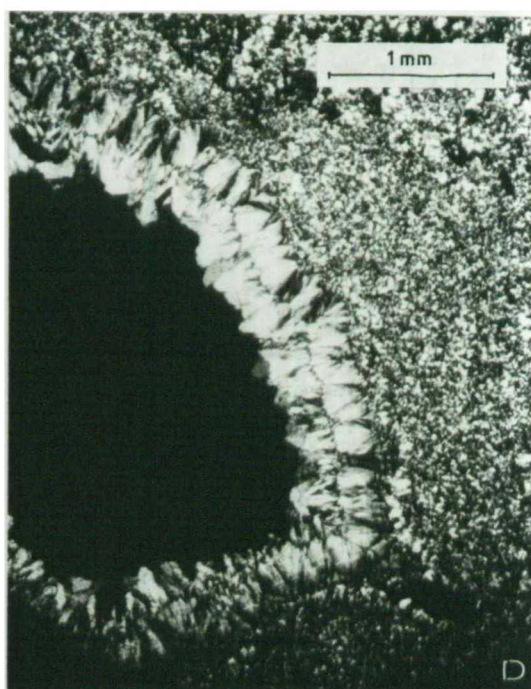
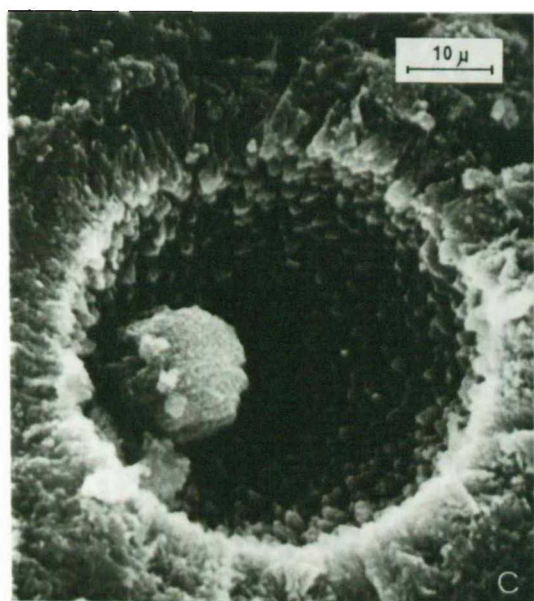
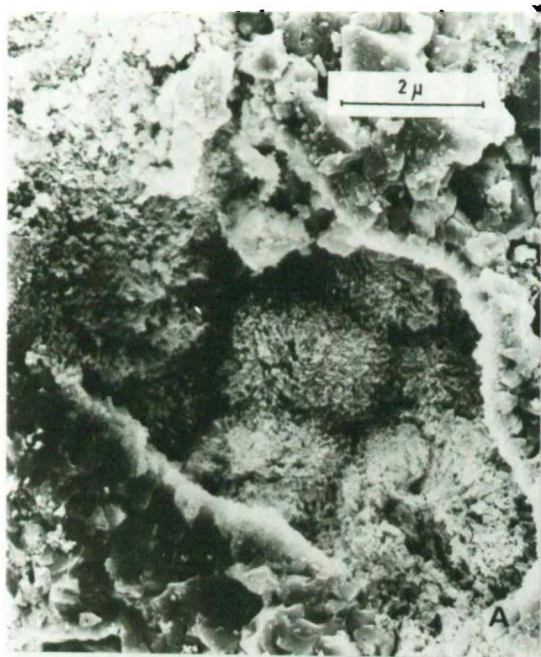


Plate 11

Plate 12

- A. *Chalcedony rosettes in a void in coalesced lepispheric flint from the Coniacian of Aquitaine.*
- B. *A skeletal chert in which the structure lacks lepispheres and is composed entirely of skeletal fragments and chalcedony. Archaeological specimen from Pontnewydd Cave, Wales.*
- C. *Detail of a hollow silicified foraminifera. Note how the silica has replaced the syntaxial calcite overgrowths on the inside of the prism structure of the foram wall.*
- D. *Thin section of a silicified bivalve fragment showing the typical radiating fibrous habit of the silica.*
- E. *Thin section of Brandon black flint containing a fossil fragment. This photograph was taken on the "feather edge" of the section and it is possible to pick out the individual grains of the lepispheres. Dark anisotropic background is due to the small size of the grains in the interstitial chalcedony.*
- F. *Detail of E.*



usually resulting in a radiating habit (e.g. pl. 11D), particularly in sponge spicules. At other times, the shell microstructure may be finely replaced. The optical properties usually correspond to those of quartz although the brown colouration of chalcedony s.s. (see Appendix) occurs in rare cases.

The lepisphere-chalcedony mixture comprises the bulk of the flint in most specimens. The ratio of the two varies from an open lepispheric framework, in which the lepispheres are only just in contact (but still form a self-supporting framework) to a totally coalesced lepispheric structure in which interstitial chalcedony is almost totally absent, and the lepispheric nature is only visible where lepispheres protrude into rare voids in the fabric (pl. 10D). In rare cases, such as in some flints from the Craie de Villedieu (Jarvis et al., 1982), these lepispheres have retained their original opal-CT mineralogy, presumably because of the shallow burial history of the area.

Individual lepispheres are about 5-20 μ in diameter and composed of a number of equant anhedral grains about 2-5 μ across, which interlock with smooth, often slightly curved compromise boundaries (pl. 11A) where individual grains can be seen in thin section (e.g. pl. 12E and F), they display the optical properties of quartz but with a very marked undulose extinction pattern, in cases simulating fibrous quartz. Within any one specimen, lepisphere size is constant suggesting that growth occurs simultaneously throughout the whole of the flint. This implies that the flint did not grow radially outwards from a central nucleus. Also, the coalescence rather than displacive growth of lepispheres suggests that flints must have grown by replacement rather than displacement of the of the host carbonate. In this case, it is likely that the original

non-carbonate constituents of the host (clays, phosphates etc.) would be quantitatively preserved within the flint, although their detailed chemistry may vary in response to the abnormal chemical environment there.

The fully coalesced lepispheric state occurs particularly within the centre of nodules, and in sheet flints or flints in more porous (i.e. bioclastic) chalks. Where this occurs, the boundaries of the lepispheres are not visible and the fabric appears as an extensive mass of anhedral grains (pl. 11C). This fabric has been described many times before. In thin section studies it is usually referred to as granular microcrystalline quartz (e.g. Wilson, 1966; Orme, 1974; Knauth and Epstein, 1975, 1976; Knauth 1979) and has been described as granular silica by Oldershaw (1968) and "novaculite" texture by Folk and Weaver (1952), based on SEM studies. These latter authors differentiate this fabric from "spongy" silica, which corresponds to type II and recrystallised type IV chalcedony of this study (see below). Micheelsen (1966) has described this as "flint grain" texture and has demonstrated that these grains are composed of piles of plates of quartz with an average thickness of 60 nm, parallel to (0001), covered by monolayers of Si-OH groups (see pl. 11E). These plates themselves consist of sub-grains of .2-.3 μ size, separated by low angle boundaries and finely divided twin faults on the (1210) plane. Both the sub-grain boundaries and the twin faults are also the sites of Si-OH groups.

The boundary of lepispheres with the chalcedony is usually gradational and in etched specimens the surface of lepispheres is often granular, representing the remains of the chalcedony which

has dissolved more readily than the coarser grains of the lepispheres (pl. 11A). The chalcedony itself (here termed type 1 chalcedony) is extremely fine grained fibrous α -quartz, forming radiating bundles, sheaths and spherules (pl. 11D, 12A). Individual fibres may be up to about 50 nm across and 2μ long, and are usually orientated with their long axis perpendicular to the surface from which they grew. In the rare cases where it is coarse enough to be visible in thin section, it displays approximate quartzose optical properties, but with refractive index and birefringence slightly lower than quartz (possibly the result of superposition of grains). The fibres show straight extinction, and are elongated in the direction of the fast ray. In reflected light, it displays a pale "opalescent" blue colour as a consequence of light scattering effects associated with the multiple grain and sub-grain boundaries.

The transition from lepisphere growth to chalcedony growth is a very important change in precipitation style. Lepisphere shape is controlled by the twinning laws of rapidly precipitated opal-CT (Florke et al., 1975; von Rad et al., 1978) but the morphology of the chalcedony suggests free precipitation of quartz from solution (Folk and Weaver, 1952; Folk and Pitman, 1971). However, the gradational boundary between the two, and comparable oxygen isotopic composition (see next chapter), suggests that the chalcedony also was originally precipitated as opal-CT. As explained in chapter 2, silica precipitation in cherts is probably caused by the introduction of dissolved carbonate into solution (i.e. chalk dissolution) which results in rapid precipitation of opal-CT lepispheres by a kinetic bridging mechanism. If this is the case, it seems likely

that the change in morphology from "catalysed" precipitation as lepispheres, to "free" precipitation as chalcedony fibres occurs on completion of carbonate dissolution, when the addition of dissolved carbonate ions ceases and silica precipitation continues at the normal rate for precipitation from saturated solution.

If true, this has important implications. The rate controlling step for silica precipitation could not have been silica supply, but the rate of carbonate dissolution (see chapter 6), a high rate favouring a greater lepisphere density. For this reason, coalesced lepispheric flints preferentially form in the centre of flints, or in higher permeability environments (e.g. in local porous beds, along sheet flints etc.) where more intense mixing/diffusion can cause more rapid dissolution of calcite. This also implies a time gap between lepisphere precipitation (which defines the position of the final flint) and the time that the flint became solid enough to resist reworking without disintegration (determined by precipitation of type-1 chalcedony "cement"). It also explains why even in the most open-structure lepispheric flints, the lepispheres produce a self-supporting framework since by the time they have completed growth, there is no fine grained carbonate available to support them.

One further interesting point about the chalcedony growth is that in almost all flint, it completely fills just about all of the microporosity. In other words, there has always been sufficient silica available to complete flint growth. This rule is broken only in regions of massive flint growth where silica constitutes about 30-40% of the rock (e.g. the Maastrichtian Romontbos Flints), suggesting that if similar quantities of silica were deposited with

the typical white chalks of southern England (2-4% silica at present), there must have been a considerable flux of dissolved silica back into the oceanic reservoir.

4.5 WHITE BODIES

4.5.1 Petrology and Origin

White bodies form smooth rounded objects with occasional protruberances, generally concentrated towards the heart of their host, but they may sometimes be large and poorly shaped, or highly flattened parallel to bedding (e.g. see pl. 8B, and 9B, C and D. Plate 4A represents a particularly characteristic type). In size they vary from small, almost insignificant objects to large, eye catching features which often receive an undue share of written (and indeed oral) descriptions of the whole object (e.g. Montbell, 1953; M.L. Coleman Num. Pers. Com.).

In thin section, white bodies appear similar to normal black flint but are characterised by a brown colouration in plane polarised light and a refractive index and birefringence much less than those of quartz. The interstitial chalcedony is particularly susceptible to this change and appears much darker than the enclosed lepispheres (pl. 13E). The effect may also be apparent in the chalcedony over a greater area than the same effect in lepispheres, and this may result in an outer pale coloured rim around many white bodies. In some cases, aggrading neomorphic crystal growth has produced an internal region of drusy quartz in the centre of the most intense white bodies.

These anomalous optical properties are essentially those which define chalcedony s.s. and they have been the subject of much speculation in the past. Early workers assumed a certain amount of

Plate 13

- A. *Void in a chalcedonic chert showing large rosettes of type 4 chalcedony and interstitial type 1 chalcedony.*
- B. *Detail from A. Note the lines of pores (once fluid filled) which result from exsolution of structure bound water during recrystallisation. cf pl. 11F.*
- C. *Lepispheres in a severly recrystallised interstitial chalcedony from a white body in Clandon flint.*
- D. *Detail from C. Note how the chalcedony has become plated onto the surface of the lepispheres leaving water filled voids in the misfits.*
- E. *Thin section micrograph across the edge of a white body. The dark colour (which is brown in the original specimen) is due to light scattering associated with the water filled pores. Lepispheric character is also visible because of the pseudo-anisotropy of the fine grained interstitial chalcedony. Ppl., section approx. 10 microns thick.*

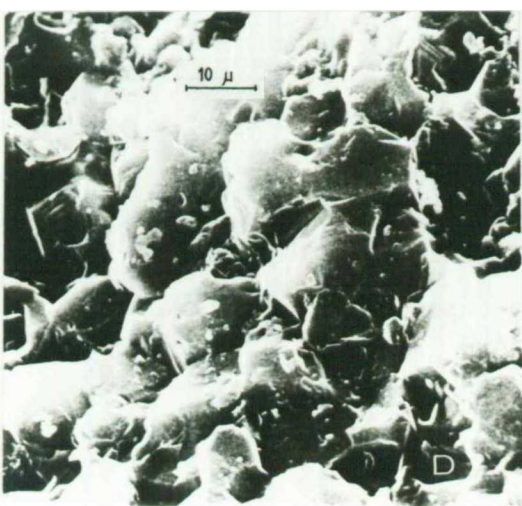
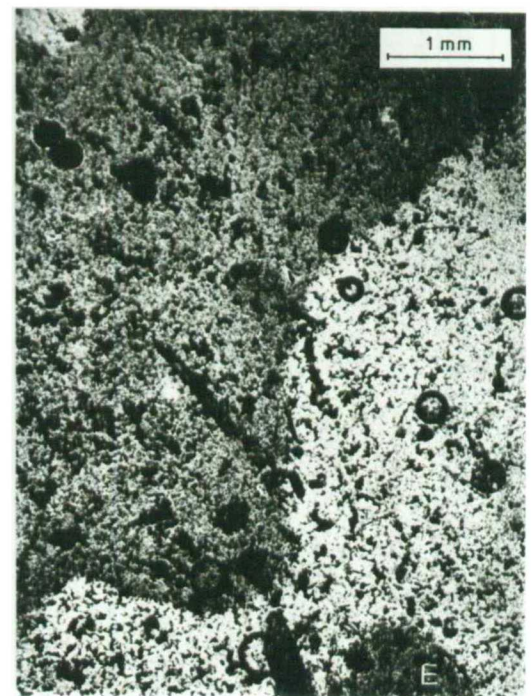
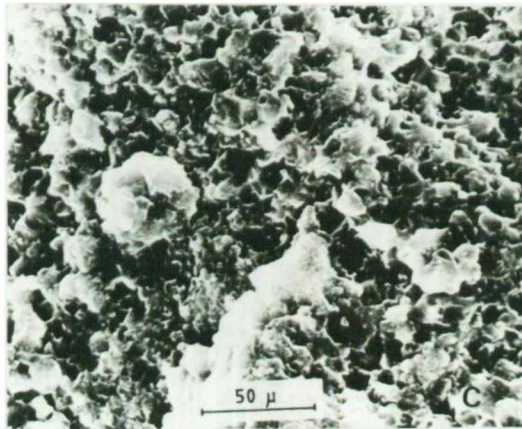
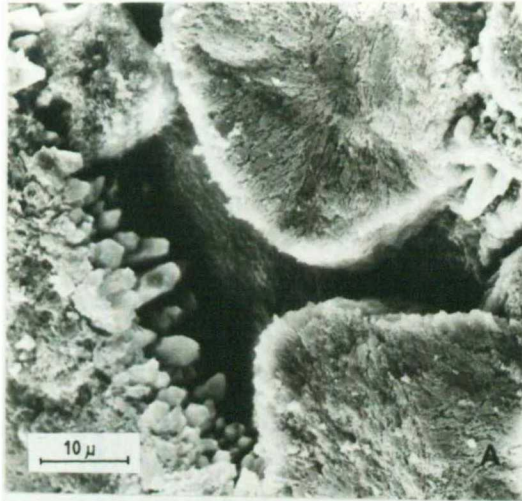


Plate 13

admixed opal to explain the low refractive index but this has been discredited now (e.g. Weymouth and Williamson, 1951; Midgley, 1951; Pelto, 1956; Micheelsen, 1966). Folk and Weaver, (1952), have pointed out the presence of small spherical microscopic water-filled pores in this material, .02 to .3 μ m in diameter and have demonstrated that the density and refractive index vary in proportion to their abundance. In addition, Pelto (1956) has postulated the presence of water along angular misfits between bundles of fibres, associated with a strained state of the material here to explain other properties of chalcedony. The important difference therefore between normal silica and the brown silica of white bodies is the presence of water-filled microscopic fluid inclusions in the latter.

The interstitial chalcedony (type II chalcedony of this work and Clayton, 1984) is particularly susceptible to dissolution and frequently disappears altogether during the etching process. This is in contrast to the lepispheres which are usually more resistant to etching. Presumably, the anomalously rapid dissolution of the chalcedony is the result of the numerous pores which offer a larger surface area for dissolution than is normally available. When short etching times are employed to preserve the chalcedony, it has an "opaline" white colour, rather than blue, as a consequence of the light refraction effects of the pores which masks the scattering effects associated with the small grain size.

In the SEM (pl. 13D), the lepisphere/chalcedony fabric can still be clearly seen but there are obvious signs of recrystallisation which has produced a coarser, more obviously crystalline fabric to the chalcedony and a structural ordering of the surface of the lepispheres. In etched specimens (pl. 13C) the water-

filled pores are accentuated and a spongy texture is visible. This is comparable to the spongy texture of chalcedony demonstrated by numerous authors (e.g. Folk and Weaver, 1952, Pitman, 1959; Kaibara, 1964; Oldershaw, 1968) but is distinct from the original unrecrystallised (type 1) chalcedony. The development of such pores is perhaps better seen in a large sheaf of coarser chalcedony in plate 13 A and B, which is the recrystallisation product of the fabric in pl. 11F (termed "type IV chalcedony" by Clayton, 1984). Presumably, similar pores in the lepispheres are present within the grains so the silica is less susceptible to etching than the more disordered precursor.

Clearly, the development of white bodies in flint represents a recrystallisation of the silica to a greater structural order, accompanied by the growth of numerous water-filled pores. These are presumably fed during recrystallisation by exsolution of the structure-bound water in the dissolved silica. This possibility is confirmed by the thermogravimetric curve for white body flint which shows a lower structural water content. It would be expected that this would be accompanied by an increase in the content of loosely bound molecular water but the grinding process breaks down the newly formed pores so this is not found. The I.R. absorption spectrum also usually shows a change associated with the recrystallisation which is reflected in a decrease in importance of the broad 3400 cm^{-1} absorption peak and sometimes a slight shift of both this peak and the internal -OH group absorption (3650 cm^{-1}) to slightly shorter wavelengths (i.e. greater bond energy reflecting greater structural order).

White bodies in flint usually reflect inhomogeneities in the

original sediment. In some cases this reflects local high concentrations of organic matter (pyrite grains may sometimes be found within the white bodies), but in other cases, white bodies reflect bioturbation structures or fossil sponge skeletons. These reflect permeability variations in the original sediment which are already known to play an important part in controlling the zone of silicification. It seems probable therefore that the sites of white bodies were controlled by some anomalous property of the pre-existing silica, which developed in response to variation in the original sediment. The recrystallisation process consists predominantly of the exsolution of structure-bound water, suggesting that the original water content is probably an important factor. This in turn is dependant on the rate of growth of the silica crystal (Dodd and Fraser, 1967; Jones, 1978, and references therein), rapid growth resulting in greater structural disorder, a higher water content and less stable forms of silica. White bodies form by recrystallisation of the metastable silica, i.e. that with the greatest structural disorder and highest water content, and this will represent the parts where silica precipitated and/or opal-CT recrystallised to quartz, most rapidly. It will be shown in the next chapter that white body formation post-dated the opal-CT - quartz inversion.

Similar exsolution of structural water occurs in pure quartz grains, both in nature (resulting in milky quartz) and in laboratory deformation experiments (see references and discussion in Jones, 1978). In both cases, this results in a change to more brittle deformation behaviour. The early stages of the process can also be induced in black flint by heating to 200-300°C and this too

results in a change of mechanical behaviour: a fact known since Paleolithic times (e.g. see Seeley, 1975; Robins et al., 1978).

4.5.2 Banded Flints

Occasionally in flints the recrystallisation in white bodies is not simple, but produces a striped or banded pattern of alternating light and dark zones. Such "banded flints" are much beloved of amateur fossil collectors, but not of museum curators who are frequently asked to identify the non-existent species (C.J. Wood, pers. com.).

The bands formed may be flat or gently curved and stop abruptly at the edge of the white body. Frequently the bands tail-off centrally into the trace of a burrow or central canal of a sponge and the overall shape of the white body is often determined by similar features (e.g. see pl. 6E and illustrations of Woodward, 1864). Spacing of the bands is fairly regular but they usually show a progressive increase in spacing along the length of the white body. In fresh specimens the edge of the light band facing the narrower spaced end is usually sharp, and grades into the darker material away from this edge. In reworked specimens however, the white bands preferentially take up pigment and appear darker so the apparent gradations are reversed.

It is obvious from the distribution and spacing of the bands that their origin is related to some form of Liesegang mechanism (see Hedges, 1932, for review of these structures). The clear relationship to inhomogeneities in the flint (particularly burrows and sponges) suggests that diffusion of some agent is responsible for initiation of the recrystallisation but if this were the case,

the bands would begin at the edge of the flint, which they do not. The other, and more likely alternative is that the original precipitation of silica during flint formation produced bands of silica which were alternately more and less susceptible to recrystallisation. As explained above, this is probably a reflection of the water content of the silica, which is related to the rate of precipitation. The Liesegang mechanism therefore probably exerted a control on the original silica precipitation rather than the recrystallisation process itself, and this was later manifested in the preferential recrystallisation of the bands with higher water content on burial. The Liesegang control of silica precipitation in this form may be the result of either the inward diffusion of silica reacting with the dissolving carbonate (i.e. silica precipitation caused by carbonate dissolution: see chapter 2), or by the diffusion and mixing of the solutions which caused the carbonate dissolution (c.f. diffusion control on flint morphology described in chapter 3).

4.6 LATE STAGE VOID-FILLING FABRICS

Any large scale voids in the flint after completion of chalcedony growth subsequently may become infilled with coarser grained chalcedonic quartz or quartz druse (e.g. pl. 98). Such voids are frequently the result of intraparticulate porosity in faunal fragments or coarse replacements of shell material, but may also reflect relic bioturbation structures in which carbonate dissolution has outstripped lepispheres formation.

Precipitation usually follows a clear sequence from fine chalcedonic quartz, typically 2-10 μ across (pl. 12D), through

coarser blocky chalcedonic quartz, into quartz druse, usually with crystals up to about 2mm (pl. 11B). Frequently this fabric lines voids within white bodies (e.g. pl. 9B), and may either partially or completely fill the available space. The reason for the association with white bodies is uncertain but it may be a consequence of the rate of carbonate dissolution at this site during replacement. The sites of white bodies may reflect places of anomalously rapid silica precipitation (see above), which is probably caused by particularly rapid carbonate dissolution. If the rate of chalk dissolution out-paces silica precipitation then a void would form at this site, and the surrounding silica would be particularly susceptible to recrystallisation into a white body. Fibrous quartz may also infill fractures in the solid flint and its' presence here and as coatings on the surface of voids imparts a resinous blue tint to the surface. Where larger areas are concerned, a waxy lustred mamillated surface may develop such as is frequently seen in broken flint specimens.

In thin sections, both the chalcedonic quartz and the quartz druse usually show quartzose optical properties, and only in the finest grain-size material is the low-relief, brown colour of true chalcedony developed. The outward coarsening grain-size is typical of free growth of crystals into space, the fibrous nature being caused by interference between neighbouring crystals. Slower growth associated with the later stages of the process produces less interference and a coarser, euhedral crystalline fabric develops (Folk and Pitman, 1971). The void infilling thus represents slow, late stage growth, following hardening of the nodule as a whole, and the isotope data of Knauth and Epstein (1975) suggests that

this occurs at the higher temperature associated with deeper burial of the sediment (see next chapter).

4.7 OTHER CONSTITUENTS

In addition to the above components, typical flints may contain minor amounts of other "ingredients" and in particular, detrital grains, authigenic pyrite, and patches of carbonaceous pigment.

4.7.1 Detrital Grains

Because flints form by replacement rather than displacive mechanisms, non-carbonate constituents in the original sediment are preserved within the final flint. Most commonly, these are detrital quartz grains but other minerals such as rare zircons and grains of possible magnetite have also been found in some Aquitanian flints. All detrital quartz grains so far found have been angular-sub-angular in shape, in contrast to the generally accepted view that detrital quartz grains in the Chalk are millet-seed shaped and so suggest an arid continental climate during the Cretaceous.

4.7.2 Authigenic Grains

Grains of authigenic minerals found in flint commonly include phosphates, "glauconite" and pyrite. As explained in chapter 3, granular and pelletal glauconite and phosphate forms very early in the diagenetic history of chalks, and where flints have formed in a glauconitic or phosphatic chalk, silicification has clearly post-dated the formation of these minerals. The difference in concentration of these minerals within and outside the flint will therefore reflect

the amount of compaction which has affected the host sediment since flint formation (or more precisely since the lepisphere framework became self-supporting).

The presence of pyrite grains within flint is a little surprising since widespread pyrite formation apparently postdates silification (see chapter 3). In detail, however, the pyrite occurs in localised patches, particularly strung out along bedding traces (pl. 9C), apparently picking out sites of early, anomalously high concentrations of organic matter. It would appear that rapid diagenesis associated with these organic concentrations initiated local sulphate reducing conditions above the level of widespread anoxia.

A further interesting point concerning the pyrite distribution in flint is that small pyrite grains are usually surrounded by a small zone of recrystallised flint (i.e. a white body: pl. 9C) sometimes with an internal zone of neomorphic druse adjacent to the pyrite itself. It is unclear if this is an effect of the pyrite itself or, whether the two have a common cause (e.g. intense localised organic matter decay), although the latter is more likely.

4.7.3 Carbonaceous Matter

Although the suggestion of many authors that the dark colour in flints is due to organic matter has now been discredited (e.g. see discussion in Micheelsen, 1966), concentrations of carbonaceous matter do occur in many flint specimens. These frequently occur in horizontal dark bands, about 5mm thick, probably the remains of soft bodied fauna (e.g. pl. 9D, left), but may also pick out bioturbation structures (pl. 8A). In thin section, the dark

colouration can be seen to be caused by numerous tiny black specks, usually less than 1μ in size, presumably composed of carbon or refractory organic matter. In some cases the black bands restrict the development of white bodies and cortex but sometimes the reverse is true.

Additionally, rare black or dark brown possible organic ghosts of dinoflagellates may be visible in some specimens (e.g. see Deflandre, 1934) and B. Tocher (pers. com.) has found an anomalously good preservation of dinoflagellates in flint when compared with the enclosing chalk. This is presumably because once enclosed in silica, the organic walls of dinoflagellates are protected from later diagenetic alteration.

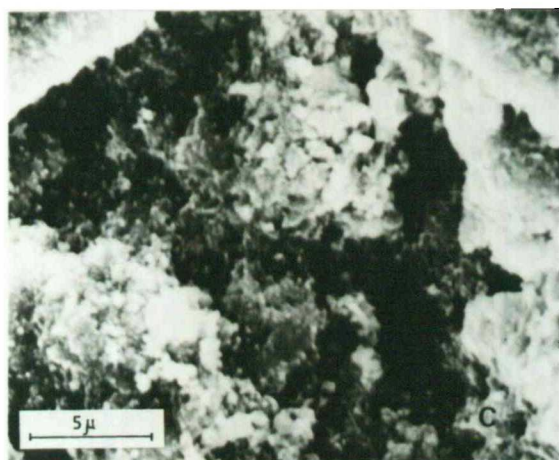
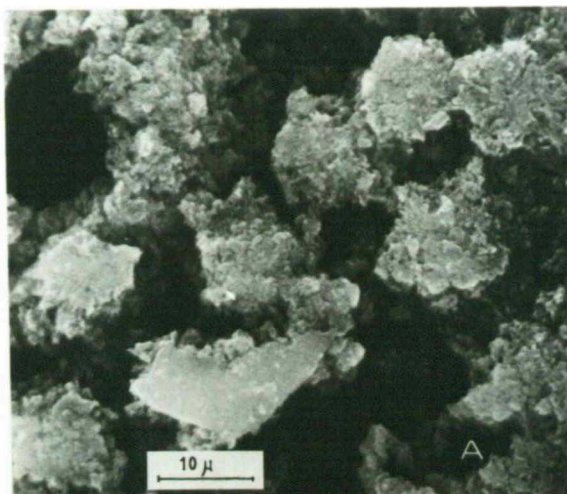
4.8 CORTEX AND PATINA FORMATION

The term cortex is here used to describe the white or grey altered flint found within the crust. Many authors use the term "patina" for this material but the term is probably best reserved for alteration effects in man-made artefacts rather than natural flint (see Appendix 1). The mechanism is the same however.

The cortex of flint is clearly an alteration product of normal flint and can usually be seen to encroach on the normal fabric (pl. 9E). In the SEM the cortex exhibits large scale dissolution of the interstitial chalcedony, leaving free standing corroded lepispheres (pl. 14A), and more advanced stages are characterised by progressive dissolution of these also (pl. 14C). Ultimately, a friable "chalky" material is all that remains (e.g. see description in Fairburn and Robertson, 1972). The generation of secondary porosity produces an abundance of water filled pores

Plate 14

- A. *Unetched specimen from the cortex of a flint. Note how the interstitial chalcedony has completely dissolved, and the corroded nature of the lepispheres.*
 - B. *Thin section micrograph of the same specimen seen in plane polarised light. The cortex appears dark because of the light scattering effects of the voids. Individual lepispheres are just visible along the boundary between the cortex and the black flint.*
 - C. *Closer view of the cortex seen in A. Lepisphere at top centre is barely recognisable.*
 - D. *A skeletal lepispheric chert collected by pre-neanderthals in north Wales.*
 - E. *Plane polarised light optical micrograph of a skeletal lepispheric chert from Aquitaine. Lepispheres are visible in lower part. Most of skeletal fragments are silicified echinoderm fragments.*
-



(c.f. chalcedony s.s.) and the cortex appears almost black in thin section (pl. 14B).

Although dissolution is obviously an important feature of cortication, it cannot be the only process involved since there is frequently a thin, apparently unaltered zone of black flint outside the cortex, adjacent to the crust (pl. 9E, middle and upper specimens), and it is difficult to imagine dissolution occurring inside this zone but not affecting it. In extreme cases, the cortex may even be banded, similar to the banding in the white bodies of banded flints (pl. 6F, 9E). It would appear that silica recrystallisation has occurred before dissolution and, as in white bodies, the strings of fluid inclusions in the chalcedony have controlled subsequent dissolution. One important difference however is that recrystallisation of the cortex has left the lepispheres unaltered, retaining quartzose optical properties: only the more susceptible chalcedony is altered (pl. 14B). This effect also explains the apparent loss of water associated with cortex formation (see Buurman and Van Der Plas, 1971; and discussion in Shepherd, 1972) since water which would have been measured as within the structure is now present in lines of pores, and any slight dissolution will result in these being open to the outside. The water would therefore be registered as atmospheric water, absorbed on the surface rather than structure-bound hydroxyl groups.

The cause of the recrystallisation is unclear at present but would appear to be related to some initiating agent in the pore waters of the enclosing chalk sediment. The original silica is highly disordered and metastable with respect to ordered silica with fluid inclusions, so it is not difficult to imagine some form

of chemical "seeding" to initiate the recrystallisation process. This occurs rapidly when flint specimens are reworked, but the presence of recemented fractures in flint which displace the cortex (see pl. 9E, top) suggest that the process also occurs at depth. Presumably the thin, apparently unaltered zone adjacent to the crust represents a region in which the exsolved structural water is lost to the outside rather than forced into fluid inclusions. In some cases, the early stages of the recrystallisation process can be seen pervading the whole flint to produce a silky white tint to fracture surfaces. The banding, where present, must represent a more complicated process, probably involving a Liesegang mechanism associated with the inward diffusion of the "seeding" solution.

This two stage mechanism of cortication has many implications. Firstly, flints of differing lepisphere/chalcedony ratio will show greatly differing alteration rates, coalesced lepispheric types being more resistant to dissolution. This is of great interest in a civil engineering context where seemingly identical flint aggregates may show vastly different susceptibilities to corrosion by chemically active high-alumina cements. Secondly, flints which have undergone recrystallisation (white body formation) will be very susceptible to incipient dissolution (the chalcedony is easily dissolved) but not to lepisphere corrosion. White bodies formed in coalesced lepispheric flints are highly resistant to cortication. The effects of heating (natural or artificial) and even freezing (such as during glacial periods) will also affect the water distribution in flint and therefore the weathering/alteration characteristics of the material, and this is of interest in archaeological studies where proof of heating and freezing of flint

has important social implications to stone age civilisations.

4.9 STRUCTURE OF FLINT CRUST

The chalky crust frequently found around the outside of flints varies greatly in importance from thin, barely visible rinds, to being the dominant silica type present in many incipient flints (see chapter 3).

Structurally, these crusts consist of a mixture of silicified skeletal fragments, massive and spherulitic silica, and varying amounts of corroded relic calcite grains. Preservation of skeletal fragments in silica is much more common and detailed than in the main flint and the crust can often be seen to be composed almost entirely of silicified foraminifera, sponge spicules, and sometimes radiolarians and diatoms also (e.g. pl. 15D). In some cases, even individual coccoliths may be faithfully preserved in silica (see pl.15A and B). The abundant preservation of these here indicates that this material is not merely an alteration product of black flint but forms under a different chemical environment.

In addition to replaced skeletal grains, silica is also present as massive aggregates of opaline appearance and as curious, rather problematic spherical objects. The massive silica is apparently structureless and non-crystalline (e.g. pl.15B and C) although no opal has been found in X.R.D. determinations. The spherical objects (pl.15C) bear a superficial resemblance to lepispheres but in detail (pl.15F) can be seen to be composed of radiating silica fibres rather than bladed or anhedral grains. These objects bear a strong resemblance to chalcedony spherulites (e.g. see Aubry, 1971; and pl. 12A of this study), but at other times they appear

Plate 15

Structure of the Flint Crust

- A & B. *Silicified and partly silicified coccoliths from the crust of Brandon flint.*
- C. *Enigmatic spherulitic structures in an apparently amorphous groundmass. XRD however showed no amorphous silica hump for this specimen.*
- D. *Boundary of crust and cortex (lower) seen in reflected light. Acid etched specimen of Bridgewick flint series. Note how the lepispheric nature of the cortex passes over into a foram/radiolarian dominated material in the crust.*
- E. *Acid etched chalcedonic chert from the Santonian of the Dordogne.*
- F. *Detail of a spherulite from C. The structure is essentially radial rather than the bladed habit of opal-CT lepispheres or blocky habit of quartz lepispheres.*

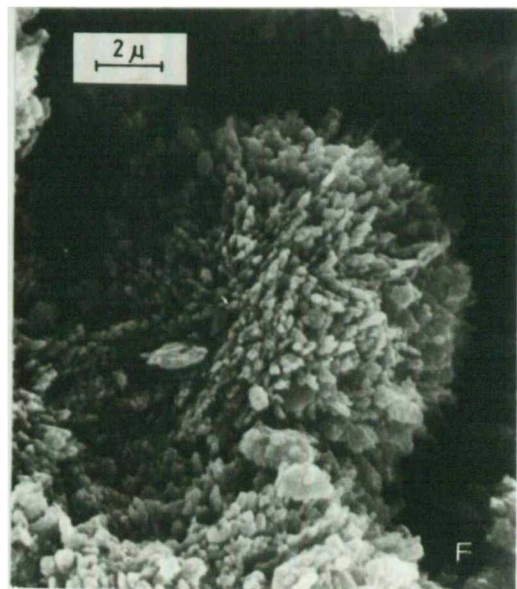
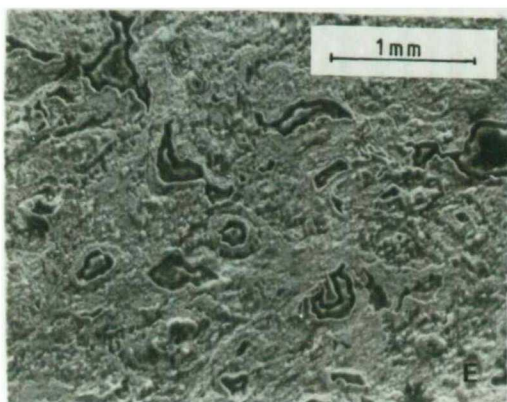
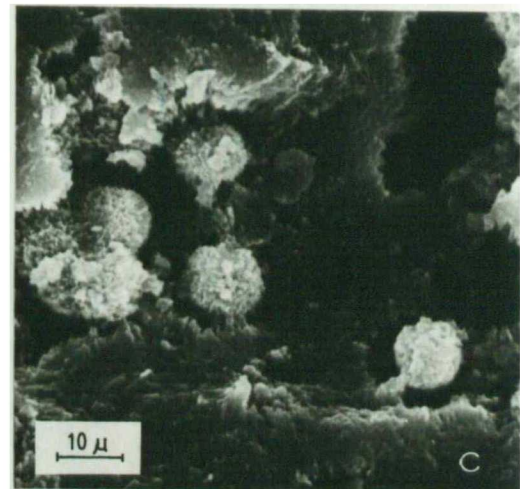
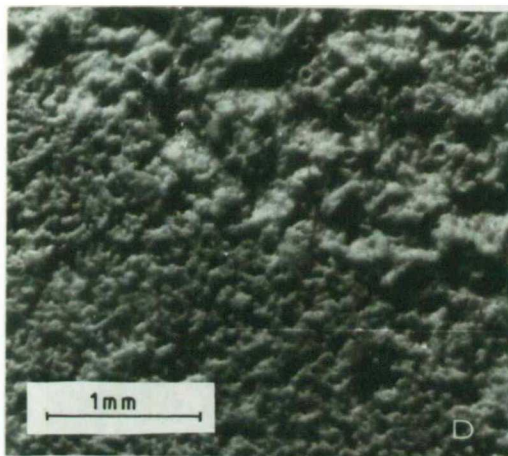
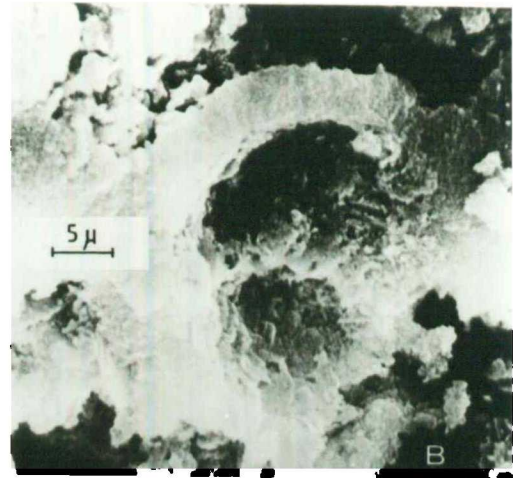
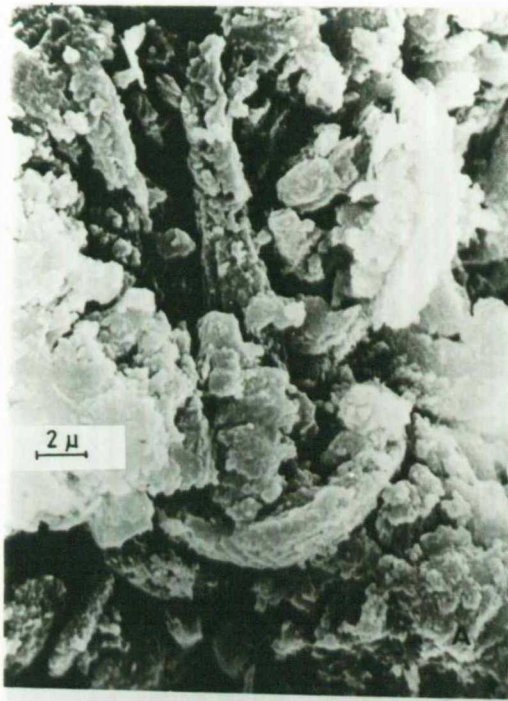


Plate 15

to be growing at the expense of the massive silica. Similar objects from Polish flints have been figures by Michniak (1980) but their origin here is also obscure. More detailed study is hindered by the dissolution which has affected the crust contemporaneously with cortex formation, but this study will be necessary before the silica fabric here can be understood.

The abundant silicification of skeletal fragments but absence of lepispheres suggests that only the early stages of flint formation are represented in the crust. However, the abundance of massive silica suggests that silica supply was not the limiting factor so presumably the crust represents silicification under conditions which were not as intense as those which produced true flints. This is of course compatible with the occurrence of the crust at the transition of flint and unreplaced chalk, and implies that incipient flints are not just juvenile flints, but completed growth in an environment not conducive to normal flint formation.

4.10 THE STRUCTURAL CLASSIFICATION OF FLINTS AND CHERTS

The skeletal fragment-lepisphere-chalcedony chert fabric characterises just about all Cretaceous flints, and most other Phanerozoic nodular cherts. However, larger scale siliceous replacements, such as the chert beds in the Lower Cretaceous Greensands of southern England, the Tertiary "Meuliere" of central France, and many of the large scale replacements in the Cambrian Durness Limestone of Scotland, are characterised by a totally different texture. These cherts consist dominantly of large sheafs and bundles of chalcedony (type IV), which is similar in properties to, but coarser than, the interstitial chalcedony in flints (pl. 11F,

13A and B, 15E). In these types, lepispheres are generally absent, and Clayton (1984) suggests the term "chalcedonic chert" to distinguish these from the "lepispheric chert" type which characterises flint. Structurally and visually the rock corresponds to that described as "chalcedony" (Fr. "chalcedoine") of many authors although the application of these terms is rather subjective. The growth mechanism for this morphology is not known at present.

Within the broad grouping of cherts into lepispheres or chalcedonic type, subdivisions are possible, based on the relative abundance of constituents. This results in, for example, "open lepispheric" (pl. 10C) or coalesced lepispheric cherts (pl. 10D), chalcedonic cherts (pl. 11F), or skeletal chalcedonic (pl. 12B) or skeletal lepispheric cherts (pl. 14D and E). It is very rare to find lepispheric and chalcedonic chert together.

In any one locality, the chert type tends to be fairly constant, and this classification has proved of use in source-typing studies of derived flints (Clayton, 1984, and unpublished data). It is also of use for differentiating cherts of different susceptibility to corrosion in cements, or to heat treatment in archaeological studies, and also has implications for understanding variations in diagenetic style in different sedimentary environments.

4.11 SUMMARY

The complex genetic and diagenetic history of flints is summarised in fig 4.4.

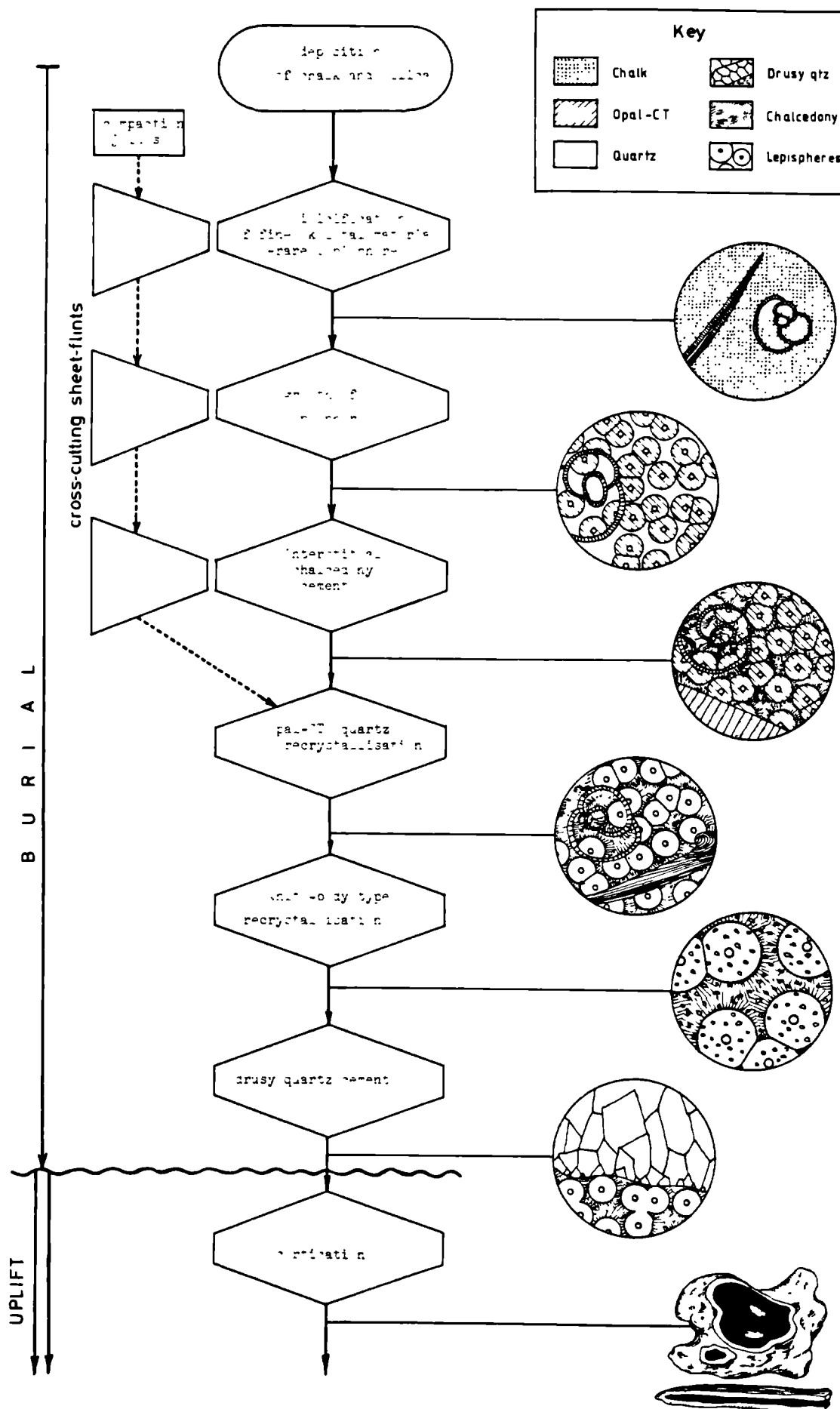


Figure 4.4 Summary of flint diagenesis

Silicification starts with the centripetal replacement of skeletal fragments, particularly of microfossils, and may continue in coarser skeletal fragments until quite late during the growth history of flint. Although this must start very early in the diagenetic history of the chalk, it postdates at least the early stage of syntaxial overgrowth on foraminiferal walls.

Precipitation of numerous opal-CT lepispheres marks the main stage of flint formation. Lepispheres tend to be of similar size over the whole of the chert but tend to be more densely packed towards the centre of the flint where silicification was most intense. Where most densely packed, the lepispheres coalesce rather than displace each other and this together with the similar size of all the lepispheres, suggests that silicification occurred simultaneously throughout the whole volume of flint rather than by radial displacive growth. Such a mechanism, barring purely chemical effects, will quantitatively preserve any pre-existing non-carbonate grains. Reworking of the flint at this stage would be expected to disaggregate the lepispheres rather than result in a hard clast which probably explains the general absence of reworked flints.

At some stage during lepisphere growth the morphology of silica precipitation changes, and all remaining voids are filled with an interstitial microfibrous chalcedony cement. This change in morphology may correspond to the end of carbonate dissolution and represents silica precipitation by a free growth mechanism rather than by an enhanced rate of precipitation (as lepispheres) brought about by dissolved carbonate catalysis of the nucleation

reaction. In almost all cases there was adequate silica available to entirely fill the interstitial voids, implying a large excess of silica in contemporary pore-waters. At some stage following chalcedony growth, the opal-CT recrystallised to quartz. This preserved the fibrous morphology of the chalcedony and the gross lepispheric-chalcedonic fabric but recrystallised the lepispheres internally to a granular micro-crystalline fabric.

Late stage recrystallisation, associated with deeper burial, affected particularly the more rapidly precipitated silica around bioturbation structures preserved in the centre of the flint. This produced a series of lighter coloured "white bodies" in which the silica is characterised by a higher structural order and numerous sub-microscopic fluid-inclusions. Where Liesegang phenomena affected the rate of silica precipitation in the initial growth stages of the flint, this later stage recrystallisation resulted in a banded flint. Contemporaneous with and subsequent to this recrystallisation episode, any remaining fractures and voids became partially or wholly infilled with coarse chalcedonic quartz and druse.

Finally, probably during uplift, some "seeding" agent in surrounding pore-waters may have initiated structural recrystallisation of the silica of the flint leading to the formation of a white "cortex" around the periphery. Silica dissolution rapidly follows this recrystallisation and may ultimately break the flint down to a powdery white "rotten" flint.

This growth sequence is characteristic of almost all the flints which are found in the Upper Cretaceous Chalk of Western Europe

and provides a framework in which to interpret the chemical data from flints. The effect of this diagenetic history on flint chemistry is the subject of the next chapter.

5. TRACE ELEMENT AND STABLE ISOTOPE VARIATIONS IN FLINT

5.1. INTRODUCTION

Geochemical studies of flint fall conveniently into two divisions: (1) variation of trace element concentrations within flints; and (2) hydrogen and oxygen stable isotope variations within the silica of the flint. The former of these is important to define the chemical environment at the time of silicification. A knowledge of the mineralogical association of specific "tracer" elements within the flint is essential if trace element variations around the flint are to be interpreted in terms of the chemical environment in which silicification occurred. Conversely, isotope studies may give information about the diagenetic changes affecting the silica itself, and knowing this it may be possible to use the original isotopic composition as a monitor of Cretaceous bottom water temperature (e.g. Kolodny and Epstein, 1976) or of pore water variations during diagenesis (e.g. Kolodny et al., 1980).

These two approaches are considered together in this chapter which sets out to provide a chemical background with which to interpret more complicated data in the succeeding chapters.

5.2. TRACE ELEMENT VARIATIONS

There is a major dearth of data on the chemistry of cherts, and almost all of the few data which are available (e.g. Barrett, 1981; Rangin et al., 1981) concern deep sea bedded cherts (primarily

radiolarian cherts) which have a very different origin to "nodular" replacement cherts such as flints. The few analyses of flints which have been published generally account for only one or two samples, frequently without detailed descriptions of petrography or stratigraphic context (e.g. Weymouth and Williamson, 1951; Micheelsen, 1966; Sabine, 1967; Blankenberg et al., 1979). More detailed data have been published by Sieveking et al., (1972) in connection with an archaeological study but these authors did not discuss in detail the mineralogical association of the elements reported.

Trace elements in flint may be located in any of a number of chemical environments:

- 1) In saline microscopic fluid inclusions, such as trapped connate waters.
- 2) Within or adsorbed onto the silica grains themselves.
- 3) As relic grains of other minerals, (e.g. clays, calcite grains etc) inherited from the original sediment.
- or 4) As authigenic phases associated with the chemical environment which led to silicification.

It is not possible to differentiate these latter two situations by analysis of individual flints in isolation but this problem will be considered in detail in chapters 6 and 7. It is intended here only to provide a framework with which to interpret trace element data in more specific cases of silicification. It is convenient to start with an investigation of trace elements associated with fluid inclusions.

5.2.1. Trace Elements Associated with Trapped Pore-waters

As explained in chapter 4, the silica in flint is partially hydrated and frequently includes a number of microscopic fluid inclusions. As the flint grew in a saline (i.e. marine) environment it might be expected that these inclusions may contain a significant NaCl content.

To test this, part of a large flint (CL1/30) from the Coranguinum Zone (Santonian) of West Clandon Pit, Surrey, was calcined at 1000°C to dehydrate the structure and then ground in an agate disc mill. Samples were removed for analysis at convenient intervals and each was subjected to a distilled water extraction to determine the water soluble trace element fraction exposed in each grain size. In theory, if a trace element is associated with pore-waters a sigmoidal curve of concentration against grinding time should occur as the grain size of the powdered sample approaches the fluid inclusion size and releases the water soluble component (fig. 5.1a).

Only two elements were detected in the solution: Na and Ca (table 5.1). The amount of these extracted for each grain size is shown graphically in fig. 5.1b. The calcium curve is very variable and probably is predominantly caused by dissolution of fine grained relic carbonate (now thermally degraded to CaO because of calcination), rather than a calcium mineral precipitated from pore waters during dehydration. However there is a clear positive relationship between grinding time and extractable Na, suggesting the presence of saline fluid inclusions in the original flint. The maximum Na concentration extracted is about 145 ppm which compares with a total Na of about 260 ppm in the flint (see below section 5.2.2).

Table 5.1
Distilled water leach on Cl1/30 fractions

Sample No.	T (mins)	log T	Conc.
Ca (1)	0.25	-1.386	310
Na (1)	0.25	-1.386	75
Ca (2)	0.50	-0.693	395
Na (2)	0.50	-0.693	90
Ca (3)	1.00	0.000	335
Na (3)	1.00	0.000	85
Ca (4)	2.00	0.693	255
Na (4)	2.00	0.693	95
Ca (5)	4.00	1.386	490
Na (5)	4.00	1.386	120
Ca (6)	8.00	2.079	295
Na (6)	8.00	2.079	105
Ca (7)	16.00	2.772	450
Na (7)	16.00	2.772	125
Ca (8)	32.00	3.466	440
Na (8)	32.00	3.466	145

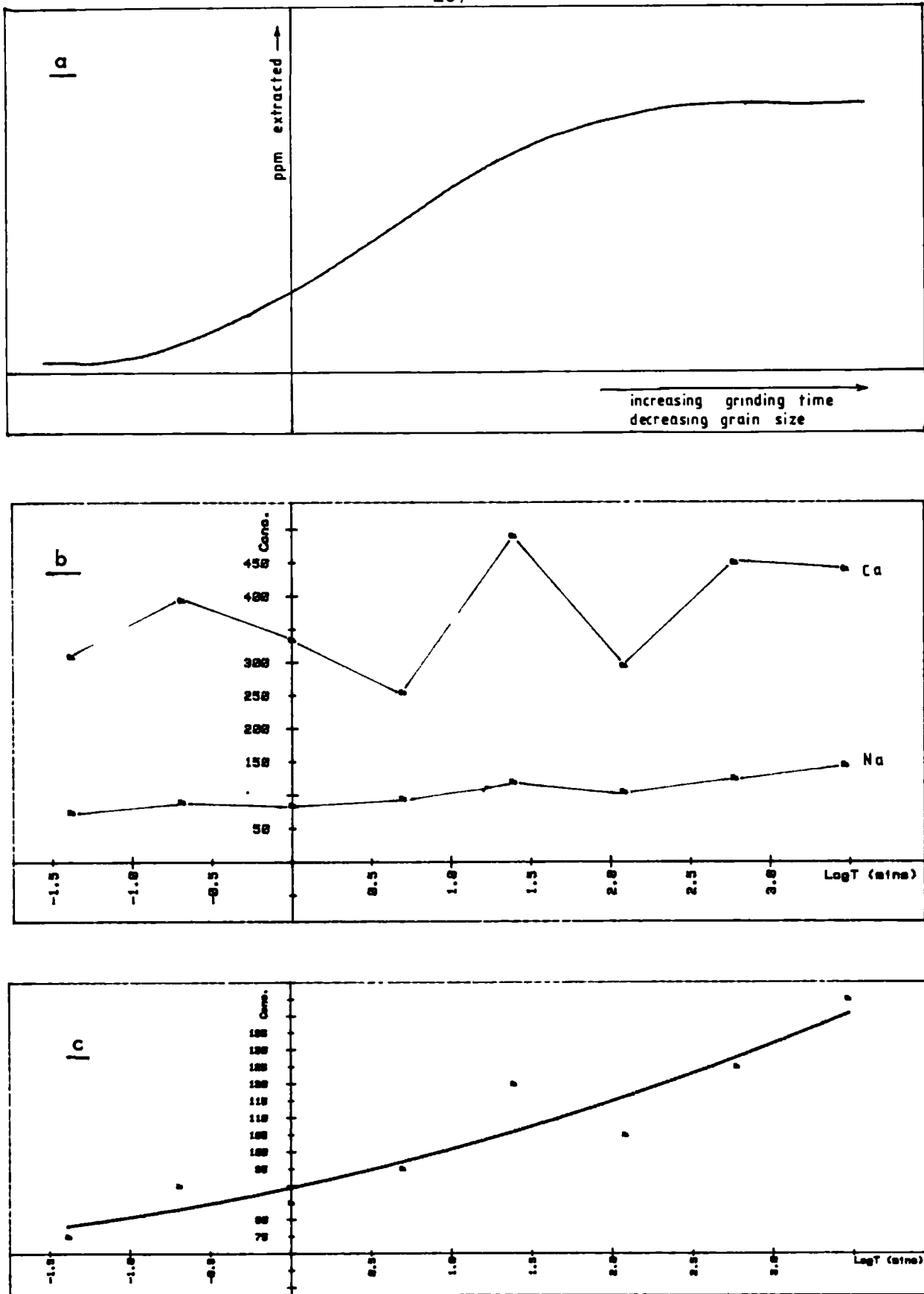


Figure 5.1 Distilled water extractable fraction as a function of grain size (ie grinding time) in calcined sample of flint CL1/30.
a: theory, b: Na and Ca concentrations, c: detail of Na curve.

Clearly, this inclusion-released Na may account for a substantial proportion of the total Na in the flint.

One possible error in the above analysis could be contamination from the grinder. However, following the untimely death of the agate disc during the grinding of a subsequent sample it was possible to test this by measuring the Na content of the agate. This turned out to be only 650 ppm, so it would be necessary for over an eighth of the sample to be contamination to give the observed increase in the analysis. Such a degree of wear of the agate would have been clearly visible were it the case, so contamination cannot account for the observed Na trend.

As a further test of the validity of this interpretation it is possible to estimate the salinity of the fluid inclusions, assuming that all of the sodium in the flint (260 ppm) can be assigned to the inclusions. If it is assumed that about half of the OH^- in the flint is present as molecular water (i.e. about 1% by weight), and that this accounts for all 260 ppm Na, then the water must be about 26 ppt (parts per thousand) Na, equivalent to about 66 ppt NaCl. Bearing in mind the somewhat random choice of 1% total H_2O in the fluid inclusions this figure is in remarkably good agreement (less than a factor of 2 too high) with the 35 ppt of modern, and probably Cretaceous sea-water. In practice it is probable that at least some Na is associated with clay minerals in the flint (see next section below) so the calculated salinity will be in even better agreement with the expected value.

5.2.2 Trace Elements in Other Phases

a) Effect of "White Bodies"

The small grainsize of the constituent silica phases prohibits hand picking of the pure end members but it is possible to investigate their trace element content by indirect means. The most dramatic variation in flint structure is associated with silica recrystallisation to form white bodies, and this conveniently produces an easily visible change in appearance of the flint (from black to white). A series of sub-samples arranged according to colour will therefore represent a sequence of increasing degree of white body-type recrystallisation with lighter tint.

To determine trace element variations associated with white body formation the main part of flint CL1/30 (the same specimen as that used for the fluid inclusion study) was coarsely crushed and then a number of chips hand picked according to their colour. The resulting sequence varies from pure "clean" black flint (I), through slightly cloudy black flint, to fully developed white body (VIII). However, it is important to note that this sequence does not vary systematically: samples I to V are basically black with varying stages of cloudiness (i.e. incipient recrystallisation principally of the interstitial chalcedony), VI and VII are predominantly white with vague areas of relic darker colouration, and VIII is a very coarsely crystalline pure white body.

The trace element composition of these samples is given in table 5.2, and the variation shown graphically in fig. 5.2. There is no clear trend for any individual element with changing colour except possibly Ca which shows a higher concentration in the white bodies. Most of this Ca is easily removed if the ground sample is treated with dilute hydrochloric acid before digestion so it

Trace element variations in flint CL1/30

Sample No.	Ca	Mg	Na	Sr	Mn
I	1150	480	265	4	1.5
II	750	420	240	2	1.0
IIIa	935	590	255	3	1.0
IIIb	65	380	265	3	1.5
IV	965	580	185	2	0.5
V	1190	470	270	3	2.5
VI	1760	470	300	4	2.0
VII	2435	460	210	9	2.5
VIII	1590	190	570	5	1.5

Sample No.	Fe	P	Al	P
I	45	85	450	345
II	50	75	370	330
IIIa	60	71	445	320
IIIb	75	83	470	335
IV	85	81	395	240
V	100	100	350	300
VI	70	75	360	285
VII	80	150	405	305
VIII	120	60	355	270

Table 5.2b
Linear correlation coefficients - flint CL1/3:

[illegible]

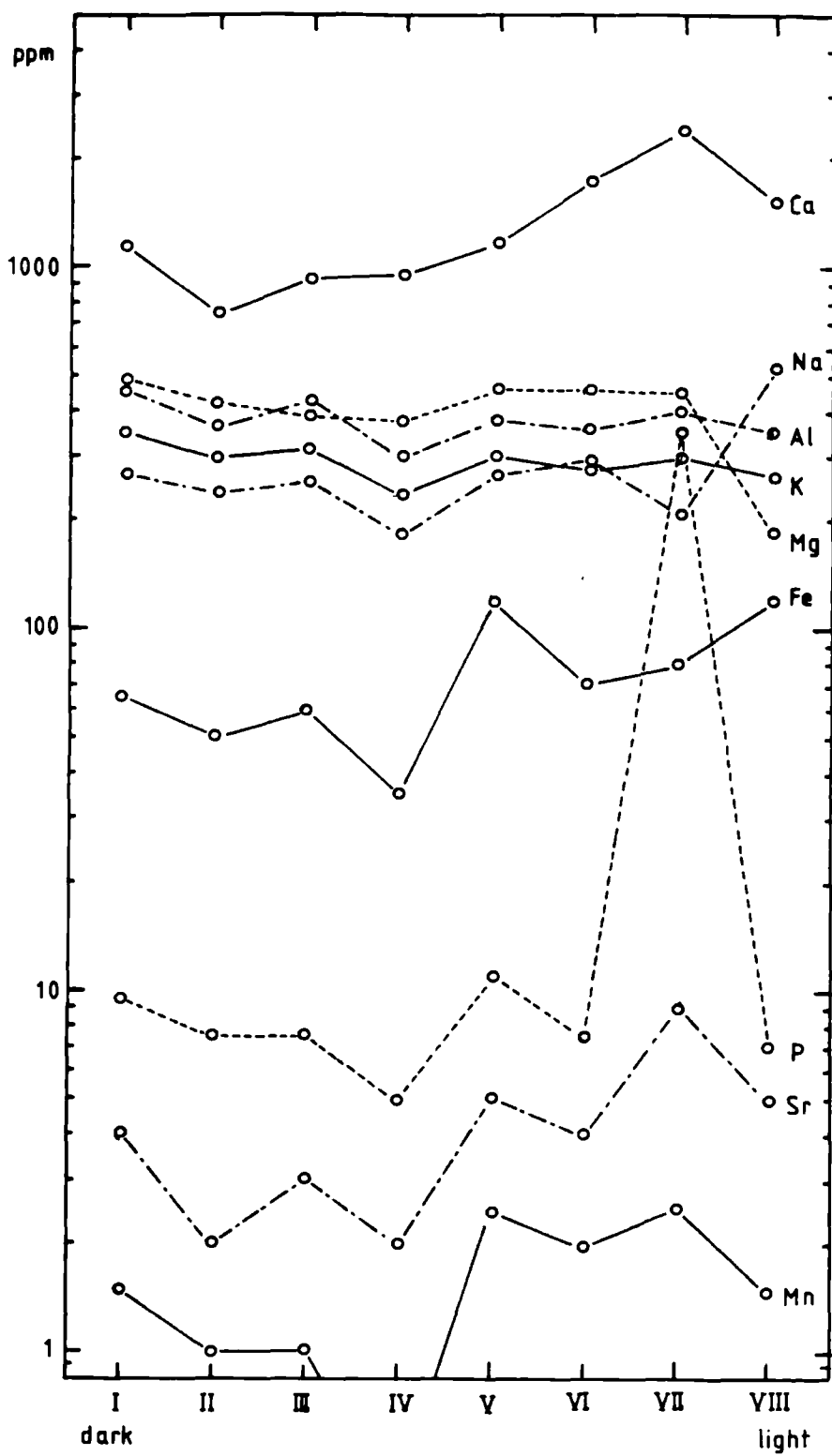


Figure 5.2 Variation of trace element concentrations with colour in subsamples of flint CL1/30, West Clandon Pit, Surrey.

seems reasonable to attribute it to relic calcite in the flint. The higher concentration of relic calcite in the white bodies is probably fortuitous since white bodies tend to form towards the centre of the flint where the original calcite would be more readily preserved. The silicification process, of necessity, involves carbonate dissolution which will in part be controlled by diffusion of the dissolved carbonate away from the site. As flint growth was simultaneous throughout the whole volume of the nodule (as evidenced by the uniform size of the lepispheres, see chapter 4), loss of dissolved carbonate during replacement will be less efficient at the centre of the flint than at the edge, favouring preferential preservation of carbonate at this site.

All of the other elements, at least in the black flint, show a very high degree of covariance (table 5.2b) This is particularly well seen in the K-Al curve (fig. 5.3a) which reflects a correlation coefficient of 0.96 ($n=8$), and in the P-Sr curve (fig 5.3b.) with $R^2=0.89$. This high degree of covariance between elements of very different chemical properties, and the absence of a systematic variation as the silica structure varies, implies that these elements do not reside predominantly in silica mineral phases.

The comparatively high aluminium content with closely associated potassium strongly suggests the presence of illitic clay minerals, and the association of Fe, and to a lesser extent Mg with this probably reflects a glauconitic (s.l.) component to these clays. The correlation of Na with Al in most of the samples probably indicates incorporation of a little Na in the clay structure (? smectite) superimposed on the background of Na in trapped connate waters.

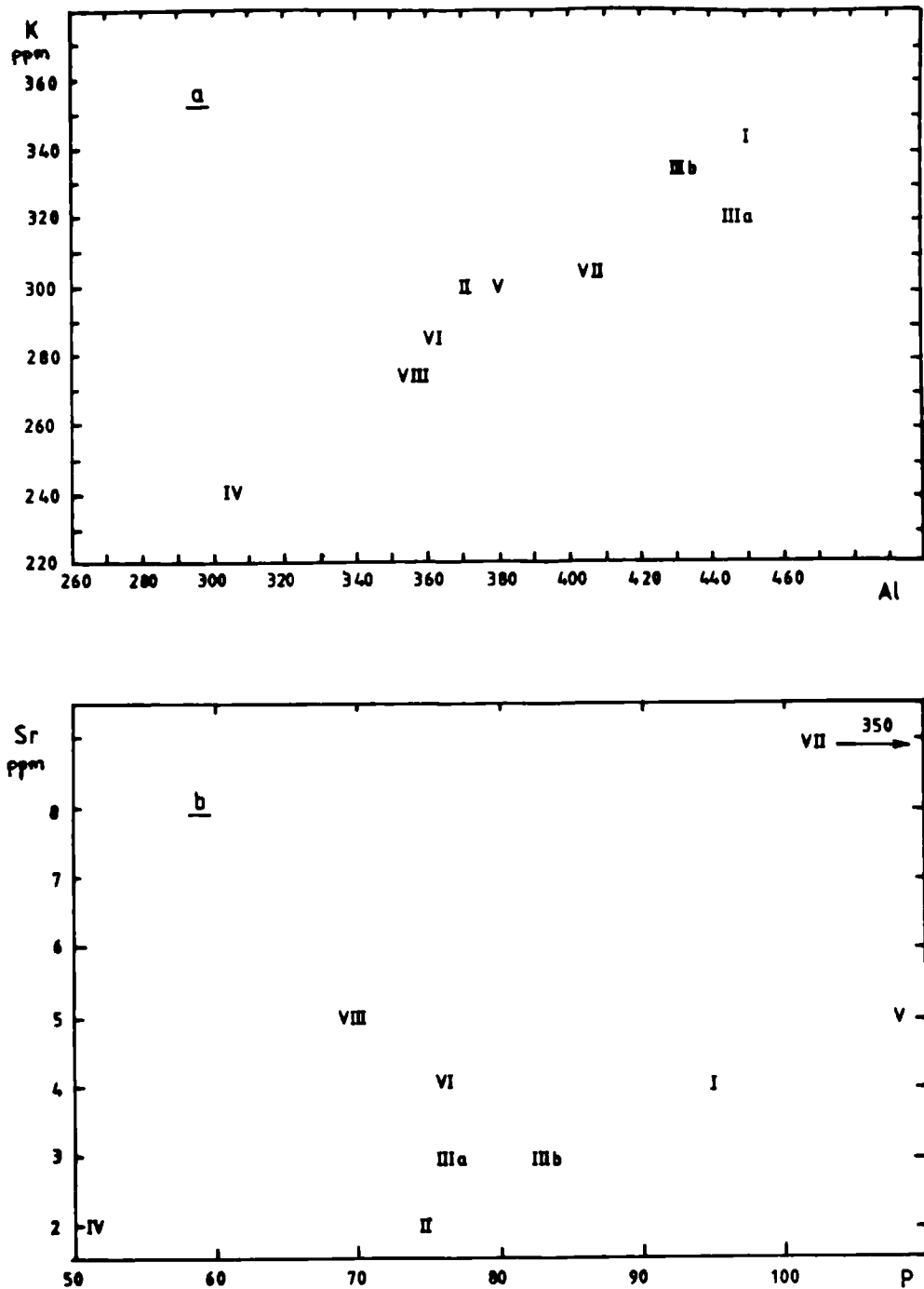


Figure 5.3 Variations of K with Al (indicating illites) and Sr with P (indicating that the Sr is not present in phosphates) in flint CL1/30. West Clendon Pit, Surrey.

The association of phosphorus with the clays is rather unexpected since it is unlikely that this element would be included in the clay lattice in this quantity (more than 10% of the Al content). However the presence of phosphates in the Chalk is well known (see section 3.8) so it seems reasonable to attribute the P in the flint to the presence of phosphates. The anomalous P content of sample VII probably is due to accidental sampling of a coarser phosphate grain, such as a fish bone or tooth, or maybe a burrow lining of fish scales.

The close association of Sr and Mn with the other curves may reflect the incorporation of these elements either into the clays or the phosphates. However, the absence of anomalous levels of these elements associated with the high P content of sample VII rules out phosphates as the prime source. Small amounts of these elements will also be present in the calcite lattice but the calcite content of this flint is generally too low to account for significant Sr or Mn.

The assignment of elements to specific minerals above is based only on covariance between the elements. However, this distribution is entirely compatible with the non-carbonate mineralogy of the host sediment which consists of a mixture of illite, smectite, and a mixed layer illite-smectite with about 30% glauconite layers (see chapter 7). If this trace element assignment is correct, then it implies that the trace element content of flint is inherited directly from the non-carbonate fraction of the original chalk. The variations in absolute concentration of the elements therefore probably represents variations in the original chalk.

b) The Brandon Flint

To investigate further the distribution of trace elements within flints, a two-dimensional study was undertaken. A specimen of black flint from the Turonian of Taflins Quarry, Brandon, Suffolk (BDN) was sawn in half and diamond drill cored at a number of points over its surface. The sample distribution is shown in fig. 5.4 and the chemical data given in table 5.3. Analytical precision for these data is not as good as in other analyses because of the smaller sample size (pooled 2σ based on pairs of analysis was between 1.6% and 6.6 % for all elements other than V and Mn; 19.4% and 9.5 % respectively - see Appendix 3).

The linear regression coefficients (table 5.4) and selected cross-plots (figs 5.5 a-d) show a similar pattern to the Clandon flint described above except that the higher calcite content (i.e. Ca) of the Brandon flint is reflected in a significant Sr and Mn component contributed from relic carbonate. Although there are one or two "wild" points, probably reflecting isolated detrital or authigenic grains of "exotic" minerals, aluminium shows a good correlation with K and Fe (in clays?) and to a lesser extent Mn (which is partly associated with Fe also). There is again a reasonable correlation of Mg with Fe, probably reflecting a "glauconite" component. P and Na appear to be essentially independent of other elements probably reflecting their presence as phosphates and in trapped connate waters respectively.

The spatial distribution of these components is best seen in the contour diagrams (fig 5.6 a-d). Although the number of data points is inadequate for the construction of reliable contours (e.g. the patterns are highly sensitive to individual high concentrations)

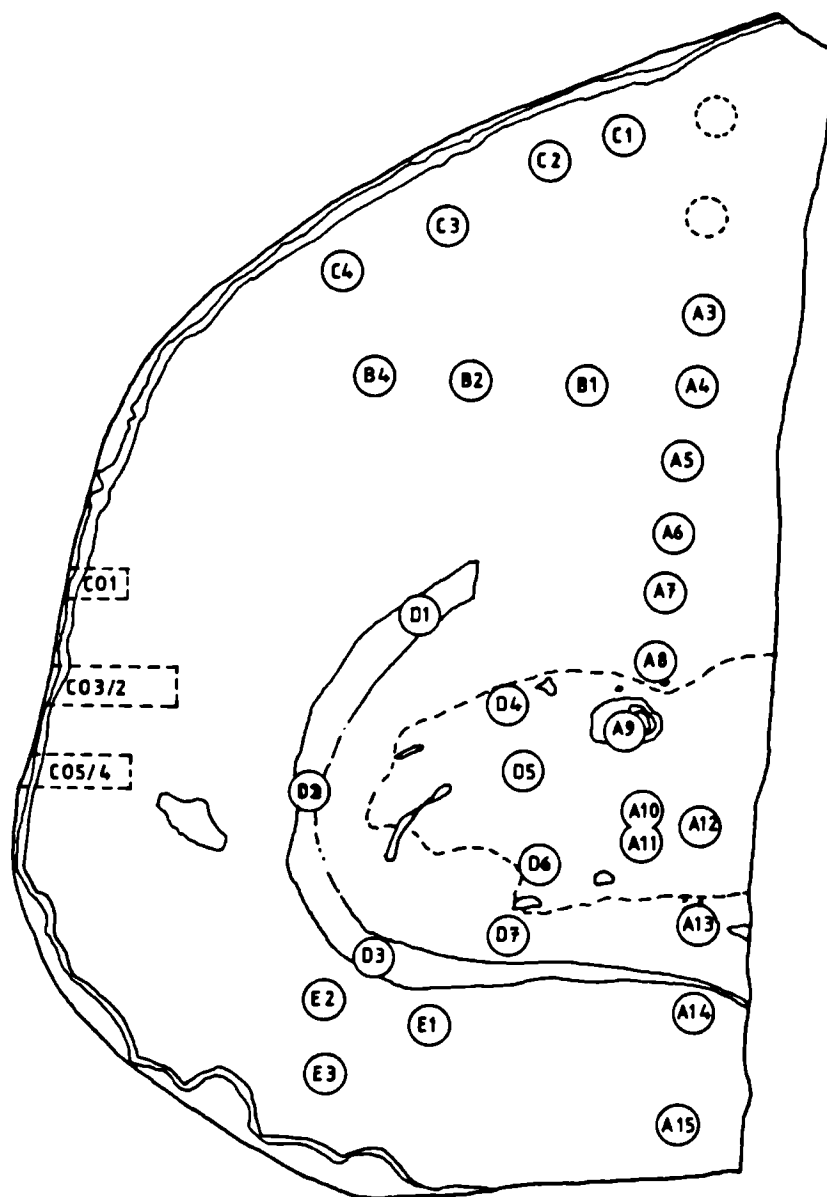


Figure 5.4 Sample distribution for two-dimensional study of flint BDN. Brandon flint series, Brandon, Norfolk.

Table 5.3
Micro elements in Prandion film. ppm

Sample No	Ca	Mg	Na	Cr	Mn	Fe	P	Al	K
A3	1111	130	200	6	2.1	290	220	720	290
A4	655	110	200	8	3.0	260	220	200	400
A5	1135	155	310	9	11.0	290	220	770	465
A6	2000	655	655	9	2.0	150	170	500	270
A7	730	42	570	3	1.1	135	130	530	345
A8	670	37	555	6	0.5	135	115	510	270
A9	7090	82	290	30	4.0	315	175	620	320
A11	1595	201	260	13	12.0	340	270	720	435
A12	2670	425	230	20	29.0	575	555	1180	505
A13	1200	130	300	40	3.5	560	85	885	500
A14	600	330	565	5	2.0	175	125	530	310
A15	415	80	600	5	3.0	240	170	530	290
B1	1700	325	270	16	19.5	440	525	880	450
B2	4630	1620	295	23	33.0	1465	800	1025	755
B4	2405	725	220	14	22.5	720	475	1050	495
C06	4000	1500	185	25	29.0	365	280	540	260
C1	500	425	170	15	11.0	305	280	530	330
C2	590	1550	205	29	22.5	650	390	580	585
C3	1050	1270	205	20	12.0	525	345	940	455
C4	310	400	200	19	12.0	290	260	650	420
D1	1900	890	300	15	13.5	255	250	735	435
D2	140	40	175	8	4.0	140	170	585	250
D4	500	150	175	10	6.5	160	185	520	395
D5	820	210	160	9	5.5	135	115	510	290
D6	1310	500	179	11	15.5	220	195	605	440
D7	2070	415	175	12	12.0	190	175	625	400
E1	600	170	165	16	5.0	130	180	515	335
E2	115	15	150	9	2.1	140	160	480	265
F3	330	90	175	8	4.0	110	170	500	295
D3	245	40	170	8	4.5	155	170	560	350

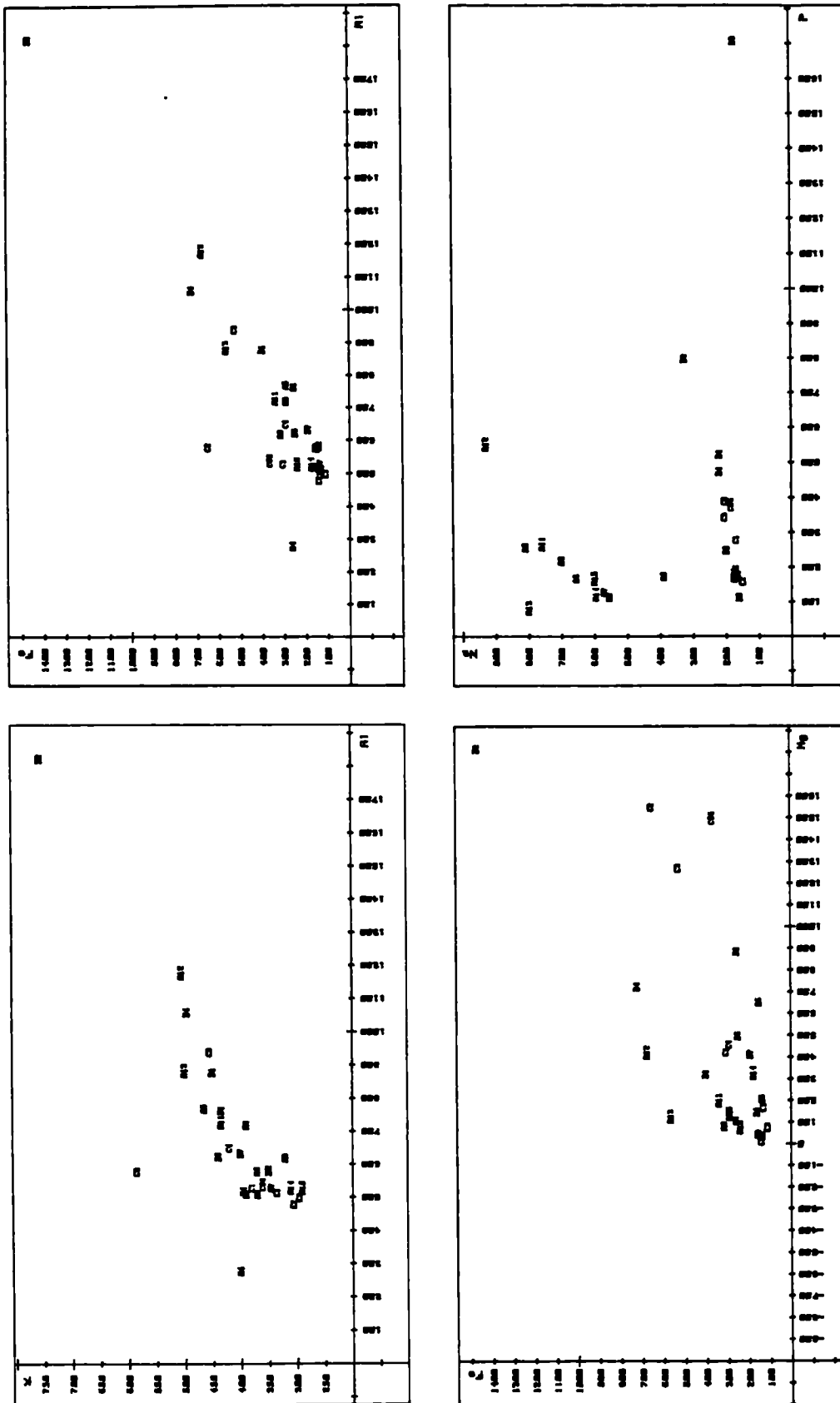


Figure 5.5 Comparison of selected trace elements in Brandon flint. See text for details.
All values in ppm

these diagrams do serve to highlight the variability in the distribution of specific mineral groups.

Calcium (fig 5.6a) represents the distribution of relic carbonate in the flint which, as explained above, occurs preferentially towards the centre of the flint. In the case of the Brandon specimen, Ca is concentrated in two main areas towards the centre of the flint, possibly suggesting two main centres of silicification, and that the overall flint is of a coalesced form. A similar pattern is apparent in the Na diagram (b) reflecting preferential incorporation of saline pore-waters in the silica around the main growth centres. These sites were probably the areas of most rapid silica precipitation so it is not surprising that this is where most water is trapped in the structure. The lower of these Na rich areas has become the centre of white body formation although this is not well developed in the Brandon flints. There is a possible causative relationship here in that the "wet" flint is more susceptible to recrystallisation, but this does not explain the absence of white bodies at the upper site.

The aluminium distribution diagram (fig. 5.6c) is a guide to the variation in clay mineral content of the flint, largely inherited from the precursor chalk sediment (see above). Clays are concentrated in two main areas which occupy similar positions to the silicification centres picked out by Na and Ca. The resulting pattern bears a striking resemblance to bioturbation structures in unreplaced chalk (cf. pl 2D and F). Burrows in the chalk are usually visible only because of variations in the clay mineral content of the chalk so a similar pattern preserved in flint suggests that the trace element distribution was inherited directly from burrow structures in the

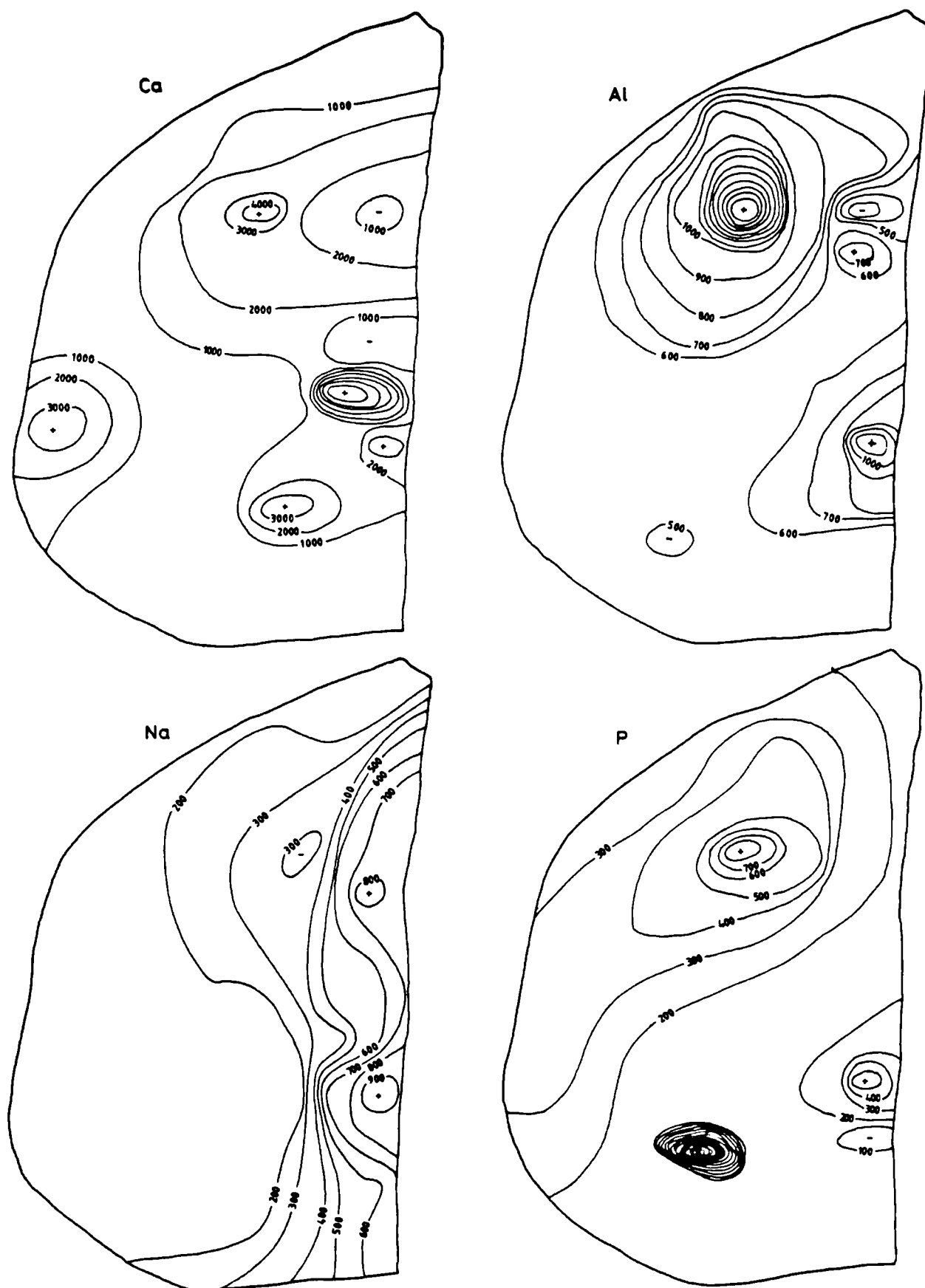


Figure 5.6 Distribution of representative trace elements in Brandon flint specimen BDN. See fig. 5.4 for sample distribution.

original sediment. The coincidence of these relic "burrow " structures with the centres of silicification are further evidence that silicification is intimately associated with bioturbation in the chalk (see chapter 3).

Phosphorus (fig. 5.6d), a reflection of phosphate minerals, shows a similar pattern to Al although there is a superimposed P peak in sample D3, which probably reflects the inadvertant sampling of biogenic phosphate grain (cf. sample CL1/30 VII). This sample also has a lower Al content possibly reflecting dilution of the clay bearing chalk by the phosphate grain. The similarity to the Al distribution suggests that the phosphates in flint are derived from the original chalk, so barring extensive reworking, phosphate growth in the chalk must, in the main part at least, have pre-dated silicification.

5.2.3 Clay Mineral Dilution During Silicification

From the above data it is apparent that the non-carbonate fraction of the chalk is preserved in the flint. Furthermore, once enclosed in flint these minerals are protected from subsequent compaction which affects the enclosing sediment. The dilution of clay minerals in the flint reflects, therefore, the porosity of the host sediment at the time of silicification (fig. 5.7) and can be used to determine the depth of silicification in the chalk sediment. In practice, this method is very sensitive to subsequent clay mineral diagenesis in the host sediment which may alter the apparent dilution and so is not very reliable.

Despite the limitations, the clay mineral dilution effect may be of use if flints can be found in a chalk which contains a high

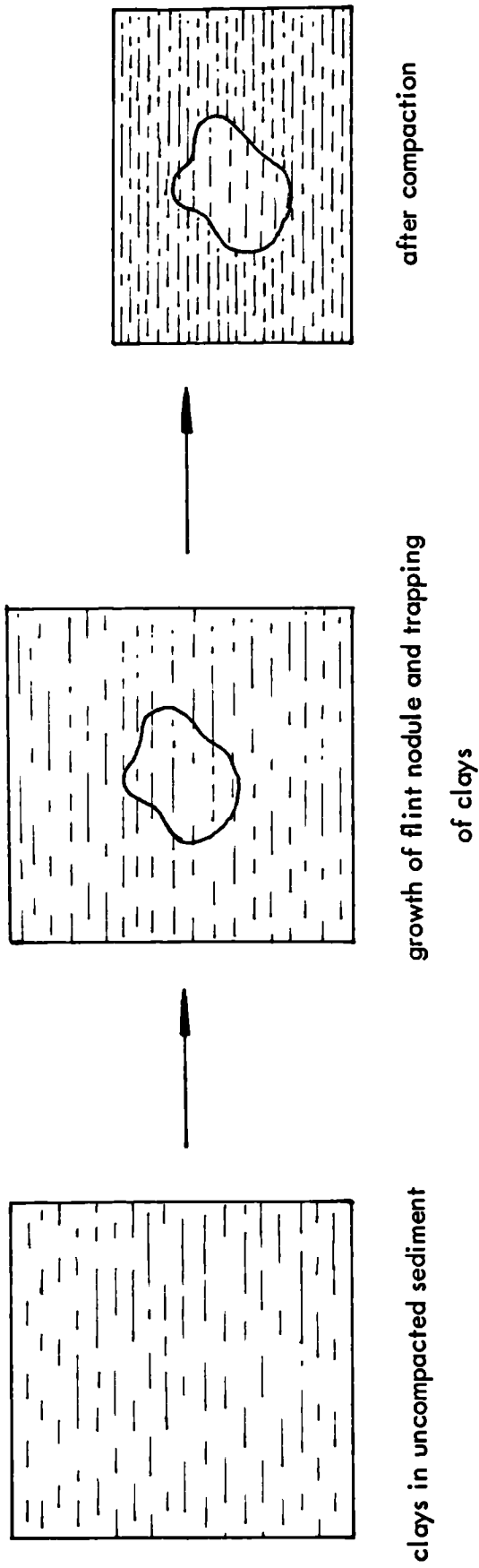


Figure 5.7 Schematic representation of the dilution effect caused by differential compaction of flint and chalk.

proportion of clay minerals, in which case subsequent diagenesis will have a comparatively small effect. Unfortunately such cases are rare but one example has been found at Malincourt, near Cambrai in northern France. The Upper Turonian here represents a shallow water facies of the Paris Basin and the slightly tuffaceous chalk contains a high glauconite content which is preserved in rare flints. Two flints were collected, each with samples of the surrounding chalk, and these were analysed for their potassium content as a tracer for glauconite (table 5.5). In each case a number of sub-samples were analysed as a guide to intra-flint variations in glauconite content.

The two flint samples gave mean K contents of 522 and 499 ppm respectively, compared to 1166 and 1091 ppm for the enclosing chalks ($\sigma=3.9\%$ based on nine analyses of a similar chalk). This corresponds to dilution factors of 0.448 and 0.457. The mean porosity of the chalk was determined by the method of Jeans (1980) as 41.35% so assuming a negligible porosity for the flint, the porosity at the time of silicification can be determined as 73.7% and 73.2% respectively for the two flints. In more detail, allowing for the variation between sub-samples of flint and slight variations in porosity, values of between 71.6% and 75.3% can be obtained.

These "initial" porosities are very high indeed and suggest that silicification occurred very early in the diagenetic history of the chalk, before significant compaction had occurred. There are few reliable data on the compaction rate of chalks but experiments by R. Mortimore (pers. com., 1980) suggest that these figures indicate that the flints were almost certainly solid enough to resist compaction by about 10 m depth of burial. However, any subsequent modifications to the K content of the host sediment may cause errors in these estimates. Also, it is uncertain if the flints formed in such an

Table 5.5

Potassium distribution in Malincourt flints and chalks

	Flint		Chalk		Initial Porosity %	
	K-ppm		K ppm	porosity %	Mean	Range
1.	536	} 522	1093 } 1166 1239 }	41.49	73.7	72.1 - 75.3
	527					
	519					
	534					
	492					
2.	471	} 499	1099 } 1091 1071 } 1104 }	41.54	73.2	71.6 - 74.6
	527			41.02		

atypical facies are characteristic of flints as a whole. These points will be considered in more detail in chapters 6 and 7.

5.2.4 Chemistry of the Cortex and Crust

The chemistry of the cortex and crust of flint has not been studied in any detail but it is relevant to mention it here for completeness.

Table 5.6 gives selected trace element data for two flints from the Turonian Bridgewick Flint Series (fig. 3.3), of Bridgewick Quarry, Sussex. As the cortex is merely an alteration product of black flint there should be no significant chemical difference between the black flint and the cortex. This is indeed the case except for a slightly higher Ca (and associated Sr) concentration in the cortex. This probably reflects slightly less efficient replacement of the host calcite around the periphery of the flint and is unrelated to the cortication process.

Clearly there are no major chemical changes associated with cortication. Despite this however, there must be some degree of change in the oxidation state of at least one component during cortication since the cortex of many Bridgewick Flints takes on a characteristic purple colour, typical of MnO_4^- staining. Interestingly, the Mn concentration in the cortex is below the detection limit of the method used (5 ppm in this case) suggesting that if Mn is the cause of the colour then only very slight traces are required.

In contrast to the cortex, the crust would be expected to be significantly different in chemistry, in that it formed in the unique chemical environment at the very edge of the silicification zone. In the Bridgewick flints this is not the case (table 5.6) but these flints have a very silica-rich crust so do not differ significantly from the cortex.

Table 5.6

Analyses of black flint (bl), white body (wt), cortex (cc) and crust (cr) of two flints from the Bridgewick Flint series, Bridgewick Quarry, Sussex.
(- : not detected)

Sample	Ca %	Mg ppm	Na ppm	Sr ppm	Mn ppm
BR1/4 bl	.331	80	285	5	-
-*- wt	2.810	410	100	43	12
-*- cc	.530	130	340	12	-
-*- cr	1.457	210	321	19	5
BR1/1 bl	.154	120	281	4	17
-*- cc	.340	50	295	7	-
-*- cr	1.477	341	311	24	5

Sample	Fe ppm	F ppm	Al ppm	I ppm
BR1/4 bl	80	110	571	354
-*- wt	90	105	441	325
-*- cc	238	175	741	335
-*- cr	350	200	845	390
BR1/1 bl	110	171	545	311
-*- cc	231	171	730	345
-*- cr	385	250	1040	475

Table 5.7

Trace elements in flints and flint crusts from West Clarendon Pit
(ppm unless stated)

Sample	Ca %	Mg	Na	Sr	Mn
13 flint	.341	80	241	5	4.5
13 crust	19.0	951	318	387	180
21 flint	.410	81	270	5	4.0
21 crust	29.8	1017	251	417	216
30 flint	.075	480	265	2	1.0
30 crust	20.3	521	274	314	146
Host chalk	-	2730	170	595	750

Sample	Fe	F	Al	I
13 flint	50	85	390	275
13 crust	477	225	1790	466
21 flint	155	102	295	255
21 crust	104	361	1921	525
30 flint	50	75	370	301
30 crust	1070	132	1210	699
Host chalk	390	260	875	235

More dramatic differences between flint and crust chemistries are apparent where the crust has a low silica content, such as in flint samples from the Clandon Pit (see above). The chemical data for three crust-flint pairs from Clandon are given in table 5.7, together with figures for a typical chalk from the same quarry. The variations are best seen in a series of elemental cross-plots (fig. 5.8) in which the trace element differences can be related to mineralogical variations. As the crust forms at the boundary between flint and chalk, the composition of the crust in terms of any element pair should fall on a mixing line between the pure flint and chalk end-members (solid lines in fig. 5.8). The relative enrichment or depletion of any element can then be represented by constructing tie-lines between the theoretical and measured concentrations (broken lines in fig 5.8).

For the three flints analysed, there are systematic differences between the theoretical and measured composition (fig 5.8), suggesting that similar diagenetic reactions have occurred in the crust of all three flints. This is best seen in the K-Al diagram which shows that the crust is highly enriched in a K-bearing clay mineral. The ratio of K to Al for the extra mineral is similar to that for the original flint (i.e. all three crusts and the original flints fall along the same line) suggesting that the extra may be clays physically pushed out of the flint during the opal-CT - quartz recrystallisation. Any degree of chemical purging would almost certainly result in a change of chemistry which is not the case. A similar pattern is seen in the Fe-Al diagram although Fe is a little more variable in its behaviour. Such a physical purging of clay minerals from the flint structure will obviously affect the dilution ratios discussed above, but in view of the quantitative insignificance of the crust

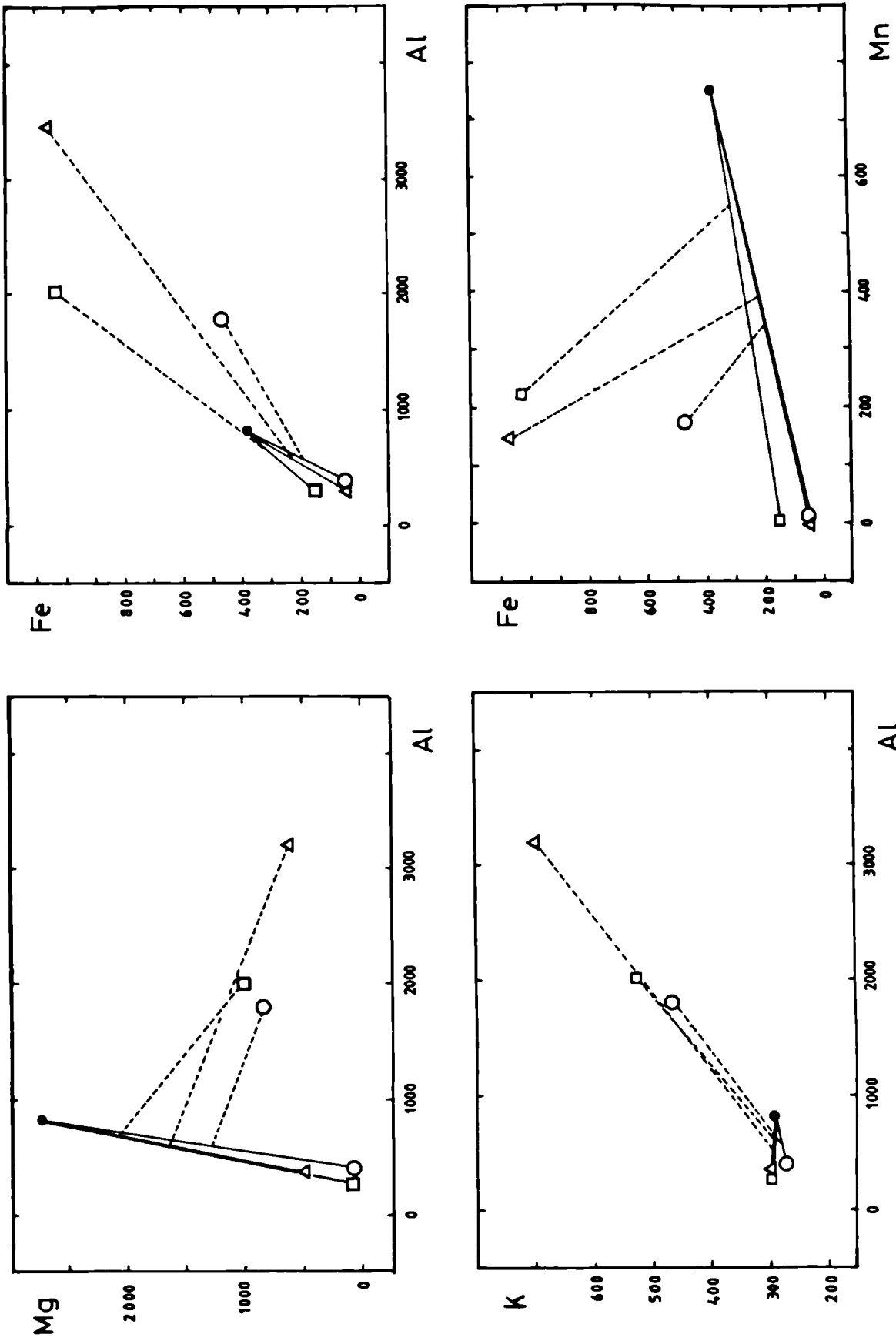


Figure 5.8 Comparison of trace element concentrations in flints and their crusts. Solid lines are tie lines between flint conc. and host chalk (solid circles), broken lines connect crust concentrations with theoretical concentrations based on simple mixing of chalk and flint. ppm.

compared with the flint as a whole, this error will not be great.

The simple physical purging model cannot be applied to Mg or Mn since these elements show a relative depletion in the crust over their theoretical contents. However, in each case the actual values still fall between the two end members so this effect may be the result of preferential preservation of some (Mg and Mn poor) carbonate components during replacement. More data will be necessary to resolve this problem.

In summary, it can be said that the trace element content of flint reflects the chemistry of the original sediment rather than chemical variations in the silica itself. Although flint chemistry cannot be used as a guide to the diagenesis of flints after they form, it may be of use to determine the chemical environment in which the flint formed. This will be the subject of subsequent chapters. However, in order to investigate diagenesis of the silica itself it is necessary to consider the oxygen and hydrogen stable isotope variations in some detail.

5.3 STABLE ISOTOPE VARIATIONS

5.3.1 Background

The use of stable oxygen isotope ratios in carbonates to determine palaeotemperatures is well established (e.g. see review by Savin, 1977) but extensive diagenetic alteration usually makes this method unsuitable in pre-Mesozoic sediments and of almost negligible value for pre-Cambrian rocks. In contrast, the greater durability of cherts has great potential in these cases. Consequently, the oxygen isotope composition of cherts has received considerable attention in recent years as a potential tool in palaeoclimatic studies (Knauth 1973; Knauth and Epstein 1975, 1976; Kolodny and Epstein, 1976; Perry et al., 1978 and Knauth and Lowe, 1978).

Despite its obvious importance, little detail is known about the effects of diagenesis on the isotopic composition of cherts other than that the opal-CT-quartz transition results in a systematic decrease in $\delta^{18}\text{O}$, reflecting recrystallisation at higher temperature during burial (Knauth and Epstein, 1975; Kolodny and Epstein, 1976; Pisciotta, 1981). Quartzose cherts from a variety of sediment types which show an overall progressive depletion in ^{18}O with increasing age (Degens and Epstein, 1962)

have been variously interpreted as indicative of an increasing degree of post-depositional exchange between cherts and ^{18}O depleted ground waters (Degens and Epstein, op.cit); changing isotopic composition of sea water (Perry, 1967; Perry and Tan, 1972); or a higher temperature of early oceans (Knauth, 1973; Knauth and Epstein, 1976; Knauth and Lowe, 1978). However, no one has yet reported attempts to resolve this problem by detailed analysis of a single group of cherts.

By far the most extensive work to date has been that of L. Paul Knauth (Knauth, 1972; Knauth and Epstein, 1975, 1976; Knauth and Lowe, 1978; and others). Based on the $\delta^{18}\text{O}$ and δD of a large number of on-land exposed cherts Knauth (1972; Knauth and Epstein, 1976) was able to differentiate a number of elongated fields for cherts of different ages, which trend sub-parallel to the meteoric water line (fig 5.9). These fields apparently originate from a line defined by $\delta\text{D} = -6\delta^{18}\text{O} + 137$, which Knauth interpreted as the locus of cherts in equilibrium with ocean water of various temperatures. The temperature dependence of the quartz-water fractionation is not well known below 250°C because of kinetic problems in crystallising quartz at low temperatures in the laboratory, but Knauth and Epstein (1975) were able to estimate

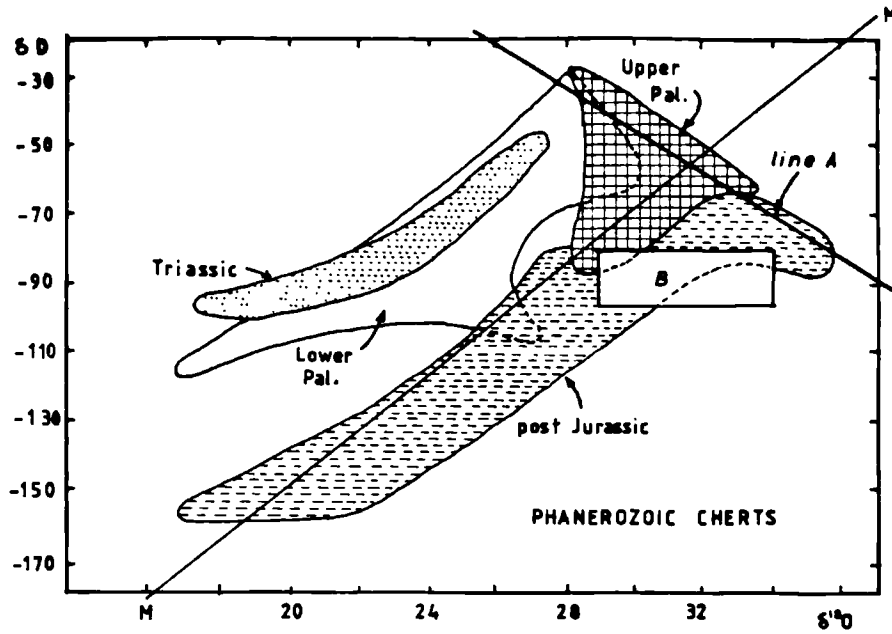


Figure 5.9 δD vs $\delta^{18}O$ for cherts of various ages. *M* represents the meteoric water line, *A* is possible locus of cherts in equilibrium with marine waters of various ages. After Knauth, 1973. *B*: this study.

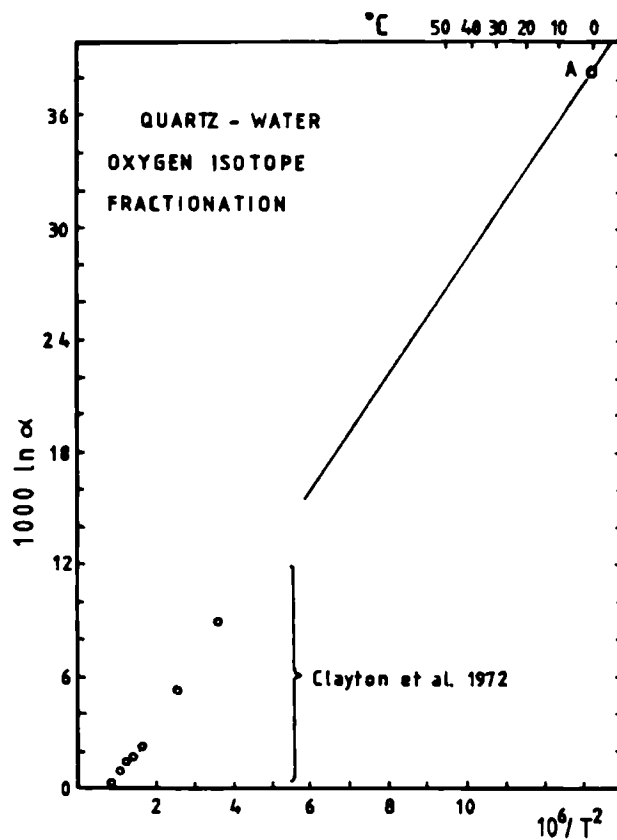


Figure 5.10 Temperature dependance of the quartz-water oxygen isotope fractionation. After Knauth and Epstein, 1975.

this by extrapolating the high temperature data of Clayton et al., (1972) to the composition of a chert believed to have grown at about 0°C (fig 5.10, this work). This yielded the empirical equation

$$1000 \ln \alpha_{\text{water}}^{\text{qtz}} = 3.09 (10^6/T^2) - 3.29$$

from which it was possible to deduce oceanic temperatures of up to 70°C for the pre-Cambrian (Knauth and Epstein, 1976).

The trend parallel to the meteoric water line (fig 5.9) is compatible with the suggestion of Degens and Epstein (1962) that the lighter $\delta^{18}\text{O}$ values are due to increasing degree of equilibration with meteoric waters. More recently however, Knauth (1979) has proposed that it is indicative that the cherts formed at the mixing interface of marine and meteoric waters, analagous to large scale dolomitisation (Hanshaw et al., 1971; Land, 1973; Badiozamani, 1973). Unfortunately, all isotopic work carried out so far has been carried out in the absence of a firm petrographic basis so it is not possible to compare these cherts with oceanic cherts (e.g. those of Knauth and Epstein, 1975) which, although similar in many respects, implicitly must be assumed to have a different origin.

5.3.2 Relevance of Flints to Other Cherts

The petrographic description given in chapter 4 offers a good basis on which to study in detail the effects of diagenesis on a comparatively simple group of cherts. It has already been demonstrated that Upper Cretaceous flints - at least in terms of growth history - are comparable in most respects with deep-sea cherts (i.e. growth of opal-CT lepispheres with later recrystallisation to quartz), and yet, conversely (and somewhat perversely) a small number of flints have been included as "on-land" cherts by Knauth and Epstein (1976)

and Kolodny and Epstein (1976). Furthermore, all the samples analysed for this study fall below Knauth's "line-A", and a significant distance along his "meteoric water trend" (fig 5.9).

Three main questions are apparent from the preceeding discussion of flint petrography: (1) is it possible to differentiate the constituent phases of black flint (lepispheres, chalcedony and skeletal fragments) isotopically ? (2) what is the effect of recrystallisation to form white bodies? and (3) are there any subsequent overprinting effects ? As it is well established that drusy vein and void filling quartz have very light $\delta^{18}\text{O}$ values as a result of growth during deep burial (Knauth and Epstein, 1975; Lancelot, 1973) this material will not be considered further here.

It is relevant to consider the effect of white bodies first.

5.3.3 Effect of White Body Formation

To determine the effects of white body formation on the isotopic composition of flint a specimen of tabular flint from West Clandon Pit was sampled to give specimens of the white bodies and from the black flint (specimen CL2/7, samples A-J (Fig 5.11)). The adjacent slab of flint from the same specimen is shown in plate 8B.

The oxygen and hydrogen isotopic composition of these samples are given with other structural information in table 5.8. The analytical precision of the $\delta^{18}\text{O}$ determinations is poor (.72, .09 and .12‰ difference between replicate analyses of three samples which gave a reasonable yield), but despite this there is a clear depletion in ^{18}O of between 1 and 4‰ in the white bodies relative to the black flint. This is better seen in fig. 5.12 where the "structural" water content of the flint is used as a monitor of the

extent of recrystallisation. Formation of white bodies involves the exsolution of structure-bound water into microscopic fluid inclusions (chapter 4) which are broken down during grinding resulting in an apparent decrease in water content of the sample as a whole. Such reactions are reflected in fig 5.12 as a clear distinction between the original black flint and the white bodies which are characterised by lower H_2O and ^{18}O contents.

There are two possible explanations for the decrease in $\delta^{18}O$ in the white bodies: either recrystallisation occurred at a higher temperature than the opal-CT to quartz transition, or it took place in equilibrium with isotopically lighter pore waters. This latter possibility seems unlikely in this case, since there has been little diagenetic alteration of the chalk which could have significantly affected $\delta^{18}O$ of the pore waters subsequent to the opal-CT to quartz transition.

If recrystallisation took place at a higher temperature than the previous change, then the temperature dependence of the quartz-water fractionation would leave the new silica depleted in ^{18}O . If this is the case, then the temperature can be estimated from the equation of Knauth and Epstein (1975; fig 5.10, this work). Assuming that pore-water $\delta^{18}O$ was approximately that of normal seawater (-1‰ ; Shackleton and Kennett, 1975), the mean $\delta^{18}O$ for white bodies (30.6‰) corresponds to a temperature of about $24.5^\circ C$. This compares well with temperatures quoted by Knauth and Epstein (1975) for deep burial drusy quartz void infillings (quoted as $32^\circ C$ based on $\delta^{18}O_{H_2O} = 0\text{‰}$, equivalent to $28^\circ C$ assuming $\delta^{18}O_{H_2O} = -1\text{‰}$) which are known to be intimately associated with white body formation. However, a possible complication here is the reservoir effect which would

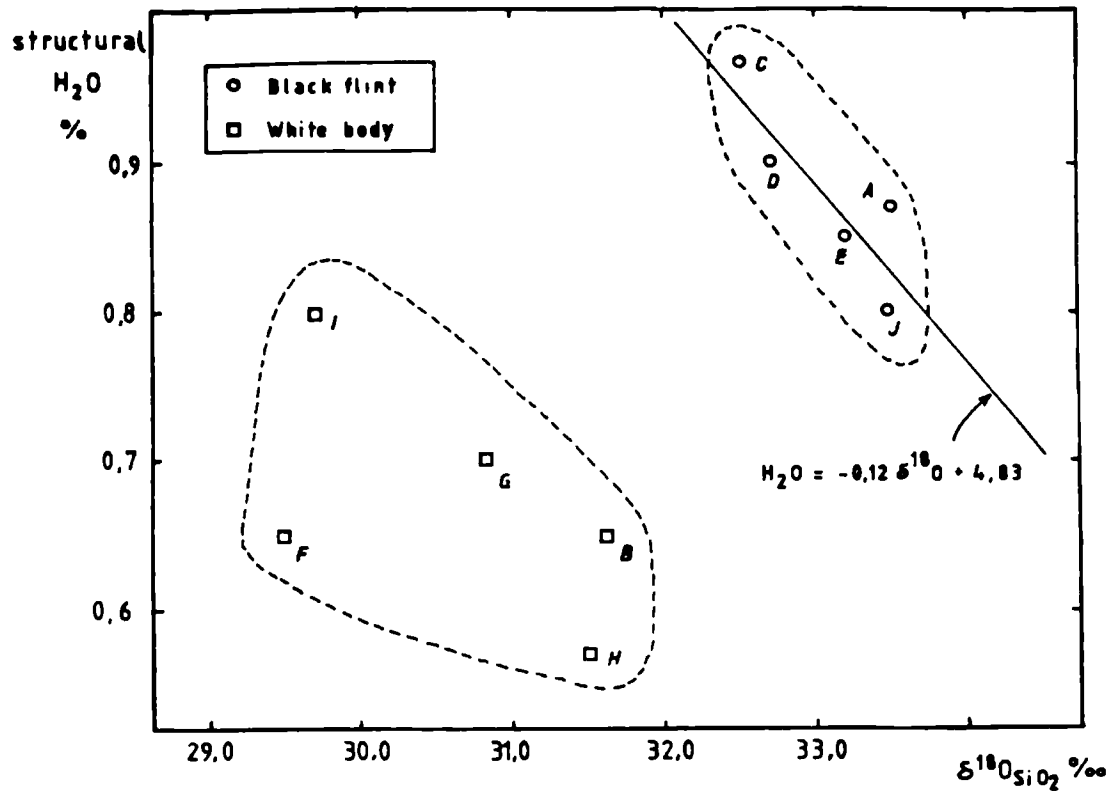


Figure 5.12 Variation of $\delta^{18}O$ with structural water in flint CL2/7, West Clandon Pit, Surrey.

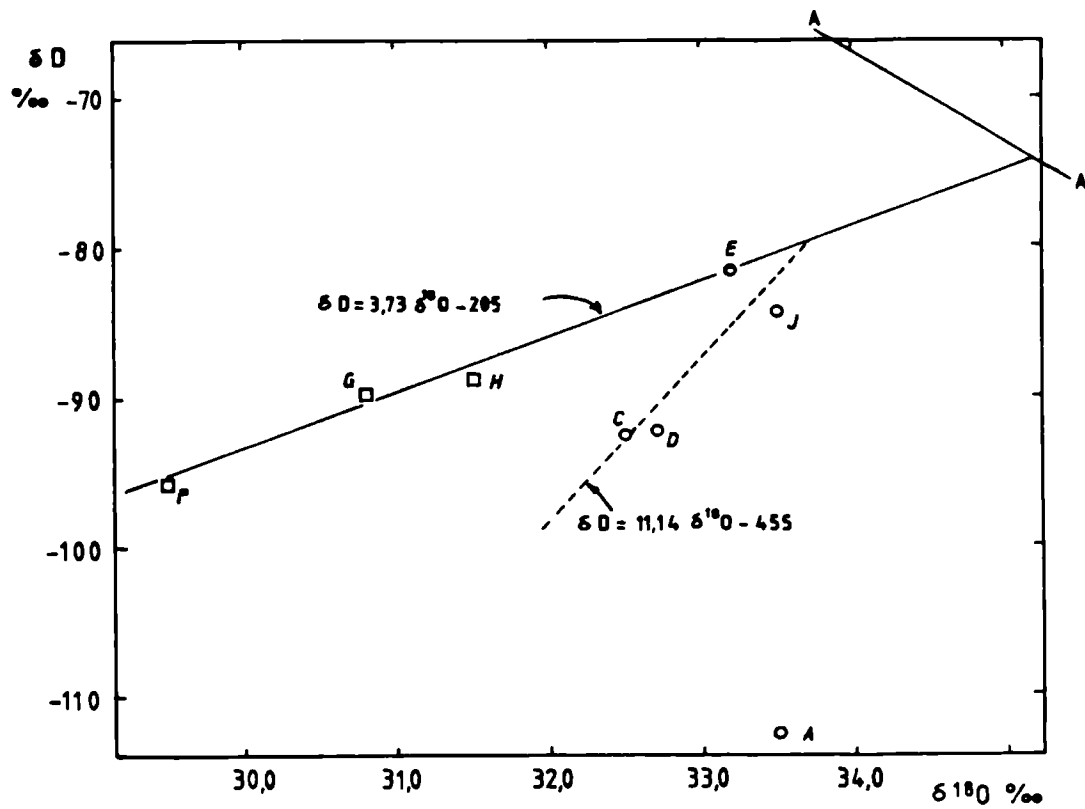


Figure 5.13 δD vs $\delta^{18}O$ in flint CL2/7

occur if there was inadequate exchange of the trapped water in flint with the surrounding pore waters. As the silica becomes isotopically lighter, the balance of the ^{18}O must be taken up by the pore waters within the flint. If the system is closed with respect to external pore waters then subsequent recrystallisation will take place in equilibrium with pore waters which become progressively enriched in ^{18}O . The net effect will be to buffer the effect of temperature on the ^{18}O of the silica, and the above temperatures must be considered as minimum estimates. It is possible that the range of $\delta^{18}\text{O}$ for the white bodies is not a reflection of recrystallisation over a range of temperatures but the effect of differing degrees of buffering at a single temperature.

To find out more about the variation in the stable isotope ratios in the flint, δD was determined on the same samples. These analyses were carried out during the development of the isotope extraction line so only 7 of the samples were successfully analysed. An eighth sample (A) was analysed but produced a δD value of -112.4‰ which is substantially lower than any other flint analysed and so is believed to be erroneous. Analytical precision is difficult to ascertain but is believed to be within $\pm 1\text{‰}$ (see Appendix 4).

The δD values are compared with $\delta^{18}\text{O}$ in fig 5.13. There is again a clear distinction between the white and black flint. Also shown on this diagram is "line A" of Knauth (1972) which supposedly represents the $\text{H}_2\text{O} - \text{SiO}_2$ equilibrium curve (see above). The position of the CL2/7 samples below this line would suggest some degree of fresh water participation during chert genesis if the hypothesis of Knauth (op.cit) is correct.

With only four data points, the apparent line defined by the white bodies (F, G & M) and black flint sample E must be considered tentative. However the range in values ($\sim 4\%$ in $\delta^{18}\text{O}$, 12% in δD) is well outside analytical error so this line must have some significance. This suggests that the recrystallisation process which caused the lower $\delta^{18}\text{O}$ and H_2O values is accompanied by a concomitant decrease in δD . If this is purely a temperature effect (i.e. no reservoir buffering) then the apparent temperature dependence of δD can be estimated as $-0.89\text{‰}/^\circ\text{C}$ over the temperature range $18\text{--}34^\circ\text{C}$. However, this variation is really representative of the temperature dependence of the isotopic fractionation between the hydrogen of molecular water and the hydrogen of the mineral hydroxyl groups, and is, for no apparent reason, of the opposite sense to the water-hydroxyl fractionation for all other hydroxyl bearing silicates so far determined (see Savin & Epstein, 1970; Friedman and O'Neil, 1977). This seems very unlikely in view of the overall similarity in bonding style between the minerals and their OH groups, and suggest that some other process must control δD in cherts.

As an alternative, the apparent temperature effect can be explained in terms of a closed system model. The formation of white bodies involves primarily the exsolution of structure-bound hydroxyl groups into molecular water filled fluid inclusions (chapter 4). There is therefore a fundamental change in the relative size of the hydroxyl hydrogen reservoir with respect to the molecular water reservoir within the flint. If for example the flint starts with equal amounts of hydroxyl hydrogen and water hydrogen, the transfer of 50% of the isotopically lighter hydroxyl hydrogen to water will result in a substantial decrease in the overall δD of the water

(equivalent to about 30‰ assuming the water starts with $\delta D = 0\text{‰}$ and hydroxyl hydrogen starts as -90‰ , typical value for black flint). If the system now comes to equilibrium, even allowing for a large temperature controlled decrease in δD the hydroxyl group will still end up more depleted in D because it has come to equilibrium with water which is itself depleted in deuterium.

If reservoir buffering is the cause of the hydrogen isotope variations, then the spread of $\delta^{18}O$ in the samples cannot easily be attributed to buffering of the oxygen isotope system since the most highly buffered sample with respect to hydrogen (sample F) would be the least buffered with respect to oxygen. A possible alternative here is that the oxygen system is indeed buffered, but that the variations in δD are the result of a kinetic isotope fractionation involving the preferential loss of the light isotope from structural sites in the silica, without subsequent re-equilibration with molecular water. Unfortunately, it is not possible to resolve this problem with the data currently available, although it is likely that the solution lies in the bonding state of the hydroxyl groups and molecular water within the flint. Possibly δD represents in part the isotopic composition of molecular water physically adsorbed on the chemisorbed hydroxyl layer.

5.3.4 Stable Isotope Variations in Black Flint

In addition to the clear distinction between the black flint and white bodies, figure 5.12 also suggests a possible inverse relationship between $\delta^{18}O$ and structure bound water concentration within the black flint samples. If real, this would suggest that the "wettest" silica (ie the interstitial chalcedony: Chapter 4)

has a lower average $\delta^{18}\text{O}$ than the remaining silica (ie the lepispheres). However, with the current data set it is unwise to attach much reliance to this relationship, although it will be considered in a little more detail below.

The black flint samples are also shown on the $\delta\text{D}-\delta^{18}\text{O}$ plot (fig. 5.13), and ignoring sample A (see above) lie on a very poorly defined trend along $\delta\text{D}=11.1 \delta^{18}\text{O}-455$. With only four data points and the possible errors involved this correlation scarcely can be considered significant but it is important to note that all of the black flint samples fall on or below the line defined by the white bodies. This strongly suggests the variations in the isotopic composition of the black flint samples are the result largely of processes acting subsequent to white body formation during deep burial.

In order to confirm the above relationship, and to investigate in more detail the isotopic variations in black flint, a number of sub-samples from the main Brandon specimen (BDN - see section 5.2.2) were analysed.

The specimen was sampled by coarsely crushing a slab of flint and HF etching the resulting flint chips. This enabled hand picking of samples with different lepisphere-chalcedony ratios. All samples contain about 5% skeletal fragments. The amount of silica affected by the etching process is negligible compared with the total volume of each chip so there will be no significant effect of this process on the isotope ratios.

The results of the isotopic determinations together with T.G. data are given in table 5.9. These data are of higher precision than the CL2/7 samples with a mean difference in $\delta^{18}\text{O}$ between replicates of 0.05‰.

Table 5.9
Structural data and isotope ratios in
Brandon flint "BDN"

Sample	% leps	At.H ₂ O %	St.H ₂ O %	§180	§D
1	40	.30	1.00	32.85	-82.0
2	45	.21	1.25	32.54	-86.0
3	50	.32	1.38	32.47	-89.5
4	60	.30	1.10	32.38	-86.0
5	55	.21	1.31	32.37	-89.3
6	60	.20	1.29	32.60	-85.8
7	65	.24	1.22	32.64	-85.5
8	70	.22	1.10	33.00	-83.0
9	80	.40	1.62	32.28	-93.9
10	85	.26	1.18	32.55	-90.8
11	85	.32	1.44	32.35	-93.4

Table 5.10
Initial isotope composition of Brandon
flint fractions, based on regression data

Sample	% leps	St.H ₂ O %	§180	§orig.	$\Delta \delta^{18}O - \delta^{18}O_{orig}$
1	40	1.00	32.85	32.78	.07
2	45	1.25	32.54	32.73	-.17
3	50	1.38	32.47	32.98	-.51
4	60	1.10	32.38	32.52	-.14
5	55	1.31	32.37	32.82	-.45
6	60	1.29	32.60	32.78	-.28
7	65	1.22	32.64	32.82	-.16
8	70	1.10	33.00	33.06	-.06
9	80	1.62	32.28	33.13	-.85
10	85	1.18	32.55	33.19	-.64
11	85	1.44	32.35	33.19	-.84

The oxygen isotope composition of the samples is plotted against the proportion of lepispheres in fig. 5.14. Clearly there is no correlation whatever, indicating that there is no significant difference in $\delta^{18}\text{O}$ between the lepispheres and the chalcedony. As the $\delta^{18}\text{O}$ of quartz cherts reflects the temperature of the opal-CT to quartz inversion, (see Knauth and Epstein, 1975; Kolodny and Epstein, 1976) these data imply that the chalcedony must have recrystallised from an opal-CT precursor at the same time as the lepispheres. This is in agreement with the petrographic investigations (chapter 4) which suggest that chalcedony growth had probably finished before this inversion.

Figure 5.15 shows the relationship between the structure-bound water content and the $\delta^{18}\text{O}$ of the samples. Here, also, there is a very wide scatter of data. The best fit regression line ($\text{H}_2\text{O} = -.4 \delta^{18}\text{O} - 13.8, R^2 = -0.56, n = 11$) is not at all significant although if the solitary point in the bottom left of the field (sample 4) is ignored this fit improves substantially ($\text{H}_2\text{O} = -0.5 \delta^{18}\text{O} + 17.2, R^2 = -0.75, n = 10$). There is no obvious reason why sample 4 should be anomalous although it does fall a little way along the "white body" line if δD is considered (see below). Possibly therefore the low H_2O and $\delta^{18}\text{O}$ values are the result of a small degree of recrystallisation. The trend of the remaining samples may be taken as a possible indication that a higher structural water content correlates with a lower $\delta^{18}\text{O}$ (cf. CL2/7 samples) but in the absence of better data little reliance can be attached to this association.

The data for the Brandon flint are added to the $\delta\text{O}/\delta^{18}\text{O}$ data for sample CL2/7 in fig. 5.16. Also shown on this figure is the trend of the meteoric water line, and "line A" of Knauth (op. cit.).

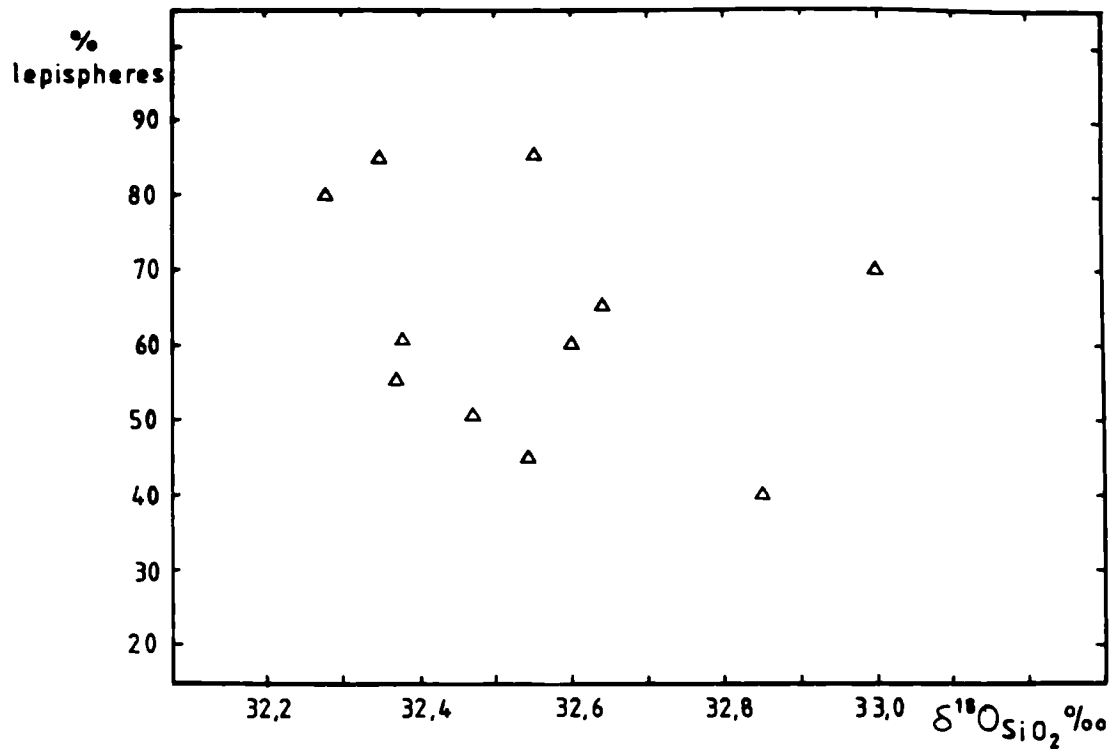


Figure 5.14 $\delta^{18}\text{O}$ vs % of lepispheres in subsamples of Brandon flint BDN, Brandon, Norfolk.

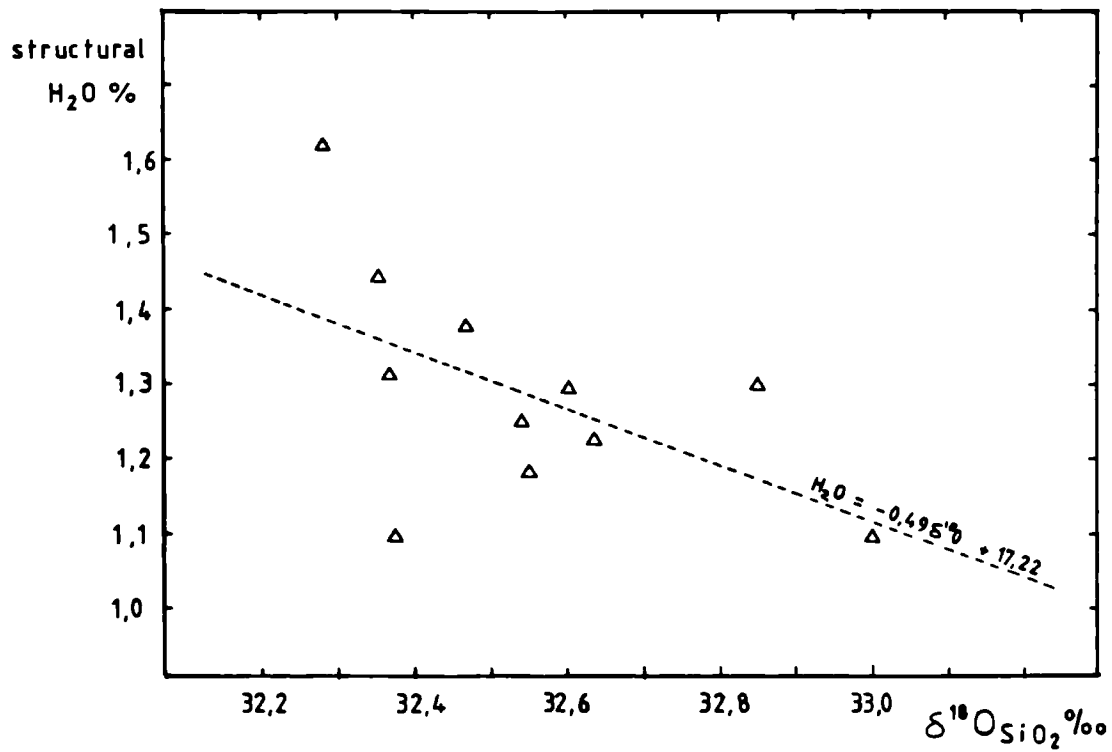


Figure 5.15 Structural water vs $\delta^{18}\text{O}$ in Brandon flint

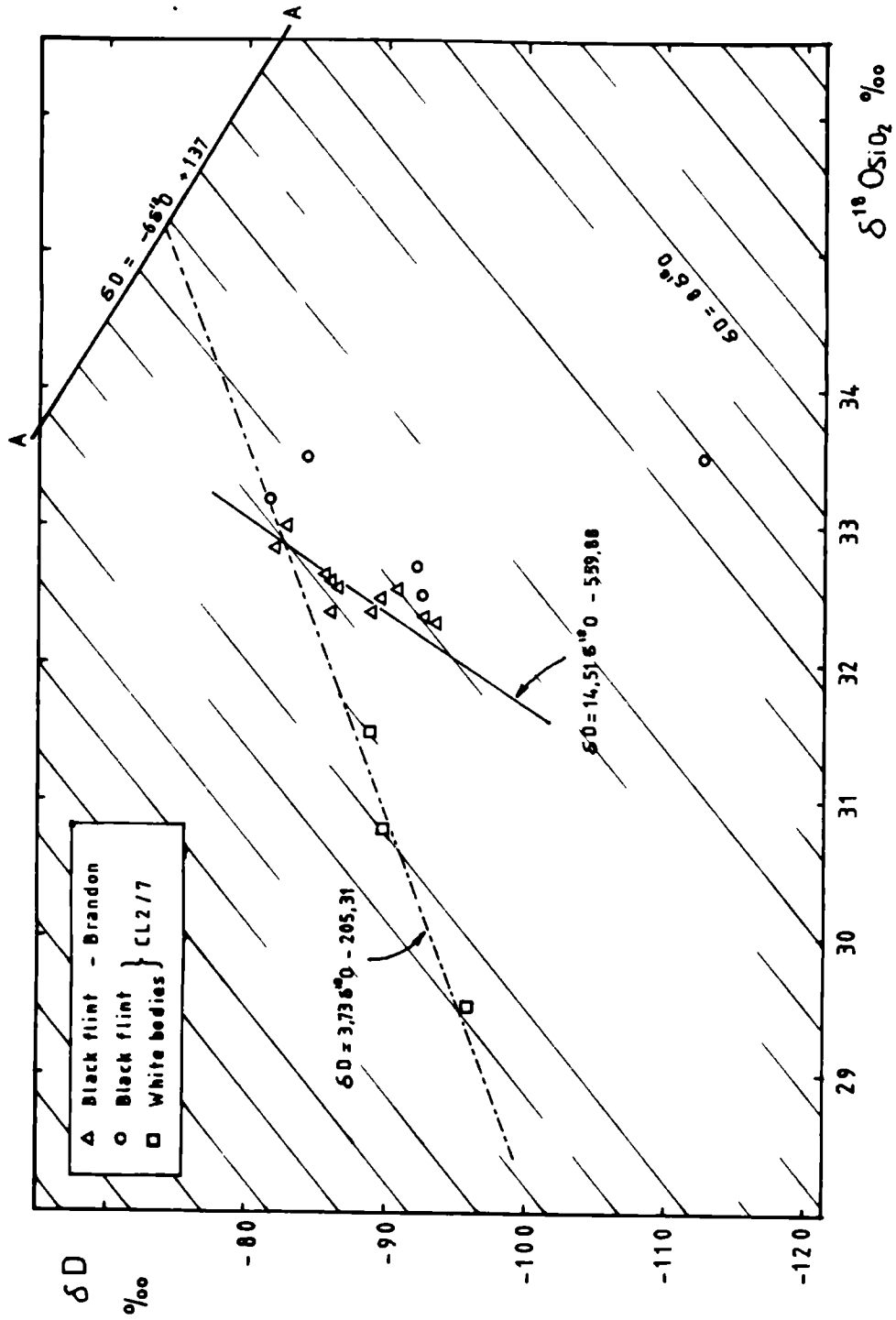


Figure 5.16 δD vs $\delta^{18}O$ for all flints analysed for this study. Pervasive oblique lines are drawn parallel to the meteoric water line. 'A' is line A of Knauth (1973).

To within analytical error, all of the Brandon samples fall below the line defined by the white bodies of CL2/7, and occupy a field in approximately the same position as the black flint samples. The best fit regression line through the Brandon samples ($R^2 = 0.66$, $n = 11$) has a slope of 14.5 which, within the analytical errors involved is not too dissimilar to the slope of 11.1 obtained for the CL2/7 black flint samples. The slight offset of the two lines (BDN has slightly lighter $\delta^{18}O$) possibly is the result of analytical error since the analytical procedure changed slightly between measurement of the two data sets (in particular the BDN samples were "pre-fluorinated" to remove structure-bound water and atmospheric contamination, prior to the main fluorination: see Appendix 4 for details).

The spread of these data points, below the meteoric water line, is of great significance since it suggests that the current isotopic composition of the black flint was acquired after the recrystallisation which formed the white bodies. The alternative possibility, that the white bodies formed from a highly specific sub-group of the black flint, (roughly equivalent to the composition of samples BDN 1, BDN 8 and CL2/7 E) is very unlikely as, in all other respects these samples are structurally no different from the other samples which did not form white bodies.

It is known from petrographic and oxygen isotope evidence (chapter 4 and section 5.3.3 above) that white bodies formed by local recrystallisation of the flint structure during burial, after the opal-CT - quartz inversion, so any subsequent alteration to the isotope composition of the remaining black flint suggests either a subsequent structural reorganisation of the silica (during still deeper burial or during uplift), or some degree of re-equilibration

with isotopically light pore waters. The first of these possibilities seems unlikely since the change in isotopic composition appears to be unrelated to any of the thermogravimetric or optical properties of the silica, which would almost certainly be affected by any structural change in the silica. The second explanation, equilibration with isotopically light pore waters, is more attractive since this need not result in any physical change to the silica.

Given that isotopic exchange is the cause of the variation in the black flint, then this probably is related to the infiltration of meteoric water during tectonic uplift since the chalk sediment has not undergone any diagenesis that could cause a substantial depletion of D and ^{18}O in the pore waters subsequent to the formation of white bodies. Stable isotope exchange is well known in more disordered forms of silica such as diatom valve silica (e.g. see Lebeyrie and Juillet, 1982) so it seems reasonable that the more ordered but still somewhat hydrated silica in flint is also susceptible.

The slope of the alteration line may be rather steeper than the meteoric water line because not all of the silica oxygen is readily exchangeable whereas the hydrogen is present entirely as water or hydroxyl groups which will readily exchange (cf. "exchangeable" and "non-exchangeable" silica in diatoms: Lebeyrie and Juillet, 1982). From the slope of the alteration trend it is theoretically possible to calculate the percentage of exchangeable silica for any given flint, although this will need more reliable data than are currently available.

If it is true that at least some of the isotopic variation in the black flint is due to partial exchange with meteoric waters

then it should be possible to regress the samples back along the alteration line to meet the white-body trend, and so to deduce the original isotopic composition, before alteration. The results from this extrapolation ($\delta^{18}\text{O}$ orig) are given in table 5.10, along with $\Delta \delta^{18}\text{O} - \delta^{18}\text{O}$ orig, the magnitude of the alteration as expressed as a shift in the $\delta^{18}\text{O}$ of the sample.

There is no clear relationship of either parameter to the lepisphere proportion (table 5.10) but, as shown in fig. 5.17, the original isotopic composition does appear to be related to the structure-bound water content of the flint. The scatter of all the data together is rather great but if only samples with less than 70% lepispheres are considered (samples 1-7) there is a clear positive relationship between $\delta^{18}\text{O}$ orig and $\text{H}_2\text{O}_{\text{ST}}$ ($R^2 = 0.84$, $n = 7$). Samples with a dense population of lepispheres are usually found towards the centre of flints, and are consequently more susceptible to recrystallisation (chapter 4) so it is perhaps not surprising that samples rich in lepispheres fall away from the main trend. However, even samples 9 and 11 are not altered significantly, and assuming only samples 8 and 10 are anomalous the correlation is still good ($R^2 = 0.82$, $n = 9$).

If true, the possible correlation of $\delta^{18}\text{O}$ orig with $\text{H}_2\text{O}_{\text{ST}}$ has important implications. Firstly, the absence of a correlation of any parameter with the lepisphere/chalcedony ratio suggests that after initial precipitation, these two phases behave similarly. In other words the nature of the opal-CT - quartz transition is independent of the original precipitated morphology. Secondly, the correlation of $\delta^{18}\text{O}$ with $\text{H}_2\text{O}_{\text{ST}}$ suggests that the rate of this inversion is an important factor in determining the isotopic composition of the black flint. The water content is a measure of the structural

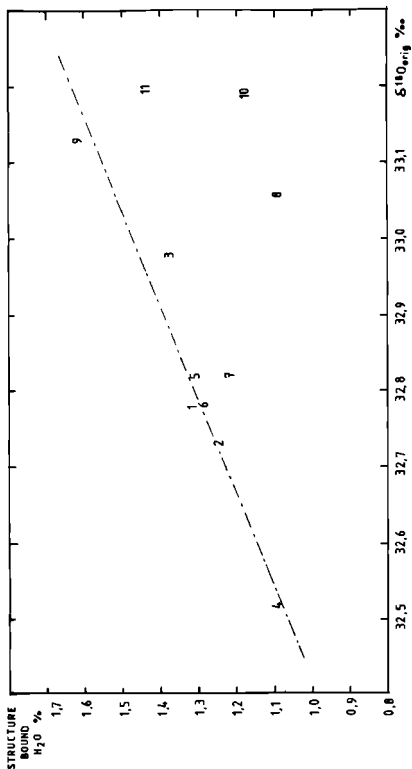


Figure 5.17 Relationship of structure-bound water content to $\delta^{18}\text{O}$ of black flint after correcting for late diagenetic isotopic overprinting.

disorder of the silica (see chapter 4), which is itself controlled primarily by the rate of precipitation, or in this case the opal-CT - quartz inversion. A lower H_2O content in samples suggests slower recrystallisation and this results in a lighter $\delta^{18}O$. This may be caused either by the recrystallisation continuing until greater depth (i.e. higher temperature) or possibly to a decreased significance of the reservoir effect (i.e. slower recrystallisation allows greater exchange with pore-waters outside the flint nodule).

Although more data are required to test the models proposed above, it is clear that the $\delta^{18}O$ of a chert is not controlled only by the temperature of the opal-CT to quartz recrystallisation, or by the isotopic composition of the pore-waters in which it formed. In the first instance, $\delta^{18}O$ is dependant on the rate of the opal-CT - quartz inversion as well as the temperature and pore-water isotope ratios. Following this, further recrystallisation may lower both $\delta^{18}O$ and δD , and the extent of this appears to be controlled in part by the degree of isotopic exchange with surrounding pore waters during the change.

Finally, during uplift, the recrystallised silica is then susceptible to isotopic exchange with meteoric waters. Possibly the apparent "meteoric water" trend of Knauth (1972) is really a function of these latter two effects.

6. GEOCHEMISTRY OF PARAMOUDRAS

6.1 INTRODUCTION

Paramoudras are large columnar, barrel or pear shaped flints, characterised by a cemented chalk interior containing a central pyritised, and sometimes glauconitised, vertical burrow (fig. 6.1). Although the flint in paramoudras is atypical, in that it occurs as vertical cylinders rather than horizontal sheets, these objects offer a unique opportunity to study flint formation in close association with all the other major diagenetic changes affecting the chalk, i.e. pyritisation, glauconitisation, phosphatisation and calcite cementation.

The origin of paramoudras is not known with any certainty, but the well-cemented chalk interior and abundant pyrite, both associated with the central burrow, suggests that sulphate reduction of organic matter in the burrow is a key reaction. The possibility that other organic matter oxidation reactions have also had an effect cannot be discounted but the contribution of these is probably not great (chapter 3). For instance, apart from a few rare silicified fossil fragments, which may be the result of very localised aerobic decay, widespread carbonate dissolution near the burrow is absent, suggesting that aerobic oxidation was only important very near to the sediment surface where the CO_2 released could diffuse back into overlying seawater. In addition, the paramoudra clearly formed very early in the diagenetic history of the chalk (see above), and in a comparatively organic-poor sediment such as this, very little if any, organic matter would have been preserved down into the zone of bacterial fermentation.

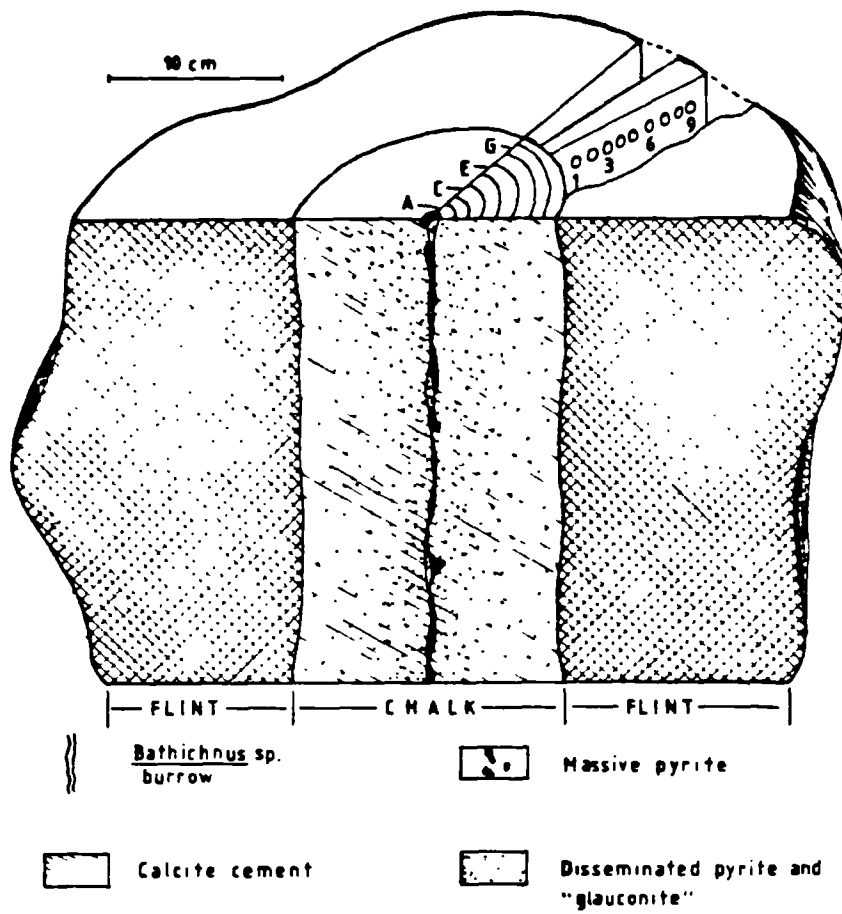


Figure 6.1 Sample distribution from paramoudra CA/1.

Upper Campanian, Caister St. Edmunds, Norfolk.

The major driving force for paramoudra formation would therefore appear to be sulphate reduction of organic matter in the central burrow. It should be possible to determine the precise chemical affects of these reactions on the surrounding sediment by looking at the trace element distribution in this area. The paramoudra described here as a test case comes from the Upper Campanian of a quarry near Caister St. Edmunds in Norfolk, England. Trace element and carbon[&]/oxygen isotope analysis have been carried out on a sequence of 7 samples from the lithified chalk interior (A-G), the inner crust of the flint (H), 9 from the flint (Nos. 1-9) and of the host sediment at the same stratigraphic level (CA/4). In addition preliminary sulphur isotope determinations were carried out on pyrite from the central burrow. The sample distribution is shown in fig. 6.1 and the data are given in table 6.1 and 6.2 and figures 6.2 and 6.3.

6.2 MINOR AND TRACE ELEMENT CHEMISTRY

6.2.1 Chalk Interior

a) Pyrite and Carbonate Chemistry

As would be expected, the concentration of iron within the paramoudra shows an overall enrichment over that in the host, reflecting the authigenic pyrite content. This is concentrated around the central burrow - the source of the sulphide. Although the sample density is not great, the "sawtooth" distribution pattern may reflect a certain amount of liesegang-like banding resulting from mixing of the inward diffusing iron ($? Fe^{2+}$) and outward diffusing sulphide (see Hodges, 1932). A more detailed analysis would be necessary to confirm this however. The sulphide is

Table 6.1a
Minor element composition of chalks and host
sediment for the Caister paramoudra

Sample	Mg	Na	Sr	Mn	Fe
CA/1A	1725	235	875	260	2410
CA/1B	1660	185	870	250	1820
CA/1C	1590	210	850	245	1610
CA/1D	1638	170	880	241	1675
CA/1E	1565	170	870	275	1565
CA/1F	1500	165	880	250	1680
CA/1G	1485	190	905	265	1310
CA/1H	1485	205	845	125	1700
CA/4	1425	275	926	296	975

Sample	F	Al	I	SiO ₂ %
CA/1A	715	630	145	.600
CA/1B	202	585	185	.617
CA/1C	247	571	170	.615
CA/1D	247	575	155	.607
CA/1E	275	521	145	.577
CA/1F	275	525	145	.576
CA/1G	215	565	155	.569
CA/1H	255	675	175	-
CA/4	770	1247	250	.761

Table 6.1b
Trace elements in Caister paramoudra chalks
(- : not determined)

Sample	Fe	Co	Cd	Cr	Cu
CA/1A	2410	7.6	4.4	12.6	1.7
CA/1B	1820	6.7	2.5	11.0	1.1
CA/1C	1610	6.7	2.3	8.9	1.3
CA/1D	1675	6.7	2.0	9.4	1.2
CA/1E	1565	6.7	2.5	8.7	1.2
CA/1F	1680	7.0	2.7	5.8	1.1
CA/1G	1310	3.2	2.2	2.2	1.1
CA/1H	1700	12.1	4.3	10.5	1.5
CA/4	975	-	1.5	6.4	1.0

Sample	Li	Ni	Ti	V	Zn
CA/1A	2.2	8.6	24.1	7.4	30.8
CA/1B	1.5	6.7	20.6	6.2	18.6
CA/1C	1.2	7.0	20.5	5.7	25.0
CA/1D	1.6	8.7	21.5	6.6	22.7
CA/1E	2.2	7.0	21.0	6.2	15.2
CA/1F	1.6	7.0	21.7	6.3	14.6
CA/1G	1.6	7.1	23.2	6.5	13.9
CA/1H	2.7	25.9	22.2	6.4	17.0
CA/4	1.4	2.5	30.1	5.2	14.4

Table 6.2a
Minor elements in CA-1 flint samples

Sample No.	D (cm)	Ca	Mg	Na	Sr
1	8	2010	50	1350	8.0
2	9	2750	48	1730	8.9
3	10	3390	55	1280	10.7
4	11	4050	65	1310	12.5
5	12	3470	62	1270	10.1
6	13	3270	55	1750	9.7
7	14	2100	47	1350	6.6
8	15	767	37	1350	3.7
9	16	416	32	1510	1.0

Sample No.	Mn	Fe	P	Al	I
1	0.0	184	175	262	193
2	0.6	591	125	254	150
3	7.0	1510	257	239	204
4	15.7	777	297	264	153
5	0.6	295	217	245	237
6	0.7	112	121	274	210
7	0.2	125	72	284	297
8	1.5	175	76	294	289
9	1.0	146	74	293	283

Table 6.2b
Trace elements in CA-1 flint samples

Sample No.	D (cm)	Fe	Ba	Co	Cr
1	8	184	17.2	0.4	1.0
2	9	591	0.8	0.8	1.0
3	10	1506	4.5	1.2	2.3
4	11	777	9.7	1.5	2.7
5	12	295	0.0	0.5	1.4
6	13	112	3.7	0.5	2.7
7	14	125	11.4	0.5	2.2
8	15	175	1.3	0.5	1.3
9	16	146	3.2	0.6	0.7

Sample No.	Li	Ni	Ti	V	Zn
1	1.4	0.4	8.7	1.2	3.0
2	0.7	4.0	10.5	1.5	2.7
3	0.7	3.3	10.3	1.7	11.0
4	2.1	7.1	10.5	1.4	5.9
5	1.4	2.9	10.4	1.4	2.2
6	1.4	2.3	10.5	1.2	2.1
7	1.4	5.1	9.5	1.6	2.7
8	2.0	1.7	9.5	1.5	2.2
9	1.5	1.5	10.7	1.0	1.0

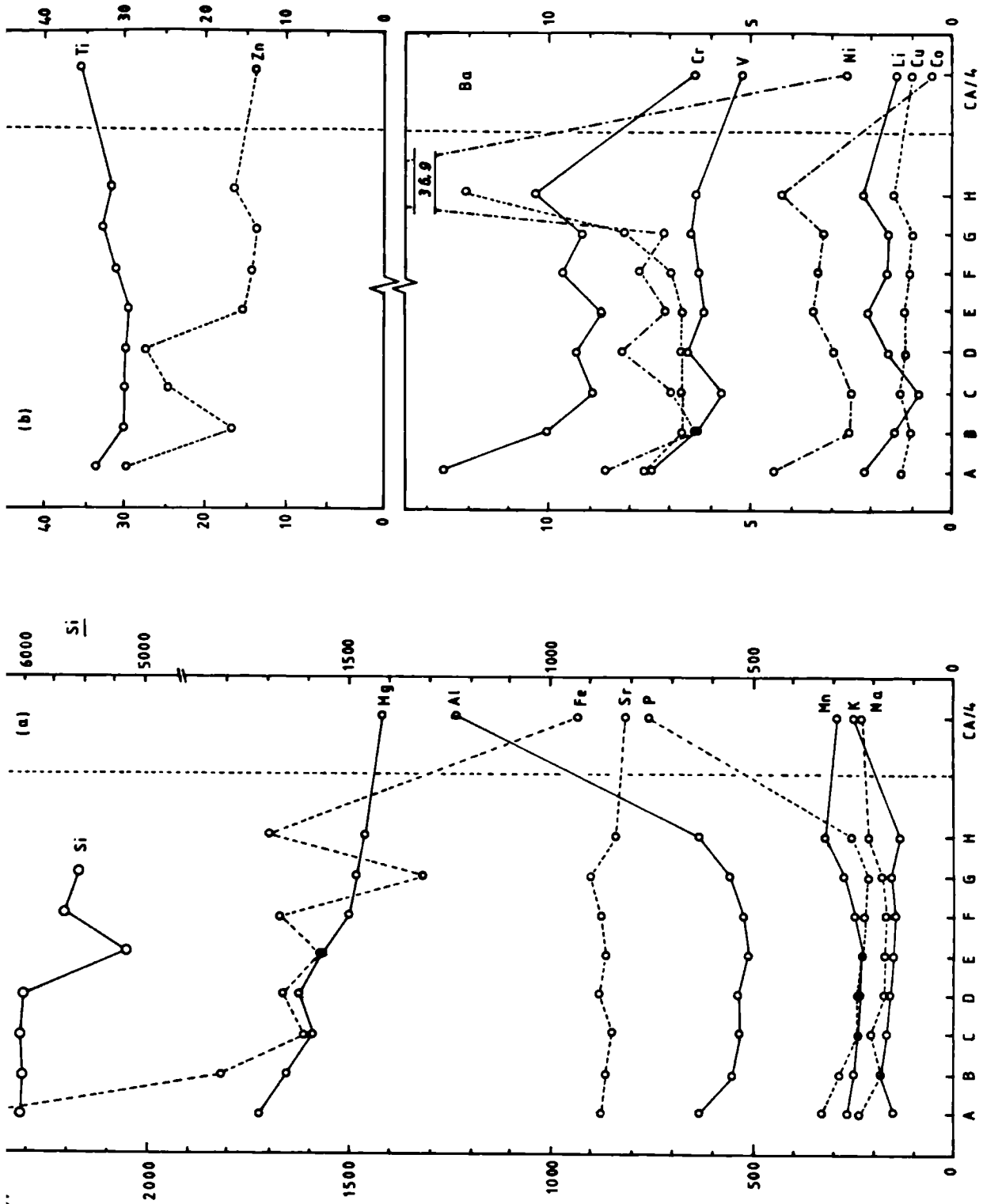


Figure 6.2 Minor and trace element variations in the chalk core of paramoudra CA/1.

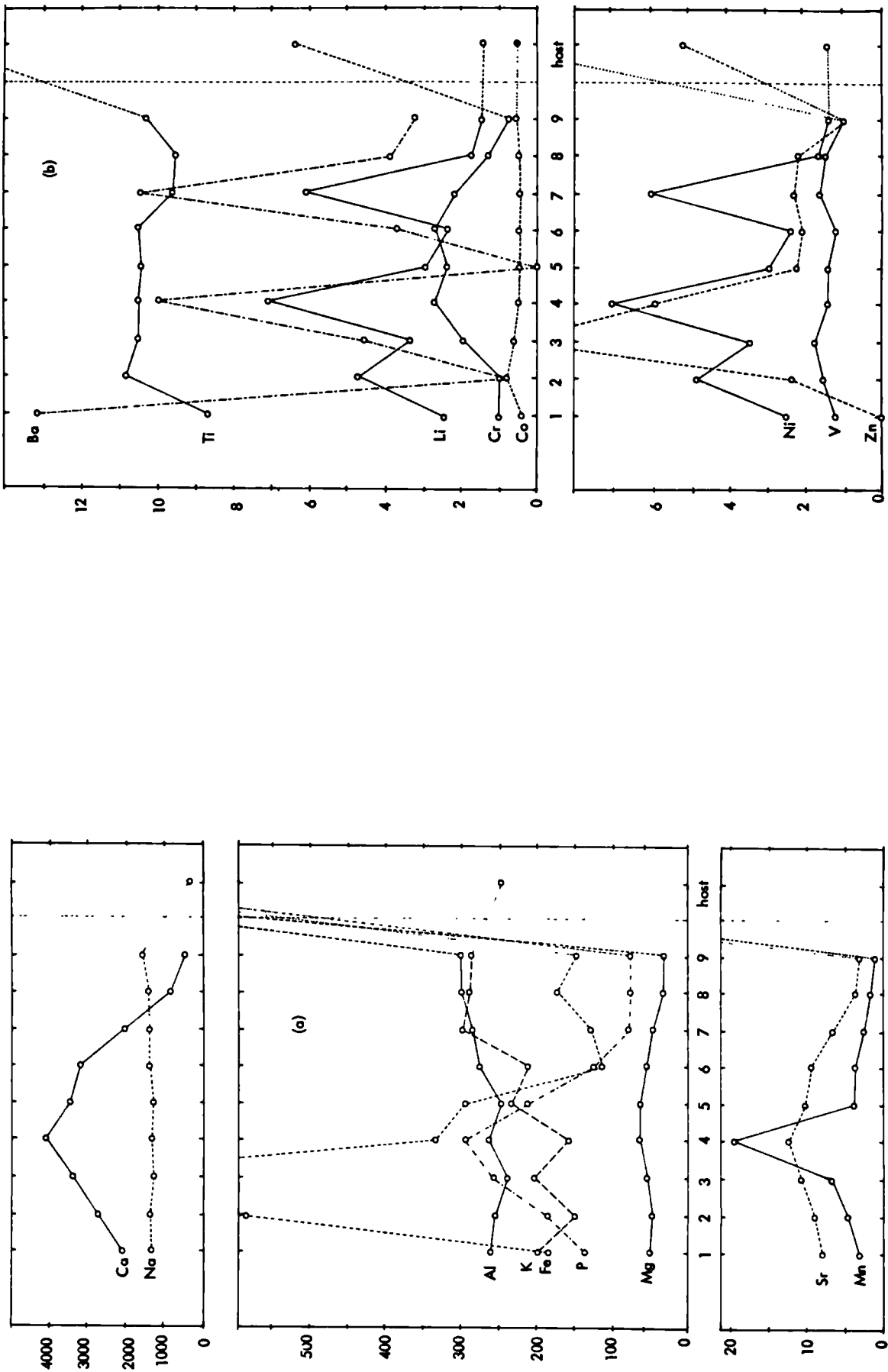


Figure 6.3 Minor and trace element variations through the paranoudra flint. All values in ppm.

associated with a concentration of Cr, and to a lesser extent with V and Cu, reflecting the incorporation of trace elements into the sulphide lattice.

The effects of sulphate reduction in the burrow are reflected also in the precipitation of a calcite cement in the central core of the paramoudra and this results in an enrichment in magnesium over the host concentration. The higher Mg contents of the central samples reflects in part a higher concentration of cement here reflecting the source of HCO_3^- ions which probably caused the cementation. In addition, there may also be an overprint due to the formation of authigenic minerals here. Strontium, which should also be associated with the calcite lattice, shows no such variation suggesting that the cement contains a similar Sr concentration to the host sediment (about 825ppm).

The strong depletion of aluminium within the paramoudra is a reflection of the dilution of clay bearing host sediment by the cement. In addition, the effects of differential compaction after cementation will cause variations, and additional Al may have been added as authigenic minerals (such as glauconite) around the central burrow. The Al concentration shows a minimum in samples C-F with higher concentrations at either end, and this is best interpreted as a mixture of two components (fig. 6.4). Aluminium in detrital (ie pre-existing) phases is diluted by cement when incorporated in the paramoudra (fig. 6.5), the effect being greatest where cementation is most intense: towards the central burrow. Superimposed on this is an authigenic component, which is also concentrated around the central burrow.

From the magnitude of the dilution, it should be possible to estimate the amount and distribution of cement within the core, and from this the minor element chemistry of both the host carbonate and the cement can be calculated. Such estimates involve a large degree of extrapolation and the final figures can be considered only as semi-quantitative at best, but it is useful to make some first

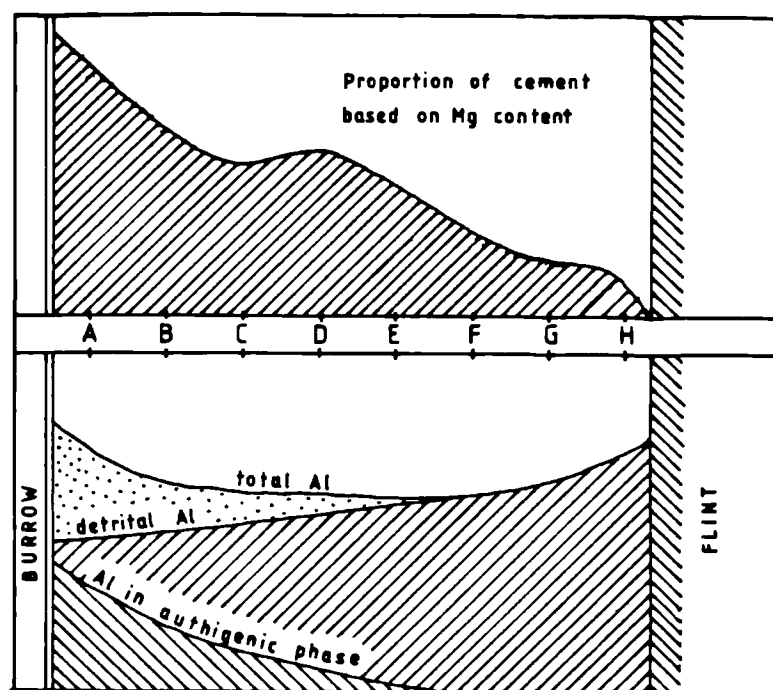


Figure 6.4 Explanation of Al distribution in the chalk core of the paramoudra.

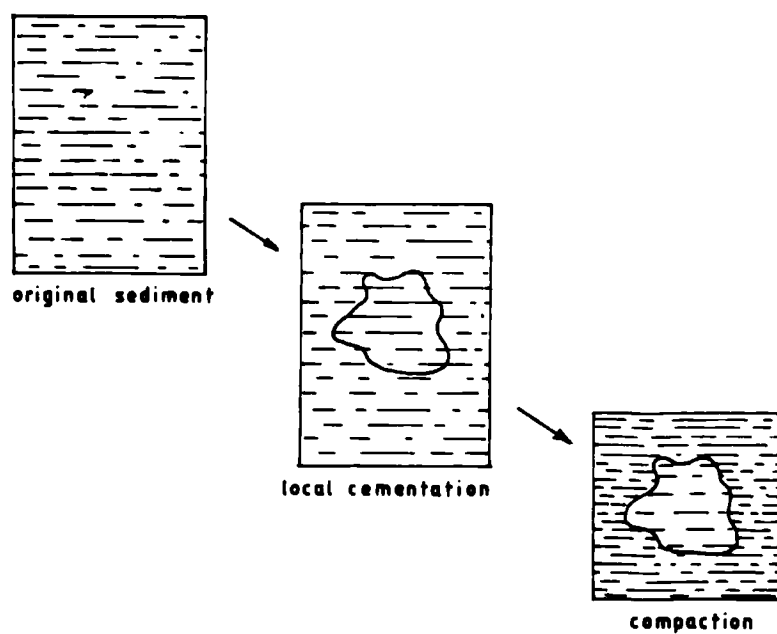


Figure 6.5 Schematic representation of the clay mineral dilution effect associated with local cementation or silicification.

order calculations in order to get an idea of the reactions involved.

By extrapolation of the detrital Al curve, it is possible to estimate the magnitude of the dilution as about .34 of the normal content at B, to .46 at G. Although this extrapolation is somewhat arbitrary, it will be adequate for approximate calculations. Given the host porosity, it is now possible to estimate the apparent "porosity" around the diluted host, ie the space now occupied by cement + pore-space (fig.6.5). Chalks of the sort in which the paramoudra grew typically have a present day porosity of about 40% (ie 60% rock matrix: Jones et al. In press) and dilution by the above factors gives "apparent porosities" at the time of cementation of 80% at B and 73% at G. The 7% difference here reflects probably greater compaction during and since lithification at G rather than at B.

The proportion of cement at each place can be estimated directly from the Al dilution figures and gives figures of 66% by weight at B to 54% at G. In addition, the present day porosity can be estimated from specific gravity measurements (see Jeans, 1980 for methods) and varies from 37% at B ($\rho=1.71\text{gcm}^{-3}$) to 29% ($\rho=1.92\text{gcm}^{-3}$) at G. From the present day porosities and the cement volume calculations, the total volume not occupied by host carbonate can be calculated as 78.6% at B to 67.3% at G. By comparison with the estimated porosity at the time of lithification it is now apparent that the sediment porosity has undergone a 1% reduction at B and a 5.1% reduction at G, subsequent to lithification. Approximately half of the 7% difference in initial porosities can therefore be explained by subsequent differential compaction, the remaining 3% being related to differential compaction during lithification.

b) Other Diagenetic Reactions

The increase in Mg from G to B reflects in part the increase in cement over this interval, and in part the presence of an authigenic mineral phase here (cf A1). Assuming that the authigenic contribution at G is negligible (as was assumed for A1), the two may now be differentiated. Sample G contains 54% by weight of cement of unknown Mg content and 46% by weight of host sediment containing 1425ppm Mg. The Mg content of the cement must therefore be about 1536ppm.

Such a low Mg content for the cement would appear to rule out the possibility that the cement was originally high magnesian calcite since, although the high Mg \rightarrow low Mg transition would result in a purging of Mg, it is difficult to imagine the process being this efficient. Similarly, the low Sr content would make aragonite an unlikely mineralogy, so presumably cementation occurred by the precipitation of low-Mg calcite.

The authigenic Mg content can now be estimated from the available data. At B, the carbonate is composed of 66% cement of 1536ppm Mg, and 34% host sediment containing 1425ppm, giving a predicted Mg content of 1498ppm. The difference between this and the measured 1660ppm must therefore be due to the introduction of 162ppm of Mg in an authigenic phase (probably^b_k the glauconite visible in the field).

It is also possible to calculate the theoretical content of the other minor elements at B and G to determine the authigenic contribution of these (fig. 6.6). As would be expected, Al and Mg show comparable distributions when plotted graphically, and these by definition, drop to zero at G.

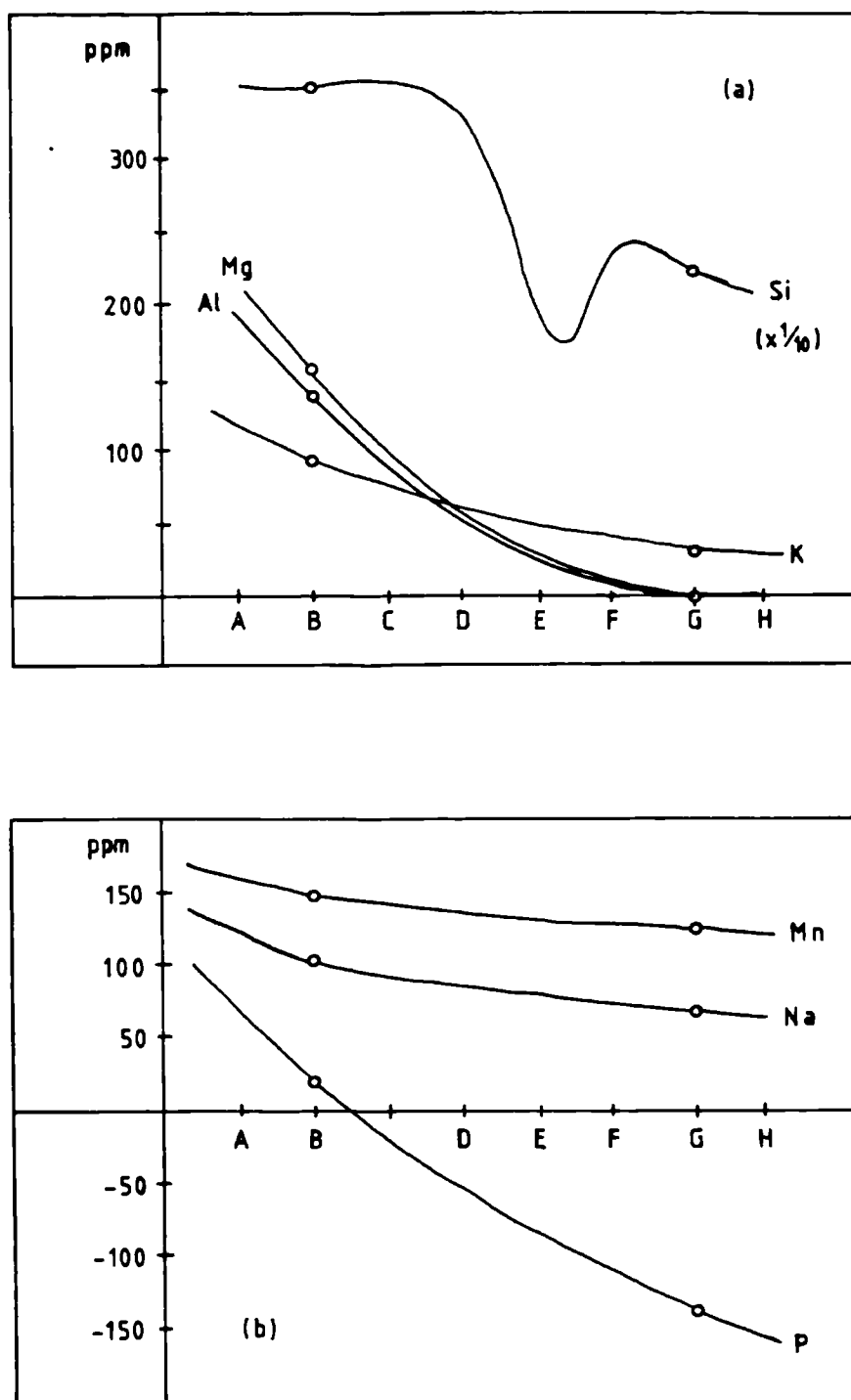


Figure 6.6 Distribution of authigenic components in the core of the paramoudra as calculated from dilution data and measured concentrations.

More interesting are the silica and the potassium curves which, in addition to an authigenic component concentrated towards the centre, have an additional excess appearing towards the outside of the core (i.e. at G). The silica probably largely represents the precipitation of quartz throughout the whole core (c.f. paramoudras which are siliceous all through - chapter 3) and this is, of course, greater in a zone around the central burrow (c.f. pl. 4B). Precipitation of silica here probably reflects the release of dissolved carbonate from the burrow (see the "kinetic-bridge" mechanism discussed in chapter 2).

The K curve also clearly reflects an excess of the element towards the outside. However, if the K curve is traced into the flint (fig. 6.3), it can be seen that this "excess component" shows the highest concentration distally from the burrow. This is rather unlikely, and a better interpretation is that there is a diagenetic purging of K from a ?clay phase as a result of the reactions occurring in the burrow. If this is the case, the excess of K in the paramoudra over that predicted from the host must be attributable to subsequent depletion of K in the host. This, then implies that the host sediment was not yet undergoing these reactions at the time the paramoudra formed, or in other words, the paramoudra formed around a locally reducing burrow in a generally more oxidising environment.

X-ray Diffraction of the insoluble residue from the core (dissolution in 2 N acetic acid, buffered with Na-acetate at pH=3.95), kindly carried out by D. Smith at King's College, revealed the presence of quartz, illite, smectite, and a mixed layer illite-smectite containing about 40% "glauconite" layers. Clearly, the

inner concentration of K, Al, Mg, and part of the Si must be present in the glauconite component. It is difficult to attribute a specific mineral to the K-depletion, but the most likely source is from the "glauconite" layers themselves. Glauconite contains a significant proportion of iron in the three-valent (ie oxidised) state so could not have formed under fully sulphate reducing conditions. Most likely, it formed under the suboxic conditions, after dissolved oxygen had been used but before the onset of truly reducing conditions. The K-depletion could then be associated with breakdown of the newly formed glauconite under the intense action of sulphate reduction. Possibly, this reaction served also as a source of Fe for the pyrite which post-dated glauconitisation and formed in the host after the paramoudra finished growing.

The other elements showing anomalous concentrations are Mn, Na and P. The Mn concentration is very difficult to interpret since Mn may be present in the diagenetic cement, clays, phosphates, or as free oxides. It is tentatively suggested that much of the Mn is incorporated in the cement, since under the conditions in which cementation occurred (ie reducing), Mn would have been mobile as the Mn^{2+} ion. It seems likely also that the anomalously high Mn content in the paramoudra compared with the host sediment is the result of re-mobilisation of Mn in the host as it too passed into reducing conditions. This was compensated for in part in the paramoudra by incorporation of the Mn in calcite before it was able to diffuse away.

Na also may be present in the cement or in clays but the situation here is complicated by the possible presence of Na in soluble

salts in micropores of the sediment, not removed by washing. Because of these uncertainties, quantitative analysis of the Na data is not attempted here.

The phosphate distribution shows a very strong concentration towards the central burrow and this probably reflects the growth of authigenic phosphates here. This may be the result of either the phosphate and/or the bicarbonate released during organic matter degradation, or of the more reducing conditions here. The negative anomaly in the outer part of the core is probably the result of subsequent growth of phosphates in the host (c.f. similar effects in K and Mn), as this too passed into more reducing conditions.

6.2.2 Flint Chemistry

The minor element variations in the flint are shown in figs. 6.3a and b. The elements fall into three main groups: those associated directly with calcite (Ca, Sr and Mg); the easily remobilised transition metals (Fe and Mn); and those present predominantly in other phases (P, Al, K and Na).

a) Calcite Association

As in most flints, Ca shows a higher concentration towards the centre, reflecting preferential preservation of carbonate here (see chapter 5). The elements Mg and Sr both show highly significant correlations with this ($R^2 = .94$ and $.98$ respectively) reflecting their presence in the calcite lattice. Linear regression analysis of these data (see table 6.3) can therefore be used to deduce the trace element content of the carbonate, and gives a content of

Table 6.3a
Linear correlation coefficients - CA/1

[illegible]

Table 6.7b
Linear correlation coefficients - CA'1

[illegible]

3550 ppm Mg and 1000 ppm Sr, both significantly higher than the known concentrations in the host. Although extrapolations of this magnitude will undoubtedly introduce large errors, the magnitude of the differences probably suggests that the calcite preserved in the flint is unrepresentative of the host carbonate as a whole. This is to be expected in view of the fact that the host chalk is composed in large part of coccoliths whereas the calcite in the flint will be fragments of macrofossils, or at least foraminifera, with little or no coccolith calcite remaining.

Extrapolation of the regression line to find the non-carbonate component gives about 30 ppm Mg and almost no Sr (2.0 ppm). After allowing for the dilution effect (calculated from the Al content - see below), this suggests virtually no Sr (10 ppm) and about 100 ppm Mg in the host, not present in carbonates. If real, the Sr content is compatible with incorporation of only a very small amount of this in clay minerals and phosphate. Subtraction of the 100ppm Mg from the host content gives 1325ppm as the Mg content of the pure calcite fraction. This is an exceptionally low-Mg calcite and attests to the selectivity of the coccoliths in excluding trace elements from the calcite lattice during growth. Interestingly this is not the case for Sr which occurs in levels up to 600ppm, despite the low level in seawater compared with Mg.

b) Iron and Manganese

The iron and manganese concentrations are replotted in fig. 6.7, together with their variation in the cemented chalk core and the theoretical concentration produced by dilution of the host by the appropriate amount. Although some of each element should be remobilised on reduction of the Mn^{4+} and Fe^{3+} to the lower oxidation state (see chapter 2), the effects of this are somewhat

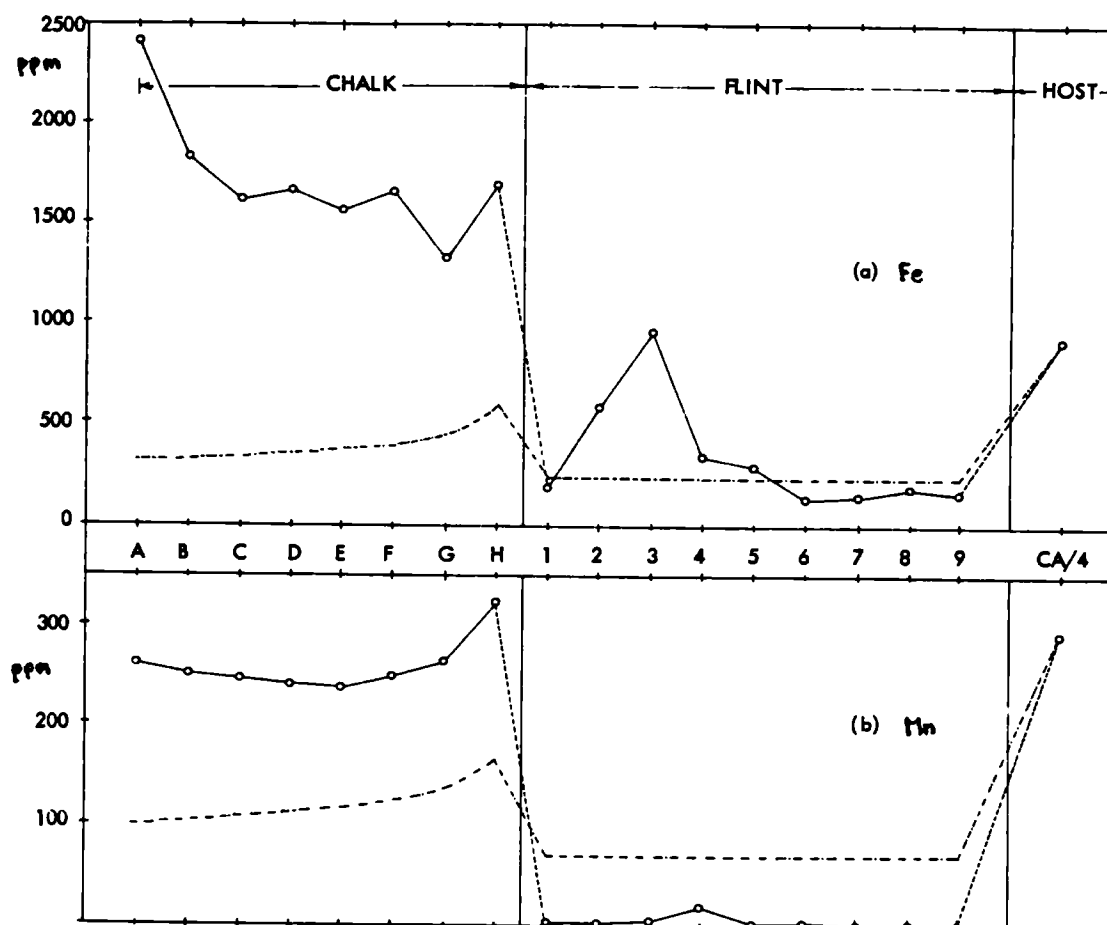


Figure 6.7 Distribution of Fe and Mn in the Caister paramoudra. Broken lines show theoretical concentrations based purely on dilution of the host concentrations.

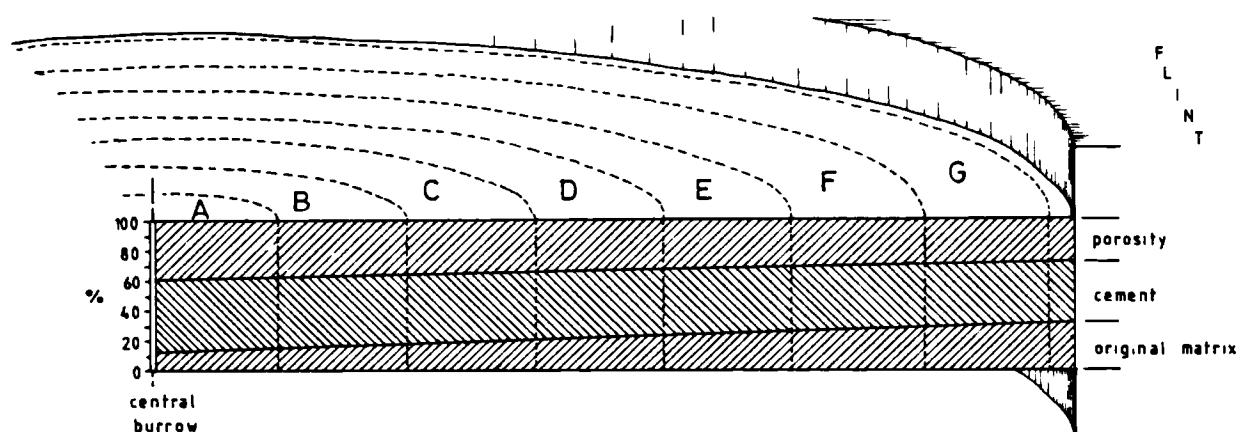


Figure 6.8 Schematic representation of the distribution of cement and porosity in the paramoudra core.

shielded by the incorporation of some of each element into structural sites in clays and the calcite lattice of the chalk.

In the flint, manganese clearly has been remobilised to a high degree resulting in a strong depletion with respect to the predicted concentration, and comparison with the Ca content gives a clue as to the mechanism of this. Fig. 6.9 shows the Ca-Mn relationship to be approximately linear below about 3500 ppm calcium (.88% calcite) but with excess Mn in the central samples where there is a higher calcite. The low, linear part of the curve probably represents Mn incorporation in the calcite and extrapolation gives a calcite Mn content of 395 ppm. This compares with a total Mn host content of 296 ppm, again suggesting that the calcite preserved in flint is unrepresentative of the host calcite as a whole. Extrapolation to the zero calcite level leaves a negligible residue (only .7 ppm), suggesting that the structural Mn content of pre-existing clays is very low indeed. The excess Mn in the centre of the flint presumably is present as an oxidised Mn mineral ($? \text{MnO}_2$), probably precipitated at the Mn redox boundary as Mn diffused out from the reducing conditions around the burrow to meet aerobic conditions to the outside.

These deductions have important implications for the Mn distribution in the cemented chalk core since they suggest that the Mn content of pre-existing clays is negligible. In addition, the Mn content in the core cannot be due to oxides since if Mn was remobilised by reduction on the inside part of the flint, it must also have been remobilised in the more reducing inner zone of the paramoudra. The Mn in the core therefore was incorporated into the host calcite and the cement, possibly with additional Mn (as Mn^{2+})

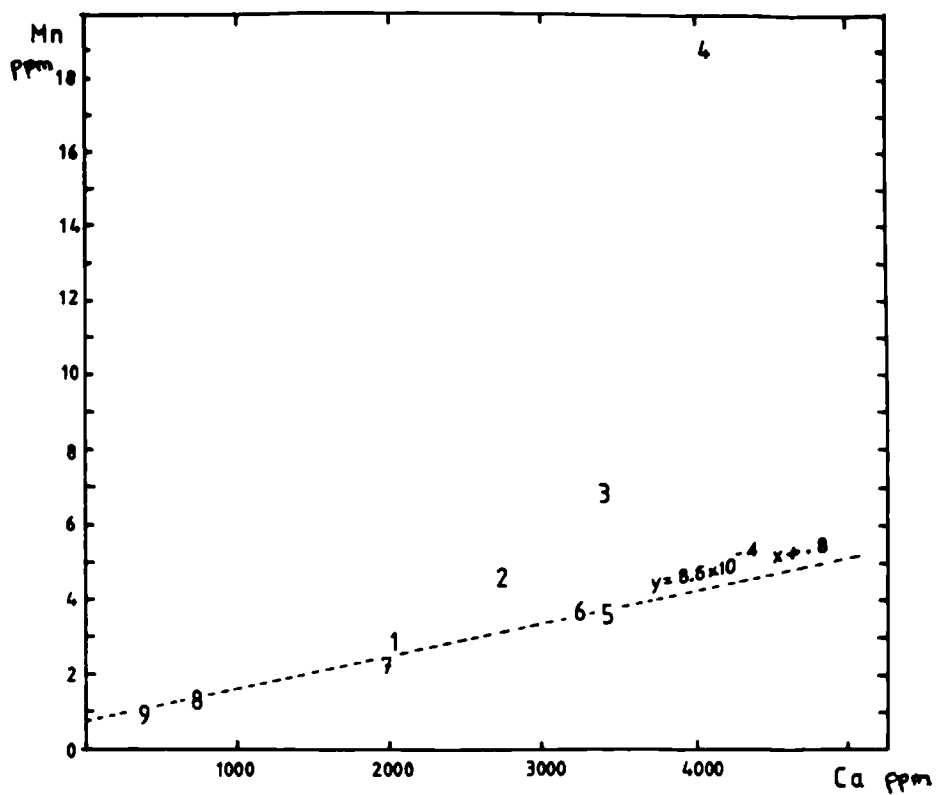


Figure 6.9 Variation of Mn with calcite (represented here by Ca) in the paramoudra flint.

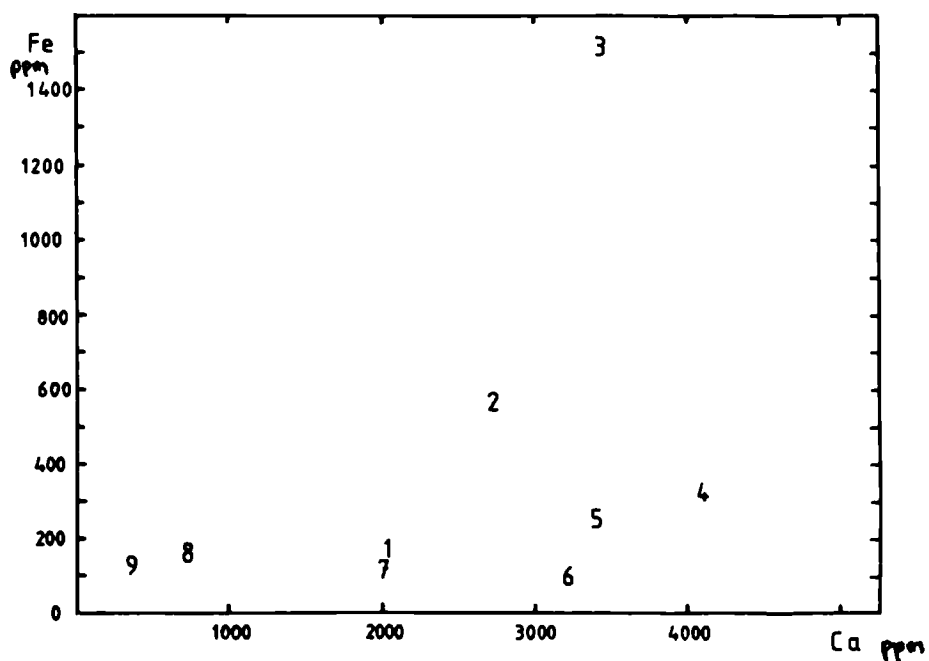


Figure 6.10 Comparison of Ca and Fe in the paramoudra flint.

in structural sites within the authigenic glauconite and/or phosphate.

The iron distribution also shows a distinct peak (in sample 3) but this does not coincide with the calcium peak implying that minimal Fe is present in the calcite. Although this iron could represent a further Liesegang-like band of sulphide precipitation (see section 6.2.1a), this seems unlikely in view of the abrupt change in concentration involved, so the peak probably represents the precipitation of iron oxides at the $\text{Fe}^{2+}/\text{Fe}^{3+}$ redox boundary. This is also suggested by the trace elements associated with the iron where there is a close association with Zn, and to a lesser extent with Li and Ni. This compares with an association of Cr and a little V and Cu with the sulphide in the chalk core (see section 6.2.1a). Also, it is worth noting that the iron oxide peak should, and does, occur within the Mn redox boundary because Mn is more easily reduced than Fe.

Another interesting point is that the background iron content, on which this peak is superimposed, is below the theoretical host dilution level implying either that some iron has been remobilised here (unlikely since this also occurs outside the Fe redox boundary) or more likely, that there has been a subsequent introduction of Fe (~ 320 ppm) to the host. The excess iron may be in the form of dispersed sulphide (see chapter 3), since this is probably the nature of the labile iron in the Chalk. This later stage introduction of iron adds more evidence that the chalk surrounding the paramoudra did not become reducing until after the paramoudra formed.

c) Non-carbonate Association

As is evident in the cemented core, aluminium shows a strong

depletion over its concentration in the host as a result of dilution, in this case by silica. The trend also shows a slight depletion towards the inner edge, reflecting the alteration of clay minerals (better seen in the K curve) and a slight drop towards the centre, reflecting slightly greater dilution here (i.e. slight compaction around the edges). This Al depletion will result in a slight systematic error in the dilution data but this is not great. The dilution coefficient is .24 at sample 8 or 9, which yields an apparent porosity of 86%. Assuming that compaction of the flint is negligible, this corresponds to the porosity of the sediment at the time the flint formed (or more precisely, when the lepisphere framework was self-supporting). This is rather high, with a porosity of 70-80% being more reasonable for such a sediment (see chapter 5), and may suggest the addition of Al to the host after flint formation. Therefore, there may be a small amount of authigenic clay formation in the host (c.f. around the central burrow), which introduces another small systematic error into the calculations, (but from the magnitude of the possible depletion, this is unlikely to be greater than about 10%).

Potassium, as explained above, shows a progressive depletion nearer the centre of the paramoudra as a result of reduction reactions in the burrow, and again this has clearly affected the host sediment subsequently to a large extent. This confirms the deductions from the chemistry of the chalk core.

The distribution of P is more complicated and would appear to be the result of a mixture of two components. A background of about 75 ppm P reflects the preservation and dilution of host phosphate at the time of silicification. After correcting for the dilution, this

would correspond to a host content of about 315 ppm, which is substantially less than the 760 ppm now present, and suggests the addition of about 445 ppm P to the host, subsequent to paramoudra formation. Superimposed on the background, and showing a poor association with the calcium peak, is a second phosphorus bearing phase, which probably represents the growth of authigenic phosphates. Their presence coincides here with the boundary between the reducing conditions of the paramoudra and the surrounding aerobic conditions, and such an environment for possible phosphate formation has been deduced also on isotopic grounds by Benmore et al., (1983). It is unclear if phosphate formed here in response to the change in Eh at this position, the pH changes associated with sulphide oxidation (see below), or the anomalously high concentration of HCO_3^- in solution here as a result of calcite dissolution. The latter alternative is the most likely since it also explains the phosphate precipitation around the central burrow where HCO_3^- was also forming by hydrolysis of CO_2 released by sulphate reduction. However, precipitation would also have been encouraged by the drop in pH at the site of flint formation and also by the generation of sulphate by re-oxidation of sulphide.

Sodium in the flint is unrelated to any of the other elements and shows a concentration higher than that of the host. As demonstrated in chapter 5, most of the Na in flints occurs in saline fluid inclusions, but it has not been possible to confirm this here because the flint samples were dissolved whole, as small cores without crushing, and there was no sample left over for a distilled water leach (see Appendix 3).

6.3 STABLE ISOTOPE VARIATIONS

The carbon and oxygen isotopic composition of the lithified chalk samples are give in table 6.4 and shown graphically in fig. 6.11. Although not very accurate due to poor reproducibility between batches of samples, these data are of high precision with reproducibility of about .02‰ for $\delta^{13}\text{C}$ and .03‰ for $\delta^{18}\text{O}$ obtained for replicate standards within each batch. The trends are therefore known with some confidence although the absolute value may be in error by up to .1‰ (see Appendix 4 for details of corrections applied for comparison of successive batches).

$\delta^{13}\text{C}$ and $\delta^{18}\text{O}$ show a very clear positive relationship ($R^2 = 0.92, n=7$) inversely related to the Mg trend for the samples (see fig. 6.2), reflecting the introduction of isotopically light cement to the host calcite. Assuming this cement is isotopically homogeneous within the core, extrapolation of the curves yields a cement composition of 1.13‰ for $\delta^{13}\text{C}$ and -1.88 for $\delta^{18}\text{O}$, and an original host composition of $\delta^{13}\text{C} = 2.63$ ‰ and $\delta^{18}\text{O} = -.05$ ‰

6.3.1 Host Calcite

The calculated values for the host are significantly heavier than its measured composition in both $\delta^{13}\text{C}$ and $\delta^{18}\text{O}$. The anomalously light values in the host at present must be the result of subsequent alteration, the most likely cause being re-equilibration with isotopically light meteoric waters, which has left the better cemented paramoudra core unaffected. The carbon isotope composition of meteoric water varies from about -5 to -11‰ (Sackett and Moore, 1966) and the oxygen composition currently varies with latitude from about 0‰ near the equator to about -6 or -7‰ in southern England where the paramoudra was collected. Partial equilibration

Table 6.4
Stable isotope data for Carsten paragonite
chalts and pyrites and Seaton Head pyrite SHF/3

Sample	$\delta^{13}C$	$\delta^{18}O$	$\delta^{34}S$	Distance
CA/1A	1.63	-1.27		0
CA/1B	1.64	1.26		1
CA/1C	1.65	1.13		2
CA/1D	1.66	1.17		3
CA/1E	1.74	-1.12		4
CA/1F	1.77	1.11		5
CA/1G	1.82	-1.04		6
CA/1H	1.74	1.01		7
CA/4	1.54	-1.54		18
11			41.4	0
12			-22.5	0
13			30.4	0
SHF/3			33.2	-

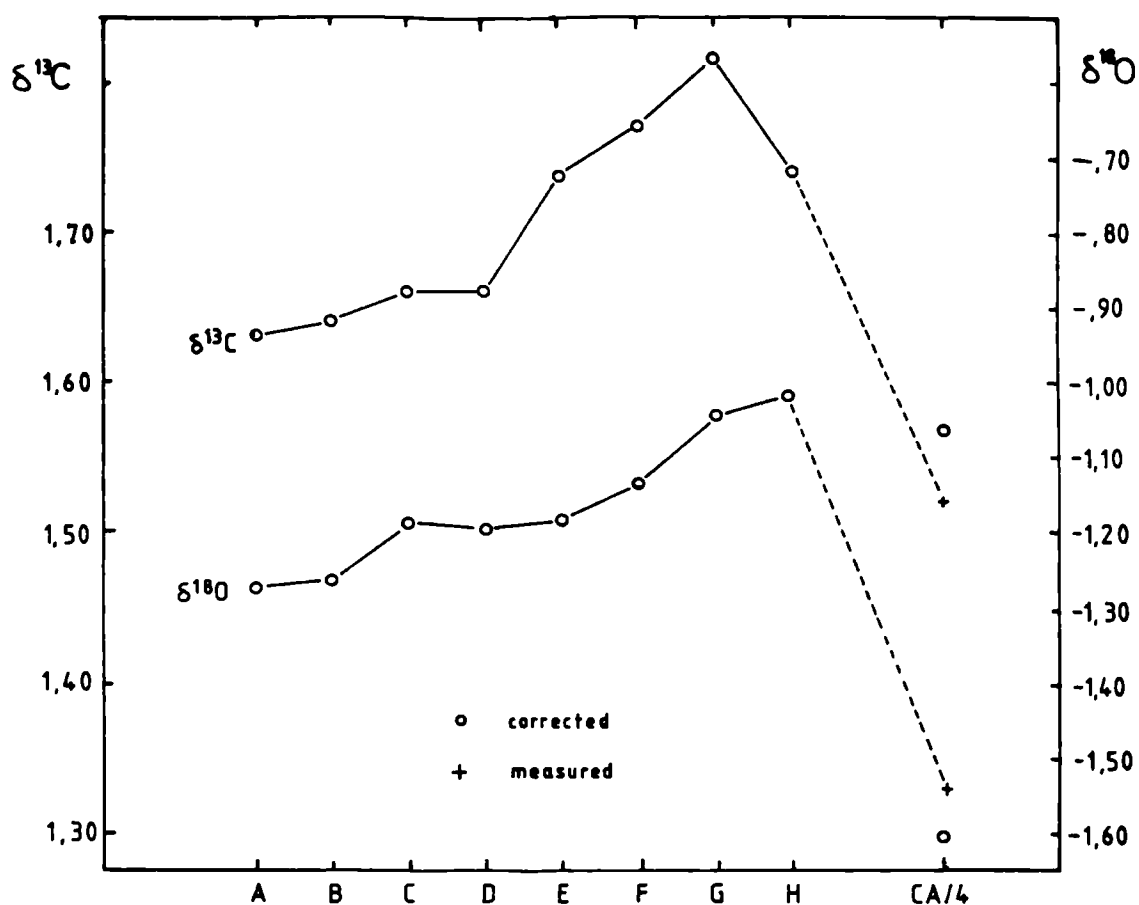


Figure 6.11 Corrected stable isotope ratios in the chalk core of the paramoudra. Curves reflect the introduction of isotopically light cement towards the central burrow (sample A).

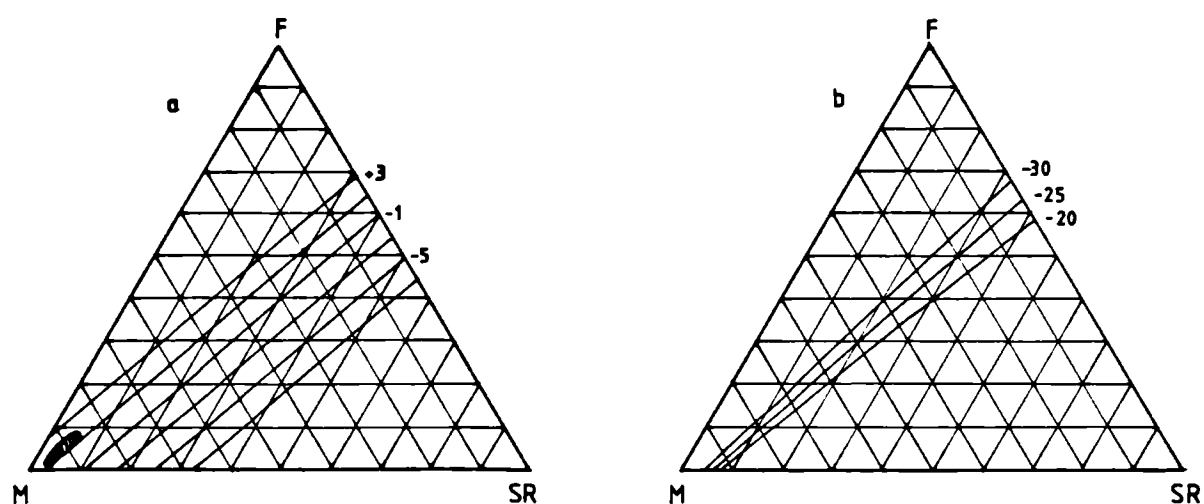


Figure 6.12 Three component mixing curves for sources of calcite in the paramoudra. a) assumes -25‰ for Sulphate Reduction component and +15‰ for Fermentation fraction. b) shows effect of variations in $\delta^{13}\text{C}$ of SR derived carbonate. Hatched area is field of the paramoudra samples.

of the chalk with water of this composition could therefore result in a significant lightening over a period of time if the ratio of water to rock is large, particularly so if this occurred during the Pleistocene when even lighter meteoric water would be expected in this area. Such a large ratio would be expected with the large flux of water which probably passes through a surface outcrop of slightly tuffaceous chalk such as this.

The calculated original composition of the host calcite is typical of Cretaceous marine carbonates. Assuming that calcite precipitation took place in equilibrium with contemporary sea-water ($\delta^{18}O_{\text{seawater}} = -1.2\text{‰}$; Shackleton and Kennett, 1975) the temperature of formation can be estimated from the equation of Craig (1965):

$$T^{\circ}\text{C} = 16.9 - 4.21(\delta_c - \delta_w) + 0.13(\delta_c - \delta_w)^2$$

where δ_c and δ_w are the oxygen isotopic composition of the calcite and water respectively. For the calcite here ($\delta^{18}O = -.05\text{‰}$) this equation yields a temperature of 13°C . This is a little lower than would be expected for a purely biogenic pelagic sediment which should reflect contemporary sea-surface temperature (estimated as $14\text{--}18^{\circ}\text{C}$ for the Campanian; Savin, 1977), but this is probably due to the incorporation of a small amount of benthic fauna, which would have grown at the lower temperatures associated with bottom waters.

The temperature dependence of the carbon isotope fractionation is very small (Emrich et al., 1970) so the carbon isotopic composition of the chalk is predominantly a function of the contemporary marine carbon isotopic composition. The value here (2.63‰) is reasonable for Upper Cretaceous sediments (Veizer et al.,

1980) and compares well with other data for sediments of this age (e.g. Fisher and Arthur, 1978; Scholle and Arthur, 1980).

6.3.2 Cement

The lighter carbon isotope composition of the core compared with the host reflects the introduction of isotopically light cement, which is compatible with a sulphate reduction origin for the carbonate. Sulphate reduction, however, yields carbonate of around -25‰ (see below) but the cement in the paramoudra has a $\delta^{13}\text{C}$ value of 1.13‰, suggesting that other (isotopically heavier) sources of carbonate are also involved.

The most likely alternative sources are primary or remobilised (? aragonitic) marine carbonate ($\delta^{13}\text{C} \sim -2.6\text{‰}$) or carbonate from bacterial fermentation reactions ($\delta^{13}\text{C} \sim +15\text{‰}$). The mixing curves for these components with sulphate reduction carbonate are shown in the form of a triangular diagram in fig. 6.12a. In order to maintain the same isotopic composition, addition of a larger amount of fermentation carbonate must be balanced by the addition of sulphate reduction cement and a decrease in the marine contribution. In the case of the paramoudra, the fermentation contribution is probably quite low since such reactions only become important at depth, after the sulphate has been used up, and as explained in chapter 2, by this time the organic content of the Chalk would have dropped almost to zero. Assuming a negligible fermentation contribution therefore, the sulphate reduction generated carbonate can be estimated to comprise between 4 and 8 % of the cement, probably around 6%..

Another possible cause of error in estimating the sulphate

reduction contribution is the isotopic composition of the CO_2 . The carbon isotope composition of the CO_2 released is a direct reflection of the isotopic composition of the organic matter undergoing decomposition. In extreme cases this may vary from as heavy as nearly -20‰ for some fully marine organic material fixed in warm water, to as light as -30‰ for material dominated by terrestrial plant matter (Sackett and Thompson, 1963). The effect of this range on the mixing diagram is shown in fig. 6.12b. For low levels of fermentation carbonate ($< 10\%$), this entire $\delta^{13}\text{C}$ range covers less than 6% variation in the relative contribution of sulphate reduction carbonate, and a maximum of about 3% difference from the mean value.

It would appear then that the cement present consists predominantly of redistributed marine carbonate, with about 6% carbonate of sulphate reduction origin and only a small, if any, contribution from bacterial fermentation.

The oxygen isotope composition of the cement is a function of temperature, the isotope fractionation factor for the mineral concerned, and the isotopic composition of the solution in which the cement grew. Knowing the fractionation factor, and assuming a normal marine value for the isotopic composition of the pore-water (-1.2‰), it is possible to estimate the temperature of precipitation from the equation of Craig (1965) as about 21°C. This is anomalously high for temperature resulting from the shallow burial inferred from the dilution data and field relations (approx. marine bottom water temperature) and there are two possible explanations for this:

- 1) The cement includes a large quantity of fermentation carbonate added at much greater depth;

or 2) Precipitation took place either out of equilibrium with pore waters or in equilibrium with local pore waters which were depleted in ^{18}O relative to sea-water.

The first of these can be discounted since, as explained above, the proportion of fermentation carbonate must be small. The alternative explanations are closely related and it is relevant to consider them together. Of the early diagenetic reactions which occur in the Chalk, only aragonite and biogenic silica dissolution happen on a wide enough scale to significantly modify the composition of the pore waters as a whole. However, the effect of both of these is to contribute proportionately more ^{18}O to the water so neither can result in ^{18}O depleted pore-waters. Because calcite is enriched in ^{18}O to an extent of about 35% with respect to the water in which it grows, precipitation of calcite cement, such as within the paramoudra can result in local depletion of the pore waters as long as ^{18}O is consumed in the calcite cement faster than it can diffuse in from outside. Rapid cementation in the paramoudra may therefore result in a local depletion of ^{18}O in pore waters around the area and successive cements will be progressively depleted in ^{18}O as a result. It is worth noting that this would probably result in an isotopically inhomogeneous cement because ^{18}O depletion would occur more rapidly where there is more cementation, i.e. at the centre. However, this effect is probably not great since there is little variation in cement content (see fig. 6.8). Similar effects to this have been observed in Jet Rock concretions (Coleman and Raisewell, In Press) and in Chalk hardgrounds (Jarvis, Bromley and Clayton, Unpublished data, and chapter 8. Unfortunately, data on the diffusion rates of ^{18}O in pelagic

carbonates is poor at present, but as this becomes available there exists the possibility of being able to quantify the rates of sulphate reduction in such situations.

6.4 MASS BALANCE CONSTRAINTS

As both the total cement content, and the proportion of it derived from sulphate reduction, are now known, it is possible to calculate the minimum amount of carbonate released from the central burrow, and therefore estimate the minimum amount of H_2S released. Calculations of this sort are important because, as shown below, it is probably the excess H_2S released in these reactions that initiates silicification at the site of flint formation.

Any given volume in the cemented chalk core of the paramoudra is composed of a mixture of pore space, original host carbonate, and cement, and the proportions of these vary systematically from the centre to the edge of the core (fig. 6.8).

The porosity varies from 37% at B to 29% at G and the cement proportion, calculated from the A dilution data, varies from 66% of the carbonate at B to 54% at G. The true cement proportion per unit volume thus varies from .42 at B to .38 at G, which, if it varies linearly, implies a mean value of .40. Since the radius of the core is 7 cm, the total volume of cement per cm of burrow can be calculated as being:

$$\pi \times 7^2 \times .40$$

which gives 61.6 cm^3 .

Assuming that the carbonate is pure calcite ($\rho = 2.71 \text{ g/cm}^3$), this is equivalent to 167 grams, or 1.67 moles.

As the cement is composed of about 6% carbonate of sulphate reduction origin, a minimum of .10 moles of CO_2 must have been released from the burrow by sulphate reduction. Assuming that the overall stoichiometry of sulphate reduction can be approximated as:

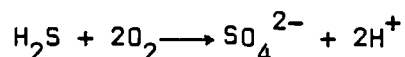


then at least .05 moles of sulphide must have been released, equivalent to .05 moles of iron monosulphide/ H_2S .

The sulphide (as FeS_2) content of the core can be estimated in the same manner as the cement calculation using the Fe content, and this comes to .43gms/cm of burrow, or .01 moles. This leaves an excess of at least .04 moles of sulphide which has been lost from the system. In practice, the precipitation of sulphide in the core would have inhibited the precipitation of an equivalent quantity of carbonate (.02 moles). It is therefore likely that at least another .02 moles of carbonate was produced over that now represented in the cement, and allowing for this, a more reliable estimate for the minimum excess sulphide lost from the system would be .06 moles. Even this may be an underestimate if there is any fermentation carbonate in the cement of the core since this would have to be balanced by a higher proportion of carbonate from sulphate reduction to maintain the same overall isotopic composition.

It would appear from the above calculations therefore that a very large excess of sulphide has apparently been lost from the system during formation of the paramoudra and it is important here to determine the cause and the geochemical significance of

the fate of this sulphide. The excess must almost certainly have been lost in the form of H_2S as this is necessary for the precipitation of carbonate (chapter 2), and as this diffused away from the burrow it would ultimately encounter the aerobic conditions which appear to have been present around the growing paramoudra. Where reduced sulphur compounds reach aerobic conditions, a mixture of bacterial and abiological oxidation reactions occur, usually dominated by the metabolic processes of the chemolithotrophic bacteria, principally the thiobacilli (Goldhaber and Kaplan, 1974). The precise reactions are not known in detail but are highly complex with elemental sulphur, thiosulphate and polythionates being generated as important intermediates (e.g. see Roy and Trudinger, 1970). However, the net result of the oxidation can be approximated as:



This will result in a local drop in pH in response to the release of hydrogen ions as a consequence of the oxidation of the excess sulphide, and this will in turn be buffered by dissolution of carbonate minerals. Attainment of a steady state, with an outward diffusive flux of H_2S balanced by the inward flux of oxygen, will therefore result in a localised zone of carbonate dissolution straddling the redox boundary. The width of this zone will then be controlled by the width of the zone of mixing (controlled by rate of supply of the reactants and local permeability variations) and the distance the newly formed hydrogen ions can diffuse before being buffered by carbonate.

As explained in section 2.4, such large scale carbonate dissolution in a chalk sediment would result in rapid silica precipitation at the site, initially in the form of lepispheres

and replacement of microfossils, and later, probably after carbonate dissolution ceases, as chalcedony. The result therefore would be a columnar flint, formed around the oxic/anoxic boundary, encasing the Fe and Mn redox boundaries.

From the Al dilution data in the flint, it is known that silicification occurred in a sediment of a maximum of about 80% porosity, so by calculating the volume of flint, it is also possible to estimate the minimum amount of carbonate which has been dissolved. Taking a mean outside radius of the flint of 17 cm (i.e. 10 cm thick flint walls) this gives a volume of flint of about 754 cm^3 per cm of burrow, equivalent to at least 150 cm^3 of calcite. This is equivalent to 409 grams or 4.1 moles of carbonate dissolved.

The minimum excess of H_2S calculated above (.06 moles) can be responsible for only .12 moles of this, leaving about 4 moles of carbonate unaccounted for. There are three possible causes of this paradox. Firstly, the estimate of CO_2 produced from the burrow reactions may be an underestimate if the cement content of the core represents only part of the bicarbonate released, rather than all of it as assumed above. Secondly, if the isotopic composition of the cement has been buffered by fermentation carbonate ($\delta^{13}\text{C} = +15\%$) rather than marine carbonate (+2.6%), then more sulphate reduction carbonate must be included to maintain the observed isotopic composition. This alone, however, is inadequate in itself since even if all the cement is of sulphate reduction origin, still only about .9 moles of sulphide would have been released, suitable to dissolve only another 1.7 moles of carbonate. The third possibility is that the sulphide oxidation reaction is only responsible for the initiation of the dissolution, and once the

silica precipitation starts, the process is self-perpetuating by the carbonate feedback mechanism (see chapter 2). It is relevant to note here that the volume of flint precipitated (754 cm^3) is equivalent to 1956 gms ($\rho_{\text{flint}} = 2.594$), or 32.5 moles. Even if only 50% of this is lepispheric silica (? precipitated whilst carbonate was dissolving), this still leaves a large excess of silica precipitating over the amount of carbonate dissolving.

6.5 SULPHIDE-SULPHATE REFLUX REACTIONS

The fate of the sulphate generated at the sites of flint formation is also of interest. As sulphate reduction was occurring in the central burrow at this time, it would be expected that the re-generated sulphate would rejoin the dissolved sulphate flux towards the burrow, eventually to be reduced again - a simple reflux mechanism. If this is the case, it should be detectable in the sulphur isotope composition of the pyrite since open system sulphate reduction results in a large depletion of ^{34}S ($\Delta \sim -43\%$) but oxidation of the sulphide so formed apparently results in a small fractionation (Nakai and Jensen, 1964). The effect of reflux between the two states therefore is to progressively deplete the available pool of sulphur in ^{34}S , and successively formed pyrite generations should have anomalously light isotopic compositions.

To test this, three samples of pyrite from within a paramoudra were analysed: a piece of the pyritised burrow itself, a larger nodule associated with the burrow; and a pyritised sponge collected adjacent to the burrow. The results (table 6.4) give values between -41.4% (the burrow) and -22.5% (the nodule) with respect to Cañon Diablo Troilite. Compared with contemporary seawater ($\delta^{34}\text{S} = +16\text{--}17\%$; Claypool et al., 1980), this corresponds to

fractionation factors of $\Delta = -38\%$ to -57% .

Open system sulphate reduction would be expected to result in pyrite of about $\Delta = -40\%$ but in a closed system this would tend towards the contemporary sulphate value (i.e. $\Delta = 0\%$). This is a consequence of the reservoir effect in which depletion of the light species from the available source results in an enrichment of the heavy species in the remaining material. Successive generations of pyrite will therefore be progressively enriched, to an extent which is dependent on the extent to which the reservoir has been depleted (i.e. Rayleigh distillation process).

The determined values for the paramoudra are within the possible range for normal sulphate reduction but, the burrow in particular, is well beyond the theoretical limit. Similar light values have been measured in sedimentary environments (Hudson, 1982; M.L. Coleman, pers. com.) but not satisfactorily explained. Even heavier values than these are usually associated with sulphate reduction in an open system (usually the result of slow sulphate reduction rates compared with the rate of sulphate supply), but from the oxygen isotope data, it would appear that the system was in fact partially restricted with respect to ^{18}O supply, in order to account for the depletion of ^{18}O in local pore-waters (see above). It is difficult, in this case, to envisage a system which is fully open with respect to sulphate and yet not open to the oxygen of the pore-waters in which the sulphate is dissolved. In short, there is a paradox in which the oxygen isotope variation suggests a confined system and yet the sulphur isotopic composition is anomalously light for such a situation. This is interpreted as suggestive of a sulphide-sulphate reflux system which results in a progressive depletion of ^{34}S in dissolved sulphur species. Further tests will be necessary to confirm this conclusively, and in particular, analysis of a series

of sub-samples, representing successive generations of pyrite, will be of use. If sulphide-sulphate reflux is the cause of the light isotopes, successive generations should also show a progressive depletion in $\delta^{34}\text{S}$, but if open system sulphate reduction is the cause, little variation, or more likely a slight trend towards heavier sulphur, would be expected to occur.

Interestingly, the $\delta^{34}\text{S}$ composition of a normal pyrite nodule, unrelated to any paramoudra, also gave a value of -33.2‰ ($\Delta = -50\%$). If reflux mechanisms are responsible for the light isotopes in the paramoudra, this value suggests that these reactions may also have some more general significance in explanations of chalk and flint diagenesis.

6.6 SUMMARY

Taking all these data together, it is now possible to propose a general model of paramoudra genesis as in fig. 6.13.

Paramoudras form around a very unusual long burrow, within which rapid organic matter oxidation is taking place. The effect of this is to deplete local pore-waters in oxygen, and in time, the burrow initiates local sulphate reducing conditions within a generally oxidising environment. Sulphate reduction of organic matter in the burrow releases sulphide ions and carboxy species, and some of the sulphide is fixed as iron monosulphides, eventually changing into pyrite. However, there is insufficient iron available to neutralise all of the sulphide released and the bulk of it is hydrolysed to H_2S which then diffuses away towards the aerobic conditions further out.

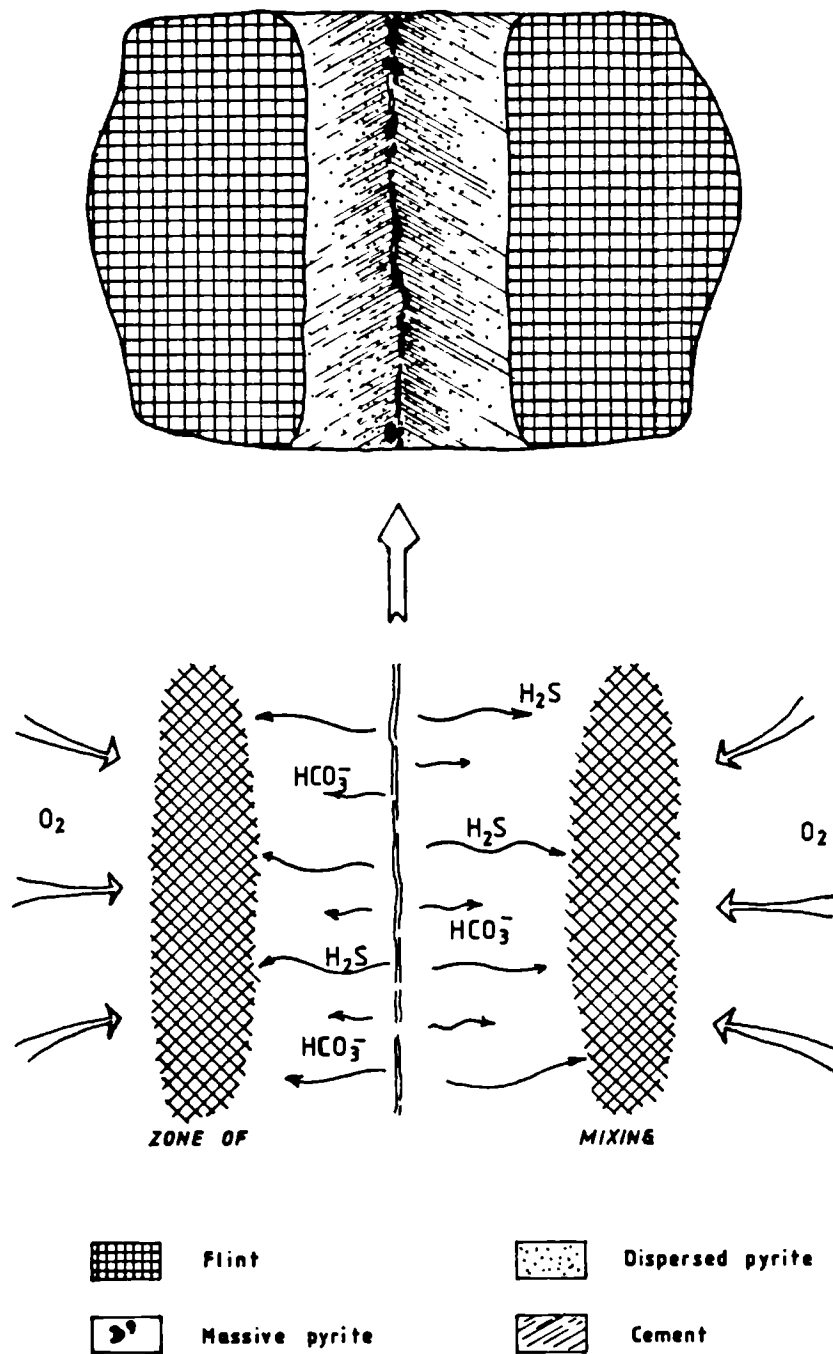


Figure 6.13 Postulated model of paramoudra formation around an isolated organic rich burrow. See text for discussion.

Meanwhile, hydrolysis of the sulphide liberates hydroxyl ions which react with the CO_2 from the sulphate reduction to form bicarbonate and carbonate, which if present in sufficient quantities may exceed the solubility product of calcite and low Mg-calcite is precipitated around the burrow. This cement contains about 6% carbonate derived from sulphate reduction, the remainder being redistributed marine carbonate.

At about the same time, or slightly before, authigenic phosphate and glauconite form adjacent to the burrow, the latter breaking down again to some extent during subsequent (possibly intense sulphate reduction) diagenesis. This results in an apparent K-depletion effect associated with the reactions in the central burrow. Similar phosphate growth and K-depletion subsequently affects the host sediment, as does additional pyrite growth.

The excess H_2S formed by hydrolysis of the sulphide diffuses away towards more oxic conditions where it is re-oxidised to sulphate and hydrogen ions by the action of thiobacilli bacteria. Part of the sulphate produced diffuses back towards the central burrow to continue in the sulphate reduction process, but the hydrogen ions diffuse only a short way and act to dissolve the chalk in an annular region around the cemented chalk core (fig. 6.13). Dissolved silica is abundant in the surrounding pore waters at this time due to the dissolution of biogenic silica, and the effect of carbonate dissolution at the oxic-anoxic boundary (approx Mn and Fe redox boundaries) is to precipitate the silica to form

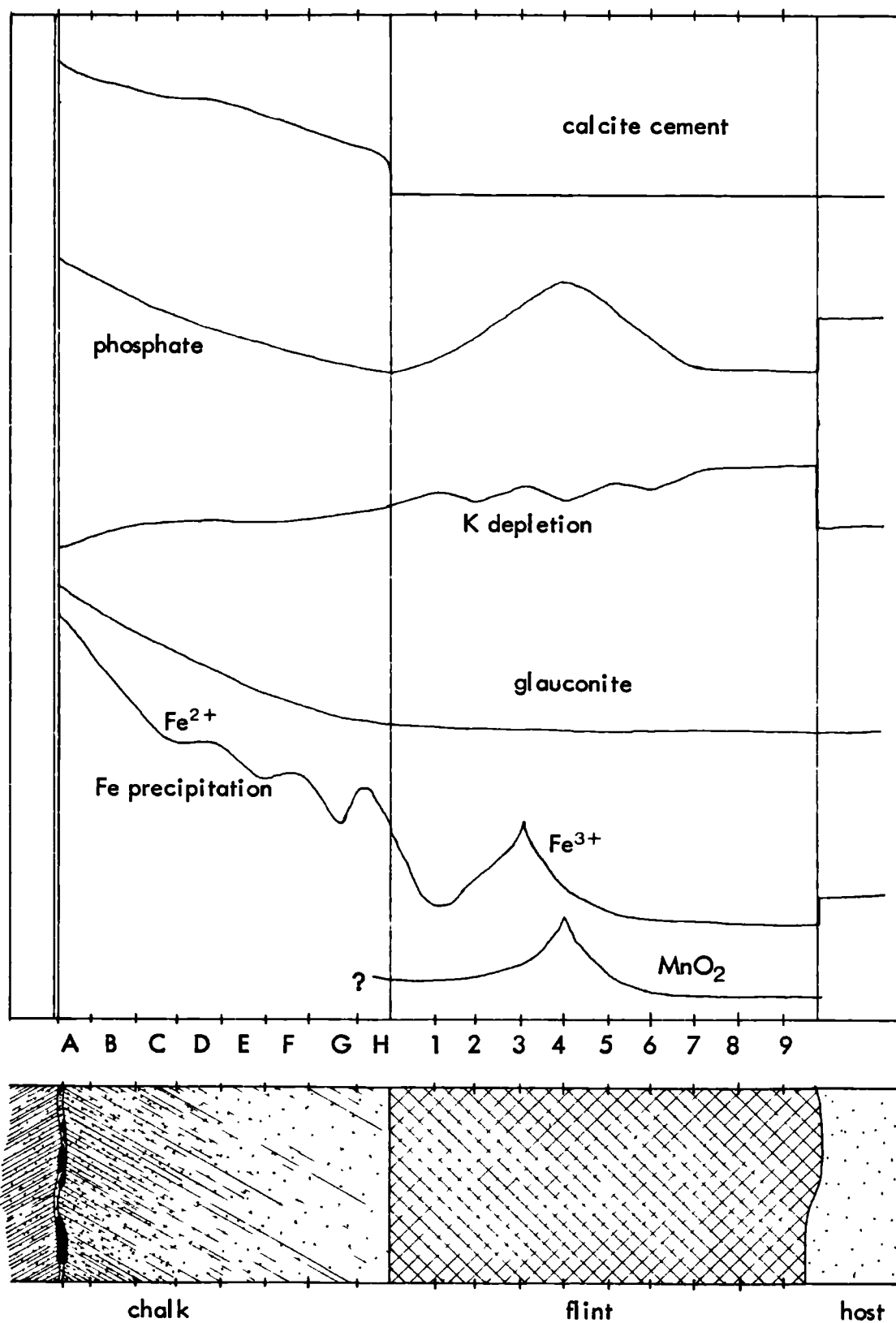


Figure 6.14 Summary of diagenetic reactions and products associated with paramoudra formation.

a flint. At the same time, more authigenic phosphate is formed towards the centre of the flint, possibly as a result of the pH and the high levels of dissolved bicarbonate and sulphate here, and this is associated with iron and manganese oxide precipitation at the iron and manganese redox boundaries respectively, within the flint (fig. 6.14).

Paramoudras clearly formed very near to the sediment surface, although their size points to a minimum depth of about 5 m. If this model is correct, then it has important implications for the genesis of nodular flint bands, which may also have formed at the oxic/anoxic boundary within the sediment, a possibility also suggested by the spatial relationships between the two flint types (chapter 3). In this case, it should now be possible to demonstrate similar timing of the above reactions in normal bedded flint series. In particular, phosphate and disseminated "pyrite" formation should post-date silicification, and if flint formation occurred at the top of the sulphate reducing zone during a break in sedimentation, it might also be expected that there would be preferential formation of pyrite immediately beneath the flint, where sulphate reduction would have been more intense. Extrapolation of these ideas to normal flint bands is the subject of chapter 7.

7. GEOCHEMISTRY OF BEDDED FLINT

SERIES

7.1. INTRODUCTION

The flint in paramoudras probably formed at the boundary between local anoxic conditions, developed around a sulphate reducing burrow, and the oxidising environment of the surrounding sediment. This occurred above the level of normal flint formation but it is likely that similar sulphide reoxidation at the main (horizontal) redox boundary was responsible for more widespread silicification (chapter 6). Indeed this is implied by the field relations between paramoudras and flint bands where the paramoudra combines with the lowest flint it meets, even if the burrow passes through it (section 3.6.2, plate 1E). Flint bands may therefore be thought of as the result of reoxidation at the base of the aerobic zone of H_2S generated by widespread sulphate reduction reactions in the sediment.

If this is the case, then it should be possible to detect the effects of the associated reactions in the diagenetic minerals around and within the flint. In particular, there should be preferential formation of iron sulphide below the flint where sulphate reduction is concentrated, additional phosphate growth may occur after flint formation, and manganese and iron may be remobilised from the sites of flint formation (cf fig 6.14).

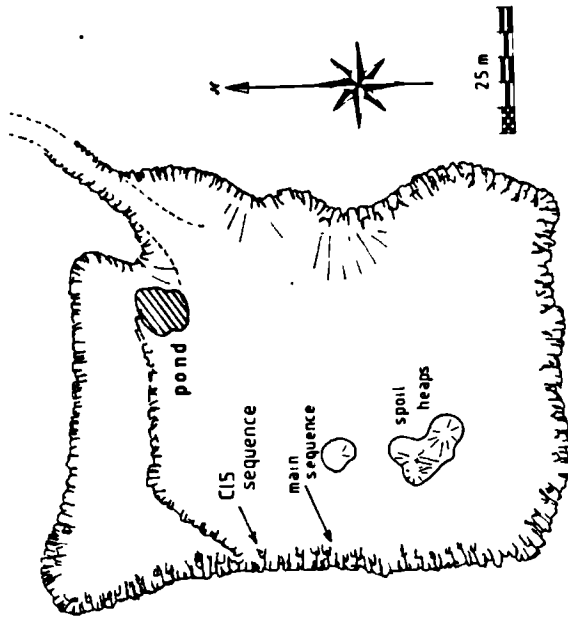
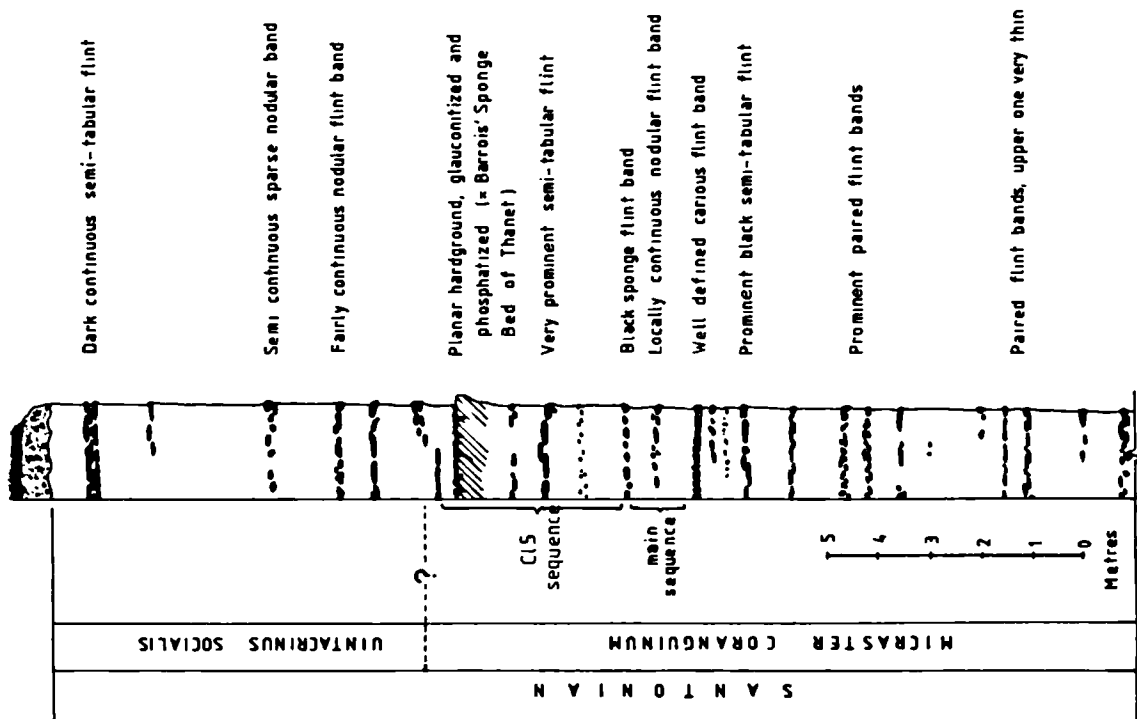


Figure 7.1 Sample locations at West

Clandon Pit, Surrey. Eiostratigraphic
zonation after A.S.Cale (pers. comm.)

To test this, detailed sampling around a flint band was undertaken, in a high Coranguinum sequence (Santonian) of west Clandon Pit, Surrey (fig. 7.1). The chalk here is exceptionally homogeneous and free from nodular beds, marl seams etc. which may disrupt any chemical trends caused by the silicification reactions. Sampling was undertaken in three vertical traverses (a,b & c) across a well formed nodular flint band (fig. 7.2) and the trace element data for the chalks and associated flints are given in tables 7.1 and 7.2 respectively. In addition, the carbon and oxygen isotopic compositions of the chalks were determined and the results of this are given in table 7.5.

7.2. CHEMICAL VARIATIONS IN THE CHALK SAMPLES

7.2.1 Variations Around the Flint Band

The minor and trace element distribution of selected elements in the Clandon Chalks is shown graphically in fig. 7.3. In these figures, the three curves for each element represent the three separate traverses across the flint and are shown together to allow easy assessment of lateral variation in the chemical trends.

Magnesium and strontium occur predominantly in the calcite lattice of the chalk sediment so the presence of any diagenetic carbonate should be reflected in variations in one or both of these elements. However, there is no systematic vertical variation in the concentration of either element suggesting that if diagenetic carbonate is present, it is of comparable chemistry to the original calcite.

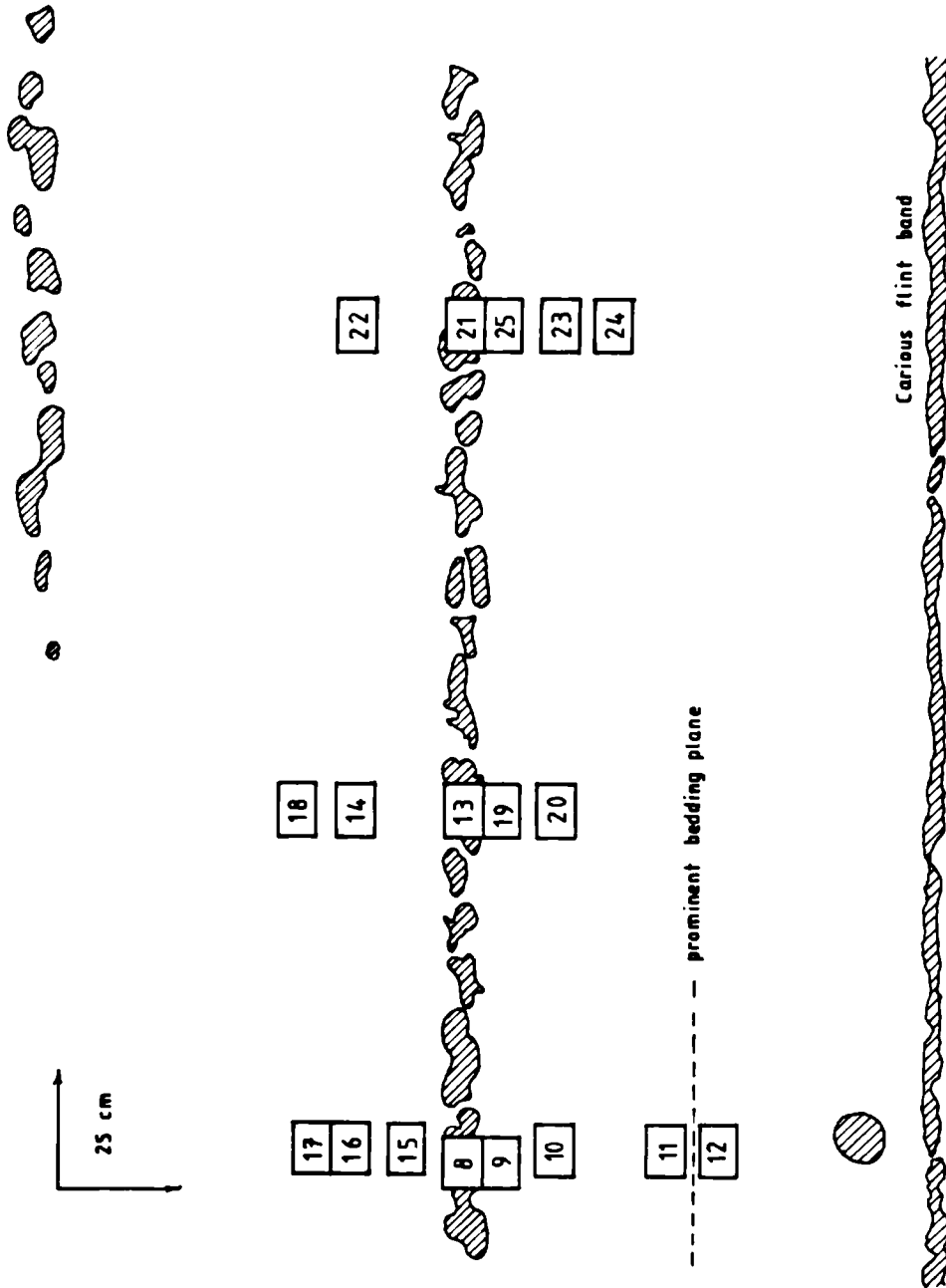


Figure 7.2 Sample distribution of the main Clandon specimens (CL 1 series).

Stratigraphic level is illustrated in fig. 7.1.

Table 7.1
Minor elements in Clandon cherts

Sample No.	Mg	Na	Sr	Mn	Fe
9	2760	195	640	505	545
10	2790	180	620	615	545
11	2530	205	620	640	705
12	2850	275	675	665	600
14	2700	195	640	640	365
15	2600	230	625	645	475
16	2770	210	650	505	445
17	2750	180	660	610	390
18	2820	175	635	645	370
19	2730	190	640	625	560
20	2860	190	630	620	545
22	2620	190	650	610	475
23	3000	170	580	730	570
24	2900	170	635	625	485
25	2950	175	665	600	500

Sample No.	P	Al	I	Ti	Si
9	285	1020	740	35.0	10600
10	315	995	720	32.0	6740
11	315	-	745	32.0	7140
12	400	1050	390	76.0	6890
14	325	840	260	30.0	5520
15	335	925	290	31.0	5940
16	375	925	260	31.5	6090
17	340	965	255	29.0	5600
18	350	810	235	26.5	-
19	310	890	255	28.5	-
20	310	985	315	33.0	-
22	275	855	265	29.0	-
23	570	970	270	27.0	-
24	280	985	330	32.5	-
25	335	870	280	31.5	-

Table 7.2
Minor elements in Clandon flints

Sample	Ti	Mg	Na	Sr	Mn
CL1/8	16.5	100	240	10	5.5
CL1/13	16.0	80	241	8	4.5
CL1/21	15.1	80	270	9	4.0

Sample	Fe	P	Al	K	Ca
CL1/8	52	108	370	250	5400
CL1/13	50	86	390	275	520
CL1/21	155	106	395	295	4100

Table 7.3
Porosity determinations on cherts

Sample	S.E.	Porosity %	Source
CL5/1	2.514	7.0	Clandon hardground
CL5/4	1.704	77.1	75cm below
CL5/9	1.781	72.9	200cm below
CL5/23	1.700	37.3	450cm below
Lanaye	1.700	77.3	Lanaye chalk, Maastricht
NC-16	2.167	20.3	Paramoudra in Lanaye chalk
CA/1B	1.714	36.9	Caister paramoudra
CA/1G	1.919	29.2	"

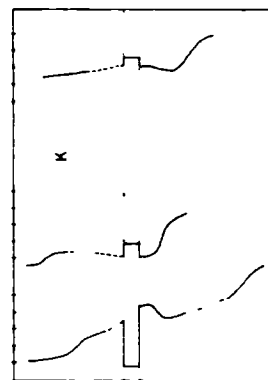
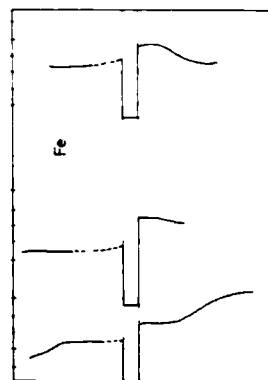
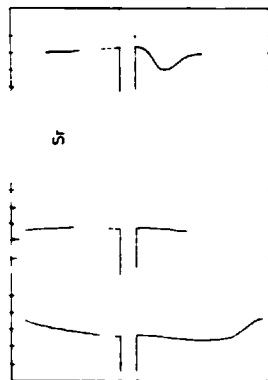
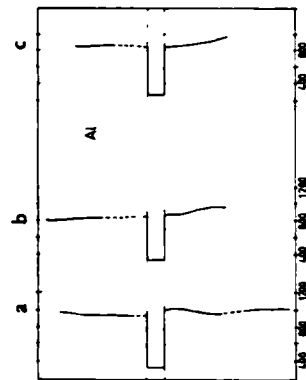
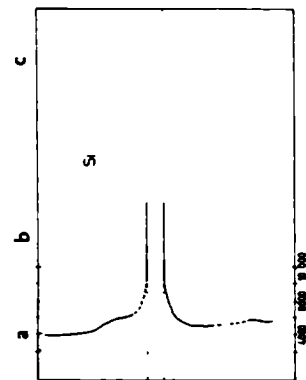
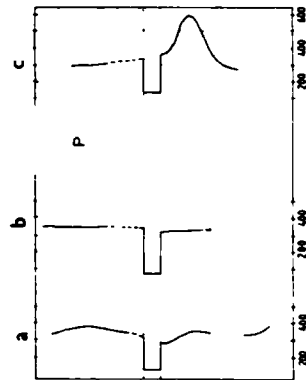
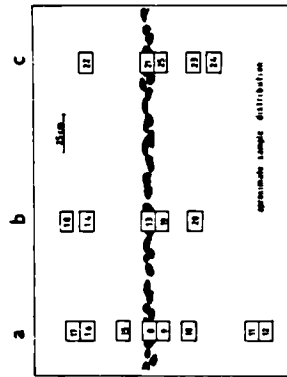
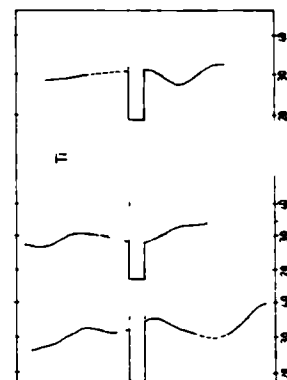
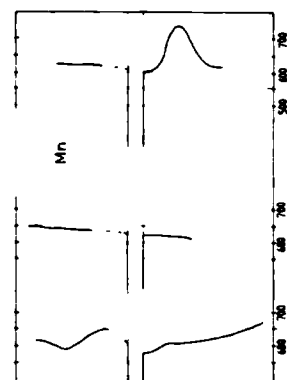
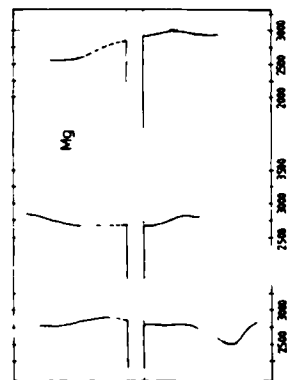


Figure 7.3 Vertical variations in trace element concentration across a flint band, West Clandon Pit, Surrey. Sample locations are given in figs. 7.1 and 7.2.



Conversely, there does appear to be a relationship between the Mg and the Na contents of the chalks. (fig. 7.4). The steep curve (2) of fig. 7.4 is only poorly defined and possibly may be the result of analytical errors. However, the curve represents an increase of Na and Mg in the ratio of 1:1 which is approximately the ratio of incorporation of these trace elements in the skeletal calcite of many macro-faunal fragments (G. Mackenzie, pers. com.) so this trend most likely represents the addition of small amounts of skeletal calcite to the samples. On the other hand, all of the samples which lie on this trend (12,15 & ?16, 9 & 17) were collected from traverse (a)(fig 7.2) which may suggest some other (diagenetic) cause. The more subtle negative relationship within the rest of the samples ($r=0.67$) is more difficult to explain. The wide range in Mg content (~ 550 ppm) is much greater than the amount of this element in clays and phosphates (see below) so it must represent variation in the chemistry of the coccolith calcite. This is possibly a consequence of oceanographic variations which have influenced the chemistry of the primary carbonate (i.e. coccoliths), but more data are necessary to test this.

Aluminium and potassium are associated predominantly with clay minerals in the chalk. Of particular interest in the Clandon sequence is the upward depletion of potassium, accompanied by similar variations in Ti, Si, to some extent Fe (but see below) and possibly a slight variation of Al (fig. 7.5). These variations are particularly apparent in traverse (a) but also occur in the other two. In the flints, a higher K content than that of the enclosing chalk is found in traverses (b) and (c) and even in traverse (a)

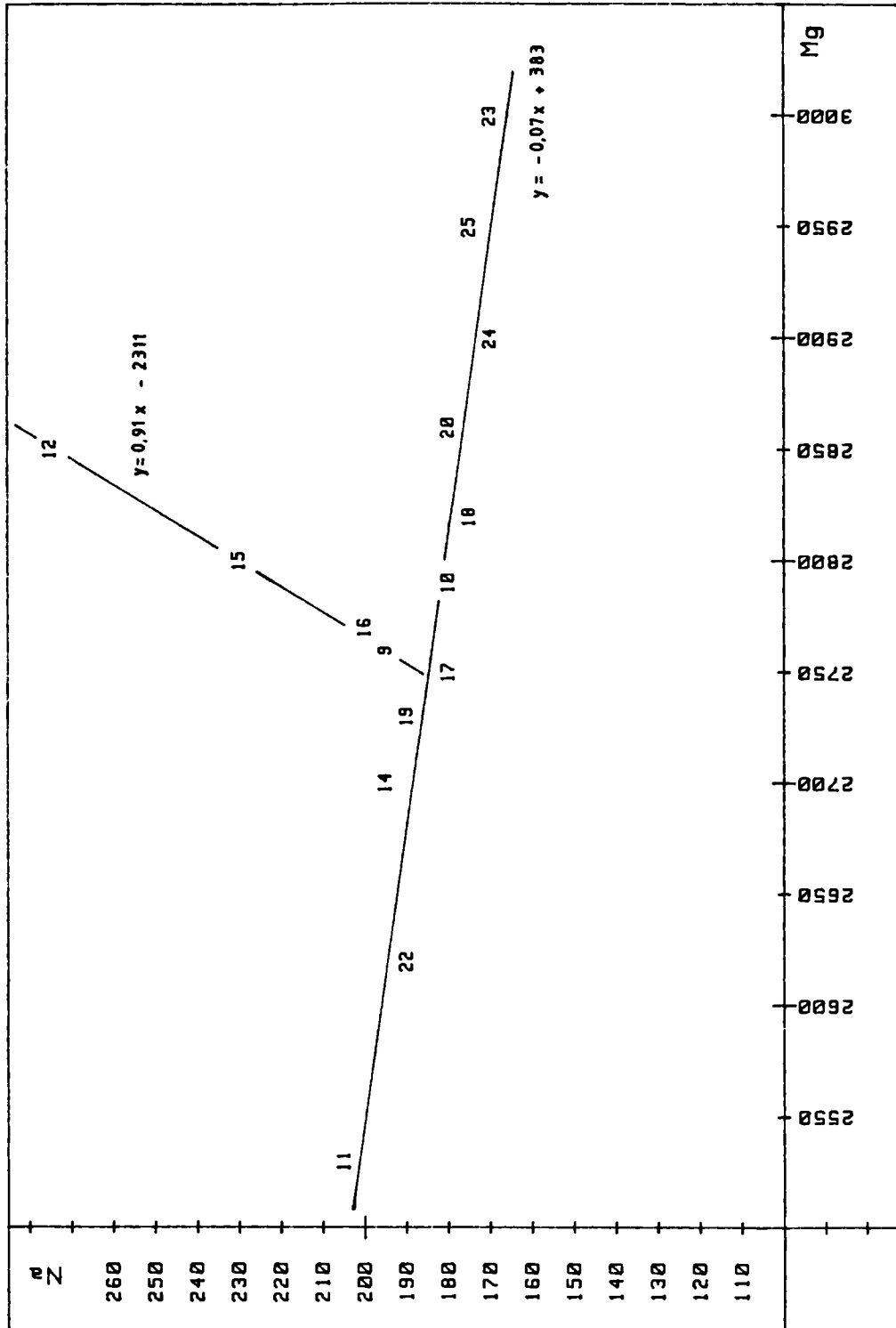


Figure 7.4 Comparison of Na and Mg in chalk samples from West Clandon Pit. *Ppm*

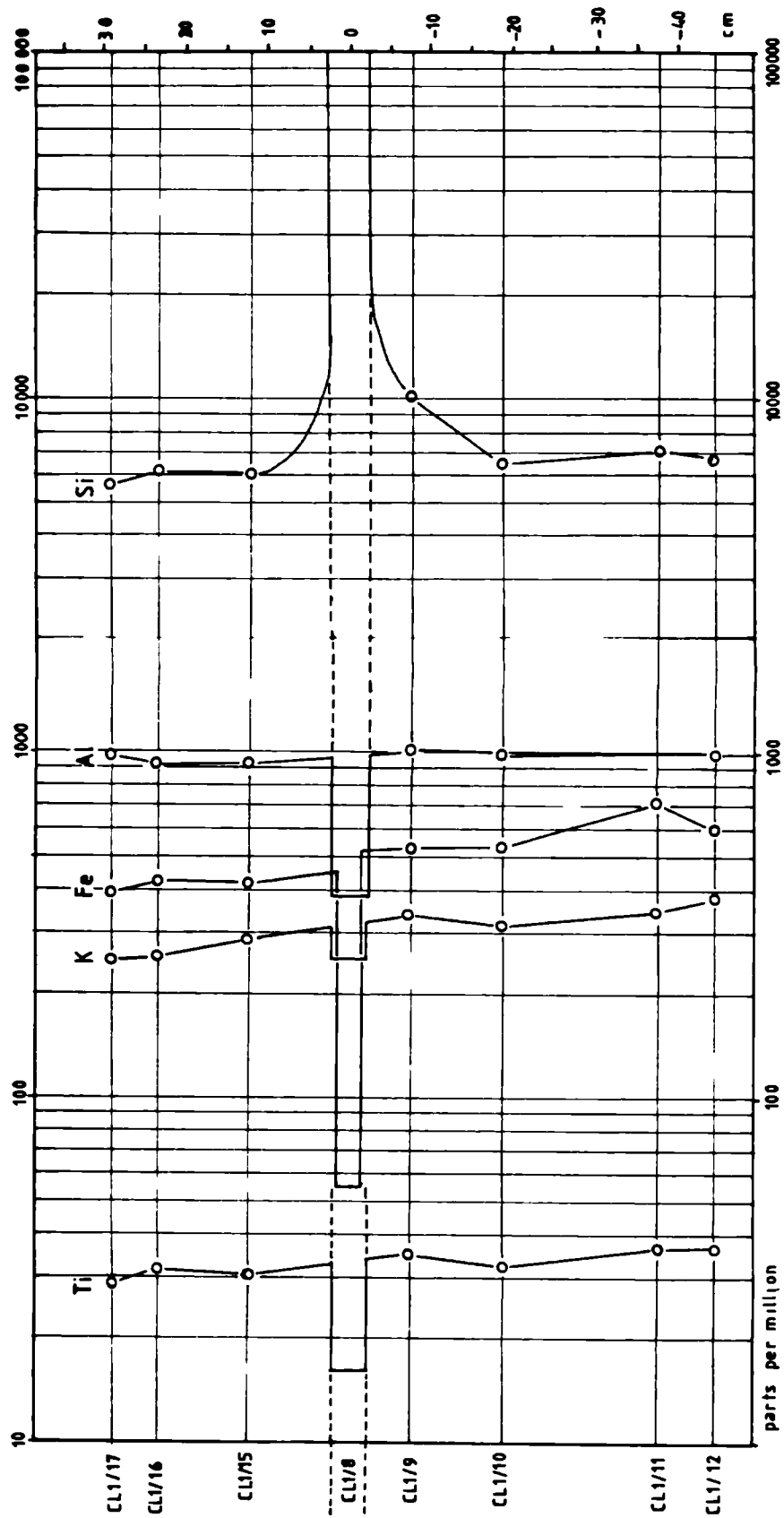


Figure 7.5 Detail of Ti, K, Fe, Al, and Si from traverse a of fig.7.3

the potassium shows less dilution within the flint than would be expected from the amount of Al dilution. This suggests that the K-trend (and associated element curves) is due to potassium depletion of some mineral(s) within the chalk subsequent to flint formation, and that the flint has protected the mineral grains preserved within it. This effect is similar to that observed in paramoudras (chapter 6) where it was apparently caused by bacterial organic matter oxidation, either during or just prior to sulphate reduction. In paramoudras it either pre-dates, or is contemporaneous with silification but in the Clandon sequence it postdates silicification and must be related to the subsequent development of reducing conditions above the flint.

The insoluble residue of the chalk here (after treatment in 2N acetic acid at pH = 3.95) revealed a similar mineralogy to that in the paramoudra: quartz, illite, smectite, and a mixed layer illite-smectite with about 30% "glaucinite" layers. If, as seems likely, the simultaneous depletion of both K and Fe is due to alteration of a single mineral, the curves presumably represent alteration of the glauconite layers since this is the only mineral with a significant content of both elements. Fe and K are depleted in the atomic ratio 7:2 suggesting that either the K is more firmly bound than the Fe, or that the change represents a transition from a glauconite structure to a true illite structure. This latter possibility is more compatible with the limited variation in Al content of the samples, and would be expected to exclude Fe but not K, which would readily be accommodated in the illite structure. This would suggest that glauconite forms early (possibly under sub-oxic or mildly anoxic conditions - see Chapter 3)

and breaks down again under more strongly reducing conditions.

In addition to the upward depletion of Fe ? from glauconite, there is a consistent difference in iron content from below to above the flint. This results in an excess of about 100 ppm Fe, present in another mineral phase, immediately beneath the flint in all three traverses. Excess Fe here is also implied by a plot of Fe against K in which the samples immediately below the flint in traverses (b) and (c) lie above the main trend (fig. 7.6). In sequence (a) the effect is masked by an anomalously high K content. The additional iron may be the result of introduction of ferroan calcite cement below the flint but as there is no comparable change in the Sr or Mg concentration this is unlikely. The introduction of ferric oxyhydroxides is also unlikely since there is no comparable Mn peak (cf. precipitation at the Fe and Mn redox boundaries in paramoudras - see 6.2.2b) so it is likely that the excess represents preferential formation of iron sulphides here. This implies a longer or more intense period of sulphate reduction below the flint compared to above, suggesting that at some time the level now occupied by the flint represented the oxic/anoxic boundary. This does not necessarily mean that the flint formed at this time, although in view of the close parallel with the formation of flint in paramoudras, it seems likely.

No clear trend is visible in the phosphorous distribution such as would suggest preferential formation of phosphates anywhere. The anomalously high P content in CL1/23 (570 ppm) probably represents incorporation of traces of biogenic phosphate particles (e.g. fish scales or teeth) in the sample.

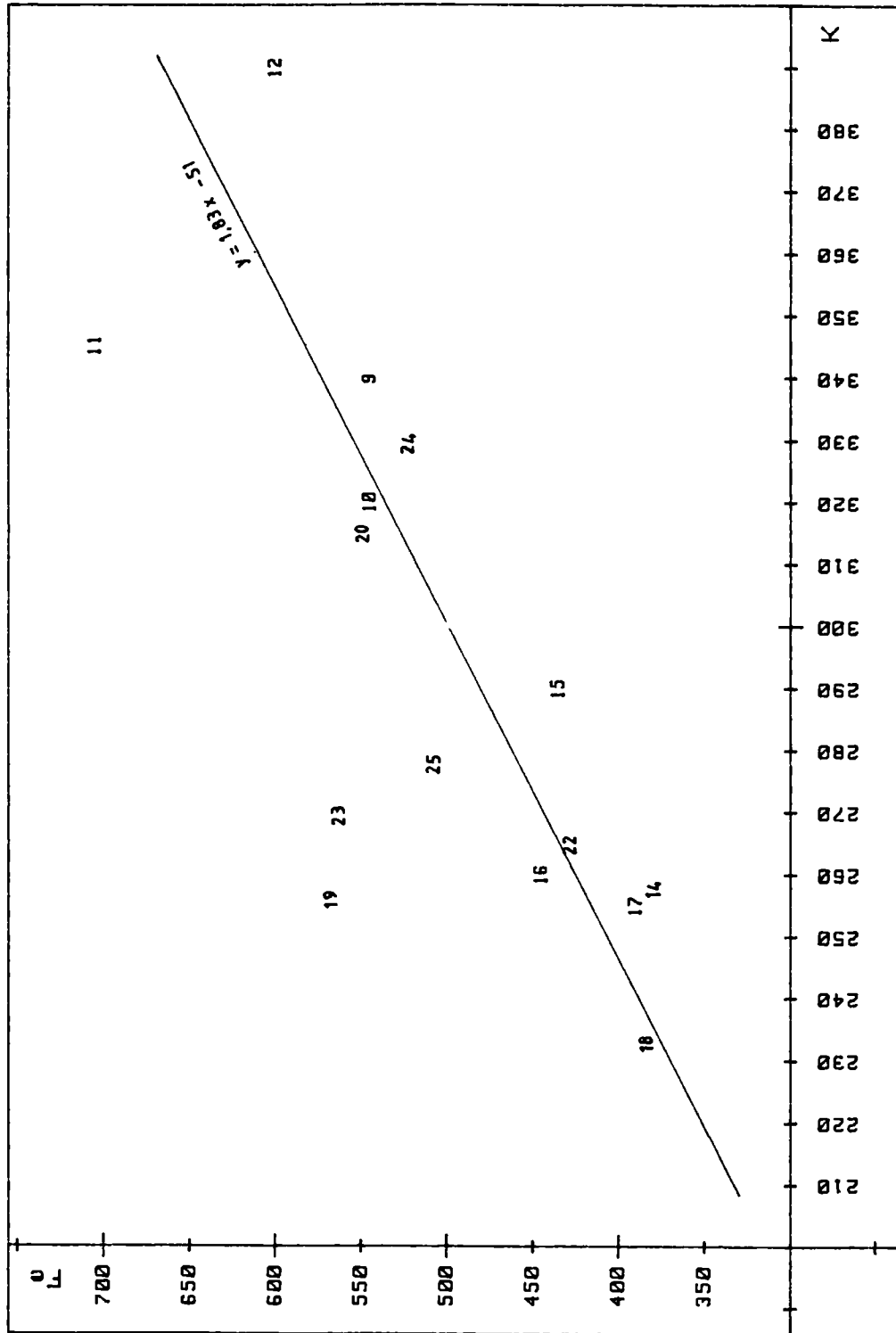


Figure 7.6 Correlation of Fe with K (reflecting ?illites) in West Clandon chalks . ppm

7.2.2 Variations Higher in the Section

If the K and Fe depletion effect is due to sulphate reduction reactions subsequent to flint formation, then it would seem likely that it is connected with formation of the hardground about 4 metres above because this is the only obvious diagenetic feature in the section other than the flints themselves. To test this, samples were collected at intervals of approximately 35 cm up to the hardground (Table 7.4, fig. 7.7). More detailed sampling was undertaken for the 2 m immediately beneath the hardground in connection with an isotopic study to determine the origin of the hardground (see chapter 8).

Cementation below the hardground is accompanied by an increase of about 200 ppm Mg and a decrease of about 200 ppm Sr. This suggests a comparatively Mg-rich cement (? similar to the paramoudra cement - 2000 ppm - see 6.2.1), but depleted in Sr with respect to the original calcite. The increase in Fe in the same samples probably reflects the growth of iron sulphides although Jeans (1980) has suggested that the cement in Chalk hardgrounds is "ferroan calcite". The increase in P reflects the authigenic phosphates visible in the field.

Al shows the predictable dilution effect, reflecting the presence of cement diluting the host sediment whilst below the lithified unit, K and Al show a close positive relationship which breaks down in the cemented chalk. Potassium again shows a decrease in concentration within the cemented chalk (cf paramoudras, Chapter 6) which is presumably associated with the bacterial reactions here (sulphate reduction or just before - see discussion in Chapter 8), although the shape of the K and Al curves probably

Table 7.4
Minor elements in high zonal cherts at
West Clendon Pit

Sample	Mg	Na	Sr	Mn	Fe
CL5/14	1250	157	464	343	653
CL5/15	1860	167	524	383	1010
CL5/16	1600	194	647	346	403
CL5/17	1557	133	604	358	401
CL5/18	1540	172	576	342	302
CL5/19	1491	172	537	328	345
CL5/20	1647	167	649	335	397
CL5/21	1622	183	610	358	380
CL5/22	1700	177	638	337	422
CL5/23	1520	162	657	326	421
CL5/24	1530	152	611	327	418

Sample	F	Al	S
CL5/14	943	698	168
CL5/15	1040	688	195
CL5/16	417	922	257
CL5/17	716	815	282
CL5/18	278	656	171
CL5/19	267	777	242
CL5/20	310	816	250
CL5/21	306	784	217
CL5/22	378	922	327
CL5/23	374	922	267
CL5/24	366	770	275

Table 7.5
Stable isotope data for Clendon cherts
(Depth is w.r.t. main flint band)

Sample	$\delta^{17}O$	$\delta^{18}O$	Depth (cm)
CL1/9	2.07	-1.90	-5
CL1/10	2.00	-1.83	-25
CL1/11	2.02	-1.91	-45
CL1/12	2.02	-1.92	-50
CL1/14	1.95	-2.07	20
CL1/15	1.99	-1.87	10
CL1/16	1.96	-1.82	25
CL1/17	1.98	-1.88	30
CL1/18	1.98	-2.06	30
CL1/19	1.97	-1.88	-5
CL1/20	1.97	-2.12	-20

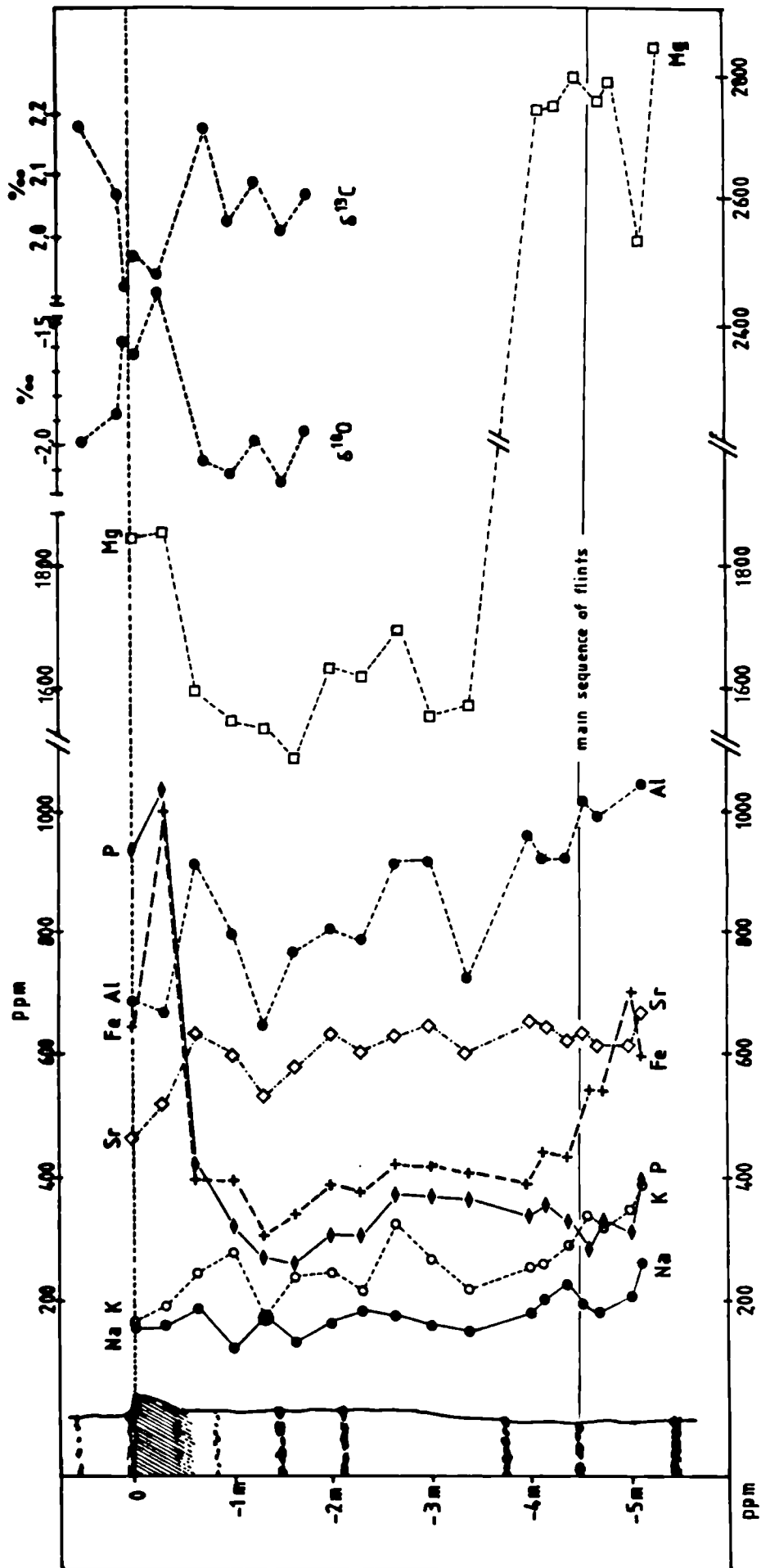


Figure 7.7 Trace element and stable isotope variations above the main Clandon

series of samples. hatched area at 0m is the Clandon Hardground.

has been modified by the addition of small amounts of diagenetic glauconite here.

Below the lithified chalk, Al and K contents vary greatly but are closely related to each other. The K and Fe depletions in the main sequence of samples are not related to any obvious lithological change although there is a slight trend towards lower K (and to a smaller extent Al) values up sequence. This possibly reflects the effect of K-depletion associated with the hardground, superimposed on more local sedimentological variations. The anomalous Fe concentration low in the sequence is unexplained.

Na and Sr also show a slight upward decrease in concentration, probably representing changes in the chemistry of the calcite component in response to oceanographic variations (temperature etc). The abrupt change in Mg between the lower and upper sequence of samples is curious. This could be due to an analytical error (e.g. poor calibration of the Mg line in the spectrometer) but there is no anomaly in the concentrations of part of a series of flints analysed at the same time, so this seems unlikely. The jump coincides with the presence of a flint band but no other elements show a dramatic change here so the association may be fortuitous. The apparent change in Mg remains unexplained.

Clearly, the well developed depletion of K and Fe in the main sequence of samples is not directly related to formation of the hardground itself although similar reactions, at least in the case of K, and probably also Fe, are associated with hardground formation. In this respect, it may be important that the main depletion effects terminate about $1\frac{1}{2}$ metres above the sampled flint band, just where there is a distinctive gap in the normal,

regular succession of flint bands. This position (approx. sample CL₅/23) is also characterised by Al, K, Mg and to a lesser extent P and Fe concentrations above the predictable background for these elements. It seems possible that this position was also once the site of early diagenetic lithification but that in this case normal sedimentation resumed before exposure of the lithified unit to form a hardground. A cemented bed here was not detected in the field but on a fresh unweathered section, such as at Clandon, this is not unreasonable.

It seems likely therefore that the unusual diagenetic effects lower in the section relates to a transient period of lithification, below the main hardground, which never developed into a fully lithified and mineralised unit. By comparison with similar reactions which occurred in the Caister Paramoudra, it is suggested that sulphate reduction, or an associated bacterial reaction, is the cause of these effects.

7.3. STABLE ISOTOPE VARIATIONS

If the effects described above are indeed due to the same reactions which occurred in paramoudras, then they should also result in changes in the stable carbon and oxygen ratios of the carbonate. To test this, the samples in sequences (a) and (b) were analysed isotopically and the results are given in Table 7.5. Similar analytical problems to those encountered while analysing the paramoudra chalks necessitated multiple analyses of each sample and selection of the most reliable determinations.

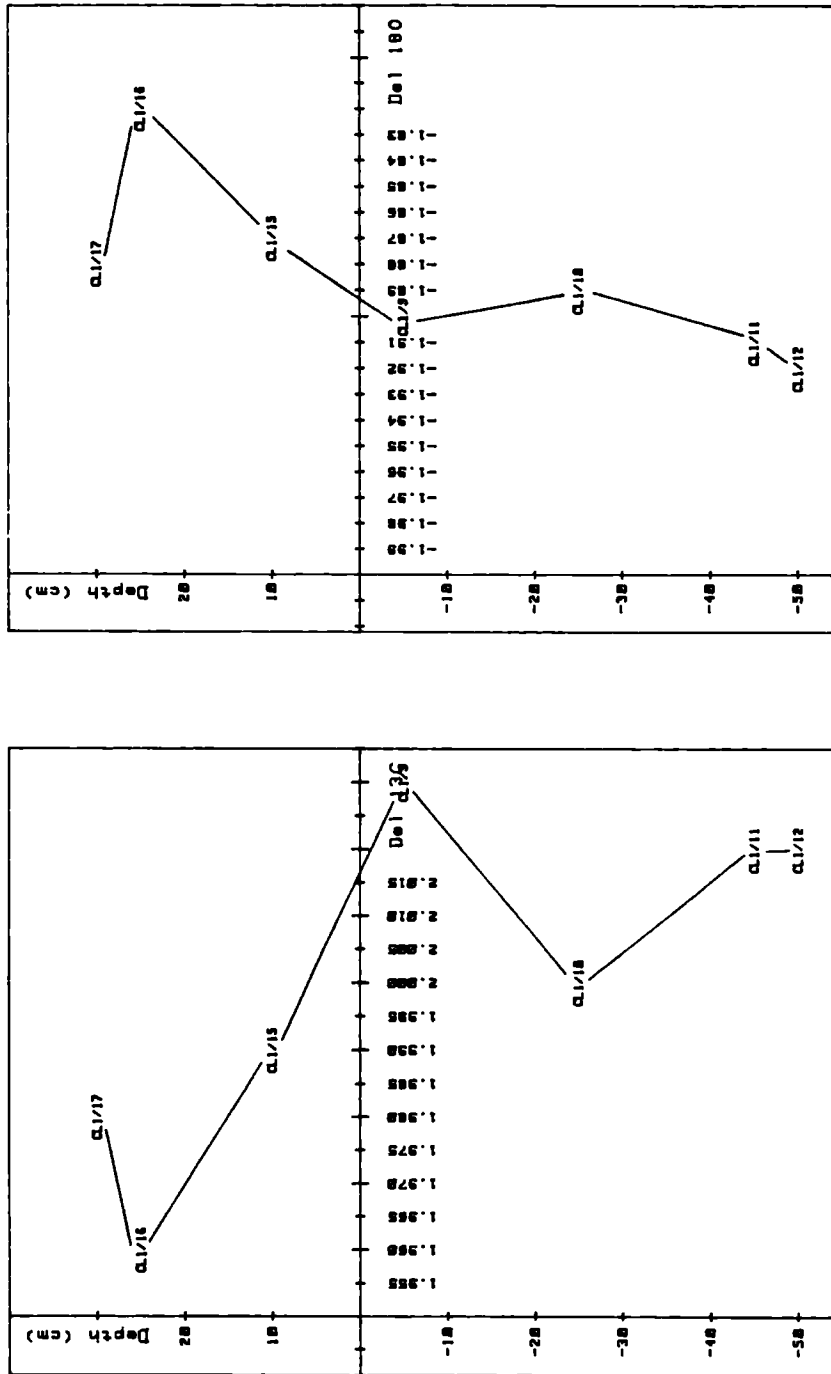


Figure 7.8a Vertical variation in $\delta^{13}C$ and $\delta^{18}O$ in West Clandon series (a)

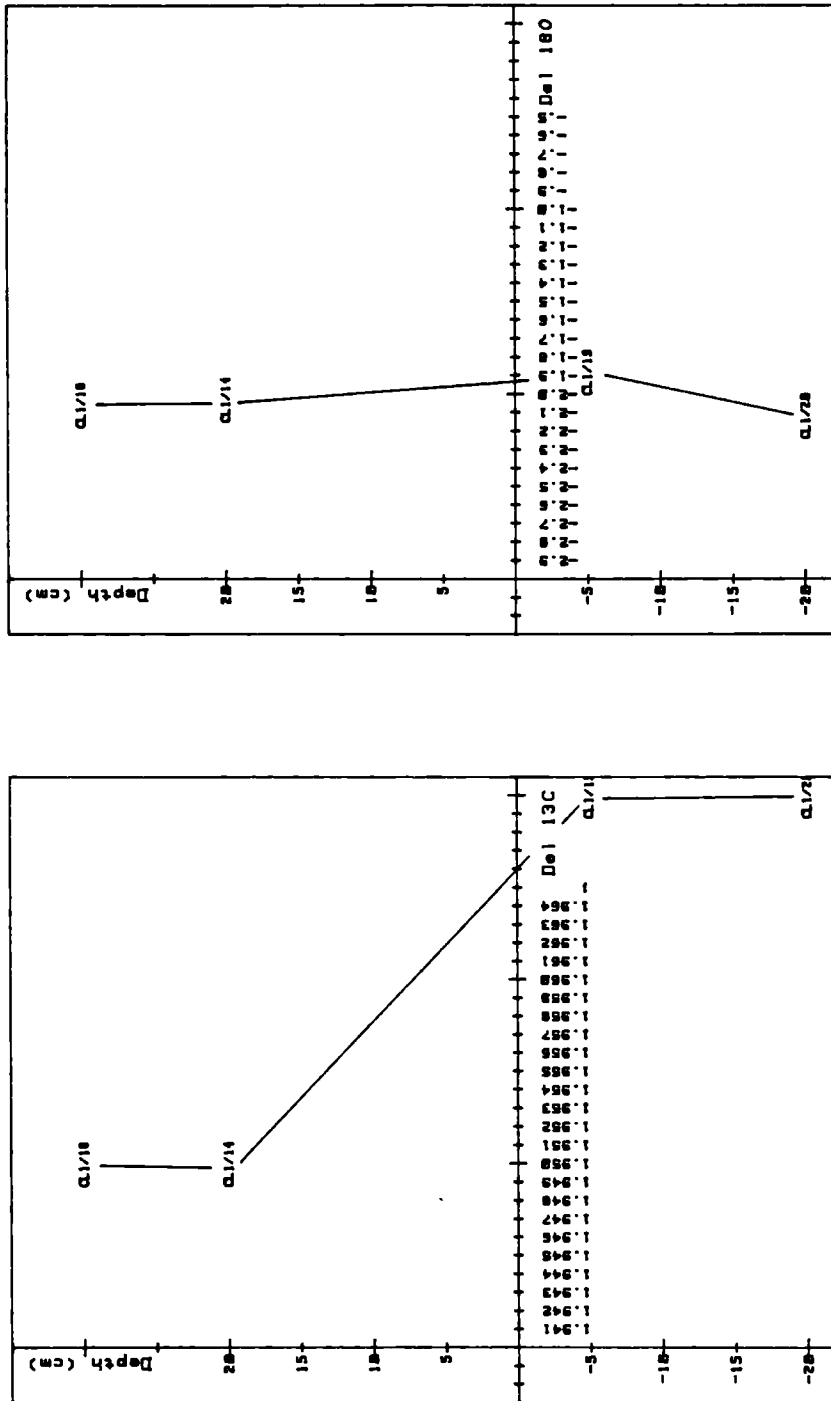


Figure 7.8b Vertical variation in $\delta^{13}C$ and $\delta^{18}O$ in West Clandon series (b)

The variations in $\delta^{13}\text{C}$ and $\delta^{18}\text{O}$ with position relative to the flint band are shown in figs. 7.8 a and b. As there are only four samples in the central sequence, the trends cannot be considered in any detail so discussion here will concentrate on the better sampled sequence (a). Although the variations are very small ($< .1\%$ in both $\delta^{13}\text{C}$ and $\delta^{18}\text{O}$), there is a clear trend towards lighter $\delta^{13}\text{C}$ and heavier $\delta^{18}\text{O}$ values higher up the sequence. This inverse relationship is also seen by comparing the two directly (fig. 7.9). It is possible that variations of this magnitude may be due entirely to analytical error (see above) but in view of the clear correlation between the ^{13}C curve and that of potassium in the same samples (fig. 7.10), it is considered likely that the trends are real. In addition, analytical errors would probably produce a positive relationship between $\delta^{13}\text{C}$ and $\delta^{18}\text{O}$ due to the correlated kinetic fractionation effects on the ^{13}C and ^{18}O in the CO_2 analysed.

All the samples of traverse (a) except CL1/9 lie on an approximately linear trend in a plot of $\delta^{13}\text{C}$ against $\delta^{18}\text{O}$ (fig. 7.9) although in view of the poor sample spread it is difficult to be confident of the validity of this correlation. Ignoring CL1/19 a similar (but even less certain) trend is suggested from the samples in sequence (b). In addition samples from both sequences together show a good positive correlation between $\delta^{13}\text{C}$ and the K content ($R^2 = .84$) suggesting a common cause of the variations. The upward depletion in K has already been attributed to diagenetic reactions (probably sulphate reduction) occurring nearer to the sediment surface, so the associated upward decrease in $\delta^{13}\text{C}$ and

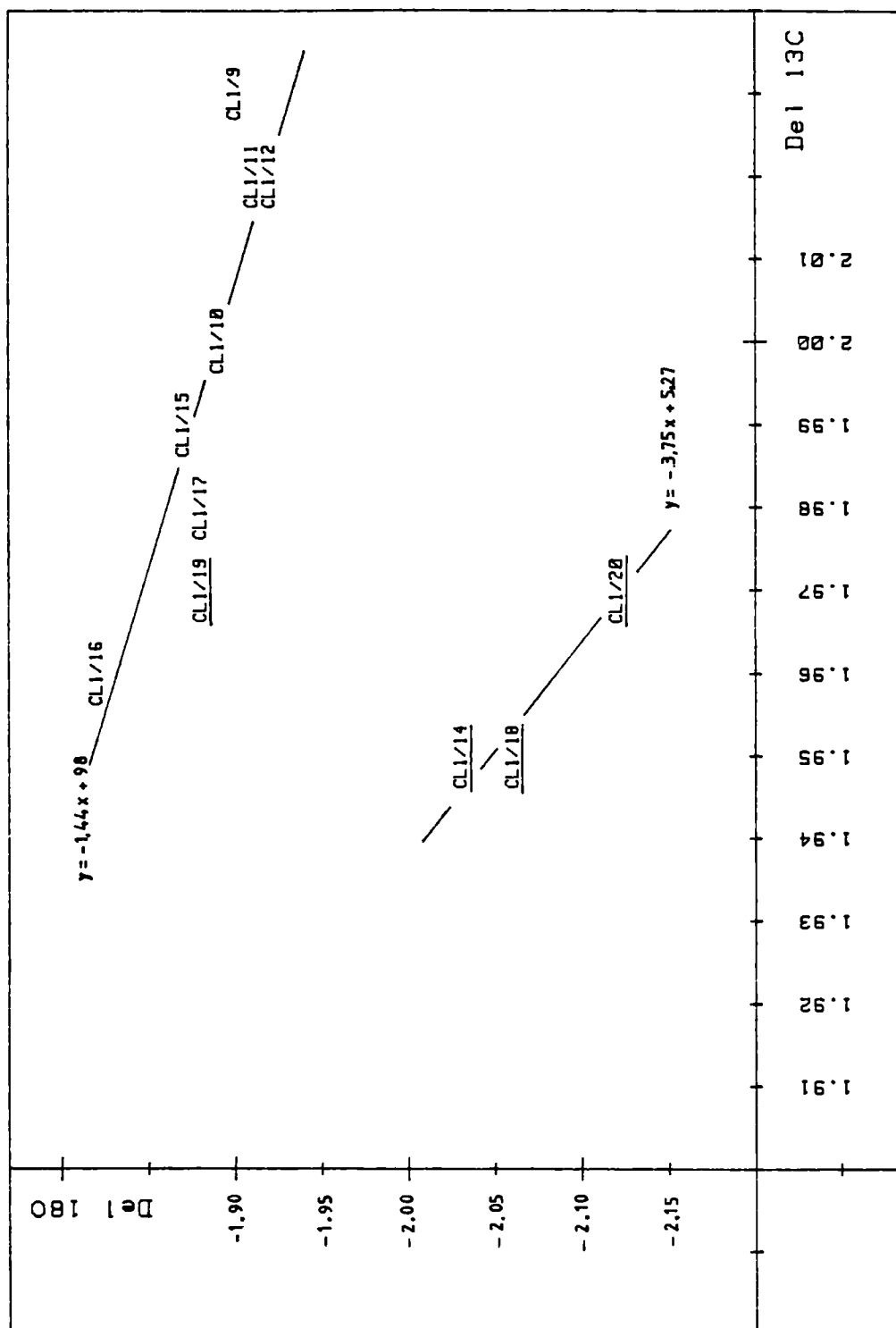


Figure 7.9 Correlation of $\delta^{18}O$ with $\delta^{13}C$ for West Clandon series b (underlined) and series a. Regression lines exclude CL1/9 and 19

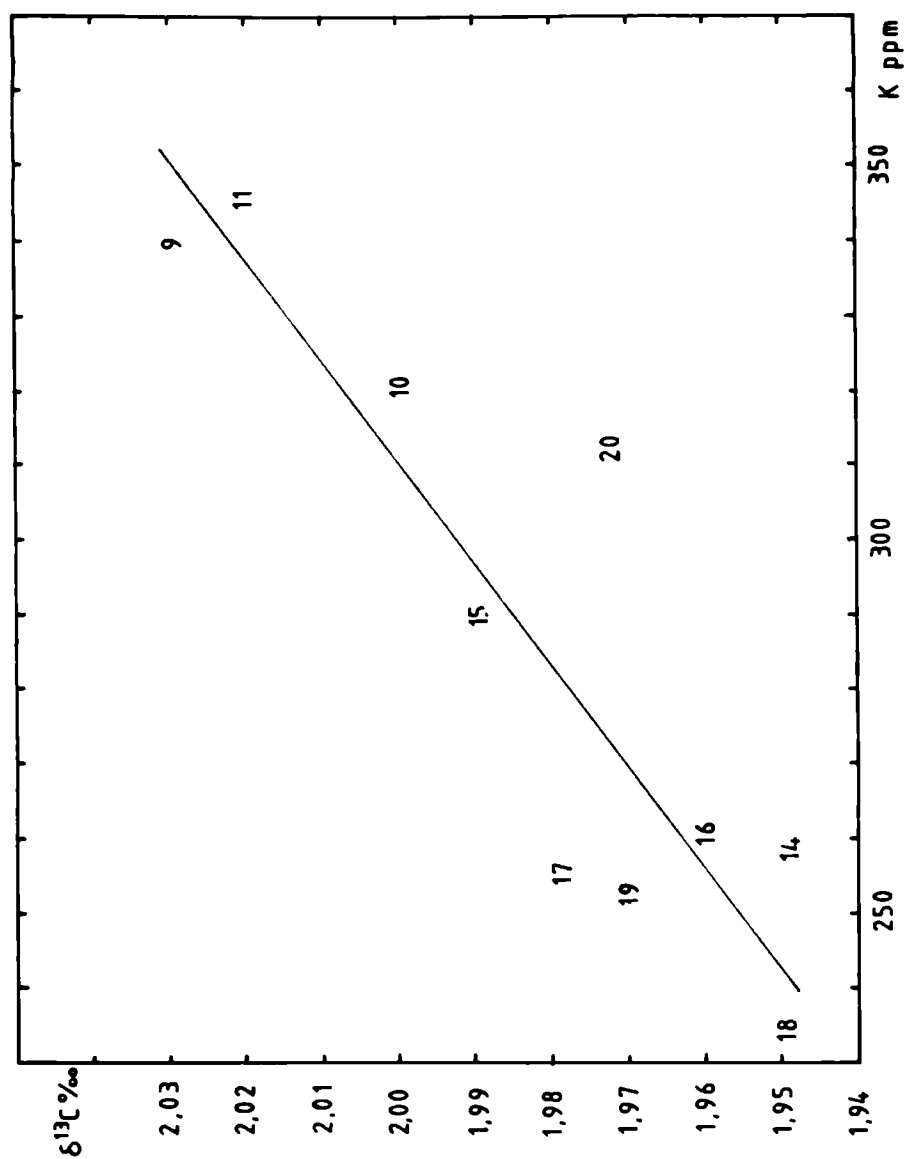


Figure 7.10 Correlation of $\delta^{13}\text{C}$ with K content (illite) in
chalks from West Clandon series

increase in $\delta^{18}\text{O}$ presumably reflects the same, or a related process. This suggests that the isotope variations are due to incorporation of diagenetic (sulphate reduction) cements similar to those in the Caister paramoudra. Similar trends occur in the lithified chalk below the hardground, higher in the section, (fig. 7.7), and it will be shown in Chapter 8 that lithification here is probably attributable to sulphate reduction cements also. As with the paramoudra cement (Chapter 6), the sulphate reduction component has been strongly buffered by pre-existing marine carbonate to produce a calcite only a little lighter in ^{13}C than the original sediment. Calcite precipitated during sulphate reduction is generally non-ferroan as any Fe is rapidly fixed as sulphides so the cements detected isotopically at Clandon are not reflected in an increase of Fe in the chalk.

An important difference between the paramoudra cement and that represented here is the inverse relationship between $\delta^{18}\text{O}$ and $\delta^{13}\text{C}$, reflecting a cement which is isotopically heavier in $\delta^{18}\text{O}$ than the host carbonate. In the paramoudra, the lighter oxygen isotope composition of the cement was attributed to exceptionally rapid precipitation of the carbonate, which resulted in the depletion of local pore waters in ^{18}O . However, the comparatively heavy cement associated with the Clandon lithification episodes suggests that this apparently did not happen, and the oxygen isotope composition of these carbonates reflects more closely the temperature of precipitation of the cement. It is heavier than the host because the precipitation temperature is approximately that of Cretaceous marine bottom waters, which were considerably colder than the surface waters in which the coccolith-rich host sediment was formed.

In addition to the above variations, the samples immediately beneath the flint band (CL1/9 and 19) apparently have been subjected to further alteration since, in both cases, they lie above the normal trend of $\delta^{13}\text{C}$ against $\delta^{18}\text{O}$ (fig. 7.9). The anomalously high K content of CL1/9 can be attributed to shielding of the sample, by the overlying flint, from the chemically active fluids above, so a similar effect would be expected in the isotopic composition. As samples CL1/9 and CL1/19 still lie close to the K - $\delta^{13}\text{C}$ curve for the Clandon chalks (fig. 7.10), it seems reasonable to assume that their carbon isotope composition is more or less normal. This implies that the anomalous $\delta^{13}\text{C}/\delta^{18}\text{O}$ ratio for these samples (i.e. above the main $\delta^{18}\text{O}$ - $\delta^{13}\text{C}$ curve for each sequence) is due predominantly to an anomalously heavy oxygen isotope ratio rather than to light carbon. By comparison with the host sediment to the paramoudra, it is tentatively suggested that this is due to exchange of the samples with isotopically light meteoric waters, but with CL1/9 and CL1/19 preferentially protected from the downward migrating meteoric waters by their respective overlying flints.

Further evidence of isotopic exchange with meteoric water derives from the estimation of the original isotopic composition of the chalks before addition of cement. Knowing the dilution factor of clays in the flint (see below - section 7.4), and assuming that the flint preserves the pre-alteration K content, the original K content of the sediment can be calculated as approximately 660 ppm. The K-depletion of the samples is proportional to the introduction of isotopically light carbon to the sediment so it is now possible to calculate the original $\delta^{13}\text{C}$ of the carbonate: about 2.2 ‰. This is typical of Upper Cretaceous Chalks (eg. Scholle and Arthur, 1980). From this, a

very rough estimate of the original sediment $\delta^{18}\text{O}$ can be obtained from the $\delta^{18}\text{O} - \delta^{13}\text{C}$ trend in fig. 7.9 giving a value of -2.9 PDB. Interpreted in terms of precipitation temperature from sea-water (Craig, 1965), and taking $\delta^{18}\text{O}$ of contemporary sea water as -1.2% (Shackleton and Kennett, 1975), this suggests a Cretaceous sea-water surface temperature of about 25°C . Inevitably, with such unreliable data, very large errors may be involved in such approximations but even allowing for an error of 1% (i.e. $\sim 100\%$ error on the $\delta^{13}\text{C} \rightarrow \delta^{18}\text{O}$ extrapolation) this does not explain the anomalously high temperature compared with the 15°C or so suggested by Savin (1977). This is further evidence (albeit somewhat unreliable) that the Clandon chalks have anomalously low $\delta^{18}\text{O}$ values, suggestive of interaction with isotopically light meteoric waters.

If this latter suggestion is correct, then $\delta^{18}\text{O}$ has been affected substantially more than $\delta^{13}\text{C}$. This is similar in type but not extent to the same exchange reactions affecting the host chalk of the Caister paramoudra in which $\delta^{18}\text{O}$ was lowered more than $\delta^{13}\text{C}$ by a factor of about 5.

7.4 CHALK - FLINT PARTITIONING

From the above discussion it is clear that the flint band formed prior to the onset of intensive sulphate reduction which occurred at a level only one or two metres above it. It is relevant now to investigate the mechanisms of the replacements, and in particular the effect of silicification on the non-carbonate components of the chalk. As will be shown, this provides greater refinement in defining the specific chemical environment of silicification.

From the overall trace element trends for the three vertical traverses sampled (fig. 7.2) and assuming that the values have not changed significantly since the flint formed, it is possible to predict the theoretical concentration of any of the trace elements at the site of the flint. From the difference between this estimate and the measured concentration of each element in the flint it is then possible to calculate the apparent dilution of each element as the carbonate host is replaced by silica. These chalk-flint "partition coefficients" (Table 7.6) can be plotted graphically between the two end members represented by Ca (which is lost almost entirely upon silicification), and Si (which increases from negligible values to about 96%). As shown in fig. 7.11a, elements associated dominantly with the original calcite will plot towards the chalk (Ca) end, elements associated with the silica will plot towards the flint (Si) end, whilst any elements associated with impurity minerals (clays, phosphates etc) will plot on some intermediate line. Furthermore, the position of this line will depend on the amount of dilution of the mineral concerned, and this can be interpreted directly in terms of the porosity of the chalk at the time of replacement (see discussion in Chapter 5).

The partition coefficients for the elements of interest are shown graphically in fig. 7.11b. As would be expected, Sr and Mg show a very strong association with calcite and a slight association with another phase, probably clays. If this is the case, the proportion of the element which is present in the impurity mineral can be estimated by comparison with the Al dilution, and suggests about 170 ppm Mg and only a few ppm Sr present in clays and

Table 7.5
Flint/chalk, bull partition coefficients
West Clendon Pit

Sample	Left	Log	Centre	Log	Right	Log
Al	.7805	-.4197	.4509	.3460	.3420	-.4659
Fe	.1166	-.9337	.0905	-1.0474	.3370	-.4724
Mg	.0360	1.4440	.0663	-1.1785	.0232	1.5502
Ca	.0138	-1.0587	.0092	2.0348	.0105	1.9782
Na	1.2310	.0902	1.2470	.0758	1.4800	.1701
F	.8197	.0361	1.0680	.0202	1.0826	.0345
Ti	.4848	.1141	.5517	.0483	.4918	-.3082
P	.3549	-.1300	.2656	.5757	.1700	-.7294
Mn	.0093	2.0107	.0057	2.1990	.0066	-2.1977
Sr	.0158	-1.8011	.0125	1.9021	.0137	-1.8637
Si	149.7	2.1725	173.8	2.2402	-	-

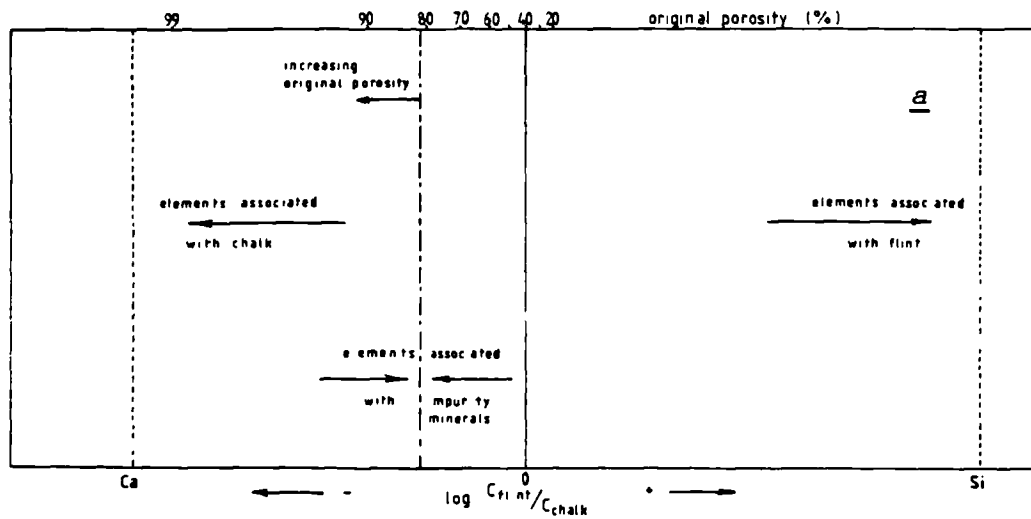
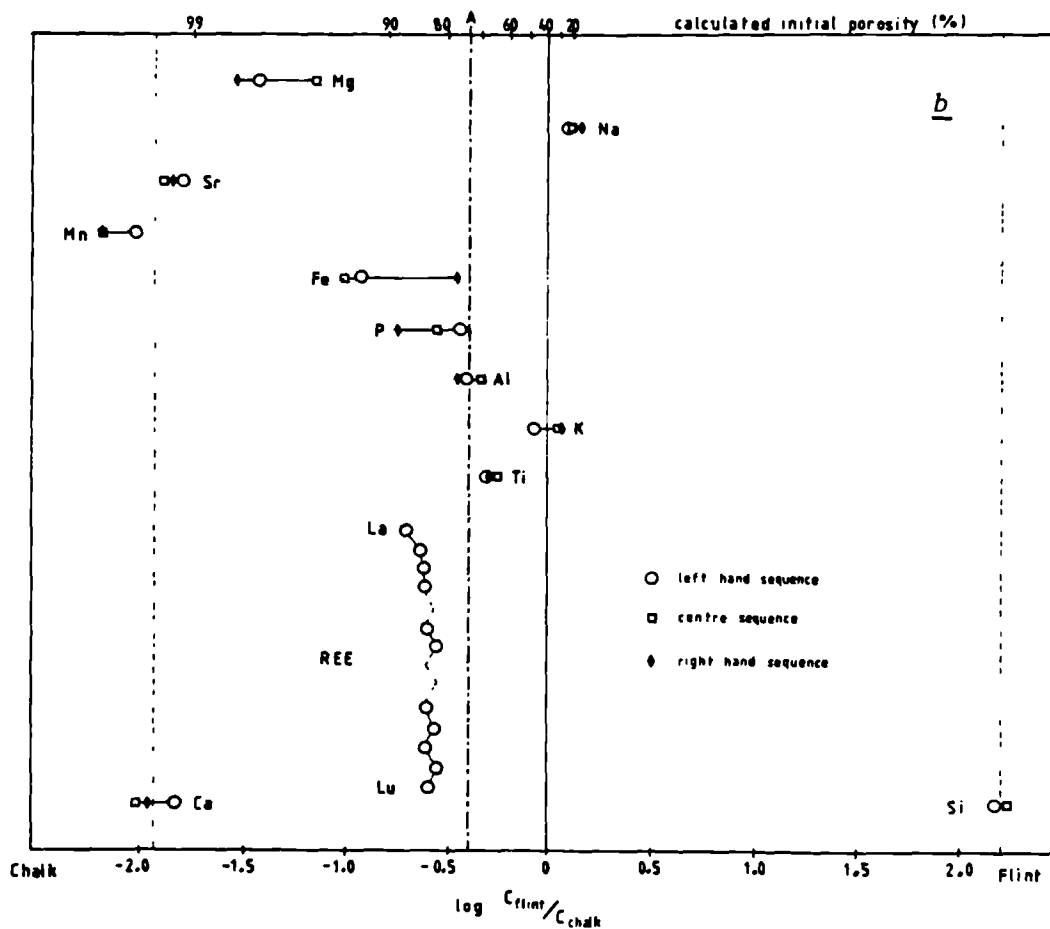


Figure 7.11 Schematic representation of chalk/flint partition coefficients. Above: theoretical. Below: West Clandon series (CL1x).



phosphates. These figures are similar to those deduced for the paramoudra samples.

Manganese also shows an association with Ca, but for all three traverses there is proportionally more Mn lost than Ca (i.e. calcite). This implies that not all of the Mn can be present in calcite or the clays and phosphates, and another Mn bearing phase must have been remobilised from the site of flint formation. By analogy with paramoudras, this presumably represents either the remobilisation of Mn oxides as the sediment became reducing, or the subsequent fixing of manganese (? as oxides) in the host, associated with the infiltration of meteoric waters.

K and Ti are known to have become depleted in the chalk subsequent to flint formation and this is reflected in the partition diagram by a shift of these elements towards the flint end member (i.e. preferential preservation in flint). Assuming that Al has not been significantly affected since flint formation, the amount of subsequent K and Ti depletion can be estimated from the difference in dilution between these elements and Al: in this case 135 ppm and 5 ppm respectively. In practice, the Al has also been slightly depleted over this range (~100 ppm), but assuming that K and Al have been depleted proportionally, then the amount of Al depletion can be approximated from the above (slightly erroneous) estimate of K depletion, and the ratio of K-depletion to Al-depletion deduced from the original curves (~ 3:2). This gives a new Al dilution of .3402 ($\log_{10} = -.400$) not significantly different from the uncorrected value (.3805, $\log_{10} = -.420$). This implies that the flint grew in a sediment of about 76% porosity.

The new K-depletion value can now be used to correct the Fe partition coefficient for the Fe depletion of the host. The Fe:K ratio of the depletion is approximately 7:2 so the Fe partition can be recalculated as 0.572 ($\log_{10} = -1.243$) much nearer to the calcite line. This could be due to either incorporation of Fe^{2+} in the calcite lattice (unlikely since the calcite is of coccolith origin which formed in the highly oxidised surface layers of the ocean), diagenetic remobilisation of iron oxyhydroxides from the site of flint formation, or introduction of iron sulphides to the host sediment after completion of flint growth. This is considered in more detail below.

The slight concentration of P in the host may reflect incorporation of a small amount of P in the host calcite, but as explained in Chapter 5 this is probably not great. A more likely explanation is the subsequent introduction of small amounts of phosphate to the host, subsequent to flint formation, similar to that which occurred in the paramoudra.

As would be expected, Na plots towards the flint end of the partition diagram reflecting its presence in saline microscopic fluid inclusions. However, it does not coincide exactly with the Si partition suggesting substantial incorporation of Na in either the calcite lattice of the host or, more likely, in clays.

7.5 THE RARE EARTH ELEMENTS

Further information on the origin of the clay minerals in the sediment can be obtained from consideration of the rare earth element distribution patterns (Table 7.7 and fig. 7.12). The bulk

partition coefficients of the REE's between the flint and the chalks of sequence (a) are included in figure 7.11b. Two features are noteworthy: the partitions fall very close to the clay mineral partition line (suggesting that the elements predominantly are associated with the non-carbonate fraction: clays and phosphates); and there is a small quantity, particularly of the light REE, present in the calcite (i.e. falling towards the Ca end of the partition diagram).

The partition pattern is better seen in fig. 7.12c. The light rare earths show a progressive increase in concentration in the chalk with decreasing atomic number, and this is apparently related to the ionic size of the element in the trivalent state (fig. 7.12d). A similar pattern has been predicted by Turner and Whitfield (1979) based on the ion capture concepts proposed by Goldschmidt (1954). In contrast, the intermediate and heavy rare earths show a bimodal distribution with Yb, Eu and Ho comparatively enriched in flint relative to Lu, Er and Dy. The latter elements follow the light rare earth trend of increasing incorporation in calcite with decreasing ionic size but the anomalous concentration of Yb, Eu and Ho remains unexplained (but see discussion on possible analytical errors in Appendix 3).

The REE patterns of the chalk and flint samples are shown in fig. 7.12 a and b respectively, normalised to average marine shale (Haskin and Haskin, 1966). The distribution curves show a pronounced Ce depletion and a slight depletion in the heavy and light rare earths relative to the intermediate elements. As explained above, this pattern is controlled primarily by incorporation of the REE's into clays and phosphates and is characteristic of Cretaceous sediments (Jarvis, In Press).

Table 7.7
Rare earth elements in Clandon flints and chalks
(HCl : hydrochloric acid leach)

Sample	La	Ce	Pr	Nd	Sm
CL1/9	5.0	3.2	.63	3.1	.63
CL1/10	5.2	3.2	.68	3.2	.60
CL1/11	9.0	3.7	.73	3.6	.69
CL1/12	5.6	3.3	.74	3.5	.71
CL1/15	4.1	2.6	.56	2.5	.53
CL1/16	5.6	3.2	.64	3.2	.67
CL1/17	4.4	2.8	.62	2.9	.51
CL1/9/HCl	4.8	2.7	.57	2.9	.61
CL1/16/HCl	4.5	2.5	.56	2.8	.61
CL1/8	5.3	3.9	.67	4.1	.87
CL1/13	.3	.4	.09	.4	.11
CL1/21	5.1	3.8	.51	3.7	.73

Sample	Eu	Dy	Ho	Er	Yb
CL1/9	.13	.53	.10	.29	.25
CL1/10	.14	.53	.10	.29	.24
CL1/11	.16	.61	.13	.37	.29
CL1/12	.15	.61	.13	.34	.26
CL1/15	.11	.45	.10	.29	.22
CL1/16	.14	.57	.13	.36	.28
CL1/17	.13	.50	.10	.30	.26
CL1/9/HCl	.13	.53	.10	.28	.24
CL1/16/HCl	.12	.53	.11	.31	.24
CL1/8	.19	.69	.14	.53	.37
CL1/13	.01	.06	-	-	.03
CL1/21	.16	.67	.13	.72	.33

Sample	Lu	Y
CL1/9	.04	5.2
CL1/10	.04	4.9
CL1/11	.05	5.7
CL1/12	.04	5.7
CL1/15	.04	4.5
CL1/16	.04	6.1
CL1/17	.04	5.1
CL1/9/HCl	.03	5.5
CL1/16/HCl	.03	5.7
CL1/8	.05	6.4
CL1/13	-	1.4
CL1/21	.06	5.8

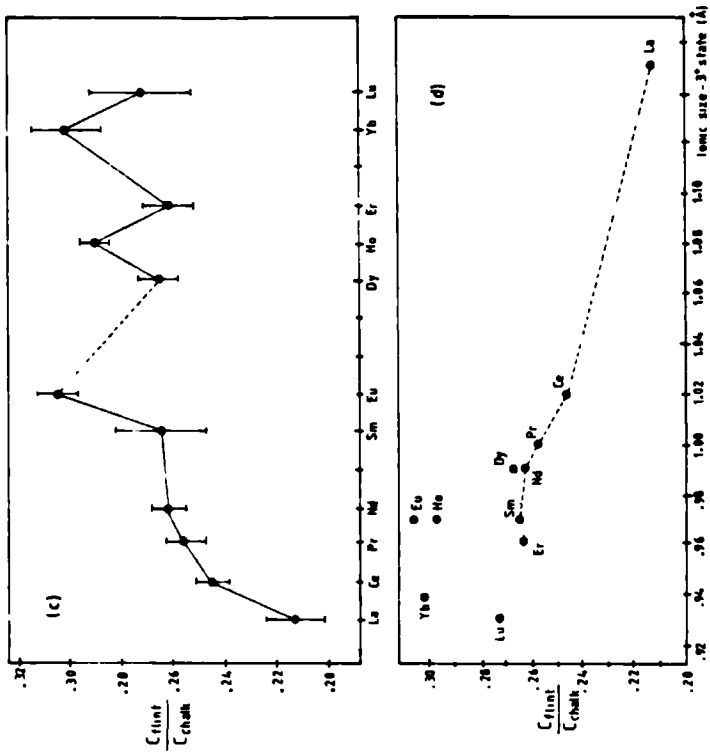


Figure 7.12 Rare Earth Element distributions

in samples from West Clandon Pit.

See text for discussion.

It is difficult to differentiate the REE pattern of the clays from that of the phosphate but some idea can be obtained from consideration of the Ce depletion. This can be quantified by comparing the actual Ce value on the shale normalised plot (Ce_{sn}) with the Ce values obtained by interpolation between La and Pr on the plot (Ce_{sn}^*). Typical deep ocean sea-water (Høgdahl, 1970; Martin et al., 1976) and planktonic foraminifera (Elderfield et al., 1981) have $\log (Ce_{sn}/Ce_{sn}^*)$ values of -0.75 whereas average marine shale which is composed dominantly of detrital material, by definition, has a $\log (Ce_{sn}/Ce_{sn}^*)$ value of zero. The cerium depletion in sea-water is caused by scavenging of Ce by deep sea ferro-manganese deposits but this leaves detrital grains more or less unaffected (Bonnet-Courtois, 1981). Authigenic clays and phosphates inherit the REE pattern of the parent sea-water (Jarvis, In Press; Fleet, In Press) so it should be possible to differentiate the authigenic components (phosphate and ? some clay) and the detrital clays from the magnitude of the cerium anomaly.

Excluding CL1/15 (which has an anomalous La content which biases the result), the chalks all have values of $\log (Ce_{sn}/Ce_{sn}^*)$ between -.39 and -.42, indicating a mixture of detrital and authigenic components. In flint, however, the anomaly varies from only -.23 to -.35 indicating a lower proportion of authigenic material in flint. This is not really surprising as it is already known that additional phosphate growth and clay mineral alteration have occurred in the chalk after silicification (see above), but it does suggest that at least some of the clay present is of detrital origin.

With more detailed analyses it may be possible to quantify the distribution of REE's further but this is not attempted with the limited data currently available.

7.6 VARIATIONS WITHIN THE FLINT

Chalk-flint partition diagrams give an idea of the mineral associations of trace elements in flint but it is also important to know the distribution of these minerals within the flint for comparison with their distribution in the chalk.

Specimen CL1/7 is a fragment of a semi-tabular flint collected at the foot of the cliff where the main series of chalk samples were collected. On morphological grounds it is believed to come from the same flint band as CL1/8, 13 and 21. The trace element concentrations from a single vertical traverse across the flint are given in Table 7.8 and fig. 7.13.

As would be expected, Ca is present in the highest concentration near to the centre of the flint, and this is reflected in the Mg and Mn distribution. Mn shows a progressive upward depletion, with a superimposed peak in sample IV, coincident with Ca peak. If this is due entirely to incorporation of Mn in the calcite lattice, the relative magnitude of the Ca and Mn peaks can be used to estimate the Mn content of the calcite: about 320 ppm. After correcting the Mn curve for the calcite-bound Mn, a residual of only between about 7 ppm (sample 7) and 2 ppm (sample V) is left. This new curve parallels the Al distribution suggesting an association with clays. If the calcite in the flint is representative of the host calcite as a whole, then these figures suggest about 250-300 ppm Mn in the chalk which is not present in either calcite or clays. However, as explained above (Chapter 5 and 6), such estimates must be treated with caution.

Mg, like Mn, shows a peak coinciding with that of calcite but there is additional Mg in the samples below this peak (I-III).

Table 7.8
Minor elements in flint CL1.7

Sample	Ca	Mg	Na	Sc	Mn
I	1310	220	270	4	4.5
II	1500	420	375	4	4.0
III	2380	600	240	5	5.5
IV	11000	730	223	13	5.5
V	1010	90	200	17	2.0

Sample	Fe	P	Al	L	Ti
I	305	85	405	375	24
II	270	80	390	310	20
III	105	135	305	290	19
IV	145	255	320	275	17
V	100	175	340	255	20

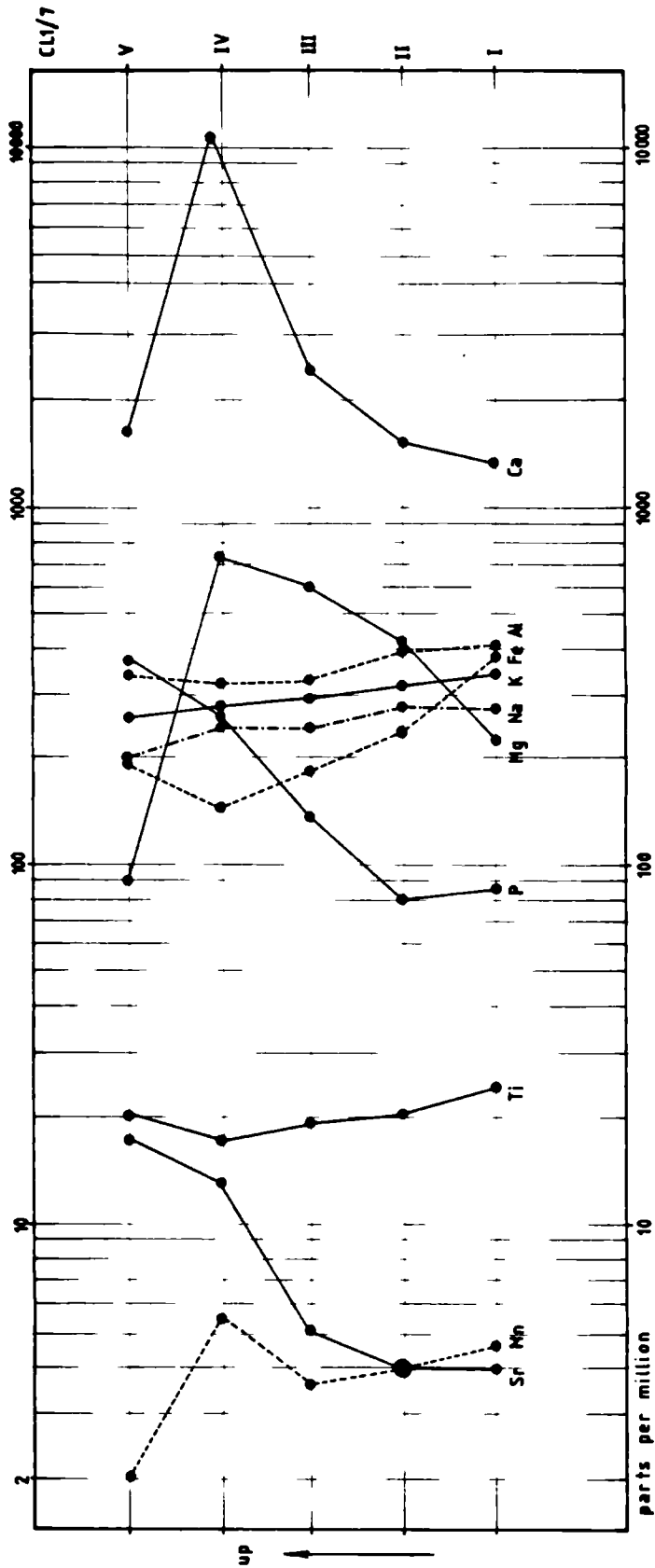


Figure 7.13 Trace element variations on a vertical traverse through flint

CL1/7, West Clandor Pit.

These data are too poor to estimate the Mg content of the relic calcite but if the Mg in sample IV is due only to calcite, this corresponds to about 1.73% Mg (~ 2.9 mole % MgCO_3) in the calcite. This is significantly different from the host sediment (~ 3000 ppm Mg) even after allowing for 170 ppm Mg in clays (see above). The excess Mg in samples I to III does not correlate with any other element so is presumably related to the formation of authigenic magnesium silicate or carbonate (? dolomitisation of the relic calcite).

Sr is known to be present in the calcite lattice but also shows a close association with the phosphorus distribution. Phosphorus is present almost exclusively as authigenic phosphates (see Chapter 5) and the upward increase in this element in the flint matches with the P distribution in the surrounding chalk (see traverse (a) of fig. 7.3). Based on samples I-IV it is possible to determine the Sr partitioning between the calcite and the phosphate, yielding figures of around 870 ppm of the Ca concentration (equivalent to 350 ppm in calcite) and .42% of the P concentration ($\sim .18\%$ of the P_2O_5 content, cf analyses of francolite, $.7 \rightarrow 1\%$ of P_2O_5 , dropping to .24% if weathered: M.L. Coleman, pers com).

The calcite Sr content is significantly less than the 650 ppm average in the host sediment. Allowing for Sr incorporated in calcite and phosphate a residual of only about 2 ppm is left, which must be incorporated in clays. This is in reasonable agreement with the value deduced from the chalk-flint partition coefficient (see above).

In addition to P, elements associated predominantly with non-carbonate components are K, Al, Na, Fe and Ti. As in the

paramoudra flint, there is slightly greater dilution of Al and Ti (in clays) in the centre of the flint compared with the edges, reflecting small amounts of compaction near the outside of the flint where the lepispheres are less densely packed. This is superimposed on a very slight upward depletion of these elements (also seen in the K-curve) which is compatible with the overall trend in the chalk sequence (fig. 7.3), and suggests that the flint was affected to a very small extent by the subsequent reactions.

Na probably is present in fluid inclusions as well as in clays (Chapter 5) so its resemblance to the Al and K curves is probably partly fortuitous. The upward depletion of Na may be associated with the diagenetic purging of Na from clays (cf. K) or the infiltration of less saline pore waters (i.e. meteoric water) from above.

The variation in iron content shows some resemblance to the clay distribution but is dominated by the anomalous high levels towards the bottom of the flint. This is most likely a continuation of the iron (? sulphide) buildup below the flint (see section 7.2.1) although this apparent trend may well be accentuated by the upward depletion of Fe from clays (? glauconite) which occurred at the same time as the K-depletion. The increase in Fe in sample V (top of flint) may be due to the formation of about 70 ppm of another authigenic mineral, but insufficient data are available to be confident of this.

7.7 DISCUSSION

From the above data and a knowledge of the reactions occurring in paramoudras, it is now possible to deduce the environment of formation of bedded flint bands.

Dilution of clay minerals within the flint suggests that the flint grew in a sediment of about 76% porosity (i.e. within the top 10 m or so of the sediment - chapter 5). Although subsequently there has been a small amount of compaction of the flint structure around the edges of the specimen, the flint has remained essentially unchanged chemically since it formed. However, relic carbonate preserved in flint is unrepresentative of the original calcite chemistry as a whole.

Postdating silicification, clay minerals in the surrounding chalk (probably "glauconite") have been progressively depleted in K, Fe, Ti and to a lesser extent Al. This is apparently related to sulphate reduction reactions (or a closely associated bacterial reaction: see chapter 6) which occurred only 1-2 metres above the flint. These reactions also produced a shift in the isotopic composition of the carbonate towards lower $\delta^{13}\text{C}$ and higher $\delta^{18}\text{O}$ values. For some reason this did not result in prominent carbonate cementation here, although the sediments show many of the characteristic chemical signatures of hard-ground formation. This suggests that the flint formed before the onset of sulphate reduction only a metre or so above, implying that the flint formed near the base of the oxic zone

In addition to the clay mineral dilution, there has been growth of authigenic phosphate in the host chalk subsequent to flint formation. By analogy with the phosphate in paramoudras,

this probably suggests that the chalk around the flint (or in this case, above it) did not become reducing until after the flint formed. Conversely, there is a build-up of iron, probably as sulphide, beneath the flint which may suggest an origin above the zone of sulphate reduction.

There is apparently a great deal of similarity between the chemical environment of flint formation in horizontal beds and around burrows in paramoudras, so it is possible to construct a general model of silicification (fig. 7.14). Flints formed above the zone of sulphate reduction but at the base of the oxic zone. In paramoudras, silicification is caused by the re-oxidation of H_2S diffusing outwards from local sites of sulphate reduction, so it seems reasonable to postulate a similar origin for bedded flints, by the re-oxidation of upward diffusing H_2S released by widespread, but not necessarily intense, sulphate reduction below.

Presumably, as in paramoudras, the regenerated sulphate from the site of silicification would then diffuse back to the site of sulphate reduction - the reflux mechanism described in Chapter 6. This should then result in anomalously light $\delta^{34}S$ values of the pyrite formed below the flint. At the time of writing it has been possible to analyse only one specimen of pyrite from this environment (SM3/P; Table 6.4) which gave a value of -33.3‰ relative to Canon Diablo Troilite, or about -50‰ with respect to contemporary dissolved marine sulphate sulphur. This is a little greater than can reasonably be expected from normal sulphate reduction (~45‰, Trudinger and Chambers 1973), and although more data are desirable, suggests that the mechanism proposed for flint formation is correct.

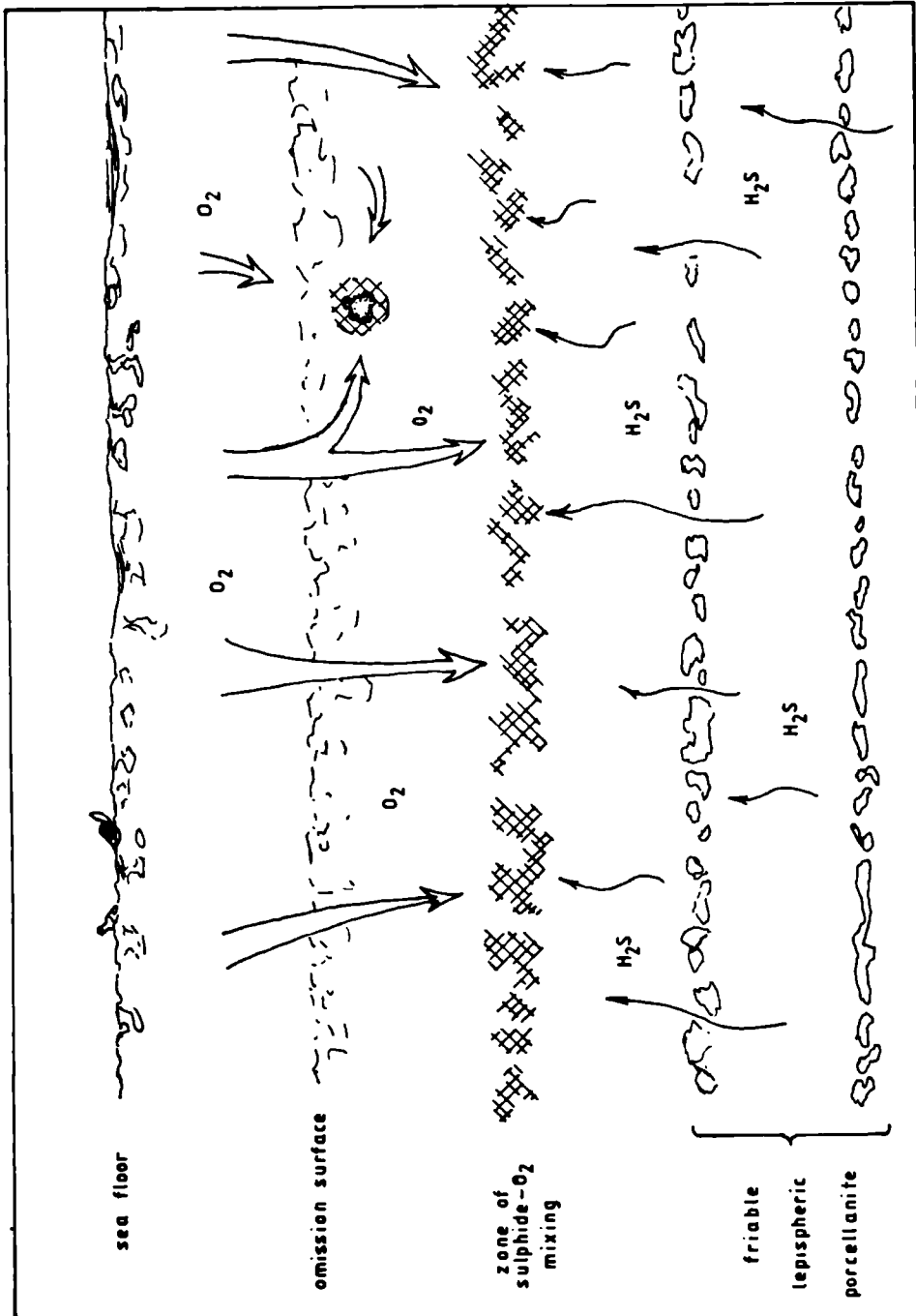


Figure 7.14 Chemical environment of flint formation in the chalk. Flints form at the O_2 - H_2S mixing zone due to bacterial re-oxidation of the sulphide.

Any model of flint formation must also be compatible with the other diagenetic reactions which occur in the sediment. Fe, Mn and phosphate diagenesis have already been discussed in some detail but models of carbonate cementation, and in particular hardground formation, have only been briefly touched on so far. It is now necessary to consider early diagenetic lithification in more detail before a general model of Chalk diagenesis can be constructed.

8. ORIGIN OF CHALK HARDGROUNDS

8.1 INTRODUCTION

In the preceding chapters it has been demonstrated that flints probably formed as a result of the re-oxidation of H_2S at the oxic-anoxic boundary, usually 5-10 m below the sediment surface. Conversely, chalk hardgrounds form only 1-3 m below the surface (Bromley, 1967, 1968; Kennedy and Garrison, 1975). Jeans (1980) has suggested a bacterial control (ammonification or sulphate reduction) for hardground formation and Jarvis Bromley and Clayton (1982) have specifically invoked sulphate reduction as the cause. This is an important apparent paradox: if flints form at the top of the sulphate reduction zone, 5 metres deep in the sediment, how can sulphate reduction be the cause of lithification at only 2 m depth? Clearly, it is necessary to investigate further the origin of hardgrounds, and particularly to confirm or disprove their genesis by sulphate reduction reactions.

Probably the best guide to the source of early diagenetic cement is the stable isotope composition of the calcite. Carbonate released by sulphate reduction of organic matter is depleted in ^{13}C by 20-30% relative to normal marine carbonate, whereas that released by bacterial fermentation is generally enriched by ^{13}C by up to 15% (see discussion in chapter 2). The incorporation of carbonate from these sources in lithified chalks therefore will result in a shift in the carbon isotope composition of the rock, although the magnitude of the effect may be greatly buffered by the incorporation of carbonate of marine origin also (see discussion

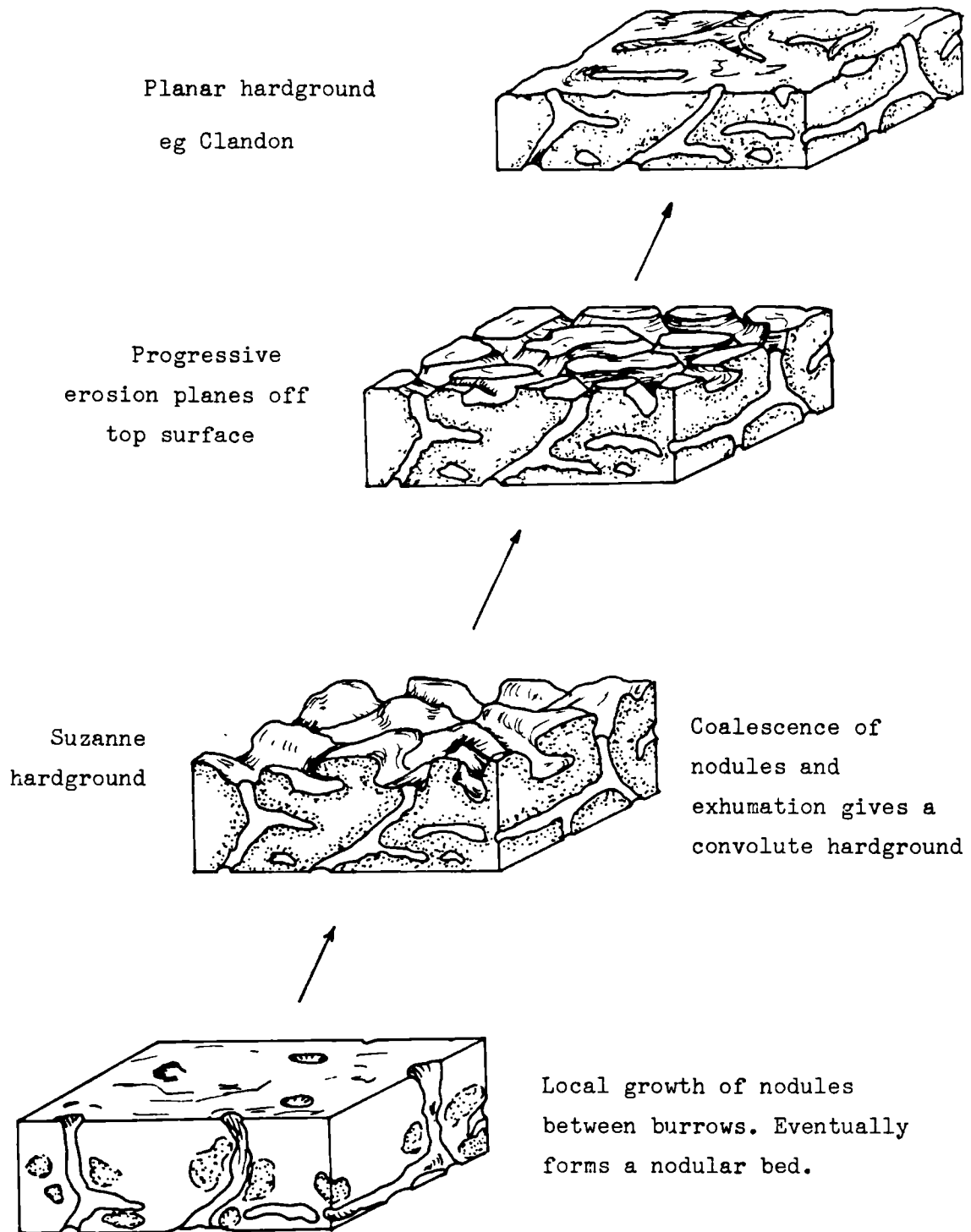


Figure 8.1 *Simplified genetic sequence of hardground types.
Borings on hardground surface not shown for clarity.
Modified after Kennedy and Garrison, 1975.*

of cementation in paramoudras: chapter 6).

In order to investigate the origin of chalk hardgrounds, three lithified units have been analysed isotopically: a poorly formed nodular bed from the "Chalk Rock" of Hertfordshire; the Clandon hardground (see previous chapter), a well lithified planar hardground from southern England and the "Suzanne Hardground" from the Somme Valley, Northern France, a particularly well preserved convolute hardground (Jarvis, Bromley and Clayton 1982).

8.2. CHALK ROCK NODULAR BED

The formation of hardened nodules, 2-10 cms across, between *Thalassinoides* burrows, marks the first stage of synsedimentary lithification in chalks (fig. 8.1). Five nodules, together with their adjacent soft chalk, were collected from a poorly defined nodular unit in the Turonian of a small pit on Home Farm, near Wallington, Hertfordshire (Bromley & Gale, 1982). This level is the lateral equivalent of the Chalk Rock (sensu Bromley & Gale, 1982) and represents the poorly developed lithification which occurred around the margins of structural highs during the generation of regional hardground complexes (chapter 3).

The $\delta^{13}\text{C} - \delta^{18}\text{O}$ relationship of matrix-nodule pairs 2-5 is shown in fig. 8.2, and the data given in table 8.1. In all cases there is a shift towards lighter $\delta^{13}\text{C}$ and $\delta^{18}\text{O}$ values in the nodules, although in some cases this is only very small. This reflects the incorporation of isotopically light cement in the nodules.

Table S.1
Variations between Chalk Rock
nodules (N) and attached chalks (C)

Sample	$\delta^{13}C$	$\delta^{18}O$
Chalk	.76	-2.07
C2	.93	-2.20
N2	.83	-2.35
C3	1.12	-2.06
N3	.92	-2.94
C4	.97	-2.03
N4	.94	-2.12
C5	1.09	-2.07
N5	.92	-2.27

Table S.2
Variations in module #1

Sample	$\delta^{13}C$	$\delta^{18}O$	Position (cm)
a	.67	-2.48	0 From Centre
b	.72	-2.41	1
c	.81	-2.00	2
d	.85	-2.16	3
e	.82	-2.43	4
f	.90	-2.47	5

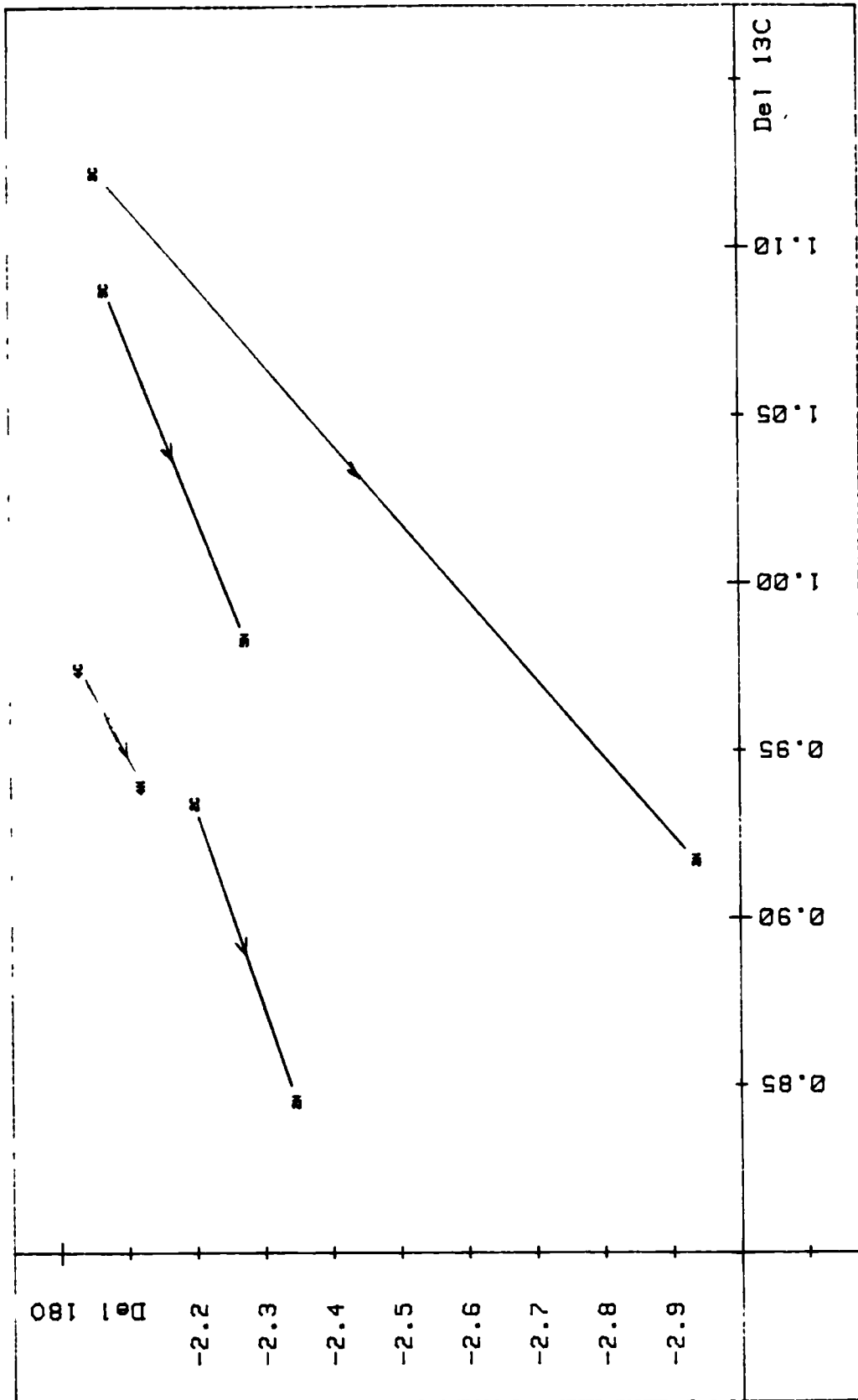


Figure 8.2 Comparison of isotope ratios in Chalk Rock nodules (n) compared with attached chalk (c).

To investigate this in more detail, nodule #1 was sampled sequentially from the centre to the edge (sub-samples a-f respectively in fig. 8.3 , both $\delta^{13}\text{C}$ and $\delta^{18}\text{O}$ decrease towards the centre of the nodule in sample A-C, but in samples d-f the $\delta^{13}\text{C}$ trend is offset to lower values and the $\delta^{18}\text{O}$ curve is reversed altogether (fig. 8.3 a & b). From isotopic determinations reported in previous chapters (6 & 7), it is known that unlithified chalks in southern England are highly susceptible to exchange with isotopically light meteoric waters, so it seems reasonable to attribute the anomalous light values around the edge of the nodule to the same effect. As in other cases, the effect on $\delta^{18}\text{O}$ is about 5 times that on $\delta^{13}\text{C}$. Presumably the host chalk has also been affected to a great extent and the magnitude of the measured differences between the nodules and their hosts (fig. 8.2) are an underestimate of the original difference resulting from lithification.

It has not yet been possible to measure the trace element concentrations within the nodule so the degree of Al dilution in the nodules compared with the host cannot be used to estimate the sediment porosity at the time of cementation. Consequently, it is not yet possible to determine how much cement is present and therefore to deduce it's true isotopic composition. However, there is little noticeable physical difference in lithification between the centre and the edge of the nodule and by comparison with hardness variations in paramoudras, the variation in cement is probably not greater than about 20%. After allowing for the effect of meteoric waters, this corresponds to a change of about .9‰ in $\delta^{18}\text{O}$ and .4‰ in $\delta^{13}\text{C}$. This indicates that the cement is probably lighter by about 2‰ in $\delta^{13}\text{C}$ and 5‰ in $\delta^{18}\text{O}$ although

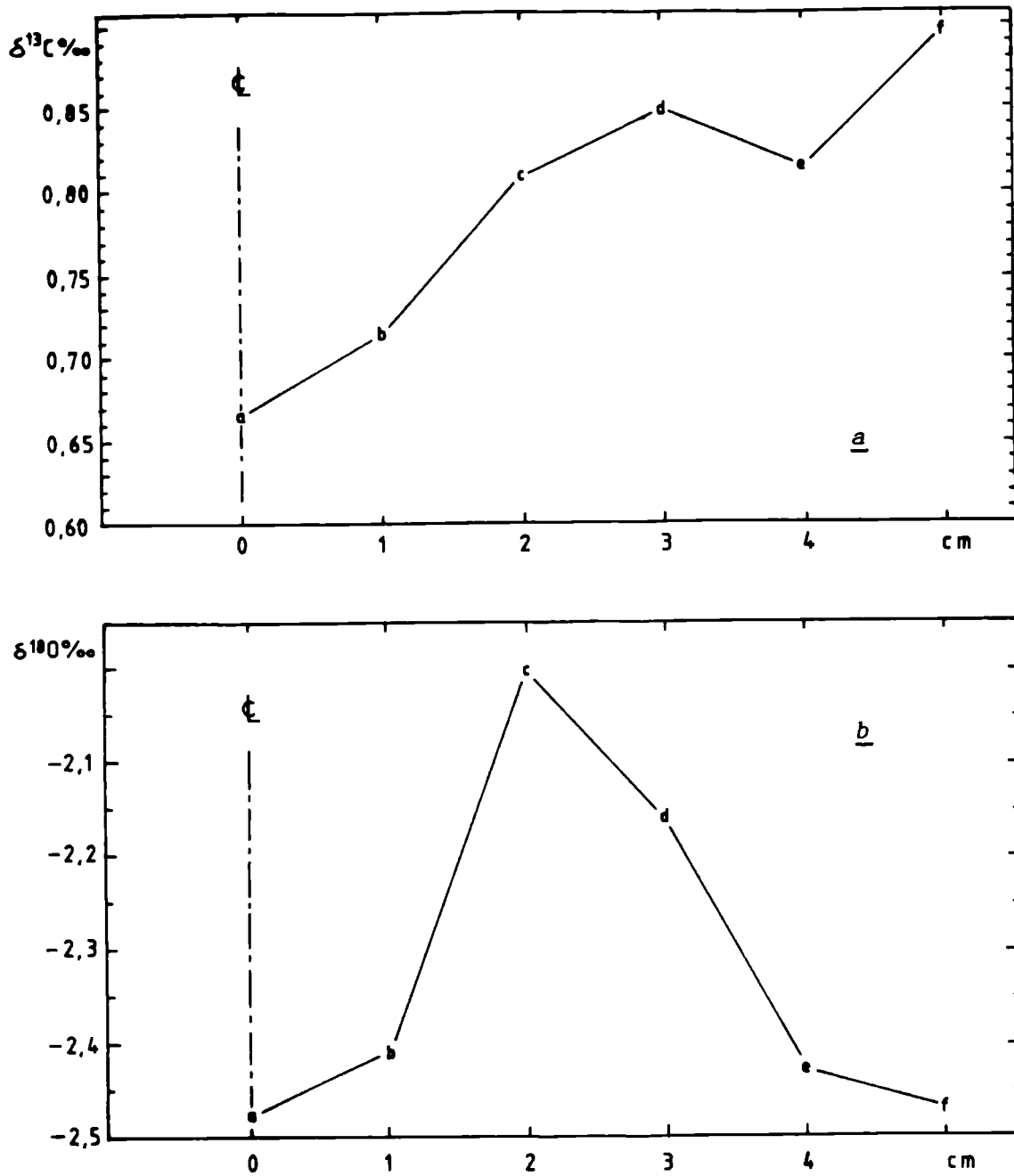


Figure 8.3 Stable isotope variations within Chalk Rock nodule No. 1. Sample a is at centre of nodule.

considerable errors may be involved in such estimates. These values are compatible with the addition of a small proportion of carbonate from sulphate reduction ($\sim 12\%$) to pre-existing marine carbonate (cf. $<10\%$ in paramoudras). The figure of 5% difference in $\delta^{18}\text{O}$ between the cement and the host carbonate suggests a cement $\delta^{18}\text{O}$ of about -7% , corresponding to a precipitation temperature of about 45°C (Craig, 1965). If the calculated $\delta^{18}\text{O}$ is even remotely correct, this temperature is anomalously high and suggests that, as in paramoudras, cementation was sufficiently rapid to deplete local pore waters in $\delta^{18}\text{O}$, leaving subsequent cements to form from abnormally light pore waters.

Although not conclusive, these data are compatible with a sulphate reduction origin for the nodules. Possible alternative reactions are aerobic oxidation or one of the sub-oxic reactions (NO_3^{2-} , Fe^{3+} or Mn^{4+} reduction) but all of these can be discounted on other grounds. Aerobic oxidation and nitrate reduction probably result in carbonate dissolution rather than precipitation (section 2.3) and Fe and Mn reduction ^{must} have been too limited in such a pure sediment to account for large scale lithification. In addition, the effects outlined above are comparable in effect and in magnitude to similar processes which formed the lithified cores of paramoudras, where the intimate association with pyrite attests to the importance of sulphate reduction.

8.3. THE CLANDON HARDGROUND

The hardground of West Clandon Pit (see chapter 7) represents a more or less isolated lithification episode during deposition of

what is otherwise a normal flinty sequence (but note the evidence for an incipient lithification episode in the chalk below this: chapter 7). The hardground is best developed in Surrey but a lithified unit occurs at this level over most of southern England (eg. Barrois'Sponge Bed in Thanet (Rowe, 1900), Whitway Rock of northern Hampshire (Hawkins, 1942)). In form, the hardground is solidly lithified with a bored, planar top, and is overlain by a thin glauconitic marl. This unit is the end product of hardground development in which penecontemporaneous erosion has completely planed off all surface topography (fig. 8.1).

Trace element variations associated with lithification have been discussed in chapter 7 but it is relevant here to discuss the isotope variations in more detail. From table 8.3 and fig. 8.4, it is clear that cementation is reflected in a decrease of about 0.2‰ in $\delta^{13}\text{C}$ and an increase of about 0.5‰ in $\delta^{18}\text{O}$. Interestingly, the greatest isotopic shift is not at the hard-ground surface itself but about 25 cm below this. The magnitude of the probable isotopic exchange with meteoric waters (chapter 7) cannot be estimated, but this effect will tend to increase the difference in $\delta^{13}\text{C}$ and decrease that in $\delta^{18}\text{O}$ between the cemented chalk and the unlithified sediment. This is because the unlithified sediment would be expected to exchange much more readily than the lower porosity and almost entirely impermeable lithified chalk. Taking this into account, the change in $\delta^{13}\text{C}$ of the cemented sediment is essentially similar to that associated with cementation in the paramoudra, and, as in the Chalk Rock nodules suggests an origin of the cement from sulphate reduction, strongly buffered by marine carbonate.

Table 8.3
Isotope variations associated with
the Clandon hardground

Sample	$\delta^{17}O$	$\delta^{18}O$	Depth (cm)
CLS '1	1.98	-1.64	0
CLS '2	1.94	-1.74	-25
CLS '3	—	—	-50
CLS '4	2.18	-2.06	-75
CLS '5	2.02	-2.10	-100
CLS '6	2.09	-1.97	-125
CLS '7	2.01	-2.19	-150
CLS '8	2.07	-1.84	-175
CLS/10	1.92	-1.58	1
CLS '12	2.18	-1.97	50
CLS '13	2.07	-1.89	5

Table 8.4
Isotope variations in the Suzanne hardground
(Depth is w.r.t. top surface of hardground)

Sample	$\delta^{17}O$	$\delta^{18}O$	Depth (cm)
SN-C1W	-0.15	-3.35	-1.7
SN-C2W	0.00	-4.04	-1.3
SN-C3W	.50	-3.22	-1.7
SN-C5W	-0.68	-5.74	-2.3
SN-C6W	-2.43	-8.15	-2.8
SN-C7W	.52	-3.46	-3.2
SN-C8E	-0.62	-3.20	-2.2
SN-C9E	-0.34	-2.24	-1.6
SZ-01W	1.32	-2.31	-30.0
SZ-02W	1.26	-2.41	-70.0
SZ-03W	1.38	-2.06	-51.0
SZ-04W	1.50	-1.73	-70.0
SZ-05E	1.84	-0.81	0.0
SZ-15W	1.08	-2.75	-60.0

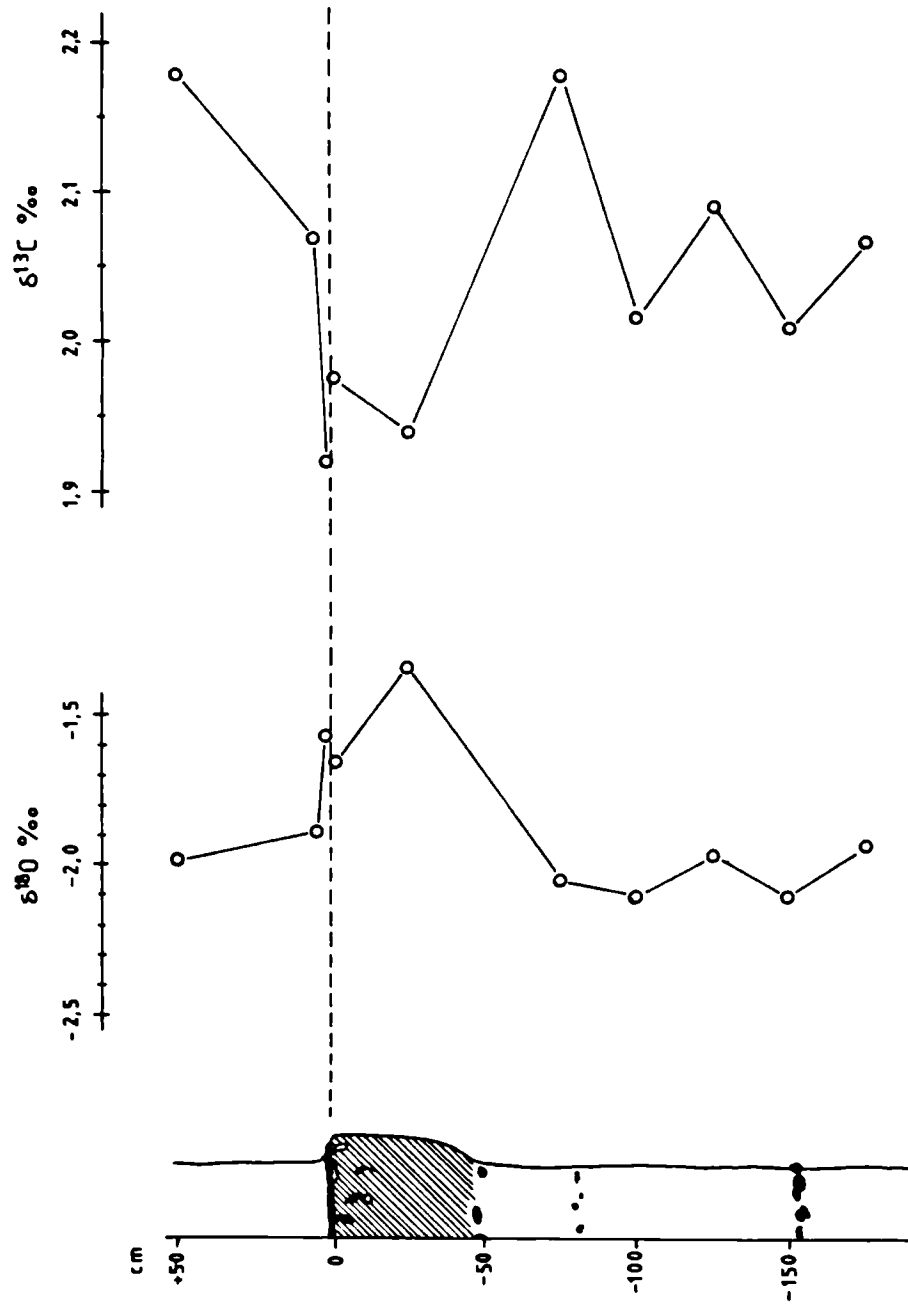


Figure 8.4 Stable isotope variations below the Clandon hardground

In contrast to the paramoudra, $\delta^{18}\text{O}$ of the lithified chalk at Clandon is higher than that of the unlithified chalk. This is probably an overprinted effect brought about by subsequent re-equilibration of the unlithified chalk with isotopically light meteoric waters (cf. paramoudras and Chalk Rock nodules). If the lithified chalk has resisted re-equilibration, (cf. paramoudras), the $\delta^{18}\text{O}$ of the lithified chalk (-1.5‰) corresponds to a temperature of precipitation of about 18°C (using the equation of Craig, 1965). In practice, only part of the carbonate here is cement so this value may be an underestimate. This temperature is considerably higher than would be expected for the shallow burial conditions under which the hardground grew (section 3.4), suggesting that, as in the Caister paramoudra, cementation was sufficiently rapid to deplete local pore waters in $\delta^{18}\text{O}$, resulting in anomalously light $\delta^{18}\text{O}$ in subsequent cements.

Above the hardground, the isotopic composition of the sediment returns to normal, but the thin marl immediately above the hardground has the isotopic character of the underlying unit rather than that of the overlying unlithified chalk. This implies that the material here is derived dominantly by erosion of the lithified unit below. The preferential preservation of such material here probably indicates that in this case, hardground formation was associated with a break in sedimentation rather than just increased current activity causing removal of the sediment.

The isotope data for the Clandon Hardground therefore are compatible in all respects with the variations in the 'Chalk Rock' nodules (see 8.2) and with variations in the sulphate-reduction-

lithified core of the Caister paramoudra.

8.4. THE SUZANNE HARDGROUND

The Suzanne hardground samples come from a small cutting near the village of Suzanne, in the Somme Valley of northern France. This hardground is typical of basal hardgrounds to erosional phosphatic chalk cuvettes (sensu. Jarvis, 1980) but is exceptional in the fine state of preservation of the bored and encrusted convoluted top surface. Indeed Suzanne's lovely rounded surfaces have attracted much admiration from all who have handled them. The hardground is currently the subject of a detailed joint ichnological, sedimentological and geochemical study by the author in collaboration with R.G. Bromley and I. Jarvis and a preliminary report can be found in Jarvis, Bromley and Clayton (1982).

Samples have been taken for isotopic analysis through the entire sequence of poorly lithified chalk, well lithified chalk, the hardground surface and overlying coarse pebble lag and phosphatic sand, although only the results of the white (i.e. non-phosphatic) chalks will be discussed here.

Figure 8.5 shows the stable carbon and oxygen isotope variations within both a bulk-sampled traverse down the lithified unit (a), and in more detail across a lithified overhanging block (b). The convoluted morphology is a result of erosion following preferential lithification between open *Thalassinoides* burrows, so the overhanging block represents the site of the main lithification reactions. The massively lithified unit below represents the downward extension of lithification,

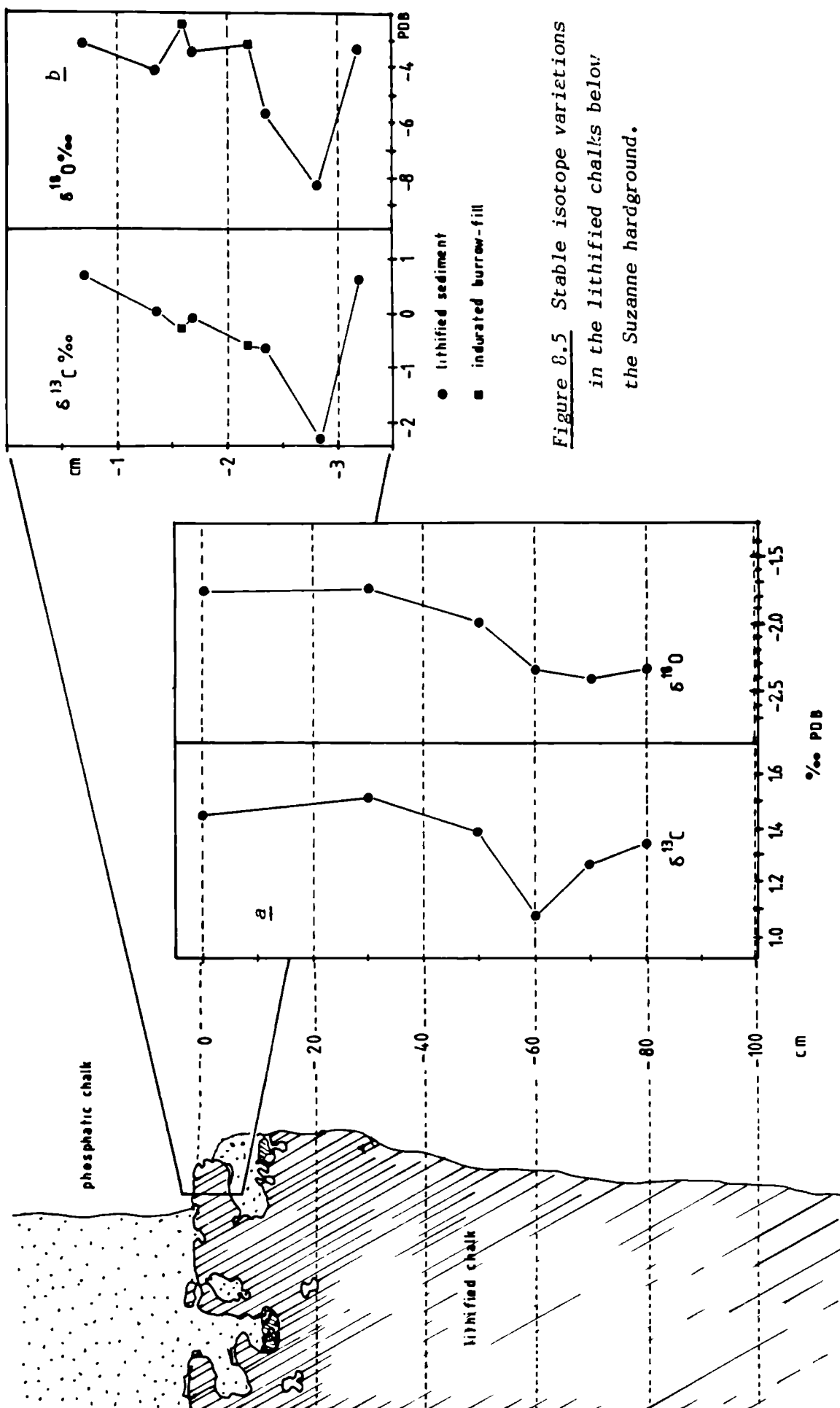


Figure 8.5 Stable isotope variations in the lithified chalks below the Suzanne hardground.

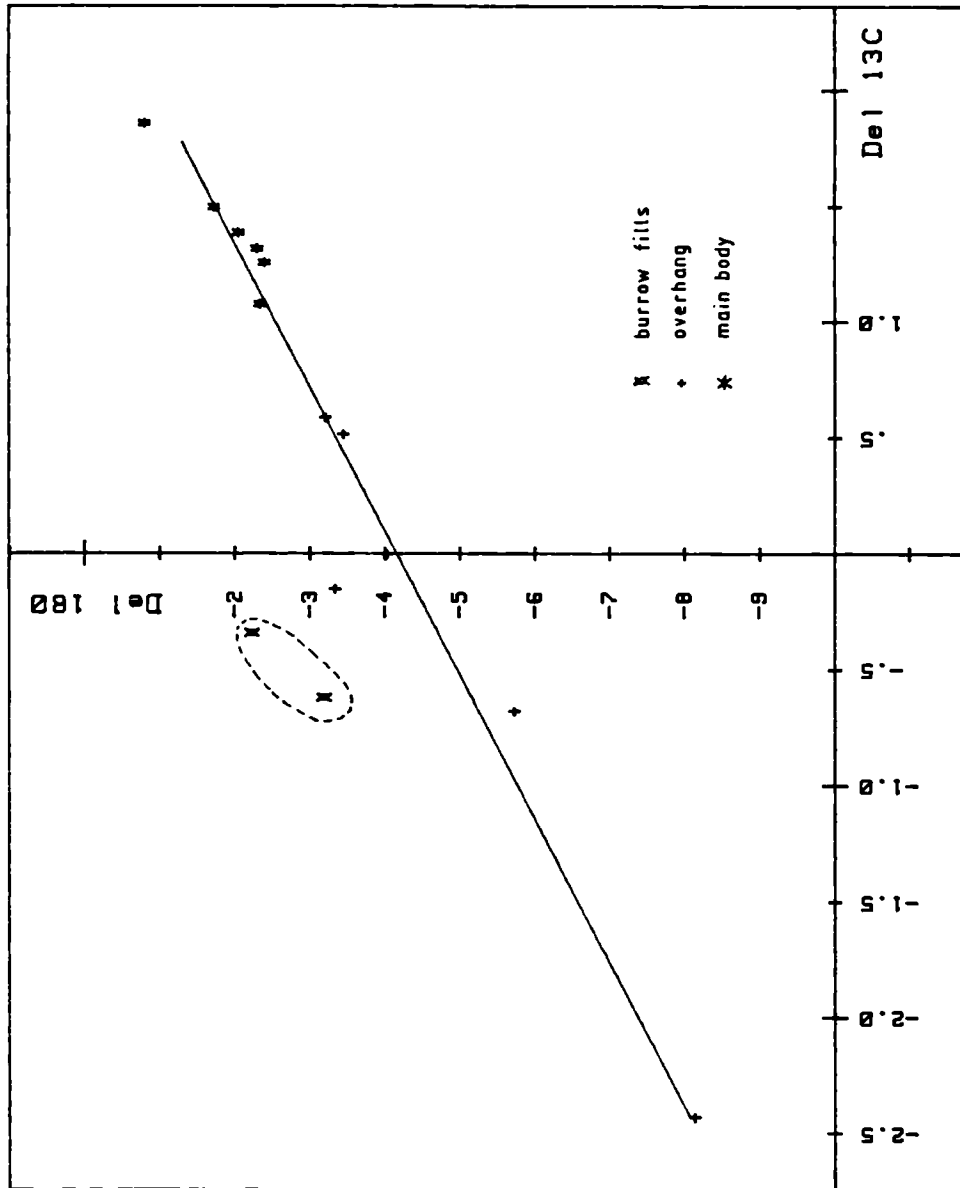
presumably caused by the migration of products from the main reaction sites.

As may be expected, the greatest variation in the isotopic ratios occurs where lithification was most intense, in the sediment between the thalassinoidean burrows, now represented by the upstanding pillars and overhanging blocks at the top of the lithified unit. Here, the carbonate is depleted in ^{13}C by 3-4‰ relative to the less lithified limestone below, reflecting the introduction of isotopically light cement. In reality, the sample analysed is a mixture of cement and pre-existing carbonate sediment (of normal marine isotopic composition), so the cement is undoubtedly even lighter than this. Such a light carbon isotope composition for the cement, combined with the abundant pyrite which occurs here (Jarvis, Bromley and Clayton, 1982), is a strong indication that bacterial sulphate reduction is an important process leading to the lithification.

The trend towards lighter ^{13}C within the lithified block is accompanied by a similar trend in $\delta^{18}\text{O}$ in excess of 8‰ relative to PDB. If precipitation occurred in equilibrium with normal marine bottom waters ($\delta^{18}\text{O} = -1.2\text{‰ SMOW}$; Shackleton and Kennett, 1975), this value corresponds to a temperature of precipitation in excess of 50°C , clearly absurd for such an environment. As in other cases of carbonate lithification in the Chalk (see above), such anomalous $\delta^{18}\text{O}$ values probably represent the depletion of ^{18}O in pore waters at the site of cementation as a consequence of the rapid precipitation of comparatively ^{18}O -rich cement. This suggestion is further backed up by the isotopic composition of the two burrow-fills analysed (fig. 8.5b, square

symbols). Although these burrows were already filled and became lithified at the same time as the rest of the sediment, the less compacted infill would have allowed freer access of isotopically normal sea water to the site of lithification. Consequently, within the burrows the usual local depletion of ^{18}O from pore waters was partially buffered and the cement precipitated here has a slightly more normal (i.e. heavier) oxygen isotopic composition (fig. 8.6). As the main source of marine derived carbon in the cement is from the surrounding sediment rather than from the overlying sea water, the same effect is not seen in the $\delta^{13}\text{C}$ curve.

Below the level of the convoluted unit isotopic variations are much less well defined, reflecting a greater degree of buffering of the sulphate reduction - derived carbonate by carbonate of marine origin. Here, the lithification is related primarily to reactions occurring higher in the sediment (see above) so it is rather surprising to observe the $\delta^{13}\text{C}$ and $\delta^{18}\text{O}$ minima 60 cm below the hardground. This may reflect either a lower degree of buffering by marine carbonate or the introduction of additional sulphate reduction products at this level. Of these, the latter is more likely since the spacing between this level and the main burrow network above (~ 50 cm) is of similar magnitude to the normal spacing between successive burrow sites which tend to occupy specific bioturbated horizons in the overall rhythmically layered chalk sediment (Bromley, 1967, 1968; Kennedy and Garrison, 1975). It seems reasonable in this case to attribute the isotopic minimum of -60 cm to low levels of sulphate reduction in the previous suite of burrows, which added to the overall pool of dissolved carbonate derived from above.



The distribution of cementation at Suzanne has important implications for isotopic variations in chalk hardgrounds in general. As explained in chapter 2 and section 8.3 above, the majority of hardgrounds in the chalk have a planar surface as a consequence of intense erosion leading to removal of the convoluted top unit, down to the base of the Thalassinoides chamber network here. This erosion represents the removal of the main centres of cementation (i.e. between the burrows) and so isotopic analyses of planar hardgrounds will reveal only the very small isotopic shifts associated with the highly buffered sulphate reduction cementation below (e.g. a shift of 0.2‰ in $\delta^{13}\text{C}$ and 0.5‰ in $\delta^{18}\text{O}$ at Clandon). Also, in the absence of this top unit, the greatest isotopic shift will occur at the site of the previous burrow suite, some distance below the hardground surface - as is indeed the case in the Clandon hardground. In general therefore, isotopic analyses of chalk hardgrounds will be non-representative of the main process of cementation as the true diagenetic history can only be understood properly by observation of the morphologically and palaeontologically more complex convoluted hardgrounds.

8.5 DISCUSSION

It is well established that most hardgrounds form between 0 and 5 m below the sediment surface, usually within Thalassinoides chamber networks at 1-2 m depth (Bromley 1967, 1968; Kennedy and Garrison, 1975; Jeans 1980), and from the above discussion it is clear that this occurs within the zone of bacterial sulphate

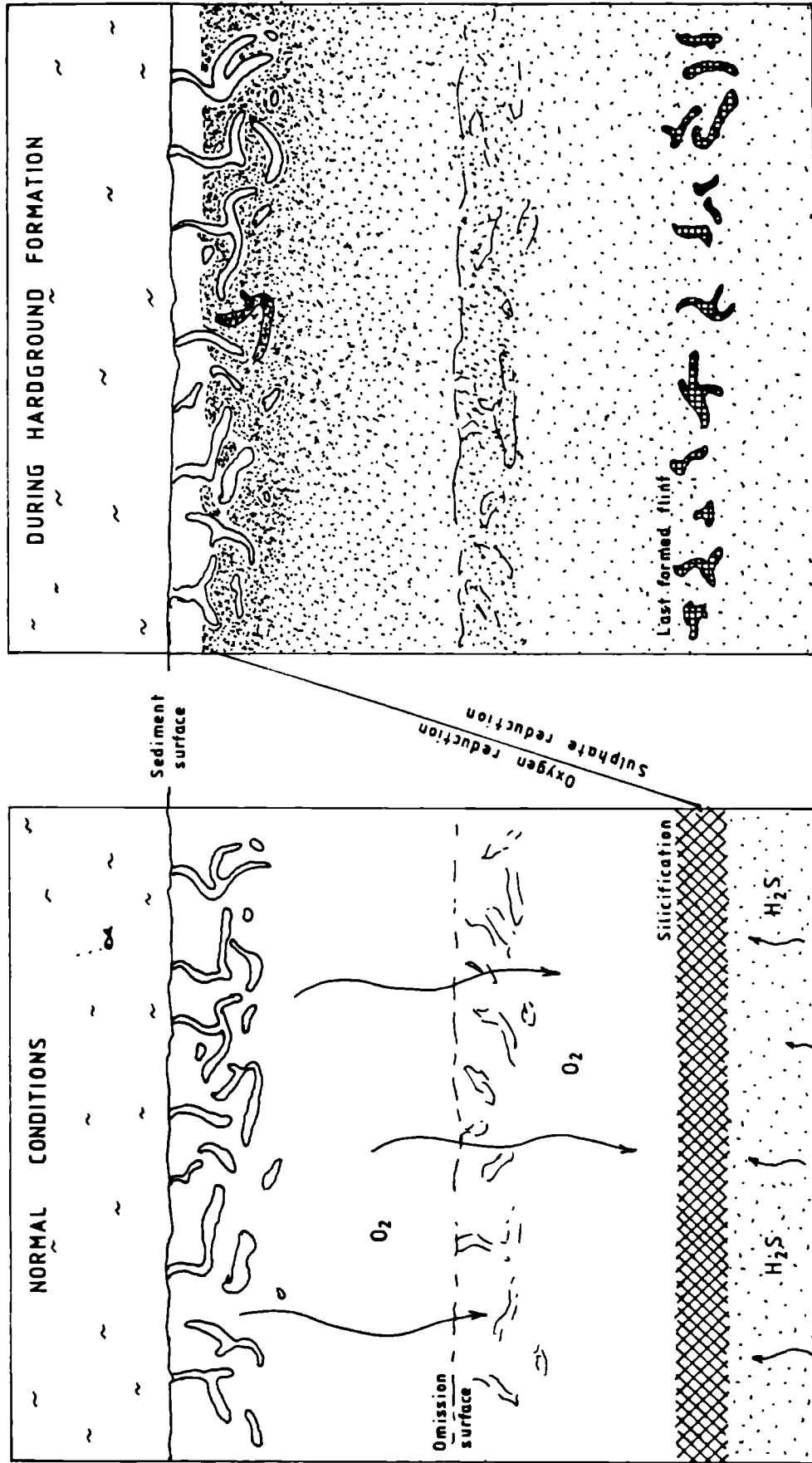


Figure 8.7 Suggested cause of lithification during periods of regional hardground formation.
 Lower oxygen content in bottom waters causes sulphate reduction nearer surface.
 Density of speckling reflects intensity of sulphate reduction.

reduction. However, it was argued in chapters 6 and 7 that flint bands form below this level (at 5-10 m depth) but at the top of the sulphate reducing zone. This is an apparent paradox which must be explained if hardground and flint formation are to be combined in any model of chalk diagenesis.

Sulphate reduction in sediments occurs below the zone where other, more readily utilised oxidants (i.e. O_2 , NO_3 etc) are available (see chapter 2). By far the most important of these is O_2 so, in practice, the initiation of sulphate reduction at depth is controlled by the maximum depth of the aerobic zone which is usually controlled by the extent and depth of bioturbation. The development of sulphate reducing conditions anomalously near to the surface, such as was apparently occurring at the time of hardground formation, is therefore a reflection of a reduction in depth of the base of the aerobic zone in the sediment. This may be caused in two ways: either the available oxygen was consumed more rapidly due to an increase in the organic carbon content in the sediment (effectively a faster sedimentation rate which causes proportionately less of the organic matter to be oxidised at the sediment water interface), or a lower availability of oxygen in the overlying marine bottom waters. The first of these is unlikely since, if anything, hardgrounds represent periods of reduced sedimentation (Kennedy, and Garrison, 1975; Bromley and Gale, 1982). It would appear therefore that elevation of the oxic-anoxic (or more precisely the sub-oxic-sulphate reducing) boundary would have been the result of reduced oxygen content of contemporary marine bottom waters.

9. SYNTHESIS, DISCUSSION AND CONCLUSIONS

9.1 MECHANISM OF FLINT NUCLEATION

From the preceeding discussions it is possible to construct a general scenario of early diagenetic conditions in the Chalk.

Oceanic bottom waters were generally well oxygenated and sedimentation rates were low. In some areas (e.g. the Northern Province of England) the sediment was extensively reworked by bottom currents, but in most places almost all traces of primary lamination were destroyed by intense bioturbation. This bioturbation frequently extended down several metres and in most cases kept the surrounding chalk well oxygenated, while emplacing organic matter at depth within the sediment.

Any biogenic opal deposited with the chalk would have readily dissolved and, if enough silica were available, would have raised dissolved silica concentrations to well above saturation for crystalline silica. Such high concentrations of silica in solution are the result of a dynamic equilibrium between the dissolution of disordered silica and the precipitation of a more ordered silica, rather than a true thermodynamic equilibrium (see discussion in section 2.4.2), and so are only metastable. Locally, aerobic organic matter oxidation within the microenvironments of shell fragments, caused carbonate dissolution which, in turn, had a local "seeding" effect on the dissolved silica (Holdaway and Clayton, 1982). This gave rise to isolated partially silicified fossils, particularly Inoceramus and belemnites, but probably had little effect on the overall concentration of silica in solution which was maintained well above saturation by continued dissolution of biogenic opal.

As sedimentation continued, burrows were infilled and bacterial activity rapidly depleted pore waters of oxygen. Organic matter oxidation continued utilising dissolved nitrate (from seawater) and Fe and Mn oxides and hydroxides (introduced by detrital clays) as the ultimate electron acceptors. The limited supply of these oxidants would soon have been depleted so the sediment would have passed rapidly into sulphate reducing conditions. Sulphate reduction would not necessarily have been intense but would have been widespread below the aerobic zone where organic matter was abundant in the old burrow networks. Meanwhile, above this level, anomalous concentrations of organic matter would have induced local sulphate reduction. These conditions led first to glauconitisation under a mildly reducing (? suboxic) environment (or in local microenvironments), and then to pyrite formation under true sulphate reducing conditions.

Widespread sulphate reduction generates large amounts of dissolved sulphide which, in a clastic sediment, would result in extensive pyrite formation. In the Chalk, however, the limited supply of iron would have been inadequate to account for the majority of the sulphide formed, so

the excess sulphide would have diffused towards more oxic conditions, probably as H_2S . Where this H_2S met suitable conditions, it would have oxidised to sulphate probably through the action of the Thiobacilli bacteria, liberating hydrogen ions as a by-product. These released ions could have led to dissolution of carbonate along the H_2S-O_2 mixing zone, and, as before, this in turn would have led to precipitation of silica from saturated solution as a consequence of the seeding action of the dissolved carbonate ions

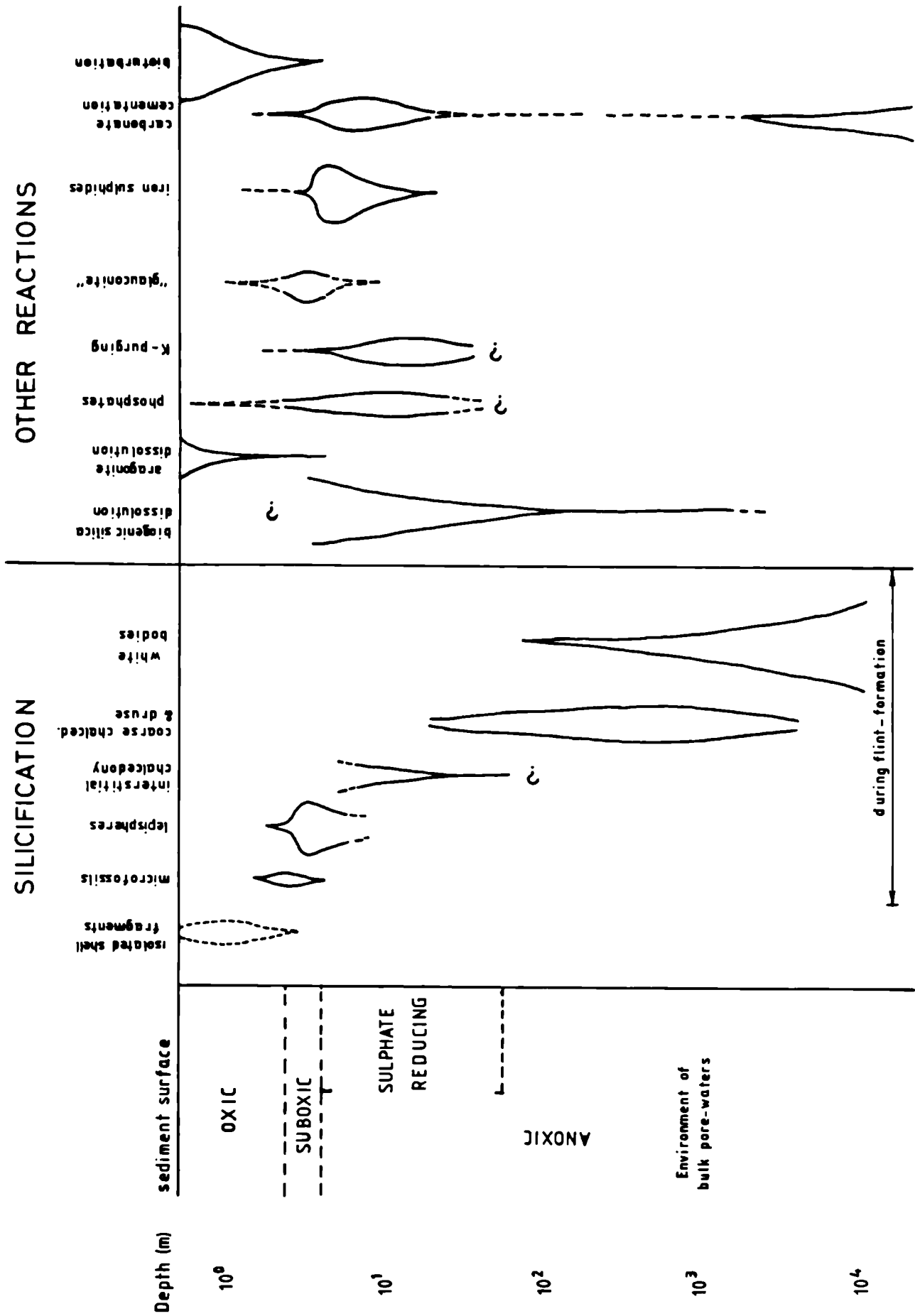


Figure 9.1 Summary of diagenetic reactions in the chalk

(section 2.4.2). Meanwhile, the newly regenerated sulphate probably diffused back to the sites of sulphate reduction to be reduced once more - a sulphate-sulphide reflux process.

Higher in the sediment, similar reactions would occur around locally reducing conditions. Recently buried echinoids would become enclosed or infilled with flint, decaying sponges would form a casing of flint and isolated organic-rich burrows, such as Bathichnus may have generated a giant flint cylinder around them. Where sulphate reduction in burrows was sufficiently intense, the bicarbonate released was precipitated as calcite cement within the flint cylinder to form a paramoudra (fig 9.2).

The position of the oxic-anoxic mixing boundary apparently was controlled largely by permeability variations within the sediment, which are mainly the result of bioturbation. Where burrows were absent or there was negligible permeability contrast between the burrows and the host sediment, $H_2S - O_2$ mixing occurred along a smooth regular boundary and a continuous tabular flint was formed. Where permeability was more variable, silicification was more erratic and confined to areas around burrows along the oxic-anoxic boundary. This led to the formation of nodular flints, frequently within or overgrowing the chamber networks of Thalassinoides burrow networks. In general, the final shape here appears to have been controlled by migration of the carbonate dissolution front beyond the burrow walls. In extreme cases, silicification was constrained entirely by the burrow walls to produce a burrow-form or digitate flint. This normally occurred below a substantial sedimentary break or "omission" where prolonged compaction of the host sediment occurred while the burrows were kept open, leading to an enhanced permeability contrast.

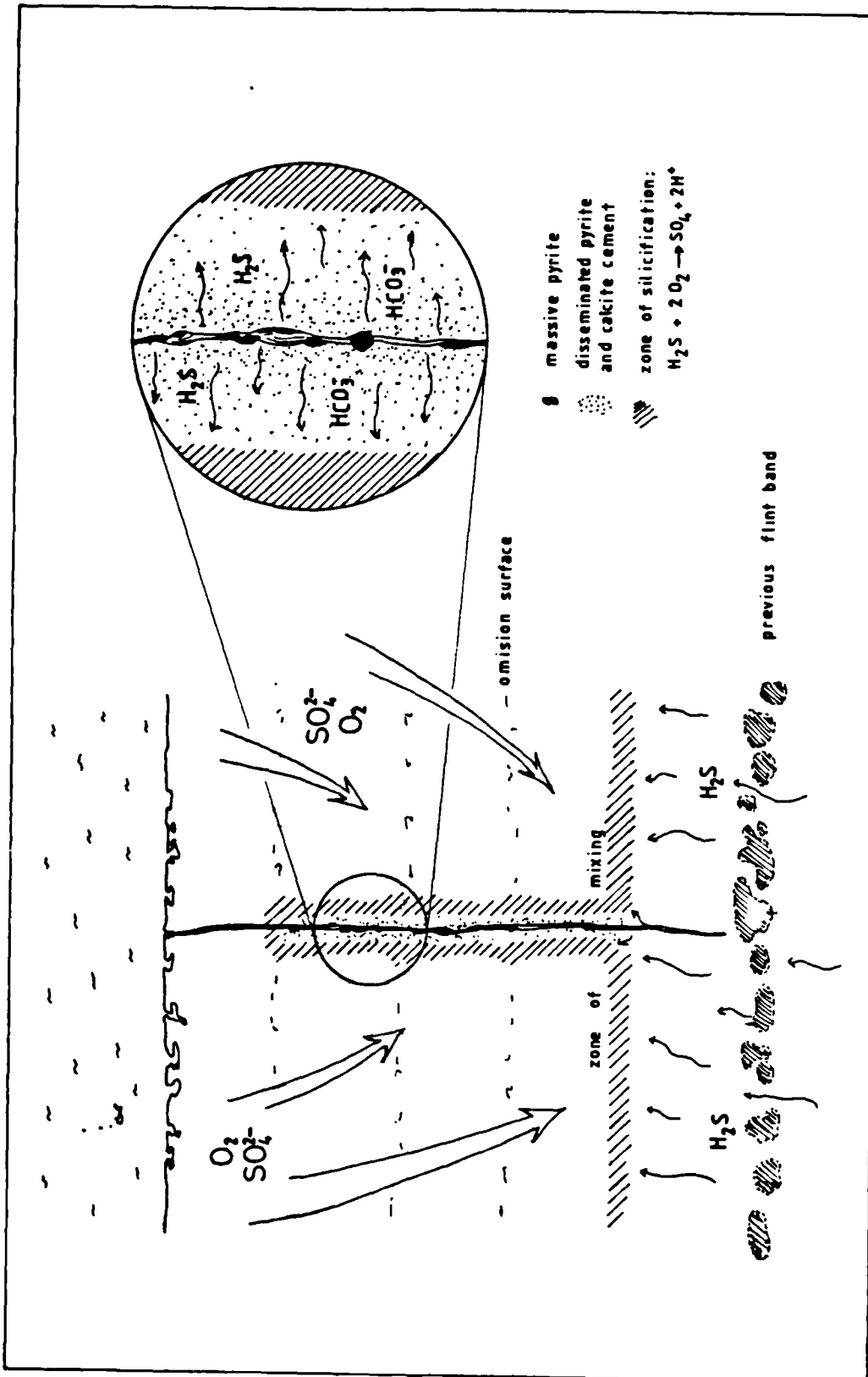


Figure 9.2 Proposed model of silicification in Upper Cretaceous chalks.

Meanwhile, $H_2S - O_2$ mixing would also occur preferentially in any fractures, such as early stage compaction joints or sub-horizontal fractures associated with inter- and intra-bed sliding. Silicification of the walls of these fractures is the probable cause of sheet flints.

Continued, or renewed sulphate reduction after flint formation had a number of effects. Sulphide precipitation occurred preferentially beneath flints, and if a flint grew in an organic rich sediment, H_2S pressure sometimes shattered the flint and precipitated pyrite in the fractures after the whole flint passed into the anoxic zone. Where two flint bands are found close together it is not uncommon for the lower one to be pyritic because the upper one restricted the oxygen supply to the burrows in which the lower flint had formed. Sulphate reduction led also to depletion of potassium from some clay minerals, and to phosphate precipitation in the anoxic sediment. Both of these effects continued after silicification and preservation of the unaffected sediment within flint is a useful guide to the timing of flint formation.

9.2 MICROSTRUCTURE AND GROWTH HISTORY (fig 9.3)

The first stage of silicification in flints is marked by the replacement of skeletal fragments, particularly foraminifera. Silicification in this case is centripetal, implying corrosion of the shell by surrounding pore waters, and is quite distinct from the centrifugal replacement of individual, isolated shell fragments occurring above this zone. Within the "proto-flint" zones, the coarser shell fragments were also peripherally replaced, but the carbonate dissolution rate was able to outpace silica precipitation, leaving a void which was preferentially infilled

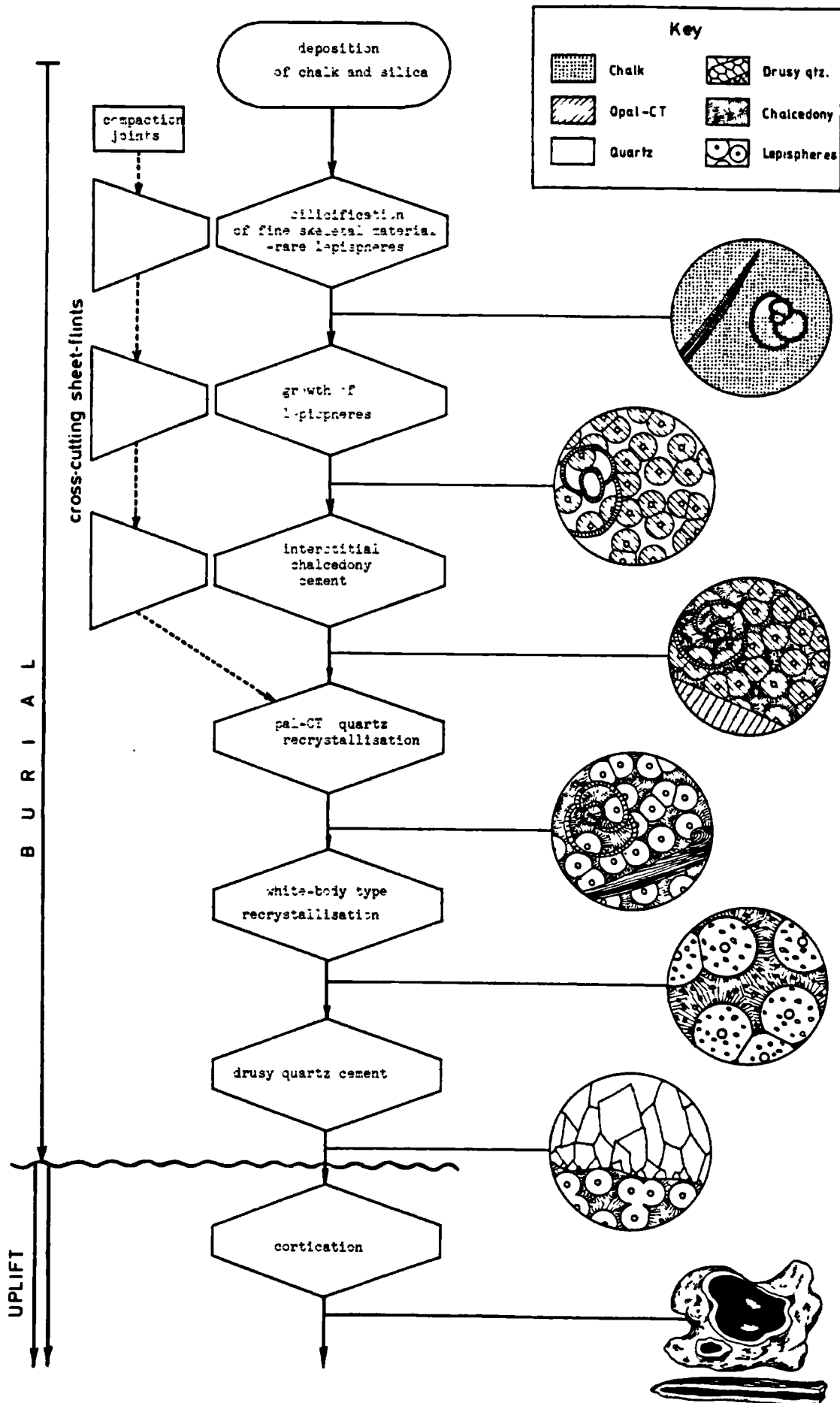


Figure 9.3 Summary of the growth history of flints

with coarse chalcedony, chalcedonic quartz and druse during later diagenesis. The presence of silica replaced syntaxial overgrowths on the prismatic walls of some foraminifera suggests that at least some carbonate redistribution had occurred by the time silicification started. This cementation presumably was associated with aragonite dissolution although the originally aragonitic macrofauna sometimes is preserved in flint.

With progressive silicification, opal-CT lepispheres were precipitated interstitially between and concomitantly with the dissolution of the host calcite grains. Lepisphere growth was initiated more or less simultaneously throughout the whole volume of the proto-flint, although the nucleation centres were more closely spaced towards the centre of the flint (ie within the H_2S-O_2 mixing zone). Continued growth of the lepispheres led to coalescence rather than lateral displacement so any non-carbonate components of the original sediment were quantitatively preserved within the flint. The lepisphere framework of flints was apparently self-supporting (ie. resisted compaction) by the time the sediment reached a porosity of 75-80%. However, reworking of the flint at this stage would probably only disaggregate the lepispheres, hence syngedimentary reworked flints are rare.

Where the silicification environment was not sufficiently intense, such as around the periphery of the mixing zone, lepisphere growth was restricted and a "crusty" framework of silicified skeletal fragments and siliceous microfossils was preserved. In some sediments, particularly those with a very high porosity, the whole flint may consist of crust, giving rise to the so called "incipient" flints. In addition, silicification was inhibited by very high concentrations of organic matter, leading either to the

preservation of burrow walls as a "chalk-meal" annulus in burrow-form flints or the formation of "carius" flints around Chondrites networks or some sponges.

Calcite dissolution continued during lepisphere growth, and a chemical gradient of dissolved carbonate was established which restricted further diffusion of carbonate away from the centre of the proto-flint. Consequently, it is normal to find preferential preservation of calcite in the centre of flints. In addition, because silicification was more intense towards the centre of flints, the silica was deposited with a greater structural disorder causing greater entrapment of pore-waters. This comparatively "wet" silica was preferentially susceptible to later recrystallisation effects (see below). H_2S-O_2 mixing effects locally resulted also in a liesegang-type interaction, leading to more intense replacement in a series of parallel bands, often constrained by high permeability zones such as burrows. Later recrystallisation sometimes picked out the "wet" (rapidly precipitated) zones to produce a banded flint.

After a period of lepisphere formation the precipitational morphology of the silica changed from the characteristic bladed twins of opal-CT lepispheres to microfibrous or micro-bladed chalcedonic opal-CT. It is probable that this reflects a transition from rapid, carbonate "catalysed", precipitation associated with calcite dissolution, to more gentle "unforced" or "free" precipitation from saturated solution after carbonate dissolution ceased. In nearly all specimens, chalcedony completely infills all interstitial void space within the shell fragment-lepisphere framework, implying that excess silica was present at the time. Presumably this excess silica diffused back into the overlying sea-water. The only case

known to the author where this is not true are the giant flints in the Maastrichtian of the type area, where in excess of 40% of the sediment volume is flint. This implies that there was originally a vast excess of silica in normal chalks which on average, now contain only 2-4% silica.

The common preservation of sponge spicules, and more rarely diatoms and radiolarians, in flint implies that much of the dissolution of biogenic opal occurred below the level of silicification. As this was probably the main source of silica (see below) it suggests that the dominant flux of silica to flints was from below, and may explain the tendency for some flint bands to develop a planar top and yet a bulbous lower surface.

The transition from opal-CT to quartz occurred after completion of chalcedony growth and resulted in a small degree of purging of clay mineral impurities from the periphery of the flint into the crust. There is some evidence from oxygen isotopes that the "wettest" silica recrystallised either sooner, or more rapidly than the more open lepispheric structure, although where lepisphere packing density exceeds 65% the picture becomes confused by other recrystallisation effects.

At some stage after the opal-CT to quartz transition, during the deepest burial of the flint, the more structurally disordered silica towards the centre of the flint recrystallised once more. This produced a quartz of greater structural order, with the previously structure-bound water exsolved into microscopic fluid inclusions, giving a white colour to the flint.

The effect of recrystallisation on the isotopic composition of the silica indicates that the system was partially closed with respect to the surrounding pore-waters. The higher temperature resulted in a depletion in ^{18}O relative to the precursor silica.

It would be expected that this would result in an enrichment in deuterium, but some form of reservoir effect, associated with partial exsolution of structure-bound water, overshadows this and the recrystallised flint actually finishes up depleted in deuterium. Because of the closed system nature of the recrystallisation, it is not possible to estimate the temperature of the reaction from $\delta^{18}\text{O}$, but as this was the last major structural recrystallisation to affect the flint it seems reasonable to attribute it to the deepest phase of burial. In Northern Province Chalks, where geothermal gradients were higher, recrystallisation is more advanced and much of the flint is totally white or grey, rather than black.

Subsequent to uplift, flints generally undergo two important changes. The most obvious of these is the development of a peripheral white cortex which, in some cases, may grow to pervade the whole flint. Cortication occurs in two stages, an initial recrystallisation, similar to that of the white bodies, followed by dissolution of the interstitial silica. It is likely that recrystallisation is seeded by an influx of (low ionic strength) meteoric water although the evidence for this is rather tenuous. Dissolution starts within the interstitial chalcedony and etches into the lepispheres. The end result is a chalky white flakey structured "rotten flint".

The second effect of uplift is the infiltration of, and isotopic exchange with, meteoric water. This results in a shift of the isotopic composition of the black flint towards lighter values of δD and $\delta^{18}\text{O}$, along a line defined by $\delta\text{D}=14.5 \delta^{18}\text{O}$. Similar exchange does not affect the structurally more ordered white bodies. A series of partially recrystallised cherts which have

exchanged with meteoric water may fall approximately on a line comparable to the "meteoric water line", a feature interpreted by Knauth (1979) as indicative of chert formation at the marine-fresh water boundary.

9.3 IMPLICATIONS FOR CRETACEOUS OCEANOGRAPHY

9.3.1 Source of Silica in Flints

The Cretaceous Chalk has always been considered as anomalous because of the apparent concentration of chert in it, and with the addition of D.S.D.P. data, the late Cretaceous-Eocene period has gained a reputation for being a period of exceptional silica productivity. Explanations for this have varied from high silica supply from contemporaneous volcanism or ocean ridge spreading (Gibson and Towe, 1971; Pomeroy and Aubry, 1977), silica supply from the drainage of large areas of lateritic terrain (Leclaire 1974; Frakes and Kemp, 1973) or even an extra-terrestrial source (Galloway, 1886). In contrast, Levitan et al. (1975) and Keene (1976) have suggested that, in the Pacific at least, the apparent concentration of silica in this period is just an artefact of the comparatively broad stratigraphical refinement of sediments of this age (see below).

Regardless of the ultimate source of the silica, and whether or not the Cretaceous seas were awash with siliceous organisms, it is important first to establish the mechanism of silica transport into the sediment where it eventually became fixed as flint. There are three possibilities for this; volcanic, diagenetic or biogenic.

Firstly, there could have been anomalous levels of dissolved silica in bottom waters, such as may result, for example, by extensive submarine volcanism. Although there is evidence of

contemporary volcanism in central Europe (eg. Valetton, 1960) and North America (Hattin 1976; Kauffman, 1977; Schultz, 1978) the degree of silicification is quite obviously totally unrelated to known volcanic areas. Also there is no evidence that such activity is capable of supplying a significant amount of silica to an area the size of the Chalk outcrop/subcrop without also introducing significant amounts of aluminium and many other elements which is not the case, so volcanism can be discounted as a major source of silica to the sediment.

A second possibility is that the silica may have been supplied by clay mineral reactions during early diagenesis. This also seems unlikely since the majority of flints occur in sediment with less than 4% clays, and the amount of silica present as flint often considerably exceeds this. SiO_2 to Al_2O_3 ratios, even of acid igneous rock, rarely exceed 4.75 (Krauskopf, 1967) and yet the ratio in normal white chalks may reach greater than 6 (Spears, 1979) and is 6.5 at Clendon, excluding the flints themselves (see chapter 7). Even if all the clay present in the Chalk was originally of acid igneous origin it would be inadequate to account for all the silica present.

The third and most likely source of silica is the entrapment of biogenic opal, particularly in the form of diatoms, radiolarians and sponges. Radiolarians, and more rarely diatoms, may occasionally be preserved in recognisable form in the crust of some flints, and must obviously have been present in the surrounding sediment, although they are by no means as common as sponge spicules. In some cases, flint crusts may contain in excess of 30% sponge spicules and calcite replaced skeletons of siliceous sponges are a very common, if rarely recognised, component of the Chalk. If the

concentration of sponge spicules in the crust is representative of the chalk as a whole then sponges alone could easily account for the amount of silica present in flints. Furthermore it is well known that biogenic opal readily dissolves when enclosed in the sediment, to form a highly saturated silica solution which is a necessary prerequisite for the model of flint formation proposed above.

Whether or not biogenic silica productivity was higher in the world's oceans during this time is rather more controversial. If tallied as the total number of occurrences for each geologic time interval, biogenic siliceous rocks appear to be substantially more abundant in Eocene and Upper Cretaceous sedimentary sequences (Davies and Supko, 1973). However, Levitan et al. (1975) and Keene (1976) have demonstrated that the apparent depositional maximum disappears if occurrences of chert and porcellanite are calculated as a percentage of time stratigraphic units. During the Cretaceous, silica accumulated predominantly in carbonates or as radiolarian mudstones concentrated in an equatorial belt in both the Atlantic and Pacific oceans (Ramsay, 1973). Accumulation rates at D.S.D.P. sites 167, 303 and 305 in the equatorial Pacific high productivity zone vary from 5 to $30\text{g/cm}^2/\text{my}$. (Polleastro, 1981), and similar rates would be expected for the Atlantic. These rates overlap the lower end of the range of opal accumulation rates for the same area during the Cenozoic (Leinen, 1979) suggesting, if anything, that silica productivity was lower during the Cretaceous than at present.

The European platform, and southern England in particular, had a latitude of this time of about 40°N (Smith and Briden, 1977). This is somewhat north of the equatorial high productivity zone, so biogenic silica productivity here would have been even lower.

Conversely, if most of the silica supply to the Chalk were fixed by sponges on the sea floor, then less of the biogenic silica would become dissolved in the water column, leading to more efficient preservation of the silica in shelf environments. This possibly could lead to a higher concentration of silica preserved in the Chalk than in contemporaneous deep sea sediments, although on a longer time scale both the oceanic and shelf environments appear to have accumulated less silica than similar environments in the Cenozoic.

The apparent abundance of silica in the Chalk probably is related more to visual appearance than to palaeoceanography. Flints are a very conspicuous component of chalk cliffs, whereas a similar concentration of diagenetic silica (2-4%) dispersed in a mudstone would usually go unnoticed. In addition, biogenic silica in shelf environments is usually greatly diluted by terrigenous material, so the absolute quantity of silica in the sediment is an unreliable guide to past biogenic silica productivity. The majority of pure carbonate shelf sediments, of all ages, also are rich in chert (e.g. Portland/Purbeck limestones, Carboniferous limestones, Durness limestones etc).

In terms of oceanic sediments, the apparent abundance of silica in Cretaceous sediments is a function of both the comparative scarcity of older sediments and the greater stratigraphic resolution which is possible in younger sediments.

9.3.2 Rhythmicity of Flint Bands

If flints form at the oxic-anoxic boundary, then the observed regular repetition of flint bands every 0.5-1.5m has important

implications for Chalk sedimentology. The most obvious interpretation is that chalk sedimentation was markedly rhythmic or cyclic on the same scale, with each phase of flint growth terminating in rapid sedimentation of a further 0.5-1.5m of sediment. However, this conclusion does not follow automatically since a modified liesegang phenomenon can also account for the rhythms: if the flint nucleation process consumes oxygen (to oxidise H_2S) this will deplete the overlying sediment of dissolved oxygen, and thus the next phase of silicification can occur only above the band of oxygen depletion. This in turn will deplete the next sediment level and so on.

One important line of evidence suggests that the liesegang effect is not the cause of the concentration of flint in discrete bands. Oxygen supply from overlying sea-water will be much influenced by only minor variations in sediment permeability, so it is almost impossible that liesegang banding could remain regular over more than a few kilometres, if that. In contrast, many flint bands may be traced over several hundreds of kilometres and even into separate sedimentary basins (such as the Northern and Southern Province basins of England: Mortimore and Wood, In Press), separated by condensed sequences containing no flints. Clearly, a liesegang phenomenon cannot explain the rhythmicity of flint bands, so it must be related to rhythmic or cyclic sedimentation of the host sediment. Flint bands apparently reflect breaks in sedimentation.

The concept of rhythmic sedimentation in the Chalk is far from new. The early theories of flint formation ^{from} _^ silica gel all called upon a rhythmic phenomenon to explain flint bands, and due

largely to the discoveries of the D.S.D.P. it is now becoming widely accepted that pelagic sedimentation often shows a strong rhythmic component, apparently related to the Milankovitch orbital parameters, (eg. De Boer, 1982 and references therein). These ideas have also been applied by Felder (1981) to explain cyclic variation in meso-fauna in the Dutch Maastrichtian, and numerous authors have drawn attention to apparently rhythmic variations in other features of the Chalk, such as hardgrounds (Kennedy and Garrison, 1975) or chalk-marl couplets (Mortimore 1979). In this respect it is interesting to note that the alternation of chalk and marl beds in the Cenomanian of southern England occurs on the same scale as flint bands. Presumably this is another manifestation of the underlying rhythmicity of Chalk sedimentation, although here the flints are absent.

The implications of rhythmic sedimentation are of little consequence here other than to explain the localisation of flints into bands. Within this context however, variations in intensity of silicification will be influenced by the size of the sedimentary break, and the concentration of organic matter buried in the sediment cycle immediately beneath. As explained above, the overall form of the flint is controlled by permeability variations in the sediment, which are themselves a function of the length of sedimentary omission and of the local fauna.

9.3.3 Depth of The Redox Boundary

One important problem of the proposed mechanism for flint formation is that it implies that the oxic-anoxic redox boundary (or more precisely the lower limit of sulphide oxidising conditions) was, at least in some cases, many metres below the

sediment surface (for example where paramoudras occur the basal flint must have formed at a depth greater than the height of the paramoudra). Although this is rather deeper than is found in present day shelf sea sediments, it is not unreasonable for deep sea pelagic carbonates where truly anoxic sediments may occur only below 15-20m depth. This interpretation of a deep redox boundary is in contrast to the opinion of M.A. Arthur (pers. com. 1983) who has suggested a depth of only a few centimetres for the chalks in chalk-marl interlayers but, on the other hand, flints do not form in this environment anyway.

The depth of the redox boundary is controlled by two factors: the concentration of biodegradable organic matter in the sediment, and the availability of dissolved oxygen to the sediment. The Chalk represents an unusual facies in that it is a widespread pure pelagic carbonate which formed in comparatively shallow epicontinental seas. Although the sedimentation rate was slow by comparison with most shelf sediments, it was faster and the fauna more diverse than for most deep sea sediments. It can be predicted therefore, that the redox boundary would occur higher than in deep sea pelagic carbonates (because of the higher sedimentation rate and richer fauna) but substantially lower than in most shelf sediments (because of the slow sedimentation rate and extensive turnover and aeration of the sediment by the benthos). It seems reasonable to assume that during non- or low-sedimentation periods (between rhythms) the upper 1-5m of sediment were kept aerated by the extensive burrow networks, particularly Thalassinoides. These burrows would also become the centre of accumulation of organic matter (faeces and wall linings etc) but only very rarely become anoxic because they will have been well aerated. Following

the deposition of the next 1-2m "wave" of sediment the existing burrow system would become infilled, trapping comparatively large amounts of organic-rich sediment below the new redox boundary. This would pass rapidly into sulphate reducing conditions and the H_2S thus formed could lead to silicification a little below the base of the new burrow system. The mechanism to generate flint in discrete bands was therefore one of "redox-boundary jumping", related to rhythmic sedimentation and related "omission-suite" burrows.

9.3.4 Regional Hardground Complexes

Nodular beds and hardgrounds in the Chalk are also intimately related to "omission surfaces", and apparently are also related to organic matter oxidation within burrow networks (section 3.4 and Chapter B). Obviously it is important to ascertain the genetic relationship between flint and hardground formation in the Chalk where the two are so obviously closely related.

Cementation in hardgrounds appears to have initiated in the white chalk "islands" within Thalassinoides chamber systems (Bromley, 1967) and then gradually spread to produce a fully indurated unit. That this process occurred close to the sediment surface is evidenced by the rich encrusting epifaunal and infaunal crustacean populations, both of which progressively modified their behaviour during the lithification process. Detailed observation of the burrow morphologies in hardgrounds indicates that this usually happened at 1-2m depth, suggesting that the sediment was undergoing sulphate reduction only 1-2m below the sediment surface. This conflicts somewhat with the proposed model of flint formation which requires the top of the sulphate reduction zone to be at 4.5m depth.

The apparent paradox here must reflect some form of a sedimentological control on the depth of the redox-boundary in the sediment, such as a reduction of oxygen in bottom waters, or a higher organic content in the overlying sediment. However, the development of sulphate reducing conditions anomalously close to the surface during periods of hardground formation cannot be caused by the presence of a greater concentration of organic matter in the sediment since, if anything, hardgrounds represent a sedimentary break, which would allow greater time for oxidation of organic matter on the sea floor. Also, hardground formation cannot be related solely to the break in sedimentation since some hardgrounds appear to have formed very rapidly while chalks at longer sedimentary breaks have remained unlithified (section 3.4). This implies that, in order to decrease the thickness of the oxic zone, there must have been a decrease in the oxygen supply to the sediment, reflecting a reduction in the oxygen content of oceanic bottom waters.

If hardgrounds represent periods of low oxygen availability, then the occurrence of regional hardground complexes such as the Chalk Rock (see Bromley and Gale, 1982) must represent large areas of oxygen depletion on the sea floor. Furthermore, periods of regional hardground formation are concentrated in shallower water areas, and are often associated with marine regressions. For example the end Turonian regression is manifested over the London Platform as the Chalk Rock, while at the same time the basal hardground complex of the Craie de Villedieu ("Calcaire dur de la Ribochere" member of Jarvis, Gale and Clayton, 1982) was forming in the shallow waters around the southwestern margin of the Paris Basin. Also,

A.S. Gale (pers. com. 1982) has pointed out that the locus of cementation over the London Platform migrated progressively off-structure during the regression. All of these features suggest that regional hardground complexes are related to the impingement of a narrow belt of oxygen depleted waters (i.e. the oxygen minimum zone) on the sea floor (fig 9.4). Smaller isolated hardgrounds may represent local "ponds" of oxygen depleted waters, although isolated widespread hardgrounds such as the Clandon Hardground (= Barrois' Sponge Bed of Kent) cannot be explained by this mechanism. However, this model can account for the absence of true hardgrounds in deep sea sediments, where the oxygen minimum zone rarely extends.

The effect of rhythmic sedimentation on hardground development would be to produce a similar "redox-jumping" effect as occurs to form discrete flint bands (see above). With each successive sedimentation period, the most intense zone of lithification would jump up to the next suite of Thalassinoides, giving the overall appearance of discrete nodular bed units, with unlithified or poorly lithified chalk units between. This is precisely the situation in a large number of nodular chalk sections described by Kennedy and Garrison (1975).

In cases where renewed sedimentation was accomplished by a return to more normal (i.e. well-oxygenated) bottom water conditions, the effect would not be another lithified unit at the top of the sediment, but a return to flint formation, lower in the sediment. In most cases this would occur within the relic burrow system of the previously lithified unit since this would be the main source of H_2S as the sediment passed into the sulphate

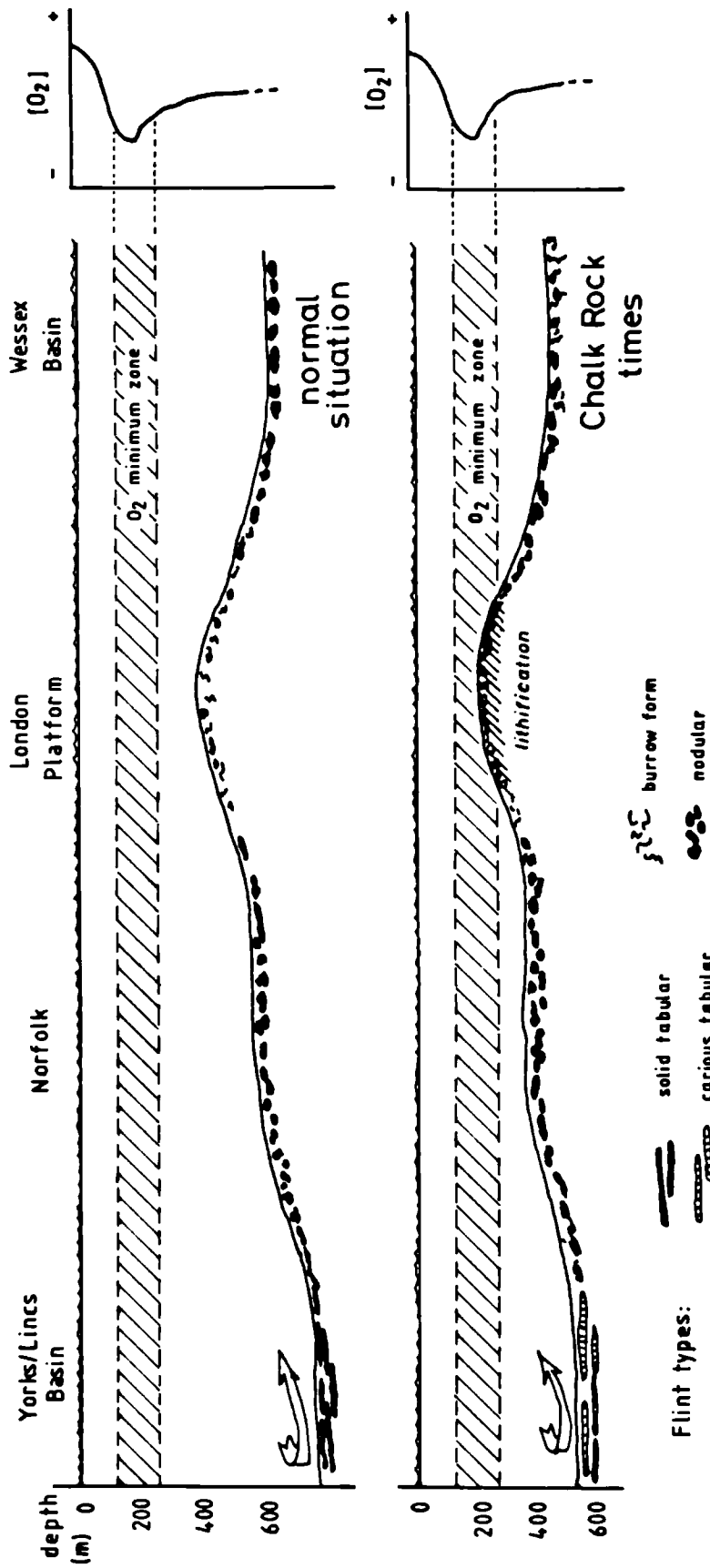


Figure 9.4 Oceanographic control of flint and hardground formation in the Chalk.

Fluctuations in the position of the oxygen minimum zone relative to the sediment surface are reflected in varying depths to the sulphate reduction zone in the sediment. Hardgrounds formed where (intense) sulphate reduction occurred near to the sediment surface.

reduction zone. This situation is particularly common in the upper parts of nodular chalk units and typical examples are shown in plates 2E and 3A and in fig 3.11.

9.4 SIGNIFICANCE OF FLINTS TO OTHER CHERTS

The models presented here explain many features of the flints in Cretaceous chalks and to some extent may be extended to replacement cherts from many other formations. The majority of Phanerozoic nodular type cherts studied by the author are of essentially the same lepispheric structure when etched, although in almost all cases the structure is complicated by more extensive burial recrystallisation and inhomogeneities in the original sediment (see section 4.10). (Indeed flints were chosen for this study because of their comparative simplicity). Such rocks include the chert nodules of the Portland and Purbeck beds of Southern England; Carboniferous Limestone Cherts; some of the mid-Jurassic cherts from the southwest Paris Basin; Upper Jurassic replaced oolites from the Dordogne; nodules in bedded cherts from the Sogno Formation of Southern Switzerland and some of the nodular cherts from the Durness Limestone.

The most characteristic feature which these cherts have in common is that they are all associated with very low clay content fine grained carbonates (or radiolarite in the case of the Sogno Formation). It is likely that only in such high porosity, low permeability sediments could a distinct sulphide-oxygen mixing zone develop which could lead to the formation of a discrete silicification zone. In coarser grained sediments, lepispheric fabric apparently could not develop, possibly because the lepispheres require isolated microenvironments (such as between coccoliths) for their formation.

Lepisphere formation is also apparently inhibited by a high clay content although the reasons for this are not clear. Lepispheres require a magnesium hydroxide nucleus for the initiation (Kastner, 1982) so it is possible that the presence of clays either inhibits the formation of lepispheres, or leads to silica precipitation on clay grains in preference. Alternatively, as the pore-waters of clay-rich sediments are characteristically richer in dissolved cations than are pure carbonates, it is possible that these may inhibit lepisphere formation (Lancelot, 1973; Isaacs, 1982).

The overall similarity in petrology of the "lepispheric cherts" suggests a similar growth history and replacement mechanism in which carbonate dissolution leads to silica precipitation from a saturated solution. The underlying chemistry of the carbonate dissolution may differ in some cases, although the close similarity in field relations points to a similar origin.

In contrast, another major group of cherts, usually represented by continuous, bedded, large scale replacements, consist almost entirely of long interlocking bundles and sheaths of coarse chalcedony fibures ("type 4 chalcedony"). This microstructure appears to be more or less mutually exclusive with lepispheric structure and Clayton (1984) has proposed the name "chalcedonic cherts" to differentiate them from the "lepispheric cherts" described above. Examples of chalcedonic cherts include the Greensand cherts of southern England (more correctly termed "skeletal chalcedonic" chert) and the Tertiary "Meuliere" of the Perigord in France.

The silica in chalcedonic cherts is similar in many ways to that in the lepispheric cherts in that it is structurally disordered and susceptible to the same secondary recrystallisation effects

(i.e. white body formation and cortication). There is also some evidence that it has passed through an opal-CT stage before recrystallisation to α -quartz, and some specimens possess a poorly silicified "crust", similar to that of flints. In contrast, although these cherts are of replacement origin, their field relations are quite distinct from those of nodular cherts such as flints, and their microstructure suggests a very different growth history.

Those points reflect a fundamental difference in origin between the lepispheric cherts and the chalcedonic cherts, although both groups are of replacement origin and distinct from the "in-situ recrystallised" bedded cherts (radiolarites and diatomites). The lepispheric cherts have enough in common with each other that it seems reasonable to assume a sulphide-sulphate reflux mechanism for their origin in the majority of examples. Clearly this is not the origin of the massive replacements represented by chalcedonic cherts, although even here the mineralizing effect of dissolved carbonate ions may possibly be the cause of silica precipitation.

APPENDIX 1 - TERMINOLOGY OF THE SILICA MINERALS

BEEKITE

Beekite is a form of skeletal replacement in which shells are replaced by concentric rings of granular silica. In thin section the structure of beekite is complex and shows a range of fabrics from true chalcedony through quartzine, lutecite and granular micro-quartz into granular quartz druse. The morphology apparently is related to a limited supply of silica at the site of replacement during rapid dissolution of carbonate (Holdaway and Clayton, 1982).

CHALCEDONIC QUARTZ

Fibrous length fast quartz, intermediate in structure between chalcedony and microquartz. Chalcedonic quartz is differentiated from true chalcedony in having the optical properties of quartz, and from microquartz by an aspect ratio greater than about 5.

CHALCEDONY

A great deal of confusion is associated with the term "chalcedony" and it has been used in different ways by a number of authors. Chalcedony s.s. is a length fast microfibrinous silica phase, commonly brown in transmitted light, and exhibiting a variable refractive index and birefringence, less than those of quartz. It is commonly biaxial positive ($2V$ up to 25°), is chemically more reactive than quartz and exhibits suppression of the low-high transition of quartz (Pelto, 1956). Length slow varieties are known as "quartzine" or "lutecite" depending on whether the fibres have straight or oblique extinction.

More recently, "chalcedony" has incorrectly been taken to

mean any fibrous form of silica (eg Shepherd, 1972), any microcrystalline form of quartz (Whitten and Brooks, 1972) or, in some cases, any fine grained quartz rock with a slight waxy appearance.

CHERT

Chert can be defined as a siliceous rock consisting predominantly of microcrystalline or cryptocrystalline silica, occurring as beds or nodular masses in sedimentary rocks (Smith, 1960). This definition excludes colloidal or opaline rocks and vein quartz etc. and contains flint, silicite, hornstone, jasper etc.

In many early works chert was considered as an impure variety of flint (eg Lyell, 1830), but the term has now become established as more general than "flint" and the term "chertification" has been introduced to differentiate chert-forming processes from more general "silicification" events (Tarr, 1938).

CRISTOBALITE

True mineral cristobalite (a colourless to white silica mineral crystallising in the tetragonal system) does not occur in sedimentary rocks, although a structurally disordered form, usually referred to as "opal-CT" is an important intermediate in the chertification process. If the term "cristobalite" is used in this sense it is desirable to make clear that it is the disordered form which is being referred to as the normal form is not stable at sedimentary temperatures and pressures.

FLINT

The term "flint" has been used to mean anything hard since the days of the Old Testament (see frontispiece), and the present form of the word has in use since the beginning of modern geology. Originally the definition of flint was based on texture (eg Bakewell in 1839 defined flint as "Siliceous earth, nearly pure", and Shepard in 1844 drew attention to it's perfect flat, conchoidal fracture), although the term has subsequently been defined in terms of mineralogical composition (Kemp, 1896), colour (Sosman, 1926) or origin (Holmes, 1926). This myriad of definitions has left flint with something of a character crisis and led to confusion on a large scale.

In theory the term is unnecessary as flint, clearly, is only a variety of chert. However, it is so well engrained in the literature that it cannot be dropped altogether. "Flint" is retained in this work only as an informal term for the chert which is derived from Cretaceous Chalk, and it is recommended that "chert" be used in preference in formal descriptions.

HORNSTONE

According to Humble in 1843, "so much ambiguity of meaning is attached to the word *hornstone* that it would be favourable to the interests of mineralogy if this term could be banished from it's nomenclature". A similar confusion surrounds the definition of hornstone as that surrounding "flint" and "chert" although in general it is taken as a particularly impure form of chert. Indeed the German word for "chert" is "Hornstein". As there is no clear distinction between "chert" and "hornstone", the former term is adopted here.

JASPER

The term "jasper" has been used from ancient times to designate any opaque cryptocrystalline variety of quartz with red, yellow, brown or green colours. Essentially it is rather a bucket term for impure cherts which owe their colour largely to inclusion of a substantial proportion of iron and manganese oxides.

KEATITE

"Keatite" is a synthetic silica phase not yet found in nature (Keat, 1954). Keatite is traditionally regarded as a high pressure phase (Sosman, 1954) although it has also been produced at lower pressures during laboratory synthesis of chalcedony (White and Corwin, 1961).

LEPISPHERE

These are small (2-20 μ) spherical aggregates of bladed crystals first described from deep sea chalks by Wise and Kelts (1972). Initially of opal-CT mineralogy, they are also found in quartz cherts pseudomorphed by low quartz. They are important components of oceanic cherts but are also known from other strata, most notably the Monterey Formation of California (Bramlette, 1946). Similar material is known to Russian workers as "opoko".

Lepispheres apparently nucleate on $Mg(OH)_2$ centres (Kastner et al., 1977), and can form in widely different conditions of temperature, pressure and pH. According to Florke et al. (1975), the morphology probably is controlled by the twinning laws of cristobalite.

LUSSATITE

This is a now obsolete term which was used to describe opal-CT (Florke, 1955; Jones and Segnit, 1971). However, this use clashed with the original definition of Mallard (1890) and potentially led to confusion with the mineral "lutecite" so the name has now been dropped and "opal-CT" or "disordered cristobalite" are used instead.

LUTECITE

Generally colourless or pale brown, subcircular aggregates of length slow fibrous quartz. Lutecite tends to exhibit elongate areas of undulose extinction rather than true fibres, with each cluster radiating from a different rather than a common centre. Extinction is oblique at up to 30° from the c-axis and represents a morphological intermediate between quartzine and true chalcedony (Cayeux, 1931).

Lutecite generally occurs as a replacement of evaporites (Folk and Pittman, 1971), but is also known as a replacement of biogenic carbonates (Wilson, 1966; Orme, 1974)

It's development apparently is controlled by the concentration of dissolved anions in the area at the time of replacement, (Holdaway and Clayton, 1982).

NOVACULITE

"Novaculite" is derived from the Latin "novacula", a razorite, and refers to a stone used for razor hones (Tarr, 1938). The name is first used by Kirwan (1796) who referred to it as a synonym for "turkey hone". The term is yet another one for a variety of chert, in this case one which is especially pure and homogeneous (eg the Arkansas novaculite: Folk and Weaver, 1952).

Characteristically, novaculite consists of equant interlocking grains of quartz, each exhibiting extreme undulose extinction, and this is shown in chapter 4 of this work to correspond to the recrystallised fabric of a coalesced lepispheric structure.

OPAL

Opal can be described as a rigid silica hydrogel containing a variable amount of water (Smith, 1960). Monroe (1964) demonstrated that fracture surfaces of opal have a spongy porous texture similar in all respects to chalcedony. It is now generally believed that most opal is structurally ordered on the molecular scale as low cristobalite, and potentially grades into opal-CT.

Although no rigid distinction can be drawn between opal and highly disordered opal-CT, the term is still useful, particularly for describing siliceous organisms ("biogenic opal" or "opal-A" of Jones and Segnit, 1971)

OPAL-CT

A silica phase with X-ray characteristics between those of cristobalite (C) and tridymite (T). This corresponds roughly to either low cristobalite disordered along the $[111]$ plane or low tridymite with turstratic stacking of its sheets (Wilson et al., 1974). In addition, Florke et al. have pointed out that opal is essentially a highly disordered form of the same material. With burial (?time, ?temperature) the $d(101)$ lattice spacing of opal-CT shows a progressive decrease from about 4.1\AA to about 4.03\AA accompanied by a sharpening of the associated XRD peak, attributed to a diagenetic ordering of

the structure (Murata and Nakata, 1974; Murata and Larson, 1975). Ultimately, opal-CT recrystallises to α -quartz, but it is not known for certain if this transformation takes place in the solid state (essentially a zero order reaction) or via a solution step. However, the latter appears more likely (Murata et al., 1977; and chapter 5, this work).

Opal-CT has also been described as opaline silica/tridymite (Weir and Catt, 1965), lussatite (Florke, 1955), subsidiary cryptocrystalline silica (Jenson et al., 1957), and "badly crystalline" tridymite (Buurman and Van der Plas, 1971). The terms "opal-CT" or "disordered cristobalite" are preferred.

PORCELLANITE

Porcellanite is technically any chert with the texture of unglazed porcelain, although in recent years it has become restricted to cherts composed dominantly of opal-CT.

The word "porcellanite" was first suggested by J.T.A. Peithner in 1794 (Chester, 1896), as a substitute name for "porcelain-jasper" and the term has always been applied to hard indurated clay or shale before the discovery of opal-CT cherts in oceanic sediments. The present, widespread use of the word as a description of opal-CT cherts has now superseded the original definition although it is preferable to describe this material as "opal-CT chert" or "porcellanous chert".

QUARTZINE

Length slow, straight extinction fibrous silica ("chalcedony" s.l.) which occurs as drusy overlays or colloform masses, replacing evaporites or skeletal debris. It typically occurs

as colourless or brown ragged aggregates or fibrous splays which collectively give the impression of undulose extinction. Quartzine frequently grades into true chalcedony.

TRIDYMITE

True tridymite is a colourless or white orthorhombic silica phase, which is unstable at sedimentary temperatures and pressures. The "tridymite" referred to ⁱⁿ most accounts of sedimentary rocks is really opal-CT (corresponding more to cristobalite than to tridymite in structure) and its description as "tridymite" is to be avoided.

TRIPOLI

"Tripoli" takes its name from the state in North Africa where it was first found although the name has been variously used since its inception. This material evidently was famous as a polishing agent to the Romans as "Tripolie" & is referred to as "Goldsmiths earth" in Holland's translation of Pliny's "Natural History" (Tarr, 1938).

The original "Tripoli" is a diatomaceous earth which has become slightly recrystallised, although current usage tends to refer only to a siliceous residual weathering deposit which is very porous, light in weight and has a harsh, rough feel.

VUURKLIP

According to Shepherd (1972), "vuurklip" is Afrikaans for flint although the present author has been unable to verify this.

APPENDIX 2 - THEORETICAL SETTLING RATES
FOR CHALK CONSTITUENTS

Assuming flow at low Reynolds number* (effectively slow enough to avoid turbulence) the drag force, F_z , exerted on a sphere free falling in a viscous fluid is given by (Happel and Bremner, 1965):

$$F_z = -6\pi.\eta.a.u \quad (A2.1)$$

where: η : viscosity of the fluid
 a : radius of the sphere
 u : relative vertical velocity of the particle

At terminal velocity (V), the downward acceleration due to gravity acting on the particle is exactly balanced by this drag force, hence:

$$\begin{aligned} F_z &= mg \\ &= \rho_{rel} \cdot \frac{4}{3} \pi a^3 \cdot g \end{aligned} \quad (A2.2)$$

where: m : mass of particle ($=\rho \times \text{volume}$)
 ρ_{rel} : effective density of the particle
 $(\rho_{rel} = \rho_{particle} - \rho_{fluid})$

*Reynolds number (Re) is defined as $Re = \frac{\text{fluid} \cdot u \cdot s}{\eta}$

where: ρ : density, u : relative velocity, s : surface area of particle, η : fluid viscosity

Combining A2.1 and A2.2 and rearranging gives:

$$V = - \frac{2}{9} \frac{g \rho_{rel}}{\eta} a^2 \quad (A2.3)$$

This is the Stokes Formula relating terminal velocity of a falling sphere to the viscosity of the fluid. Using this formula for a sinking coccosphere and assuming that the object is approximately spherical and composed of a mixture of about 50% water and 50% calcite:

$$\left. \begin{array}{l} \rho_{coccolith} = 1.85 \text{ kg/m}^3 \\ \rho_{sea \text{ water}} = 1.03 \text{ kg/m}^3 \end{array} \right\} \rho_{rel} = 0.82 \text{ kg/m}^3$$

$$g = 9.81 \text{ m/s}^2$$

$$\eta = 1.07 \times 10^{-6} \text{ Pa sec (at } 20^\circ\text{C assuming } 35\% \text{ salinity)}$$

$$a = 5 \mu\text{m} = 5 \times 10^{-6} \text{ m (typical small species)}$$

$$\begin{aligned} V &= - \frac{2}{9} \frac{9.81 \cdot 0.82 \cdot (5 \times 10^{-6})^2}{1.07 \times 10^{-6}} \\ &= -41.8 \times 10^{-6} \text{ m/s} \end{aligned}$$

equivalent to 200m in 55 days

In practice, most organisms will disaggregate into individual placoliths and constituent rod-like grains during settling so it is more relevant to consider the sinking rates for these. For non-spherical particles a modification to Stokes Law is required (Graf, 1971) such that:

$$mg = k(-6\pi\eta a'u) \quad (A2.4)$$

a' : nominal radius ($= \sqrt[3]{a \times b \times c}$ where a, b & c are the orthogonal dimensions of the particle)

k : Stokes number (equivalent to a "shape factor")

equation A2.3 thus becomes: $v = \frac{2}{9} \cdot \frac{g \rho_{rel} M}{k \eta a'} \quad (A2.5)$

M = volume of grain

For settling rates with Re within the Stokes Range (<0.5), placoliths can be approximated as a disk, for which:

$$K = \frac{8}{3\pi} \text{ if sinking broadside-on}$$

or
$$K = \frac{16}{9\pi} \text{ if sinking edgewise-on}$$

Taking a calcite placolith of $1\mu\text{m}$ diameter and $.5\mu\text{m}$ thick ($a' = .794\mu\text{m}$, $M = .5\pi$), equation A2.5 yields sinking rates of:

$$V = 8.12 \times 10^{-6} \text{ m/s if sinking broadside-on}$$

or
$$V = 12.18 \times 10^{-6} \text{ m/s if sinking edgewise-on}$$

equivalent to 200 m in 285 days ($\sim 9\frac{1}{2}$ months) and 190 days (6.3 months) respectively.

For a single placolith element, the shape can be approximated by a circular rod. In this case, again assuming $Re < 0.5$ and that the rod falls prolate-wise (Happel and Brenner, 1965).

$$F = - \frac{4\pi\eta a u}{\ln(a/b) + (\ln 2 - \frac{1}{2})} \quad (A2.6)$$

Equation A2.3 now becomes:

$$V = - \frac{\rho_{rel} \cdot M \cdot g \cdot (\ln a/b - \ln 2^{-\frac{1}{2}})}{4\pi\eta a} \quad (A2.7)$$

For a calcite rod of length 1μ and 0.2μ radius ($M = .04 \times 10^{-18} m^3$) this gives:

$$V = 0.45 \times 10^{-6} \text{ m/s}$$

equivalent to 200 m in 5144 days (14.1 years)

In contrast, a sinking faecal pellet, behaving as a sphere of 100μ diam. (cf Schrader, 1971) has a sinking rate given by eqtn. A2.3:

$$V = -\frac{2}{9} \frac{g \rho_{rel}}{\eta} a^2$$

and in this case: $a = 50\mu = 50 \times 10^{-6} m$

$$\rho_{pellet} = 1.19 \text{ kg/m}^3 \quad \rho_{rel} = 0.16 \text{ kg/m}^3 \quad (\text{Dillon, 1964})$$

giving $V = 8.15 \times 10^{-4} \text{ m/s}$

or 200 m in 2.84 days.

(cf 100m/day reported by Smayda, 1969)

Effect of Rotation

The above calculations are based on a free falling non-rotating particle. In practice, however, the shape of the

sinking grains will result in a rotational moment also, resulting from the upward drag force acting on oblique surfaces. For rotating particles, the potential energy due to gravity is converted to rotational kinetic energy as well as the downward translational kinetic energy such that, for a sphere, the rotation couple T_c is given by (Happel and Bremner, 1965).

$$T_c = -8\pi\eta a^3\omega \quad (A2.8)$$

or for a circular disk (up to 10% thickness), falling edgewise on:

$$T_c = -\frac{32}{3}\eta c^3\omega \quad (A2.9)$$

where: c = radius of disk

ω = angular velocity

The downward acceleration due to gravity must thus balance both the translation drag (e.g. A2.1) and the rotational drag, equal but opposing the rotational couple T_c (e.q. A2.9). At terminal velocity the fundamental Stokes equations becomes:

$$\frac{4}{3}\rho_{rel}\pi a^3g = x(-6\pi\eta aV) + y(-8\pi\eta a^3\omega) \quad (\text{for a sphere})$$

$$\text{and } \frac{4}{3}\rho_{rel}\pi Mg = x(-\frac{32}{3}\eta a'V) + y(-\frac{32}{3}\eta c^3\omega) \quad (\text{for a disk})$$

The coefficients x and y will depend on the specific hydrodynamic characteristics of the particle but in all cases an increase in ω will result in a decrease of the settling

velocity V . The above calculations therefore represent minimum sinking rates.

APPENDIX 3 - METHODS USED IN TRACE ELEMENT
DETERMINATIONS

A3.1 MINOR AND TRACE ELEMENTS

Chalk and flint samples were ground in a porcellain pestle and mortar or an agate disk mill respectively and the powders kept over silica gel in a dessicator before analysis. All chemical analyses were performed by wet chemical means after either fusion with lithium metaborate and dissolution in 5% v v^{-1} HNO_3 (for Si), or attack with hydrofluoric and perchloric/nitric acids (all other elements). In both cases the methods were essentially those of Walsh (1980). Where possible the solutions were analysed within 2 weeks of preparation to avoid the possibility of introducing contamination from the walls of the storage bottle, although tests showed that storage for up to 18 months still did not introduce substantial contamination.

With the exception of K, all trace element determinations on the solutions were carried out on a Phillips PV8210 Inductively Coupled Plasma Source (ICP) Spectrometer linked directly to a Phillips 852 computer. Potassium, initially, was determined by Atomic Absorption to improve analytical precision, although following re-calibration of the K emission line on the ICP (766.49 nm), this was found to be unnecessary. Subsequent K determinations were carried out simultaneously with the other elements.

Initial conversion of emission intensity to ppm concentrations was carried out on the ICP's control computer, and calibrated against artificial standard solutions mixed to represent the full range of natural abundances in flints and chalks. Correction for background, instrument "drift" and interelement interference (mostly spectral

overlap from the intense Ca emission lines) were carried out subsequently on a HP9845 computer, assuming that variations with time between "blank" and standard solutions run every 4-6 minutes (every fifth and sixth sample) were linear.

Analytical precision, based on multiple analyses of standard flint and chalk samples are given in table A3.1. The errors involved are, in most part, the result of instrumental rather than preparation problems (as demonstrated by multiple determinations of a number of separate preparations of single samples) but are encouraging considering the extremely low natural abundance of most of the elements determined. However, when the sample size drops appreciably below 0.5gm (such as in the .1-.3 gm samples of Brandon flint: chapter 5) the analytical reproducibility drops off markedly (table A3.2). Zr and Ba in chinks occasionally gave unexpected peaks which were not reproducible in repeat preparations although were consistent in repeat ICP determinations on the same solution. This apparent error is attributed to rare detrital zircons or authigenic barytes crystals which were not broken down during the grinding process (cf insoluble residue studies of Weir and Catt, 1965).

It has not been possible to assess the accuracy of the methods due to the lack of internationally recognised standards of comparable elemental abundance, although comparison of K determined by AA and ICP was favourable and Walsh (1980) has demonstrated good agreement for all elements in silicate rock analyses. In addition, Two samples of flint analysed for Sr content by X-ray fluorescence (by R.D.Beckinsale, IGS) produced results comparable to ICP determinations on the same powders (31.8 vs 34 and 8.7 vs 9 for XRF and ICP determinations respectively for samples K01/1 and CL1/33).

Samples were stored in a dessicator/prior to analysis to remove adsorbed atmospheric water vapour which could lead to errors in weighing. This was considered preferable to drying at a higher

	CHALK			FLINT			
	\bar{x}	2SE	n	\bar{x}	2SE	n	
SiO ₂	1.00%	1.40	8	-	-	-	
Mg	2207	2.78	10	338	4.62	10	
Na	310	2.04	"	1826	1.82	"	
Sr	580	0.66	"	21.2	0.98	"	
Mn	328	0.82	"	21.3	7.36	"	
Fe	5753	0.50	"	802	3.74	"	
P	481	1.42	"	191	3.84	"	
Ca	-	-	-	8250	1.56	"	
Al	11480	0.86	"	646	0.32	"	
K	423	2.64	9	261	3.92	"	Sample BDN
Ba	38.6	5.16	5	17.0	7.72	"	
Co	4.88	3.28	10	2.54	4.51	"	
Cr	18.6	4.50	"	147	2.34	"	
Cu	4.18	1.86	"	5.70	1.37	"	
Li	9.17	4.58	"	4.90	3.79	7	Intensity data only
Ni	20.6	3.40	"	743	1.73	"	Intensity data only
Ti	613	1.34	"	29.6	1.13	10	
V	17.3	1.56	"	2.0	5.57	"	
Zn	29.2	7.18	"	15.1	12.53	"	
	-	-	-	(14.1	3.09	9)	Recalculated
Zr	11.9	2.50	5	2.20	1.87	7	Intensity data only

Table A3.1 Analytical precision for trace element determinations on flint and

chalk laboratory standards. Ba and Zr in chalk and Li, Ni and Zr in flint based on raw intensity data rather than calibration lines. 2xStandard Error in %. Concentrations in ppm unless stated. "Chalk" is a natural chalk spiked with clay to raise element concentrations to a useful level: precision on real samples will be a little worse.

temperature where part of the structure-bound water in the silica may have been lost in a non-reproducible manner (see chapter 4). Tests showed that most of the loosely bound water vapour on flint powders is lost in the first 30 minutes in the dessicator.

Errors of ~1% may arise due to disturbance of the dessicated samples (eg opening the dessicator to remove another sample bottle).

A3.2 CARBONATE AND SILICA DETERMINATIONS

Determination of SiO_2 in flints and CaCO_3 in chalks was not carried out by direct means because of the problems in attaining sufficient accuracy in samples which are up to 99.8% pure. Where these figures were required for calculations, they were determined by difference, assuming that organic carbon contents were zero and that the analysed elements (+ structure-bound water in the case of flints) account for the remainder.

A3.3 HYDROCHLORIC AND ACETIC ACID LEACHING STUDIES

Methods to determine the trace element content of the pure carbonate fraction separate from the total by using dilute acid leaching proved unsuccessful. Even using 5% acid, significant Al could be detected in solution (corresponding to up to 200ppm in the original sediment) suggesting substantial leaching of clay minerals. Attempts to allow for this by using the Al content as an "index of leaching" and extrapolating back were severely hindered by the analytical precision of the ICP at such low concentrations.

A3.4 RARE EARTH ELEMENT DETERMINATIONS

REE concentrations in flints and chalks are exceedingly low

	Range	2xSE %
Mg	15-1820	4.12
Na	150-930	2.52
Sr	3-40	6.62
Mn	.5-53	9.50
Fe	110-1465	5.64
P	85-800	2.36
Ca	115-4600	2.38
Al	280-1825	3.26
K	290-755	1.64
Ti	32-149	2.10
V	1-8	19.4 (n=22)

Table A3.2 Standard error based on pooled standard deviation of pairs of determinations. n=26 unless stated. Flint BDN; details in chapter 5.

	a		b		c	
La	4.9	.1195	5.0	.1220	5.0	.1220
Ce	3.2	.0386	3.1	.0373	3.2	.0386
Pr	.64	.0634	.63	.0624	.63	.0624
Nd	3.1	.0816	3.1	.0816	3.2	.0843
Sm	.63	.0840	.62	.0827	.63	.0840
Eu	.13	.0807	.13	.0807	.13	.0807
Dy	.52	.0945	.53	.0964	.53	.0964
Ho	.10	.0746	.10	.0746	.11	.0821
Er	.29	.0822	.29	.0822	.29	.0822
Yb	.24	.0680	.26	.0737	.24	.0680
Lu	.03	.0492	.04	.0656	.04	.0656
Y	5.1	-	5.2	-	5.2	-

Table A3.3 REE and Y concentrations from 3 separate preparations of sample CL1/9. Column 1 is ppm in rock, column 2 is normalised to average shale (Haskin & Haskin, 1966).

although it proved possible to determine these after concentrating them by cation exchange chromatography (Strelow and Jackson, 1974).

The methods used were essentially those described by Walsh et al. (1981), although great additional effort was needed to eliminate the effects of spectral overlap, particularly for Ca. This appears to be non-linear at low levels of Ca and REE concentration. Replicate determinations on sample CLL/9, however, gave excellent results (table A3.3).

APPENDIX 4 - DETERMINATION OF STABLE ISOTOPE RATIOS

A4.1 CARBONATES: $\delta^{13}\text{C}$ & $\delta^{18}\text{O}$

Carbon dioxide for carbon and oxygen isotope ratio determination was prepared from finely ground chalk samples by reaction with 100% phosphoric acid using a method similar to that described by McCrea (1950). The resulting CO_2 was analysed isotopically on a VG Micromass-903 mass spectrometer, and the raw data corrected for instrumental and isotopic overlap effects according to Deines (1970) and Craig (1957).

Results are reported in the usual δ -notation relative to the PDB standard where:

$$\delta = \left[\frac{R_{\text{sample}}}{R_{\text{standard}}} - 1 \right] \times 1000 \text{ ‰}$$

$$R = \frac{^{13}\text{C}}{^{12}\text{C}} \quad \text{or} \quad \frac{^{18}\text{O}}{^{16}\text{O}}$$

In all samples it was assumed that the organic carbon content of the sample was too low to seriously affect the isotopic composition of the CO_2 released during acid digestion.

Samples were analysed in batches of 8 (or sometimes 16), which included, in all cases, 1-3 standard samples. In general, with care, it was possible to obtain a reproducibility between replicates within each batch of .02‰ for $\delta^{13}\text{C}$ and .03‰ for $\delta^{18}\text{O}$. However, it was found that in some cases successive batches gave results which were offset with respect to each other by up to .1‰. The reasons for this are unclear, but possibly reflect small variations in instrument analytical conditions. This was particularly apparent during analysis of the paramoudra samples (chapter 6) where 2 successive batches of samples E-H produced a similar, but offset, trend (tab.A4.1), which was discontinuous with a similar trend in

	A	B	C	D	E	F	G	H	CA/4
Batch 1 $\delta^{13}C$ $\delta^{18}O$					1.59 -1.20	1.61 -1.15	1.71 -1.06	1.56 -0.99	1.43 -1.65
Batch 2 $\delta^{13}C$ $\delta^{18}O$	1.63 -1.20	1.64 -1.19	1.66 -1.19	1.66 -1.12					
Batch 3 $\delta^{13}C$ $\delta^{18}O$					1.64 -1.13	1.68 -1.15	1.68 -1.11	1.67 -1.07	1.46 -1.64
Batch 4 $\delta^{13}C$ $\delta^{18}O$		1.64 -1.26						1.74 -1.01	1.54 -1.54
Corrected $\delta^{13}C$ results $\delta^{18}O$	1.63 -1.27	1.64 -1.26	1.66 -1.18	1.66 -1.19	1.74 -1.12	1.77 -1.11	1.82 -1.04	1.74 -1.01	Estmd. Msd. 1.57 1.54 -1.60 -1.54

Table A4.1 Spread of results for successive batches of stable isotope determinations on samples from the Caister paramoudra (chapter 6). Corrected results are normalised to batch 4 results. Samples E-H are based on mean of batches 1 and 3. Full details in text.

samples A-D. To overcome this problem, the data were arbitrarily normalised to a single batch of results which included samples B, H and CA/4 (table A4.1). Comparison of the calculated with the measured values for sample CA/4 give an idea of the probable error involved in the absolute value of the samples (.06%).

A4.2 SULPHIDES: $\delta^{34}\text{S}$

Sulphur dioxide for $^{34}\text{S}/^{32}\text{S}$ ratio determination was prepared quantitatively from powdered pyrite samples by oxidation with cuprous oxide at 1070°C (Robinson and Kusakabe, 1975). The resulting CO₂ and SO₂ were separated by fractional sublimation, and the SO₂ analysed on a VG Micromass 602C mass spectrometer. Results are given in the usual δ -notation relative to troilite from the Cañon Diablo Meteorite. Analytical reproducibility was within $\pm 0.2\%$.

A4.3 SILICATES: $\delta^{18}\text{O}$ & δD

Isotopic analyses of oxygen and hydrogen in the flint samples proved rather more problematic than analyses of the chalks and pyrites due to the labile nature of part of the structure-bound water (chapter 4). Two separate methods were used for the oxygen and hydrogen determinations.

A4.3.1 Bromine pentafluoride Extraction: $\delta^{18}\text{O}$

The basis of this method has been described by Clayton and Mayeda (1963), although a number of variations were employed for this study.

The finely ground decarbonated silica sample is reacted with BrF₅ at 550°C overnight in a nickel reaction vessel, and the O₂

released from the silica is converted to CO_2 for isotope ratio determination by passing it over hot platinised graphite rods. Tests showed that the decarbonating procedure has no effect on $\delta^{18}\text{O}$ of the silica. CO_2 samples were then analysed isotopically along with the CO_2 from carbonates (see above).

In general, the O_2 is released from three distinct sources during fluorination: the silica lattice of the quartz; from $-\text{OH}$ and H_2O groups adsorbed on the silica surface or along lattice defects; or from atmospheric water adsorbed on the nickel fluoride coatings inside the reaction vessel. Obviously it is important to eliminate contamination from this latter source, but it is desirable also to be able to analyse the structure-bound hydroxyl groups associated with the silica. Reaction conditions must therefore be a compromise between removing atmospheric water contamination and leaving indigenous water.

For the initial analyses, the sample and reaction tube were outgassed overnight at 200°C to try to remove atmospheric contamination, and the remaining sample + bound water were fluorinated together to give $\delta^{18}\text{O}$ of the total flint. Analytical precision by this method was not very good (.72, .09 and .12% difference between three separate pairs of samples) and indicates considerable contamination during the run.

Subsequent samples (eg BDN) were "prefluorinated" at room temperature for 2 hours prior to normal reaction to remove the contaminating water. This improved reproducibility considerably (see table A4.2) although it removed the structural water from the flint and to some extent may also have attacked the highly disordered surface layer on the silica grains. Attempts to collect the O_2 from the prefluorination in order to determine the $\delta^{18}\text{O}$ of the hydroxyl groups produced a scatter of results too great for reliable

	<i>range</i>	<i>mean</i>	$ \bar{x}-x $
1	32.89 32.82 32.85	32.85	.04
2	32.57 32.51	32.54	.03
3	32.43 32.41 32.56	32.47	.06
4	32.39 32.38	32.38	.01
5	32.28 32.46	32.37	.09
6	32.64 32.55	32.60	.05
7	32.64 32.64	32.64	.00
8	32.97 33.03	33.00	.03
9	32.18 32.38	32.28	.10
10	32.42 32.59 32.70	32.55	.15
11	32.31 32.39	32.35	.04
			<hr/>
<i>mean deviation</i>			.046%
<i>2x pooled std. dev.</i>			.021%

Table A4.2 Analytical reproducibility for BrF₅ extractions on samples of Brandon flint. All samples pre-fluorinated before reaction. See text for details.

interpretation.

A4.3.2 δD concentration in flints

δD determinations on the flints were less problematic than for $\delta^{18}O$ because it was easier to eliminate contamination. Ground samples were loaded into molybdenum crucibles and outgassed under vacuum at room temperature. This is sufficient to remove the loosely bound "atmospheric" water from the flint structure, but would leave the structure-bound hydroxyl groups (chapter 4). The 1st layer of physically adsorbed water is probably left behind also as this is very strongly bonded onto the chemisorbed hydroxyl layer.

The sample is then heated at 1200-1400°C in an induction furnace and the resulting gasses passed over CuO at 400°C to oxidise any free H₂ to H₂O. Above 1400°C there is a tendency for the water to break down to free molecular hydrogen and oxidise the molybdenum crucible. The water is collected and separated from CO₂ and other contaminants cryoscopically and the converted to hydrogen gas by reaction with Zn granules at 450°C according to the method of Coleman et al. (1982)

The resulting hydrogen gas was analysed on a VG Micromass 602C mass spectrometer and the usual corrections applied. Results are reported relative to the SMOW standard. It was not possible to determine the analytical precision of the method on the samples analysed because there was insufficient sample available but repeats of a separate flint sample (SH2/9) gave -87.3 and -87.4‰ respectively, and the standard deviation of 14 determinations of the laboratory standard GP-1 (a gypsum) was 0.65‰.

REFERENCES

- Aller, R.C. (1982). Carbonate dissolution in nearshore terrigenous muds: the role of physical and biological reworking. Jour. Geol., 90, 79-95
- Alexander, G.B., Heston, W.M., & Iler, R.K. (1954). The solubility of amorphous silica in water. J. Phys. Chem., 48, 453-55
- Alloway Pankhurst, E. (c.1895). The flints of the Chalk. Unreferenced manuscript of authors.
- Arkell, W.J. (1933). The Jurassic System of Great Britain. Oxford: Clarendon Press
- Aubry, M.-P. (1975). Recherches sur la nannopetrographie de roche siliceuses. Bull. Soc. Geol. Normandie. LXII pt. 2e 7-34
- Radiozamani, K. (1973). The Dorag dolomitisation model - application to the Middle Ordovician of Wisconsin. J. Sediment. Petrology. 43, 965-84
- Bakewell, R. (1839). An Introduction to Geology. 3rd edn. New Haven: Howe
- Balistreiri, L.S., & Murray, J.W. (1982). The adsorption of Cu, Pb, Zn, & Cd on goethite from major ion seawater. Geochim. Cosmochim. Acta 46, 1253-65
- Balzer, W. (1982). On the distribution of iron and manganese at the sediment/water interface: thermodynamic verses kinetic control. Geochim. Cosmochim. Acta, 46, 1153-61
- Bannister, F.A. (1932). The distinction of pyrite from marcasite in nodular form. Mineralog. Mag. 23, 179-87
- Barrett, T.J. (1981). Chemistry and mineralogy of Jurassic bedded chert overlying ophiolites in the North Appennines, Italy. Chemical Geology, 34, 289-317
- Benmore, R.A., Coleman, M.L. & McArthur, J.M. (1983). Origin of sedimentary francolite from it's sulphur and carbon isotopic composition. Nature, 302, 516-8

- Berner, R.A. (1970). Sedimentary pyrite formation.
Amer. Jour. Science. 268 pt1, 13-23
- _____ (1971). Principles of Chemical Sedimentology
McGraw-Hill, 240p
- _____ (1980). Early Diagenesis - a Theoretical Approach
Princeton: Princeton University Press. 237p
- _____ (1981). A new geological classification of sedimentary environments. J. Sediment. Petrology, 51, 359-365
- Bishop, J.K., Edmond, J.M., Ketton, D.R., Bacon, M.P. & Silker, W.B.
(1977). The chemistry, biology and vertical flux of particulate matter from the upper 400m of the equatorial Atlantic Ocean. Deep Sea Research, 24, 511-548
- Blankenberg, H.-J. & Rösler, H.J. (1979). Beitrag Zur Kenntnis über die Eigenschaften und die Genese von Flint.
Z. angew. Geol. 25, 333-337
- Bonnet-Courtois, C. (1981). Distribution des terres rare dans le depot hydrothermaux de la zone FAMOUS et des Galapagos - comparaison avec les sediments metalliferes.
Marine Geology, 39, 1-14
- Bramlette, M.N. (1946). The Monterey Formation of California and the origin of it's siliceous rocks. US Geol. Surv. Prof. Paper 212, 57p
- Bremner, J.M. (1980). Concretionary phosphorite from SW Africa.
J. geol Soc London, 137, 773-86
- Bromley, R.G. (1965). Studies in the lithology and conditions of sedimentation of the Chalk Rock and comparable horizons. Unpubl. PhD thesis, University of London
- _____ (1967). Some observations on the burrows of thalassinidean crustacea in chalk hardgrounds.
Quar. Jour. Geol. Soc.Lond. 123, 157-82
- _____ (1968). Burrows and borings in hardgrounds.
Meddr. dansk. Geol. Foren. 18, 248-50

- _____ (1970). Borings as trace fossils and Entobia cretacea Portlock, as an example. In Trace Fossils, ed. Crimes and Harper, Geol.J.Spec. Issue 3, 49-90
- _____ (1975). Trace fossils at omission surfaces. In The Study of Trace Fossils, ed. R.W. Frey, pp399-428 New York: Springer Verlag.
- _____ (1978). Hardground diagenesis. In The Encyclopedia of Sedimentology. ed. R.W. Fairbridge and J. Bourgeois, pp397-400. Stroudsburg, Penn.: Dowden, Hutchinson & Ross.
- _____ & Gale, A.S. (1982). The lithostratigraphy of the English Chalk Rock. Cretaceous Research, 3, 273-306
- _____, Schulz, M.-G. & Peake, N.B. (1975). Paramoudras: giant flints, long burrows and the early diagenesis of chalks. K. Dansk. Vidensk. Selsk. Geol. Skr. 20, pt. 10
- Brydone, R.M. (1920). The origin of flint. Geol. Mag. 1920, 401-4
- Buurman, P. & Van der Plas, L. (1971). The genesis of Belgian and Dutch flints and cherts. Geol. en Mijnb., 50, 9-28
- Calvert, S.E. (1966). Accumulation of diatomaceous silica in the sediments of the Gulf of California. Bull. Geol. Soc. Am. 77, 569-96
- _____ (1968). Silica balance in the ocean and diagenesis. Nature, London. 219, 919-20
- _____ (1971a). Composition and origin of North Atlantic deep sea cherts. Contr. Mineral. Pet. 33, 273-80
- _____ (1971b). Nature of silica phases in deep sea cherts of the North Atlantic. Nature Phy. Sci. 234, 133-4
- _____ (1974). Deposition and diagenesis of silica in marine sediments. In Pelagic Sediments: On Land and Under The Sea, ed. K.J. Hsu and H.C. Jenkyns, pp 273-99, Spec. Publs. Int. Ass. Sediment. 1
- Cambell, A.S. & Fyfe, W.S. (1960). Hydroxyl ion catalysis of the hydrothermal crystallisation of amorphous silica; a possible high temperature pH indicator. Am. Mineral. 45(3-4), 464-8

- Carr, R.M. & Fyfe, W.S. (1958). Some observations on the crystallization of amorphous silica. Am. Mineralogist. 43, 903-16
- Carroll, D. (1958). The role of clay minerals in the transportation of iron. Geochim. Cosmochim. Acta, 14, 1-27
- Carrothers, W.W. & Kharaka, Y.K. (1980). Stable carbon isotopes of HCO_3^- in oil-field waters - implications for the origin of CO_2 . Geochim. Cosmochim. Acta. 44, 223-32
- Cartz, L. (1964). An X-ray diffraction study of the structure of silicate glass. Z. kristallogr. Miner. 120, 241-60
- Cary, L.W., de Jong, B.H.W.S. & Dibble, E.Jr. (1982). A ^{29}Si NMR study of silica species in dilute aqueous solution. Geochim. Cosmochim. Acta, 46, 1317-20
- Cayeux, L. (1891). La Craie du nord de la France et la boue à Globigérines. Annls. Soc. Geol. N. 19, 95-102
- _____ (1930). Patines des silex de la craie. Bull. Soc. Française de minéral., Livrè jubilaire, 1878-1928, p60-72.
- _____ (1931). Introduction à l'étude pétrographique des Roches Sédimentaires. Ministère des Travaux Publics, Mémoires pour servir à explication de la Carte Géologique Détaillée de la France.
- Chester, A.H. (1896). A Dictionary of the Names of Minerals.
Quoted without reference in Tarr, 1938.
- Claypool, G.E., Holser, W.T., Kaplan, I.R., Sakai, H. & Zak, I. (1980). The age curves of sulphur and oxygen isotopes in marine sulphate and their mutual interpretation. Chem. Geol. 28, 199-260
- Clayton, C.J. (1984). The Flints. In Pontnewydd Cave. A Lower Palaeolithic Hominid Site in Wales. The First Report. ed. H.S. Green. National Museum of Wales. Quaternary Studies Monograph, No 1.
- _____ & Bradley, R. (In Press). The influence of flint microstructure on the formation of microwear polishes. In Sieveking, G. de G., and Newcomer, M.H. The Human Uses of Flint and Chert, Camb. Univ. Press.

- Clayton, R.N. & Mayeda, T.K. (1963). The use of bromine pentafluoride in the extraction of oxygen from oxides and silicates for isotopic analysis. Geochim. Cosmochim. Acta, 27, 43-52
- _____, O'Neil, J.R. & Mayeda, T.K. (1972). Oxygen isotope exchange between quartz and water. J. Geophys. Res. 77, 3057
- Colbeaux, J.-P., Dupuis, C., Robaszynski, F., Auffret, J.-P, Haeraerts, P. & Somme, J. (1980). Le Déroit du Pas-de-Calais: un élément dans la tectonique de blocs de l'Europe Nord-occidentale. Bull. Inf. Géol. Bass., 17(4), 41-54
- Coleman, M.L., Curtis, C.D. & Irwin, H. (1979). Burial rate a key to source and resevoir potential. World Oil, March 1979
- _____, Fleet, A.S. & Donson, P. (1982). Preliminary studies of manganese-rich carbonate nodules from leg 68, site 503, eastern equatorial Pacific. Initial Reports of the Deep Sea Drilling Project, vol 68, 481-9
- _____ & Raisewell, R. (1981). Carbon, oxygen and sulphur isotope variations in concretions from the Upper Lias of N.E. England. Geochim. Cosmochim. Acta, 45, 329-40
- _____ (In Press). Source of carbonate and origin of zonation in pyritiferous carbonate concretions. Am. Jour. Science
- _____, Shepherd, T.J., Durham, J.J., Rouse, J.E. & Moore, G.R. (1982). Reduction of water with zinc for hydrogen isotope analysis. Anal. Chem.
- Craig, H. (1957). Isotopic standards for carbon and oxygen correction factors for mass-spectrometric analysis of carbon dioxide. Geochim. Cosmochim. Acta, 12, 133-49
- _____ (1965). The measurement of oxygen isotope palaeotemperatures. In Stable Isotopes in Oceanographic Studies and Palaeotemperatures. ed. E.Tongiorgi, v.3, 1-16

- Crerar, D.A., Axtmann, E.V. & Axtmann, R.C. (1981). Growth and ripening of silica polymers in aqueous solutions. Geochim. Cosmochim. Acta, 45, 1266-81
- Cronan, D.S. & Moorby, S.A. (1981). Manganese nodules and other ferromanganese oxide deposits from the Indian Ocean. J. Geol. Soc. Lond. 138, 527,39
- Curtis, C.D. (1977). Sedimentary geochemistry: environments and processes dominated by involvement of an aqueous phase. Phil. Trans. Roy. Soc. A, 286, 353-71
- Davies, T.A. & Supko, P.R. (1973). Oceanic sediments and their diagenesis: some examples from deep sea drilling. Jour. Sed. Petrology, 43, 381-90
- Dean, R.S. (1918). The formation of Missouri cherts. Am. Journ. Sci. Ser. IV., 45(269), 411-415
- De Boer, P.L. (1983). Aspects of Middle Cretaceous Pelagic Sedimentation in Southern Europe. Production and Storage of Organic Carbon, Stable Isotopes, and Astronomical Influences. Geologica Ultraiectina, 31. Rijksuniversiteit te Utrecht.
- Deflandre, G. (1934). Sur les microfossiles d'origine planctonique conservés à l'état de matière organique dans les silex de la craie. Compt. Rend. Acad. Sci. Paris, 199, 966-8
- Degens, E.T. & Epstein, S. (1962). Relationship between $^{18}\text{O}/^{16}\text{O}$ ratios in coexisting carbonates, cherts and diatomites. Bull. Am. Assoc. Pet. Geol., 46, 534-42
- Deines, P. (1970). Mass spectrometric correction factors for the determination of small isotopic variations of carbon and oxygen. Int. J. Mass Spectrom. Ion Phys. 4, 283-95
- Devol, A.H. & Ahmed, S.I. (1981). Are high rates of sulphate reduction associated with anaerobic oxidation of methane? Nature, 241, 407-8
- Dillon, W.P. (1974). Flotation technique for separating fecal pellets and small marine organisms from sand. Limnol. Oceanog. 9, 602-1

- Dodd, D.M. & Fraser, D.B. (1967). Infrared studies of the variation of H-bonded OH in synthetic α -quartz. Amer. Mineral. 52, 149-60
- Elderfield, H., Hawkesworth, C.J., Greaves, M.J. & Calvert, S.E. (1981). Rare earth element geochemistry of oceanic ferromanganese nodules and associated sediments. Geochim. Cosmochim. Acta, 45, 513-28
- Emerson, S. & Bender, M. (1981). Carbon fluxes at the sediment-water interface of the deep-sea: calcium carbonate preservation. J. Mar. Res. 39, 139-62
- _____, Janhke, R., Bender, M., Froelich, P., Klinkhammer, G., Bowser, C. & Setlock, G. (1980). Early diagenesis in sediments from the eastern equatorial Pacific, 1. pore water nutrient and carbonate results. Earth Planet. Sci. Letters 49, 57-80
- _____, Kalhorn, S., Jacobs, L., Tebo, B.M., Nealson, K.H. & Rosson, R.A. (1982). Environmental oxidation rate of manganese (II): bacterial catalysis. Geochim. Cosmochim. Acta, 46, 1073-9
- Emmery, K.O. & Rittenberg, S.C. (1952). Early diagenesis of California Basin sediments in relation to the origin of oil. Bull. Am. Assoc. Pet. Geol. 36, 735-806
- Emrich, K., Enhalt, D.H. & Vogel, J.C. (1970). Carbon isotope fractionation during the precipitation of calcium carbonate. Earth Planet. Sci. Lett. 8, 363-71
- Eriksson, E. (1962). Ocean Mixing. Deep Sea Res., 9, 1-9
- Ernst, H. (1978). Zu bathymetrie und sedimentstrukturen der scribeikreide von Lägerdorf/Holstein (Coniac-Santon): eine quantitative analyse der foraminiferen faunen. Mitt. Geol. Päläont. Inst. Univ. Hamburg 48, 53-78
- Ernst, W.G. & Calvert, S.E. (1969). An experimental study of the recrystallisation of porcellanite and it's bearing on the origin of some bedded cherts. Am. J. Sci. (A), 267, 114-33

- Fairburn, P.E. & Robertson, R.H.S. (1972). The decomposition of flint. Scottish Jour. Sci. 1(3), 165-174
- Felder, P.J. (1981). Onderzoek van de meso-fossielen in de krijt-afzettingen van Limburg - een nieuwe mogelijkheid tot het correleren en dateren van de krijt-afzettingen. Natuurhist. Maandblad, 70 (4), 69-75
- Felder, W.M. (1975). Lithostratigrafische Gliederung der Oberen Kreide in Süd-Limburg und den nachbargebieten 1.teil: der raum westlich der Maas, typusgebiet des Maastricht. Public. Natuurhist. Genootschap Limburg, 24(3/4), 43
- _____ (1976). Sedimentatie-cyclothemmen in de kalkstenen uit het Boven-krijt van Zuid Limburg. Grondboor. en Hamer, 1
- Fisher, A.G. & Arthur, M.A. (1978). Secular variations in the pelagic realm. SEPM Spec. Publ. 25, 19-50
- Fleet, A.J. (In Press). Aqueous and sedimentary geochemistry of the rare earths. In Rare Earth Element Geochemistry, ed. P.Henderson. Elsevier.
- Fletcher, T.P. (1977). Lithostratigraphy of the Chalk (Ulster White Limestone Formation) in Northern Ireland. Rep. Inst. Geol. Sci. 77/24, 33p.
- Flörke, O.W. (1955). Structuronomalien bei Tridimyt und Cristalit. Ber. dt. Kerom. Ges. 10, 217-223
- _____, Hollmann, R. Von Rad, U. & Rosch, H. (1976). Intergrowth and twinning in opal-CT lepispheres. Contrib. Mineral. Petrol. 58, 235-42
- _____, Jones, J.B. & Segnit, E.R. (1975). Opal-CT crystals. Neues Jahrb. Mineralogie Monatsh. 8, 369-77
- Folk, R.L. & Pittman, J.S. (1971). Length slow chalcedony, a new testament for vanished evaporites. J. sediment. Petrology, 41, 1045-58.
- _____ & Weaver, C.E. (1952). A study of the texture and composition of chert. Am. J. Sci. 250, 498-510

- Frakes, L.A. & Kemp, E.M. (1973). Palaeogene continental positions and evolution of climate. In Implications of Continental Drift to the Earth Sciences, Ed. Tarling, D.H. & Runcorn, S.K. London: Academic Press. p539-559
- Francis, S., Barghoorn, E.S. & Margulis, L. (1978). On the experimental silicification of microorganisms, III: Implications for the preservation of the green prokaryotic alga Prochloron and other coccoids for the interpretation of the microbial fossil record. Precambrian Res. 7, 377-83
- _____, Margulis, L. & Barghoorn, E.S. (1978). On the experimental silicification of microorganisms, II: on the time of appearance of eukaryotic organisms in the fossil record. Precambrian Res. 6, 65-100
- Friedman, I. & O'Neil, J.R. (1977). Compilation of stable isotope fractionation factors of geological interest. In Data of Geochemistry, 6th edn. ed. M.Fleischer, Chap. KK, USGS Prof. Paper 440-KK
- Fröelich, F. (1974). Nature, importance relative et place dans la diagenèse des phases de silice présentes dans les silicifications des craie du bassin océanique de Madagascar (Océan Indien) et du Bassin de Paris. Bull. Soc. géol. France, 16, 498-508
- Fröelich, P.N., Klinkhammer, G.P., Bender, M.L., Luedtke, N.A., Heath, G.R., Cullen, D., Dauphin, P., Hammond, D., Hartman, B. & Maynard, V. (1979). Early diagenesis of organic matter in pelagic sediments of the eastern equatorial Atlantic: suboxic diagenesis. Geochim. Cosmochim. Acta, 43, 1075-90
- Gale, A.S. (1980). Penecontemporaneous folding, sedimentation and erosion in Campanian chalks near Portsmouth, England. Sedimentology, 27, 137-151
- _____, & Smith, A.B. (1982). The palaeobiology of the Cretaceous irregular echinoids Infulaster and Hagenowia. Palaeontology, 25, 11-42

- Galloway, W.B. (1886). The Chalk and Flint Formation. It's origin in harmony with a very ancient and a scientific modern theory of the world. London: Sampson, Low, Marston, Searle & Rivington. 53p
- Garrels, R.M. & Christ, C.L. (1965). Solutions, Minerals and Equilibria. New York: Harper, 450p
- Gibson, T.G. & Towe, K.M. (1971). Eocene volcanism and the origin of Horizon A. Science 169, 152-4
- _____ (1975). Origin of Horizon A: clarification of a viewpoint. Science, 188, 1221-2
- Goldhaber, M.B. & Kaplan, I.R. (1974). The sulfur cycle. In The Sea ed. E.D. Goldberg, New York: Wiley & Sons.
- Goldschmidt, V.M. (1954). Geochemistry. Oxford: Oxford Univ. Press
- Graf, W.H. (1971). Hydraulics of Sediment Transport. McGraw-Hill.
- Griffiths, D.R., Bergman, C.A., Clayton, C.J., Ohnaka, K., Robins, G.V. & Seeley, N.J. (In Press). Experimental investigation of the heat treatment of flint. In G. de G. Sieveking and M. H. Newcomer (eds.), The Human Uses of Flint and Chert. Cambridge University Press.
- Grundmanis, V. & Murray, J.W. (1982). Aerobic respiration in pelagic marine sediments. Geochim. Cosmochim. Acta, 46, 1101-20
- Håkansson, E., Bromley, R. & Perch-Nielsen, K. (1974). Maastrichtian chalk of north-west Europe - a pelagic shelf sediment. In Pelagic Sediments: On Land and Under the Sea, K.J. Hsu & H.C. Jenkyns, eds. Spec. Publs. Int Ass. Sediment. 1, 211-33
- Hancock, J.M. (1975). The petrology of the Chalk. Proc. Geol. Ass. 86 (4), 499-535
- _____ & Kauffman, E.G. (1979). The great transgressions of the late Cretaceous. Jour. Geol. Soc. Lond. 175-86
- _____ & Scholle, P.A. (1975). Chalk of the North Sea. In Petroleum and the Continental Shelf of North-west Europe, 1. Geology. ed. A.W. Woodland. Barking, Essex: Applied Science Publishers. 413-427

- Hanshaw, B.B., Back, W. & Deike, R.G. (1971). A geochemical hypothesis for dolomitisation by ground water. Econ. Geol. 66, 710-724
- Happel, J. & Bremner, H. (1965). Low Reynolds Number Hydrodynamics Englewood Cliffs, N.Y.: Prentice Hall
- Haskin, M.A. & Haskin, L.A. (1966). Rare earth in European shales: a redetermination. Science 154, 507-9
- Hattin, D.E. (1976). Stratigraphic study of Smokey Hill Chalk Member Niobrara Chalk (Cretaceous) in the type area. Geol. Soc. America Abs. with Programs, 8, 481
- Hauser, E.A. (1955). Silicic Science. New York: Van Nostrand
- Hawkins, H.J. (1942). Some episodes in the geological history of the south of England. Quart. Journ. Geol. Soc. Lond. 98, 49-70
- Heath, G.R. (1973). Cherts from the eastern Pacific, Leg 16 DSDP. In Initial Reports of the Deep Sea Drilling Project. 16, T.H. Van Andel and G.R. Heath, et al. 609-613
- _____ & Moberly, R. (1971). Cherts from the western Pacific, leg 7 DSDP. In Initial Reports of the Deep Sea Drilling Project. Winterer, E.L. and Riedel, W.R. et al., 991-1007
- Hedges, E.S. (1932). Liesegang Rings. London: Chapman & Hall Ltd.
- Hill, W. (1911). Flint and Chert. Proc. Geol. Assn. 22, 61-94
- Høgdahl, O.T. (1970). Distribution of the lanthanides in the waters and sediments on the River Gironde in France: a summary. Marine Radioactive Studies, IAEA Research Agreement Coordinated Program, Morocco, June 1970
- Holdaway, H.K. & Clayton, C.J. (1982). Preservation of shell microstructure in silicified brachiopods from the Upper Cretaceous Wilmington Sands of Devon. Geol. Mag. 119(4), 371-82
- Holmes, A. (1926). The nomenclature of petrology. In Principles of Petrology, 2nd ed. London: Murby

- Hudson, J.D. (1982). Pyrite in ammonite-bearing shales from the Jurassic of England and Germany. Sedimentology, 29, 639-68
- Humble, W. (1843). Dictionary of Geology and Mineralogy. 2nd ed. Referred to in Tarr, 1938.
- Hurd, D.C. (1973). Interactions of biogenic opal, sediment and seawater in the Central Equatorial Pacific. Geochim. Cosmochim. Acta, 37, 2257-82
- _____, Pankratz, H.S., Asper, V., Fugate, J. & Morrow, H. (1981). Changes in the physical and chemical properties of biogenic silica from the central equatorial Pacific: part III, specific pore volume, mean pore size, and skeletal ultrastructure of acid cleaned samples. Amer. Jour. Sci. 281, 833-95
- _____ & Theyer, F. (1975). Changes in the physical and chemical properties of biogenic silica from the central equatorial Pacific: part I, solubility, specific surface area and solution rate constants of acid-cleaned samples. In Analytical Methods in Chemical Oceanography, ed. T.T.R.P. Gibb Jr., Am. Chem. Soc., Advances in Chemistry Series no 147, 211-230
- _____, Wenkam, C., Pankratz, H.S. & Fugate, J. (1979). Variable porosity in siliceous skeletons: determination and importance. Science, 203, 1340-1343
- Iler, R.K. (1979). The Chemistry of Silica. Solubility, Polymerisation, Colloid and Surface Properties, and Biochemistry. Wiley Interscience, 801p
- Illies, H. (1949). Zur diagenese der südbaltischen schreibkreide. Geol. Fören. Förrhandl 71, H1, 41-50
- Irwin, H., Curtis, C.D. & Coleman, M.L. (1977). Isotopic evidence for the source of diagenetic carbonates formed during the burial of organic-rich sediments. Nature 269, 209-13

- Isaacs, C.M. (1982). Influence of rock composition on kinematics of silica phase changes in the Monterey Formation, Santa Barbara area, California. Geology, 10, 304-8
- Jarvis, I. (1980). The initiation of phosphatic chalk sedimentation - the Senonian (Cretaceous) of the Anglo-Paris Basin. SEPM Special Publication No.29, 167-192
- _____ (In press). Rare earth element geochemistry of late Cretaceous chalks and phosphorites from northern France. Proc. Int. Seminar & Field Workshop on Phosphorite. (IGCP 156), Udaipur, India, 1981
- _____, Bromley, R.G. & Clayton, C.J. (1982). Sedimentology of the Suzanne Hardground, northern France: colonisation and diagenesis of an early Campanian (Upper Cretaceous) seafloor. I.A.S 3RD EUR. MTG., Copenhagen, 1982. Abstr.
- _____, Gale, A.S. & Clayton, C.J. (1982). Litho- and bio-stratigraphic observations on the type sections of the Craie de Villedieu Formation (Upper Cretaceous, western France). Newsl. Stratigr. 11(2), 64-82
- Jears, C.V. (1968). The origin of the montmorillonite of the European Chalk with special reference to the Lower Chalk of England. Clay. Min. 7, 311-29
- _____ (1973). The Market Weighton structure: tectonics, sedimentation and diagenesis during the Cretaceous. Proc. Yorks. Geol. Soc. 39, 409-444
- _____ (1978). Silicifications and associated clay assemblages in the Cretaceous marine sediments of southern England. Clay Minerals, 13(1), 101-126
- _____ (1980). Early submarine lithification in the Red Chalk and Lower Chalk of eastern England: a bacterial control model and its implications. Proc. Yorks. Geol. Soc. 43(2), 81-157
- _____, Merrimen, R.J., Mitchell, J.G. & Bland, D.J. (1982). Volcanic clays in the Cretaceous of southern England and Northern Ireland. Clay Minerals, 17, 105-56

- Jenkyns, H.C. (1974). Origin of red nodular limestones (Ammonitico Rosso, Knollenkalke) in the Mediterranean Jurassic: a diagenetic model. In Pelagic Sediments: On Land and Under the Sea, ed. K.J.Hsu & H.C.Jenkyns..Spec.Publ. Int Ass. Sediment. 1, 249-71
- _____ (1980). Cretaceous anoxic events: from continents to oceans. J. Geol. Soc. Lond. 137, 171-88
- Jensen, A.T., Wøhlk, C.J., Drenck, K. & Anderson, E.K. (1957). A classification of Danish flints etc. based on X-ray diffractometry. Com. Alkali Reactions in Concrete, Progress Report D1, Copenhagen. 37p
- Jones, J.B., Sanders, J.V. & Segnit, E.R. (1964). Structure of opal. Nature, 204, 990-1
- _____ & Segnit, E.R. (1971). The nature of opal, I. Nomenclature and constituent phases. J. Geol. Soc. Aust., 18, 57-68
- _____ (1972). Genesis of cristobalite and tridymite at low temperatures. J. Geol. Soc. Aust. 18, 419-22
- Jones, M.E. (1978). Structure bound water in natural & synthetic quartz, it's potential importance in natural rock deformation. Unpubl. PhD Thesis, Univ. of London.
- _____, Bedford, J. & Clayton, C.J. (In press). On natural deformation mechanisms in the Chalk. J.Geol. Soc. Lond.
- Jukes-Brown, A.J. (1893a). The relative age of flints. Geol.Mag. Dec. 3rd, vol. 10, 315-317
- _____ (1893b). The amount of disseminated silica in the Chalk, considered in relation to flints. Geol. Mag. Dec. 3rd, vol 10, 541-6
- _____ & Hill, W. (1889). The occurrence of colloid silica in Lower Chalk of Berkshire and Wiltshire. Quart. Jour. Geol. Soc. Lond. 45, 403-21
- Julien, A.A. (1880). Quoted in Sollas, W.J. (1880).

- Kaibara, H. (1964). A study of the micro-texture of cherts. Univ. Kyoto, Memoirs of the College of Science, Ser.B, 30(4), 59-73
- Kamatani, A. (1971). Physical and chemical characteristics of biogenous silica. Mar. Biol. 8, 89-95
- Kastner, M. (1982). Authigenic silica in deep-sea sediments: formation and diagenesis. In The Sea, ed. C. Emiliani, New York: Wiley-Interscience.
- _____ (1977). Diagenesis of siliceous oozes I. Chemical controls on the rate of opal-A to opal-CT transformation-an experimental study. Geochim. Cosmochim. Acta, 41, 1041-59
- Kauffman, E.G. (1977). Geological and biological overview: Western Interior Cretaceous Basin. Mountain Geologist, 14, 75-99
- Keat, D.D. (1954). A new crystalline silica. Science, 120, 328
- Keene, J.B. (1976). Petrography of biogenic and authigenic silica from the Pacific Basin. Unpubl. PhD thesis, Scripps Inst. Oceanography, University of California, San Diego.
- Kemp, J.F. (1896). A Handbook of Rocks for Use Without the Microscope. New York: J.F. Kemp. 176p
- Kennedy, W.J. (1970). A correlation of the uppermost Albian and the Cenomanian of south-west England. Proc. Geol. Assn. 81, 613-77
- _____ & Garrison, R.E. (1975). Morphology and genesis of nodular chalks and hardgrounds in the Upper Cretaceous of S. England. Sedimentology 22, 311-86
- _____ & Juignet, P. (1974). Carbonate banks and slumps in the Upper Cretaceous (Upper Turonian-Santonian) of Haute Normandie, France. Sedimentology, 21, 1-42
- Kirwan, R. (1796). Elements of Mineralogy. 2nd Ed. London: P.Elmsly
- Kitano, Y., Okumura, M. & Idogaki, M. (1979). Behaviour of dissolved silica in parent solution at the formation of calcium carbonate. Geochem. Jour. 13, 253-60

- Knauer, G.A., Martin, J.H. & Bruland, K.W. (1979). Fluxes of particulate carbon, nitrogen and phosphorus in the upper water column of the north-east Pacific. Deep-sea Res. 26A, 97-108
- Knauth, L.P. (1973). Oxygen and hydrogen isotope ratios in cherts and related rocks. Unpubl. PhD thesis, Calif. Inst. Tech.
- _____ (1979). A model for the origin of chert in limestone. Geology, 7(6), 274-7
- _____ & Epstein, S. (1975). Hydrogen and oxygen isotope ratios in silica from the JOIDES DSDP. Earth Planet. Sci. Letters, 25, 1-10
- _____ (1976). Hydrogen and oxygen isotope ratios in nodular and bedded cherts. Geochim. Cosmochim. Acta, 40, 1095-1108
- _____ & Lowe, D.R. (1978). Oxygen isotope geochemistry of cherts from the Onverwacht group (3.4By), Transvaal, South Africa, with implications on the isotopic composition of cherts. Earth Planet. Sci. Letters, 41, 209-22
- Kolodny, Y. (1978). Participation of fresh water in chert diagenesis; evidence from oxygen isotopes and boron δ -track mapping. Sht. Pprs. 4th Int. Conf. Geochron, Cosmochron and Isotope Geology. USGS Open File Rep. 78-701, p228-9
- _____ & Epstein, S. (1976). Stable isotope geochemistry of deep sea cherts. Geochim. Cosmochim. Acta, 40, 1195-1209
- _____, Taraboulos, A. & Frieslander, U. (1980). Participation of fresh water in chert diagenesis: evidence from oxygen isotopes and boron δ -track mapping. Sedimentology, 27, 305-316
- Krauskopf, K.B. (1959). The geochemistry of silica in sedimentary environments. In Silica in Sediments, ed. H.A. Ireland, SEPM Spec. Pub. 7, 4-9

- Krauskoph, K.B. (1967). Introduction to Geochemistry, McGraw-Hill
- Krom, M.D. & Berner, R.A. (1981). The diagenesis of phosphorus in a nearshore marine sediment. Geochim. Cosmochim. Acta, 45, 207-16
- Lancelot, Y. (1973). Chert and silica diagenesis in sediments from the central Pacific. In Initial Reports of the Deep Sea Drilling Project, vol 57, E.L.Winterer & J.I.Ewing et al., 377-405
- Land, L.S. (1973). Contemporaneous dolomitisation of Middle Pleistocene reefs by meteoric water, North Jamaica. Bull. Marine Science, 231, 64-91
- Lebeyrie, L.D. & Juillet, A. (1982). Oxygen isotope exchangeability of diatom valve silica, interpretation and consequences for palaeoclimatic studies. Geochim. Cosmochim. Acta, 46, 967-975
- Leclaire, L. (1974). Hypothèses sur l'origine des silicifications dans les grands bassins océaniques. Le rôle des climats hydrolisants. Bull. Soc. Geol. Fr. 16(7), 214-24
- _____, Alcaydé, G. & Froelich, F. (1973). La silicification des craies: rôle des sphérules de cristobalite-tridymite observées dans les craies des bassins océaniques et dans celles du Bassin de Paris. C.R. Ac. Sc. Paris, 277D, 2121-23
- Leinen, M. (1979). Biogenic silica accumulation in the central equatorial Pacific and its implications for Cenozoic paleoceanography. Geol. Soc. Am. Bull. 90, 1310-76
- Levitan, M.A., Contsova, E.I., Lisitzin, A.P. & Bogdanov, Y.A. (1975). The origin of chert in sediments of the Pacific Ocean from data of oxygen isotopic analysis and a study of the distribution of chert. Geochem. Internat. 12, 95-104
- Liesegang, R. (1913). Geologische Diffusionen. Dresden and Leipzig.
- _____. (1914). Pseudoclase. Jahrb. Min. Geol. Pal. 39, 268

- Lisitzin, A.P. (1971). Distribution of siliceous microfossils in suspension and in bottom sediments. In The Micro-palaeontology of Oceans, Ed. B.M.Funnell & W.R.Riedel, Camb. Univ. Press, 173-195
- Lovering, T.G. & Patten, L.E. (1962). The effect of CO₂ at low temperature and pressure on solutions supersaturated with silica in the presence of limestone and dolomite. Geochim. Cosmochim. Acta, 26, 787-96
- Lowenstam, H.A. (1971). Opal precipitation by marine gastropods (mollusca). Science, 171, 487-490
- Lyell, C. (1830). Principles of Geology, Vol. 3.
- Mallard, E. (1890). Sur la lussatite, nouvelle variete minerale cristallisee de silice. Soc. Fr. Mineral. Bull. 13, 63-66
- Mantell, G.A. (1845). Notes of a microscopical examination of the Chalk and flint of the south-east of England with remarks on the animalculites of certain Tertiary and modern deposits. Ann. and Mag. Nat. Hist. 16, 73
- Marshall, W.L. & Warakowski, J.M. (1980). Amorphous silica solubilities-II. Effects of aqueous salt solutions at 25°C. Geochim. Cosmochim. Acta, 44, 915-924
- Martin, J.M., Høgdahl, O.T. & Philpott, J.C. (1976). Rare earth element supply to the ocean. J. Geophys. Res., 81, 3119-24
- Mathews, A. (1972). Crystallisation of quartz from silicic acid: a kinetic investigation using sodium carbonate solutions. In Progress in Experimental Petrology ed. C.M.B.Henderson & D.L.Hamilton, vol 2. 2-65
- McCrea, J.M. (1950). The isotopic chemistry of carbonates and a palaeotemperature scale. J. Chem. Phys. 18, 849-57
- McDonald, R.S. (1958). Surface functionality of amorphous silica by infrared spectroscopy. J. Phys. Chem. 62, 1168-78
- McRae, S.G. (1972). Glauconite. Earth Sci. Rev. 8, 397-440

- Menzal, D.W. (1974). Primary productivity, dissolved and particulate organic matter and the sites of oxidation of organic matter. In The Sea, ed. E.D.Goldberg. vol.5, Wiley-Interscience, 659-678
- Micheelsen, H. (1966). The structure of dark flint from Stevns, Denmark. Medd. Dansk. Geol. Foren. 16, 285
- Michniak, R. (1980). Petrology and origin of dark irregular chert nodules from the Lower Turonian sediments in the vicinity of the Ozarów, central Poland. Archiwum Mineralogiczne, 36, 100-16
- Midgley, H.G. (1951). Chalcedony and flint. Geol. Mag. 88, 179-84
- Millot, G. (1960). Silice, silex, silicification et croissance des cristaux. Bull. du Serv. de la Carte Geologique d'Alsace et de Lorraine, 13(4), 129-46
- Mizutani, S. (1966). Transformation of silica under hydrothermal conditions. J. Earth Sci. 14, 56-88
- Monroe, E.A. (1964). Electron optical observations of fine-grained silica minerals. Amer. Mineral. 49, 339-47
- Montbell, J. (1953). Tertiary Man Silicified. Publ. Jack Montbell. 67p. 1st Ed. (!)
- Mortimer, R. (1878). On the flints of the Chalk of Yorkshire. Proc. Geol. Assn. 5, 344
- Mortimore, R.N. (1979). The relationship of stratigraphy and tectonofacies to the physical properties of the white Chalk of Sussex. Unpubl. PhD thesis, Brighton Poly.
- _____ (1983). The stratigraphy and sedimentation of the Turonian-Campanian in the Southern Province of England. Zitteliana 10, 27-41
- _____ & Wood, C.J. (In Press). The distribution of flint in the English Chalk with particular reference to the "Brandon Flint Series" and the high Turonian flint maximum. In The Scientific Study of Flint and Chert. ed. G. de G. Sieveking & M.B. Hart, Camb. Univ. Press

- Murata, K.J., Friedman, I. & Gleason, J.D. (1977). Oxygen isotope relations between diagenetic silica minerals in the Monterey Shale, Temblor Range, California. Am. J. Sci., 277, 259-72
- _____ & Larson, R.R. (1975). Diagenesis of Miocene siliceous shales, Temblor Range, California. J. Res. USGS, 3 (5), 553-66
- _____ & Nakata, J.K. (1974). Cristobalite stage in the diagenesis of diatomaceous shale. Science, 184, 567
- Nakai, N. & Jensen, M.L. (1964). The kinetic isotope effect in the reduction and oxidation of sulfur. Geochim. Cosmochim. Acta. 28, 1893-1912
- Nygaard, E. (1982). Trace fossils in redeposited chalk, Mors, Denmark. IAS 3rd EUR. MTG., Copenhagen, 1982, Abstr.
- Oakley, K.P. (1939). The nature and origin of flint. Sci. Progress, 34, 277-86
- Oehler, J.H. (1973). Tridymite-like crystals in cristobalitic "cherts". Nat. Phy. Sci. 241, 64-5
- Oldershaw, A.E. (1968). Electron microscopic examination of Namurian bedded cherts, N. Wales (Gt. Britain). Sedimentology 10, 255-72
- Orme, G.R. (1974). Silica in the Visean limestones of Derbyshire, England. Proc. Yorks. Geol. Soc. 40(1), 63-104
- Parke, S. (1974). Glasses. In The Infrared Spectra of Minerals, ed. V. C. Farmer, Mineralogical Society Monograph 4. Chap. 21
- Peake, N.B. & Hancock, J.M. (1970). The Upper Cretaceous of Norfolk. In The Geology of Norfolk, ed. G.P. Larwood & B.M. Funnell. London: Headly Bros.
- Pederson, T.F. & Price, N.B. (1982). The geochemistry of manganese carbonate in Panama Basin sediments. Geochim. Cosmochim. Acta, 46, 59-68
- Pelto, C.R. (1956). A study of chalcedony. Am. J. Sci. 254, 32-50

- Perry, E.C.Jr (1967). The oxygen isotope chemistry of ancient cherts. Earth Planet. Sci. Letters. 3, 62-66
- _____, Ahmad, S.N. & Swulius, T.M. (1978). The oxygen isotope composition of 3,800 MY old metamorphosed chert and iron formation from Isukasia, east Greenland. Jour. Geol. 86, 223-39
- _____ & Tan, F.C. (1972). Significance of oxygen and carbon isotope variations in early Precambrian cherts and carbonate rocks of southern Africa. Bull. Geol. Soc. Am. 83, 647-64
- Piper, D.Z. (1974). Rare earth elements in the sedimentary cycle: a summary. Chem. Geol. 14, 285-304
- Pisciotta, K.A. (1981). Distribution, thermal histories, isotopic compositions, and reflection characteristics of siliceous rocks recovered by the DSDP. SEPM Spec. Pub. 32, 129-47
- Pittman, J.S.Jr. (1959). Silica in Edwards Limestone, Travis County, Texas. SEPM Spec. Pub. 7. 121-34
- Pollastro, R.M. (1981). Authigenic kaolinite and associated pyrite in chalk of the Cretaceous Niobrara Fm., Eastern Colorado. J. Sed. Pet. 51(2), 553-62
- Pomeroy, B. & Aubry, M.P. (1977). Relationship between Western European chalks and the opening of the north Atlantic. J. Sed. Petrology, 43(3), 1027-35
- Pyzik, A.J. & Sommer, S.E. (1981). Sedimentary iron monosulphides: kinetics and mechanism of formation. Geochim. Cosmochim. Acta 45, 687-98
- Raiswell, R. & Plant, J. (1980). The incorporation of trace elements into pyrite during diagenesis of black shales. Econ. Geol. 75, 684-99
- Ramsay, A.T.S. (1973). A history of organic siliceous sediments in oceans. In Organisms and Continents Through Geologic Time, ed. N.F. Hughes. Spec. Pap. Palaeont. 12, 199-234

- Rangin, C., Steinberg, M. & Bonnet-Courtois, C. (1981). Geochemistry of the Mesozoic bedded cherts of central Baja, California (Vizcaino-Cedros-San Benito): implications for the paleogeographic reconstruction of an old ocean basin. Earth Planet. Sci. Letters 54, 313-22
- Redfield, A.C. (1958). The biological control of chemical factors in the environment. Am. J.Sci. 46, 206-26
- Reeburgh, W.S. (1980). Anaerobic methane oxidation rate-depth distribution in SCAN-A sediments. Earth Planet. Sci. Letters 47, 345-52
- Reid, R.E.H. (1962). Relationships of fauna and sub-stratum in the palaeoecology of the Chalk and Chalk Rock. Nature, 194, 276-7
- Richardson, W.A. (1919). The origin of flint and chert. Geol. Mag. 56, 535-47
- Robaszynski, F. (1981). Moderation of Cretaceous transgressions by block tectonics. An example from the north and north-west of the Paris Basin. Cretaceous Research 2, 197-213
- _____, Amedro, S., Foucher, J.-C., Gaspard, D., Magniez-Jannin, F., Manivit, H. & Sornay, J. (1982). Synthèse biostratigraphique de l'Aptien au Santonien à partir de sept groupes paléontologiques: foraminifères, nannoplancton, dinoflagellés et macrofaunes. Rev. Micropal. 22, 195-321
- Robins, G.V., Seeley, N.J., McNeil, D.A.C. & Symons, M.C.R. (1978). Identification of ancient heat treatment in flint artefacts by ESR spectroscopy. Nature 276, 703-4
- Robinson, B.W. & Kusakabe, M. (1975). Quantitative preparation of sulphur dioxide for $^{34}\text{S}/^{32}\text{S}$ analyses from sulphides by combustion with cuprous oxide. Anal. Chem. 47, 1179-81
- Rosenfeld, J.K. (1981). Nitrogen diagenesis in Long Island Sound sediments. Am. Jour. Sci. 281, 436-62

- Ross, D.A. & Degens, E.T. (1974). Recent sediments of the Black Sea.
In Ross, D.A. & Degens, E.T. q.v., 183-99
- Rowe, A.W. (1900). The zones of the White Chalk of the English coast.
Part 1. Kent and Sussex, with appendices by J.W.
Gregory & Kitchir. The cliff sections by C.D.Sherborn.
Proc. Geol. Ass. 16, 289-68
- Roy, A.B. & Trudinger, P.A. (1970). The Biochemistry of the Inorganic
Compounds of Sulfur. Camb. Univ. Press. 400p
- Sabine, P.A. (1967). In Sites for the Proposed CERN 300 GeV Proton
Synchrotron. Vol.2. Geneva:CERN 201-16
- Sackett, W.S. & Moore, W.S. (1966). Isotopic variations of dissolved
inorganic carbon. Chem. Geol. 1, 323-28
- _____ & Thompson, R.R. (1963). Isotopic compositions of
recent continental shelf derived clastic sediments
of the eastern Gulf Coast, Gulf of Mexico. Bull.
Am. Assoc. Pet. Geol. 47, 525-31
- Savin, S.M. (1977). The history of the Earth's surface temperature
during the past 100 million years. Ann. Rev. Earth
Planet. Sci. 5, 319-55
- _____ & Epstein, S. (1970). The oxygen and hydrogen isotope
geochemistry of clay minerals. Geochim. Cosmochim.
Acta 34, 25-42
- Schlanger, S.C., Arthur, M.A., Jenkyns, H.C., & Scholle, P.A..
(In press). The Cenomanian-Turonian oceanic anoxic
event, 1. Stratigraphy and distribution of organic
rich beds and the marine $\delta^{13}\text{C}$ excursion. In
Marine Petroleum Source Rocks, ed. A.J.Fleet & J. Brooks.
Geol. Soc. Lond. Spec. Publ.
- Scholle, P.A. & Arthur, M.A. (1980). Carbon isotope fluctuations in
Cretaceous limestones: a potential stratigraphic
and petroleum exploration tool. Am. Assoc. Pet. Geol.
Bull. 64(1), 67-97
- _____ & Kennedy, W.J. (1974). Isotopic and petrological data
on hardgrounds from Upper Cretaceous chalks from western
Europe. Abstr. Progr. geol. Soc. Am. 6(7), 943

- Schrader, H.-J. (1971). Fecal pellets: role in sedimentation of pelagic diatoms. Science 174, 55-7
- Schultz, L.G. (1978). Mixed layer clay in the Pierre Shale and equivalent rocks, Northern Great Plains region. USGS Prof. Paper 1064-A 28p
- Seeley, M.-A. (1975). Thermoluminescent dating and its application to archaeology: a review. Jour. Arch. Sci. 2, 17-43
- Shackleton, N.J. & Kennett, J.P. (1975). Palaeotemperature history of the Cenozoic and the initiation of Antarctic glaciation: oxygen and carbon isotope analysis in DSDP sites 277, 279 & 281. In Initial Reports of the Deep Sea Drilling Project, vol. 24, 743-755
- Shepard, C.V. (1844). Treatise on Mineralogy. New Haven, 2nd ed.
- Shepherd, W. (1972). Flint. Its origin, Properties and Uses. London: Faber and Faber. 255p
- Shore, T.W. (1900). The Physical geology and early archaeological associations of the neighbourhood of Cheriton. Papers and Proc. Hants Field Club & Archaeol. Soc. 1900, 138
- Sieveking, G.de G., Bush, P., Furguson, J., Craddock, P.T., Hughes, M.J. & Cowell, M.R. (1972). Prehistoric flint mines and their identification as sources of raw material. Archaeometry 14(2), 151-76
- Siever, R. (1962). Silica solubility 0-200°C and the diagenesis of siliceous sediments. J. Geol. 70, 127-50
- Smayda, T.J. (1969). Some measurements of the sinking rate of fecal pellets. Limnol. Oceanogr. 14, 621-5
- Smith, A.G. & Briden, J.C. (1971). Mesozoic and Cenozoic Palaeocontinental Maps. Cambridge University Press.
- Smith, W.E. (1960). The siliceous constituents of chert. Geol. en Mijnb., 22, 1-5
- Sollas, W.J. (1880). On the flint nodules of the Trimmingham Chalk. Ann. and Mag. Nat. Hist. 1880, 440-58
- _____ (1905). The origin and formation of flints. In The Age of the Earth and Other Geological Studies. London: T. Fisher Unwin. Ch. 6, 133-65

- Sorby, H.C. (1861). On the origin of the so called "crystalloids" of the chalk. Ann. Mag. Nat. Hist. Ser.3, 8, 193-200
- _____ (1879). Anniversary Address. Proc. Geol. Soc. Lond. 1879
- Sosman, R.B. (1926). The Properties of Silica. Am. Chem Soc., Monograph Series. 865p
- _____ (1954). New high-pressure phases of silica. Science, 119,783
- Spears, D.A. (1979). Geochemical aspects of the Santonian Chalk of Ramsgate, England, and the origin of the chert and clay minerals. Min. Mag. 43(325), 159-64
- Stein, C.L. & Kirkpatrick, R.J. (1976). Experimental porcellanite recrystallization kinetics: a nucleation and growth model. J. Sediment. Petrol. 46, 430-35
- Stöber, W. (1967). Formation of silicic acid in aqueous suspensions of different silic modifications. Adv. Chem. Ser. 67, 161-82
- Strelow, F.W.E. & Jackson, P.F.S. (1974). Determination of trace and ultra-trace quantities of rare earth elements by ion exchange chromatography-mass spectrography. Analytical Chemistry 46(11), 1481-6
- Stumm, W. & Morgan, J.J. (1970). Aquatic Chemistry. Wiley-Interscience
- Suthill, R.J., Turner, P. & Vaughan, D.J. (1982). The geochemistry of iron in recent tidal-flat sediments of the Wash area, England: a mineralogical, Mossbauer and magnetic study. Geochim. Cosmochim. Acta 46, 205-17
- Sverdrup, H.U. (1938). On the process of upwelling. J. Mar. Res. 1, 155-64
- Tarr, W.A. (1917). The origin of chert in the Burlington Limestone. Amer. J. Sci. Ser.4, 44S, 409-52
- _____ (1926). The origin of chert and flint. Univ. Missouri Studies, 1(2)
- _____ (1938). The terminology of the chemical siliceous sediments. Nat. Res. Council, Div. of Geol. & Geog., Exhibit A of the Report of the Committee on sedimentology. 1937-8, 8-27

- Trudinger, P.A. & Chambers, L.A. (1973). Reversibility of bacterial sulfate reduction and it's relevance to isotope fractionation. Geochim. Cosmochim. Acta 37, 1775-8
- Tucker, M.E. (1974). Sedimentology of Palaeozoic limestones: the Devonian Griotte (Southern France) and Cephalopodenkalk (Germany). In Pelagic Sediments: On Land and Under the Sea. ed. K.J.Hsu & H.C.Jenkyns. Spec. Publ. Int. Ass. Sediment. 1, 71-92
- Turner, D.R. & Whitfield, M. (1979). Control of seawater composition. Nature, 281, 468-9
- Valeton, I. (1960). Vulkanische Tuffiteinlagerung in der nordwest-deutschen Oberkreide. Mitt. geol. St. Inst. Hamb. 29, 26-41
- Van Hinte, J.E. (1976). A Cretaceous time scale. Am. Assoc. Pet. Geol. Bull. 60(4), 498-516
- Van Lier, J.A., De Bruyn, P.L. & Overbeck, J.T.G. (1960). The solubility of quartz. J. Phys. Chem. 64, 1675-1682
- Veizer, J., Holser, W.T. & Wilgus, C.K. (1980). Correlation of $^{13}\text{C}/^{12}\text{C}$ and $^{34}\text{S}/^{32}\text{S}$ secular variations. Geochim. Cosmochim. Acta, 44, 579-87
- Voigt, E. (1959). Die ökologische bedeutung de härtgründe ("hardgrounds") in der oberen kreide. Paläont. Zeitschr. 33, 129-47
- _____ (1979). Wann haben sich die feuersteine de oberen kreide gebildet. Nach. Akad. Wissensch. Gatt. II. Math-Phys. 6, 1-54
- Von Rad, U., Reich, V. & Rössch, H. (1978). Silica diagenesis in continental margin sediments off northwest Africa. In Initial Reports of the Deep Sea Drilling Project, vol. 41, 879-905
- _____ & Rössch, H. (1972). Mineralogy and origin of clay minerals, silica and authigenic silicates in leg 14 sediments. In Initial Reports of the Deep Sea Drilling Project, vol. 14, 727-51
- Walsh, J.N. (1980). The simultaneous determination of the major, minor and trace constituents of silicate rocks using inductively coupled plasma spectrometry. Spectrochimica Acta 35B, 107-11

- Walsh, J.N., Buckley, F. & Barker, J. (1981). The simultaneous determination of the rare earth elements in rocks using inductively coupled plasma source spectrometry. Chem. Geol. 33, 141-53
- Weaver, M. & Wise, S.W. (1972). Deep sea cristobalite cherts and authigenic minerals. Science, 237, 56-7
- _____ (1974). Opaline sediments of the southeastern coastal plain and Horizon A: biogenic silica. Science 184, 899-901
- _____ (1975). Origin of opal-A: clarification of a viewpoint- a reply. Science 188, 1221-2
- Weir, A.H. & Catt, J.A. (1965). The mineralogy of some Upper Chalk samples from the Arundel area, Sussex. Clay Minerals, 6, 97-110
- Weymouth, J.H. & Williamson, W.O. (1951). Some physical properties of raw and calcined flint. Min. Mag. 29, 573-93
- White, J.F. & Corwin, J.F. (1961). Synthesis and origin of chalcedony. Am. Mineral. 43, 580-4
- Whitten, D.G.A. & Brooks, J.R.V. (1972). A Dictionary of Geology. Harmondsworth, Middlesex, England: Penguin.
- Willey, J.D. (1980). Effects of ageing on silica solubility: a laboratory study. Geochim. Cosmochim. Acta 44, 573-78
- _____ (1982). Partial molal volume calculations for the dissolution of aged amorphous silica in salt water and seawater at 0-2°C. Geochim. Cosmochim. Acta, 46, 1307-10
- Wilson, M.J., J.D. Russell & Tait, J.M. (1974). A new interpretation of the structure of disordered α -cristobalite. Contr. Mineralogy and Pet. 47, 1-6
- Wilson, R.C.L. (1966). Silica diagenesis in the Upper Jurassic limestones of southern England. J. Sediment. Petrology 36(4), 1036-49
- Wise, S.W.Jr. & Kelts, K.R. (1972). Inferred diagenetic history of a weakly silicified deep sea chalk. Trans. Gulf Cst. Ass. Geol. Socs. 22, 177-203

- Wollast, R. (1974). The silica problem In The Sea, ed. Goldberg, E.D., New York: Wiley & sons. 359-392
- Wood, C.J. & Smith, E.G. (1978). Lithostratigraphical classification of the Chalk in North Yorkshire, Humberside and Lincolnshire. Proc. Yorks. Geol. Soc. 42, 263-87
- Woodward, S.P. (1864). On the nature and origin of banded flints. Geol. Mag. 1(4), 145-9
- Wooster, W.S. & Reid, J.L. (1963). Eastern boundary currents. In The Sea. vol II, ed. M.N. Hill, New York: Wiley-Interscience. 253-80
- Wroost, V. (1936). Vorgänge der kieselung an beispiel des Feuersteins der kreide. Abh. Senkenb. naturf. Ges. 432, 1-68